SEDIMENTARY FACIES ASSOCIATIONS OF THE LOWER REACHES OF THE ZAYANDEH RIVER AND THE GAVKHONI PLAYA LAKE BASIN (ESFAHAN PROVINCE, IRAN)

Dissertation
zur Erlangung des Grades eines
Doktors der Naturwissenschaften

vorgelegt von
Hamid Reza Pakzad, M.Sc.
aus Esfahan, Iran

genehmigt von der
Mathematisch-Naturwissenschaftlichen Fakultät
der Technischen Universität Clausthal

Tag der mündlichen Prüfung:
11.07.2003

Referent: Prof. Dr. H. Kulke

Korreferent: Prof. Dr. C. Brauckmann
Korreferent: Prof. Dr. H.J. Gursky

Dekan: Prof. Dr. D. Mayer

Die Arbeit wurde an der Abteilung für Erdölgeologie des Institutes für Geologie und Paläontologie der TU Clausthal angefertigt.

ACKNOWLEDGMENTS

I would like to express my gratitude to my supervisors Prof. Dr. H. Kulke for introduction to genetic sedimentologic field studies, improvement of the text, his valuable guidance, support and in solving many of my problems and Prof. Dr. C. Brauckmann for paleantology studies, and correction of the thesis. The writer also wishes to thank Dr. A. Hamedani, my Iranian supervisor for his help in field, his support and encouragement.

Special thanks are given to Dr. F. Fayazi from the Teacher Training University of Tehran, Dr. R. Ajaloeian from the Esfahan University and Dr. N. Arzani from the Piam-e-Nor University for help in field studies, valuable comments, review and correction of my thesis. I am also grateful to Dr. A. Amini from the Teheran University for his assistance in field studies, and benefit discussion with him. Thanks to Dr. H. Safaei and Mr. A. Seif for satellite images processing, Dr. H. V. Moghaddam for paleontology studies and Mr. A. Afsharzadeh for his help in biology studies from the Esfahan University.

I would like to thank Dr. C. D. Sattler (XRD analyses and helping to determine clay minerals), for his support in solving many of my problems and also Dr. H. M. Schulz for his guidance and encouragement during the time that I was at the University of Clausthal. I wish to thank the technical staff of the Institute of Geology and Palaeontology of the Clausthal University for their help during laboratory works, particularly Mr. A. Schulz (for pretreatment of XRD analysis), Mr. F. Sandhagen (for SEM).

Thanks also to all undergraduate students in the Geology Department of the Esfahan University especially Mr. A. Soltani and Mr. M. Makizadeh who helped me in field measurements. I am much indepted the staff of the Research Center of Nasoz-e-Azar of Esfahan (thin section and SEM) and Atomic Energy Organization of Iran (XRD). I wish to thank Mr. M. Haghighipor in the Chemical Department of the Esfahan University for helping me to do chemical analyses of water samples. I would like to thank the Ministry of Culture and Higher Education and the University of Esfahan for financial supports.

Final word of thanks goes to my wife and my children for their patience and encouragement during this study.

ABSTRACT

The study area, located in an intramontane basin to the southeast of Esfahan, comprises aeolian, playa lake and alluvial/fluvial sedimentary environments. The playa lake is permanently fed by the Zayandeh river. The basin is well developed parallel to the Zagros orogenic belt in central Iran.

The aeolian sand field consists of two main sand forms: sand dune and sand sheet. High groundwater table, salinity, mud drapes, gravel lag deposits and vegetation are factors, which inhibit dune development, limit the migration of sand and promote the formation of sand sheets. Lithology/mineralogy composition of aeolian sands indicates that they are mostly derived from water-laid sediments of the Zayandeh river.

The playa lake includes six major sub-facies: sand flat, sand beach, mud flat, saline mud flat, salt pan and an etreme shallow delta, indicating sedimentation from shallow fresh/brackish water perennial lake to an ephemeral saline lake. Chemical analysis of water suggests that evolution of water is from Na^{+}, (Mg^{++}), Cl^{-}, (SO_4^{--}) to Na^{+}, Mg^{++}, Cl^{-}. Mineral assemblage comprise halite, carnallite, bischofite, and tachyhydrite in the centre of the salt pan.

The alluvial fan deposits can be divided into four facies associations:1. Debris-flow-dominated alluvial fan. 2. Stream-flow-dominated alluvial fan. 3. Lake 4. Overbank. These facies emphasizes a periodic deposition in a semi-arid setting with dominance of low energy conditions.

Regarding the facies it is supposed that climatic changes played an important role in sedimentation. During periods of increased run off and raising water table in the playa lake, sedimentation of alluvial and lacustrine deposits occurred. During periods of reduced run-off and falling water table, the salt pan formed and wind erosion of alluvial deposits resulted in formation of the aeolian sand field.

KURZFASSUNG

Das Untersuchungsgebiet liegt in einem reifen intramontanen Becken, das sich im Zentral-Iran südöstlich von Esfahan parallel zum Zagros-Gebirge erstreckt. Die Sedimentation umfasst äolische und alluvial/fluviatile Ablagerungsräume mit einer Playa im Beckentiefsten, die durch den Zayandeh-Fluss saisonal überflutet wird.

Im äolischen Ablagerungsmilieu sind Sanddünen und Schichtsande vorherrschend. Hoher Grundwasserstand, Salinität, Ton- und Kieslagen sowie Pflanzenbewuchs sind die Faktoren, die eine Dünenentwicklung verhindern bzw. deren Migration hemmen, dafür aber die Bildung von Schichtsanden fördern. Die lithologisch-mineralogische Zusammensetzung der äolischen Sande zeigt, dass diese aus dem fluviatilen Umfeld des Zayandeh stammen.

Die Sedimente der Playa umfassen insgesamt sechs Subfazies im Bereich eines permanenten flachen Süßwasser/Brackwasser-Sees bis hin zu einem ephemeralen Salzsee: Sandwatt, Sandstrand, Schlickebene, Salztonebene, Salzpfanne und ein extrem flaches Delta. Chemische Analysen der Wässer zeigen Ionen-Assoziationen von Na^{+}, (Mg^{++}), Cl^{-}, (SO_4^{--}) zu Na^{+}, Mg^{++}, Cl^{-} an, aus denen Halit, Carnallit, Bischofit und Tachyhydrit im Zentrum der Salzpfanne ausgefällt werden.

Die Sedimente der alluvialen Schwemmfächer können vier Faziesbereichen zugeordnet werden: 1. Schlammstrom-dominierte Schwemmfächer. 2. Fluviatil-dominierte Schwemmfächer. 3. Lakustrine Bereiche. 4. Überflutungsebene. Diese Fazies zeigen ein periodisches, niedrig energetisches Ablagerungsmilieu unter semi-ariden Bedingungen an.

Es wird angenommen, dass Klimaänderungen einen wichtigen Einfluss auf die Sedimentation ausgeübt haben. In Zeiten erhöhter Niederschläge bzw. steigendem Wasserspiegel im Bereich der Playa dominierten alluviale Schwemmfächer bzw. lakustrine Ablagerungen. Trockenperioden hingegen führten zur Ausbildung einer Salzpfanne, und durch Winderosion der alluvialen Schwemmfächer bildeten sich äolische Sandfelder.

CONTENTS

List of Figures

(Page numbers in brackets)

List of Tables

(Page numbers in brackets)

Chapter 1

Introduction

1.1 Objectives of the study

Many investigations have been done on intermontane basins during the last few decades. A certain volume of evaporite productions in the world derives from these basins. Number of oil (gas) reservoirs and some groundwater resources have been found in this type of basins. Therefore, intramontane basins, especially playa lakes, have been a very interesting subject from the viewpoint of sedimentology of evaporites and economic for geologists for several decades .

Despite economic importance of playa lakes, there are few sedimentological or geochemical data and therefore no systematic investigation on such depositional environments. A knowledge of the sedimentary processes, mineralogy, and post depositional alterations of the sediment is essential, not only to assess the present and future potential of the economic resources but also to evaluate the short-term changes and long-term evolution of the depositional system. A study of evaporite mineralogy and its relation to basin lithology, hydrochemistry, and brine evolution promotes our knowledge on terrestrial-evaporite sequences. Because of the closed nature of the studied playa lake, its sediments represent a sensitive indicator of any changes in hydrologic budget within the drainage basin. Thus, stratigraphic record in this playa lake should be a good reflection of past climatic fluctuation.

Because of these reasons and my private interest, the topic has been chosen. The main objectives of this study are:

1. To study aeolian sand forms, the provenance of aeolian sands and to identify factors, which control the migration and development of aeolian sands and sand dunes.
2. To describe the nature of interactions between aeolian, fluvial and playa lake environments.
3. To study the sub-environments of the Gavkhoni playa lake and the geochemistry of its brine.
4. To investigate sedimentology of the Zayandeh river and their development.
5. To investigate development, distribution, and stratigraphic sequence of alluvial fans.

1.2 Previous researches

Previous researches have mostly been focused on general geology, geography and pedology in a range of environments in the studied area. Aeolian sands and the Gavkhoni playa lake deposits were studied in general. On the other hand, detailed investigation of the sediments has not been done.

Krinsley (1970) studied the playa lakes of Iran, and carried out a general assessment of the Gavkhoni playa lake. The clay minerals of the Zayandeh river flood plain and the saline soils of the Gavkhoni playa lake were studied (Khademi, 1985; Foroghi, 1983; Honarjo, 1982). Nabian *et al*., (1991) published the first detailed report about potash in the brine of the Gavkhoni playa lake. Ramesht (1992) studied the Zayandeh river terraces and their effect on the special landscape of Esfahan. Tabatabaei (1996) gave the first preliminary description of the aeolian sands. He studied the source of the Varzaneh aeolian sands regarding grain size variations.

1.3 Methodology

In order to achieve the objectives, field and laboratory works were carried out in several stages during about four years to get required data. Using Landsat TM image, and topographic maps (1: 250 000 scale with 100 m counter interval) the slope of alluvial fans were measured, geomorphology of the area was studied, and location of sampling were determined. Thirty four vertical sections including trenches, pits and profiles cut by streams and ghanat (underground channel with a lot of wells, which drain and conduct groundwater onto ground surface) were utilized to study vertical and lateral activity and stratigraphy of sedimentary environments. Color variation, geometry of facies, sedimentary structures, and the nature of boundary of facies were studied. Lithostratigraphic-sedimentological sections were drawn based on vertical distribution of facies. Several photographs were taken from sedimentary structures and remarkable sedimentological features.

Based on facies variation, a total of 150 samples (each 1 to 3 kg), were collected in the study area. Among these, are 50 samples from sand dune, 15 samples from sand sheet, 50 samples from lacustrine/overbank and 35 samples from coarse-grained alluvial/fluvial

deposits. Grain size of about 150 samples was analyzed by sieving (dry and wet) at 0.5 phi intervals and hydrometer and pipette methods from gravel to mud were applied. Based on grain size data histogram and cumulative curves were drawn and statistical size parameters (mean, standard deviation, kurtosis and skewness) were subsequently calculated using the moment method. The long axis of ten largest particles of 35 samples also was measured. The roundness of 100 samples (sand and gravel size) was chiefly examined by binocular, polarizing microscope and macroscopically by visual estimation. SEM was utilized where it was felt necessary.

To measure the rate of movement of active sand dunes, stick marks with about 100 m interval were established at the foot of a few dunes. Variations of a crest line of these dunes were investigated by taking photograph during different seasons. Gradient of the lee sides and stoss sides of few arms of star dunes was measured. For determination of grain size of wind-blown material and deflated sand volume, several sampling traps were installed in suitable places around the active sand dunes (see Appendix E for procedure of installation).

For determination of mineralogical/lithological composition and finally of provenance of aeolian sands and alluvial/fluvial deposits: 1-About 60 representative samples (sand fraction) were selected for analysis of heavy minerals from N-S of sand dunes (Appendix C). 2-Carbonate content of about 40 samples (sand fraction) was undertaken using a chemistry method (Appendix A2). 3-Thin sections of about 90 samples, were prepared (0-1,1-2 and 2-3 phi fractions) (Appendix D). 4-Lithic grains (gravel fraction) composition of about 20 samples was studied.

Clay size fraction of 22 samples was separated by the means of sedimentation method. X-ray diffraction analyses were undertaken for the detection of different clay minerals (Appendix B1). Ten samples were taken to determine evaporitic minerals in salt pan using X-ray diffraction (Appendix B2).

For palaeontology studies, approximately 100 disaggregated samples (sand and mud fractions) were washed through a 0.062 mm sieve. Dried residues were separated through sieves at half-phi intervals from 0.5 mm to 0.063 mm and then shells were picked by binocular microscope.

For investigation of sedimentology and stratigraphy of sub-environments and geochemistry of the Gavkhoni playa lake brine, fourteen trenches (up to 2.5 m deep, 2 m long, and 0.5 m wide) and pits (up to 1 m deep) were dug and two sedimentological logs (up to 30 m deep) provided by the Geology Survey of Iran were utilized. Variations of groundwater table were measured in all facies of the Gavkhoni playa lake.

In order to determine the type of water and also the evolution of brines, water samples were taken from Zayandeh river and groundwater (Zayandeh river, salt pan, saline mud flat and interdunes) during both in dry and moist seasons. The brines were analyzed by atomic absorption spectrometer (Ca^{++}, Mg^{++}, Sr^{++}, Na^{+}, K^{+}, Cl^{-}), spectrophotometer (NO_3^{-}) and titration (SO_4^{--}, HCO_3^{-}) (Appendix A1).

1.4. Outline of the thesis

This thesis is divided into 6 chapters. Chapter 1 describes few subjects of the study including previous researches, methodology and the outline of the thesis. Description of geology, geography, agriculture follows in chapter 2 in general. Chapter 3 presents the morphology of the various types of sand forms (linar/seif, star, barchan, barchanoid, dikaka, and sand drift hummocks and sand sheets) and their dynamics. This part also will explain mineralogical composition, textural characteristics, and the source of the aeolian sands. Chapter 4 suggests the types of the sub-environments and facies of the Gavkhoni playa lake, including sand beach, sand flat, mud flat, saline mud flat, salt pan and also delta and brine evolution in the playa lake. Development and distribution of alluvial fans and the Zayandeh river, their morphology, development and stratigraphy will be described in Chapter 5. Chapter 6 contains the summary of the results and conclusions are presented at the end of Chapters 2, 3, 4, and 5.

Chapter 2

Geographical, geological & agricultural background

2.1 Location & topography

The study area is located in central Iran to the southeast of Esfahan city. It is surrounded by mountains, which are mainly composed of Eocene volcanic rocks in the east and the northeast, and Jurassic and Cretaceous sedimentary rocks to the south and the west. Surface elevation range with a maximum height of about 3330 m above the sea level in the northern mountains and a minimum of 1474 m in the Gavkhoni playa lake. The most important large-scale landscapes of this area are the Gavkhoni playa lake, the Varzaneh aeolian sand field, the Zayandeh river and alluvial fans (Fig. 2.1).

The Gavkhoni playa lake is a closed drainage basin and approximately occurs at the end of the study are, eastward of the aeolian sand field, with an area of about 550 km^2. The Zayandeh river, which is a permanent river about 400 km long, originates from the Zardkuh mountain (at the beginning of the Zayandeh river basin) in the west and enters to the Gavkhoni playa lake in the east. The Varzaneh aeolian sand field is located to the west of the playa lake and covers an area of approximately 140 km^2, trending N/S. Maximum elevation of the aeolian sand dunes is about 130 m. Coarse-grained alluvial fan deposits, derived from the surrounding mountains, cover most of the study area, especially to the north and the northeast.

2.2 Tectonic setting

The Iranian Plateau (Central Iran, Urumieh Dokhtar magmatic and Sanandaj-Sirjan zones) lies between the Alburz and the Zagros zones (Krinsley, 1970). The northern part of the Sanandaj-Sirjan zone contains a series of depressions that are well developed parallel to the southwestern boundary of the Urumieh Dokhtar magmatic assemblage and the northeastern margin of the Zagros orogenic belt. The study area, as an intramontain basin, is one of these depressions (Alavi, 1994).

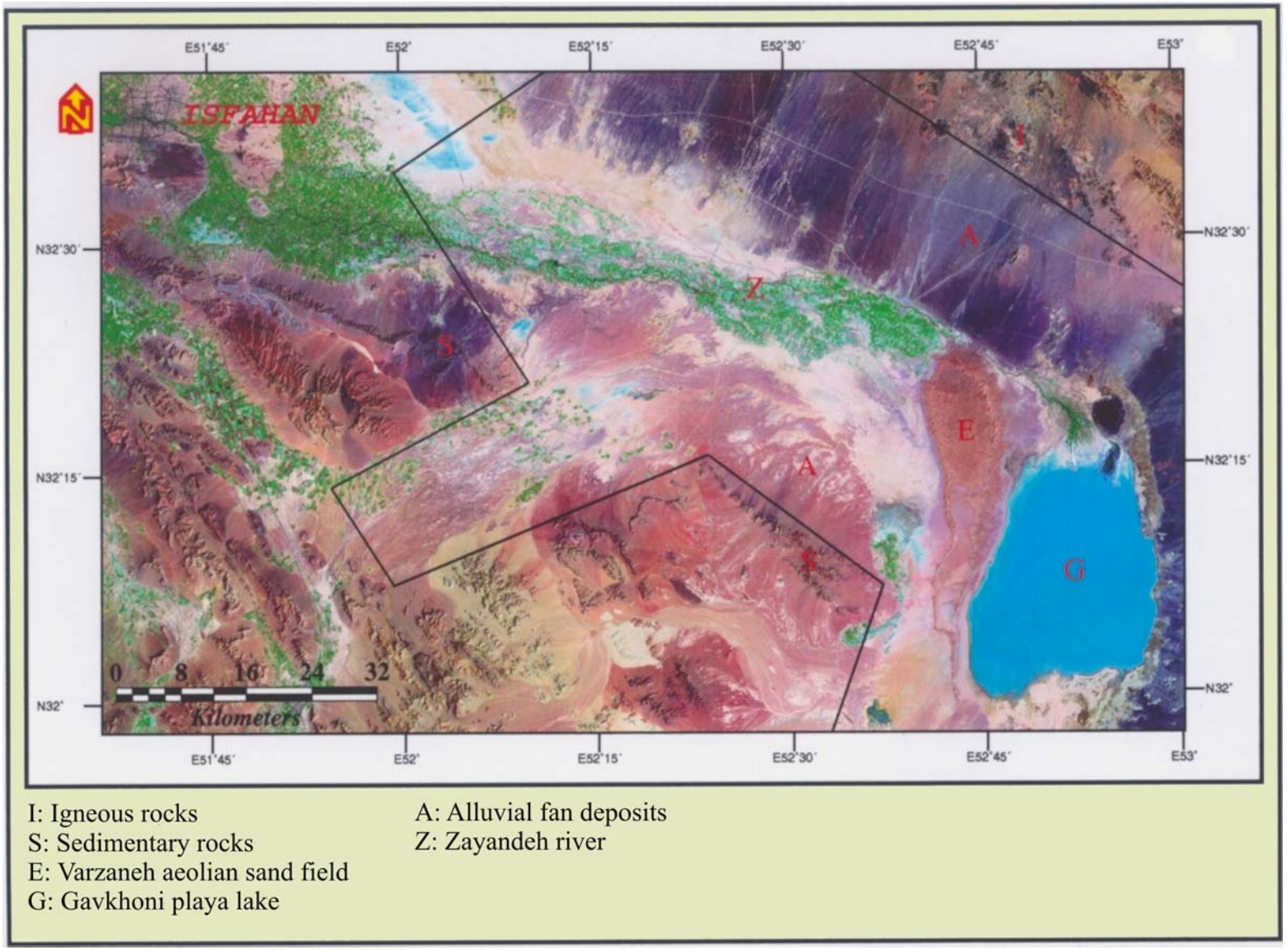

Fig. 2.1 False color-Landsat TM image showing approximate situation of the study area (indicated by black lines) and the major geological features of the lower reach of the Zayandeh river drainage basin.

Geological evidence suggests that during Paleozoic, Iran (Sanandaj-Sirjan, Central Iran and Alborz zones) formed the northern part of the continental platform of Arabia as a part of Gondwana land (Stoecklin, 1968b in Berberian, 1983). It was detached from Arabia along the main Zagros thrust line in the Late Paleozoic time or possibly the Early Triassic with formation of a new oceanic trough (Alpine ocean) between them, following extensional tectonics and rifting (Fig. 2.2 A).

Due to the Late Jurassic compressional movements, as a result of continuing subduction of the oceanic crust underneath the Sanandaj-Sirjan zone, the whole region underwent folding, faulting, magmatism and uplifting before deposition of the lower Cretaceous sediments. In the Late Cretaceous time, the whole Sanandaj-Sirjan zone underwent strong orogenic movement and magmatism. These conditions were a result of continuing subduction of oceanic crust underwent Iran. During this time the first depression parallel to the northeast of the Sanandaj-Sirjan zone formed and Cretaceous deposits folded weakly (Figs. 2.2 B & C).

Following the Late Cretaceous orogenic movement, immense volumes of lava were extruded during Eocene time and the Urumieh-Dokhtar magmatic zone was formed. This resulted in graben and/or half graben basins (e.g. Gavkhoni depression) during Eocene in response to crustal spreading along the northeastern part of the Sanandaj-Sirjan zone (Fig. 2.2 D).

In Neogene time, this graben and/or half graben basin was filled mostly by molasse–type erosional sediments. These sediments were folded and faulted during Oligocene and subsequently during the Late Plio-Pleistocene phase of the Alpine orogeny.

Recent coarse-grained alluvial fan deposits derived from the surrounding mountains, playa, aeolian sands and deposits covered the central deepest part of the depression in Quaternary time (Fig. 2.2 E). The Middle Miocene beds provided a source of salt for saline playa lake. The sedimentary infill of the basin consists of approximately 6 km of a Cenozoic and Quaternary deposits (NIOC, 1975; Berberian, 1983).

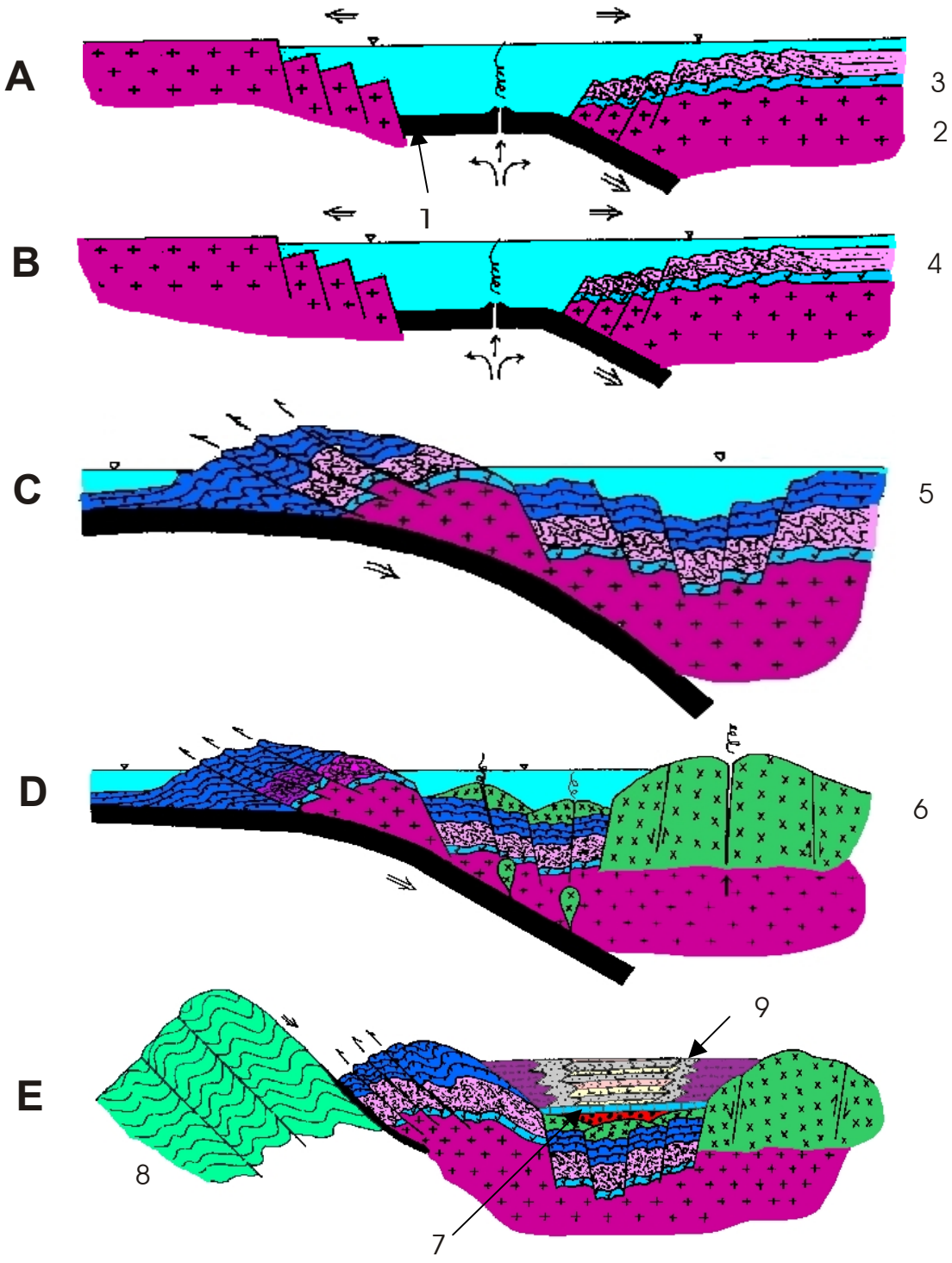

Fig. 2.2 Schematic hypothetic representation stages of sedimentary development of the intramontane basin of the Gavkhoni playa lake (modified from NIOC, 1975; Berberian, 1983; Tabatabaei & Makoui, 1994).

1. Oceanic crust. 2. Basement and platform cover (Infracambrian to Triassic). 3. Middle Triassic deposits. 4. Rhetain-Liassic deposits. 5. Baremian-Aptian deposits. 6. Eocene submarine volcanism. 7. Evaporite–clastic deposits (Oligocene). 8. High Zagros deposits. 9. Playa lake, alluvial and aeolian sands deposits (Miocene to Quaternary)

2.3 Lithostratigraphy of the Gavkhoni playa lake drainage basin

Lithology of the drainage basin can be divided into the three types of deposits: 1-Sedimentary rocks 2-Igneous rocks 3-Metamorphic rocks. Sedimentary rocks outcrop mostly in the west, the southwest and the northwest. Igneous rocks (mainly volcanic) outcrop in the east and the southwest. Metamorphic rocks extend mostly in the northwest of the playa lake. It is described the lithology of the basin from Precambrian to Quaternary as follow (Fig. 2.3).

Precambrian:

Schist, gneiss, metamorphosed volcanics, dolomitic limestone, amphibolite, marble, quartzite, phyllite.

Cambrian-Silurian:

Salt and pyritic marls with intercalation of sandstone, shale with intercalation of limestone.

Silurian- early Devonian:

Sandstone, dolomite with volcanics at the base.

Devonian:

Limestone, dolomitic limestone.

Devonian-Carboniferous:

Limestone, sandstone, quartzite.

Permian:

Limestone, dolomitic limestone, limestone locally bearing coaly shale, sandstone, dolomite, shale, sandstone, conglomerate.

Permo-Triassic:

Marly reddish limestone, limestone.

Lower-middle Triassic:

Vermicular limestone and oolitic limestone, yellow dolomite, marl, dolomite, dolomitic siliceous limestone, shale, sandstone.

Late Triassic:

Shale, sandstone, limestone, massive dolomite, dolomitic limestone, red sandstone, conglomerate with volcanic intercalation (locally).

Early Jurassic:

Shale, sandstone, conglomerate, limestone, radiolarite limestone, andesitic volcanic, argillaceous dolomitic limestone, sandy dolomite, argillaceous dolomite, tuff, sandy limestone, black shale, limestone with chert layers, granite, granodiorite.

Early Cretaceous:

Limestone, shale, sandstone, conglomerate, yellow dolomite, sandy dolomite, gray limestone, argillaceous marl, black shale with limestone, gray shale, reef limestone, argillaceous limestone, marl, sandy limestone, calcareous shale.

Late Cretaceous:

Shaly limestone, sandy limestone, marl, shale, glauconitic sandy limestone, marly limestone, dolomite, dolomitized limestone, limestone, calcareous shale.

Eocene:

Basaltic andesite, andesitic basalt, latite, dasite tuff, brecia ignimbrite, andesite, rhyolitic tuff, rhyodacite , basal conglomerate, conglomerate with sandy tuff, sandstone with intercalations of volcanic, siltstone with evaporitic intercalation, dolomitic limestone, limestone, radiolarite.

Eocene-Oligocene:

Dolerite.

Oligocene:

Rhyolitic lava, red conglomerate, sandstone, marl with andesitic basalt.

Oligocene-Miocene:

Limestone, basal conglomerate, marly limestone, sandy limestone, marl, acidic dike, rhyolitic pyromeride, gypsiferous marl.

Miocene:

Conglomerate sandstone.

Miocene-Pliocene:

Sandy limestone, conglomerate, sandstone, sandy marl, gypsiferous marl, marl with sandy limestone, agglomerate, granodiorite, andesite.

Pliocene-Pleistocene:

Conglomerate, sandstone, diorite, granite, granodiorite, trachy dacite, trachy andesite.

Pleistocene-Holocene

Clay pan, mud flat, sand dune, recent alluvial, river deposits, travertine, gypsiferous marl, marl.

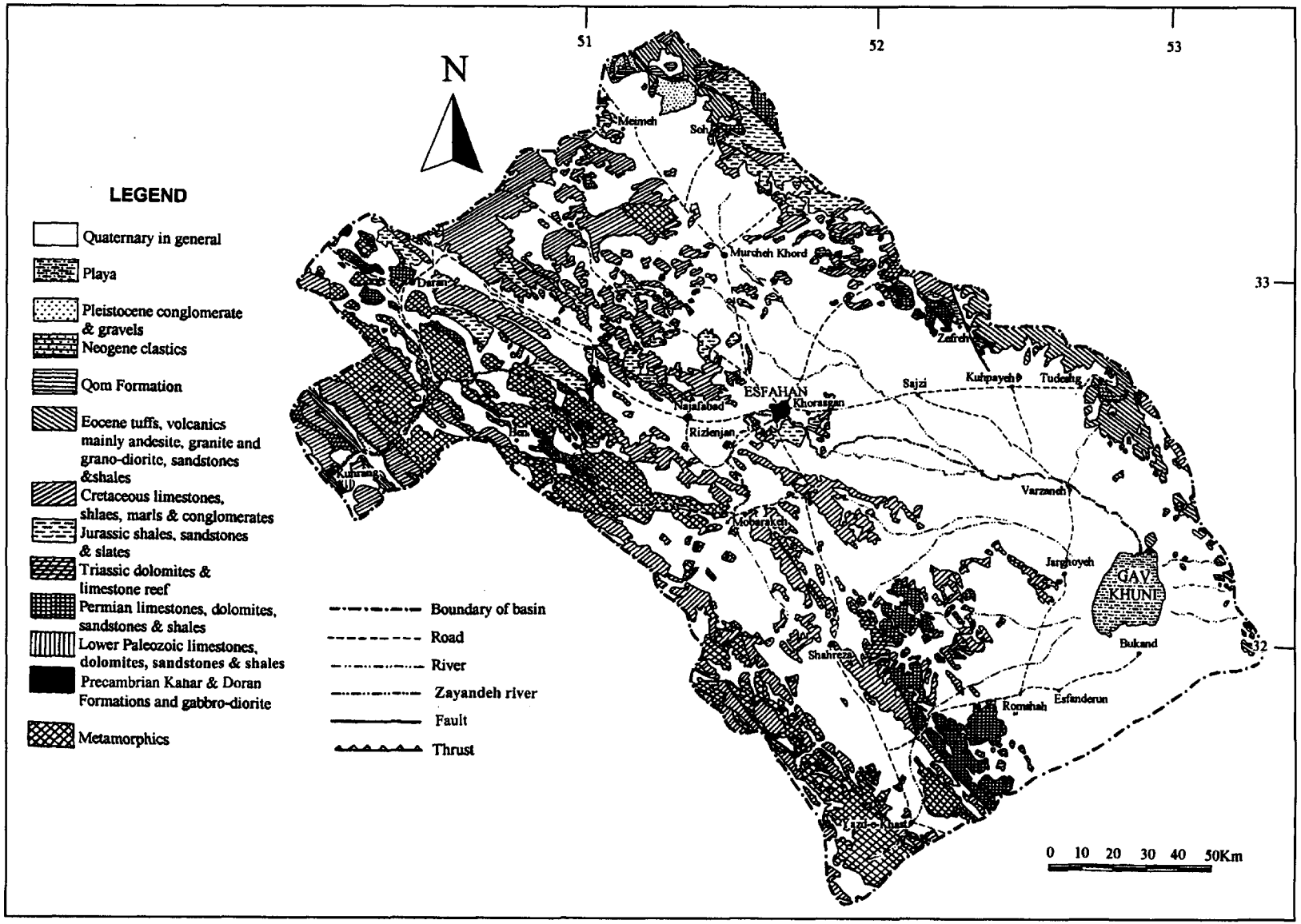

Fig. 2.3 Simplified geological map of the Gavkhoni playa lake drainage basin, showing deposits exposed in the study area (modified from NIOC, sheet 4 (1978) and sheets 2 and 5 (1977)).

2.4 Climate

Generally, the study area is located in the intertropical convergence zone, which approximately comprises one third of the world. This zone is classified into three sub-zones of extremely arid (4%), arid (15%) and semi arid (14.5%) climate (Nickling, 1994) (Fig. 2.4).

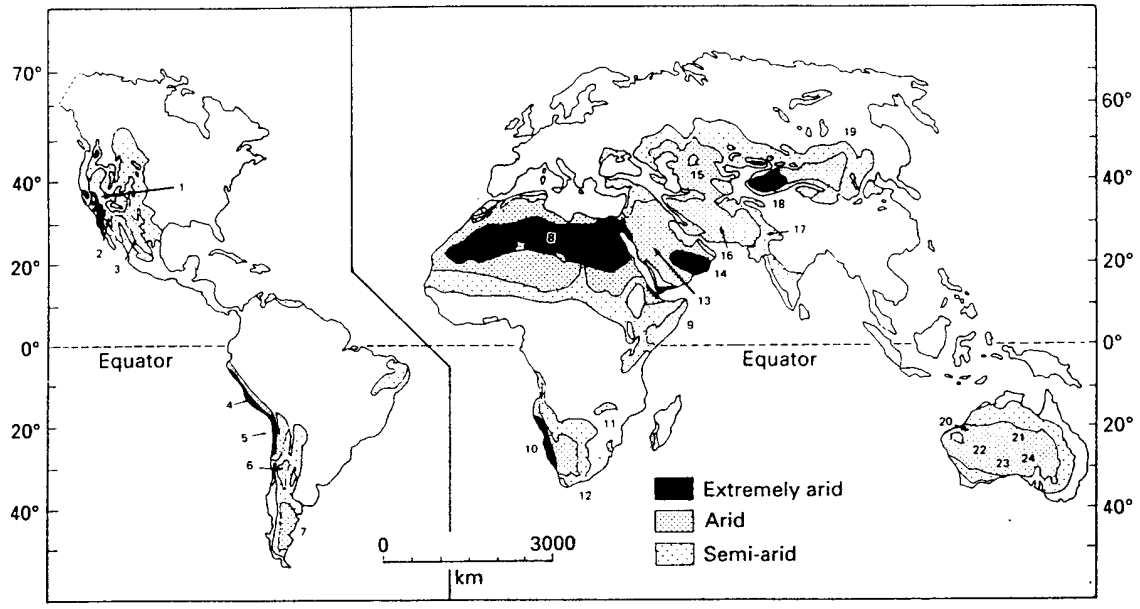

Fig. 2.4 Distribution of world dry lands; the study area (No. 16) includes an arid region (after Nickling, 1994 in Pye, 1994).

In the Varzaneh station, temperature varies between –17°C in winter and +42°C in summer. Average low temperature is 1.8°C in January and average high temperature is 39°C in July. Mean temperature is 9.30°C in spring and 20°C in autumn. The mean temperature is about 24°C during the hot season (June to September), and 5.5°C during the cold season (January to March) with annually 16°C. Average maximum humidity is 54%, minimum 27% with an annual average of 40.5%. Evaporation is very high, especially in summer, but variable within different seasons. Average evaporation rate is about 3265 mm/y (averaged over 10 years, unpublished data, Iranian Water Organization, 1999).

Moist winds bring considerable precipitation during winter to the northern slopes of the Alborz mountains, which effectively prevent the movements of moisture to the south.

Similarly, the Zagros mountains act as barrier to the moisture of the westerly winds. Rainfall is quickly reduced southwards and the eastwards. The air from the southeastern monsoon, after having passed through India, reaches Baluchistan and Iran almost completely dry. It is stable and dry when it descends from the Makran mountains. Therefore, the interior area lies within a vast rain shadow, and becomes increasingly arid from the west to the east and from the north to the south. For this reason, the study area, located in this region, has a desert climate (Krinsley, 1970). Annual mean precipitation exceeds 600 mm in the northwest corner of the Zayandeh river drainage basin (Kuhrang 3974 m elevation), but decreases up to 80 mm in Varzaneh. Maximum and minimum annual rainfall recorded there is between 153 and 32 mm. Average rainfall occurs 48 % in winter, 29% in spring, 2% in summer and 21% in autumn in the Varzaneh station (averaged over 25 years unpublished data, Iranian Water Organization, 1999).

Data from the Varzaneh station supported by observations in the field suggest that the westerly winds are dominant throughout the year (mainly 9 months). Wind frequency increases from January onwards and reaches maximum in March. It decreases from April to November and again increases in December. The dominant westerly and the northwesterly winds blow in May, southwesterly ones in March and April, the southeasterly and the easterly ones in June and July, and the northeasterly ones in July. Minimum mean wind speed is about 1.2 m/s in November and maximum 3.1 m/s in February and March. Minimum mean wind speed is recorded in autumn (October-November). Maximum wind speed across the area is about 28 m/s blowing during March, and April. The frequency of dominant wind direction varies between 12% (November) to 24.6% (March and May). The frequency of wind in March and April is higher than in the other months. The maximum frequency of calm wind is in November (71.7%) and autumn (68%). The minimum frequency of calm wind is in April (about 38.7%) and spring (42%) (over 36 years, unpublished data, Iranian Meteorology Organization, 1999) (Fig. 2.5).

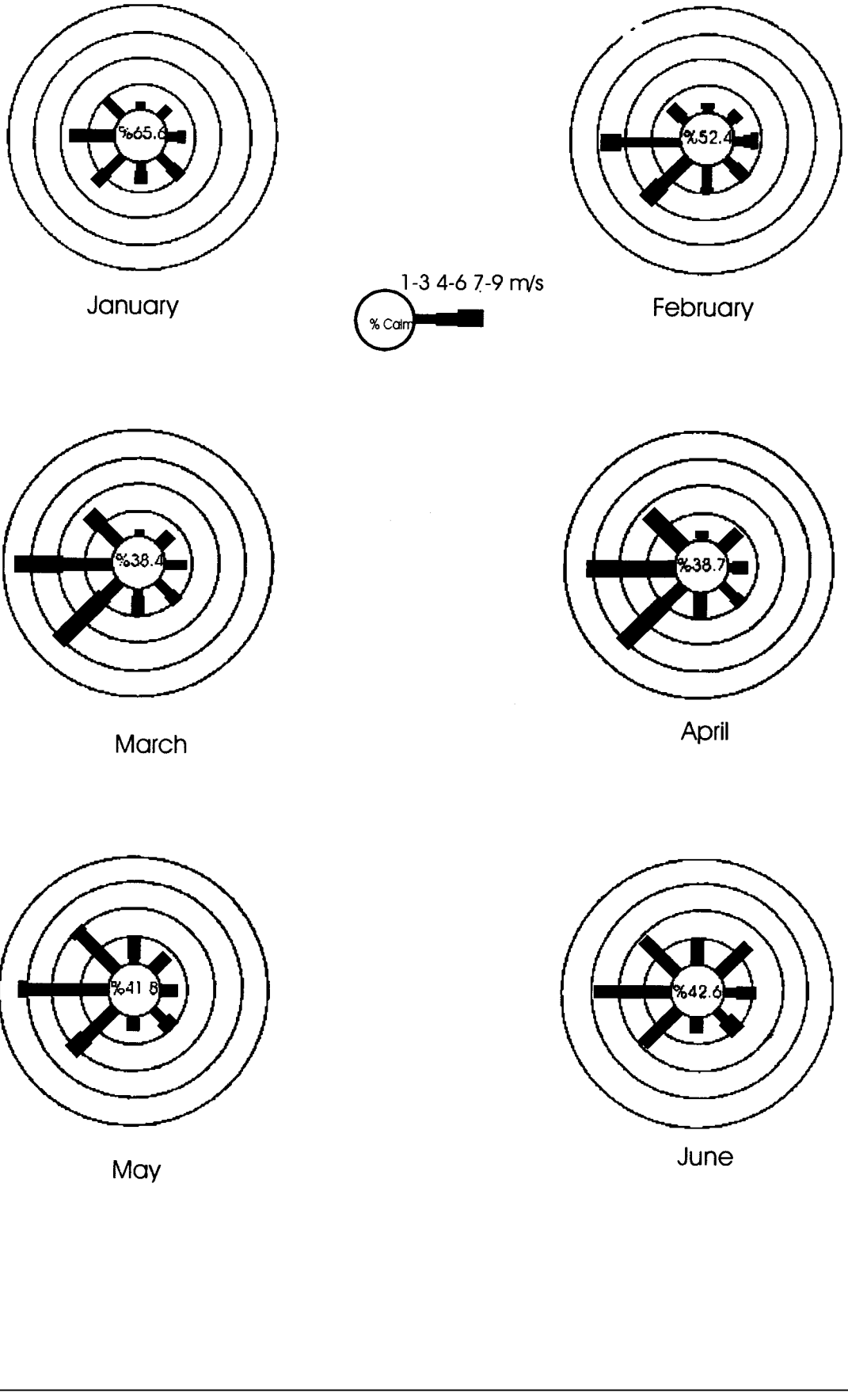
%65.6
January
1-3 4-6 7-9 m/s
% Calm
%52.4
February
%38.4
March
%38.7
April
%41.8
May
%42.6
June

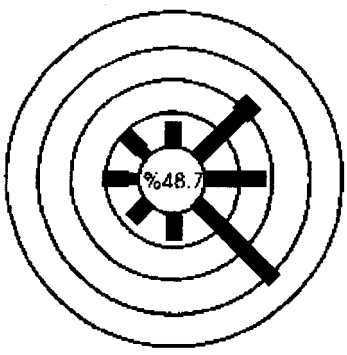

July

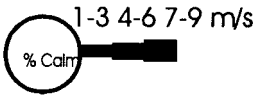

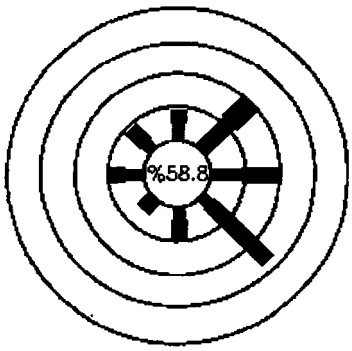

August

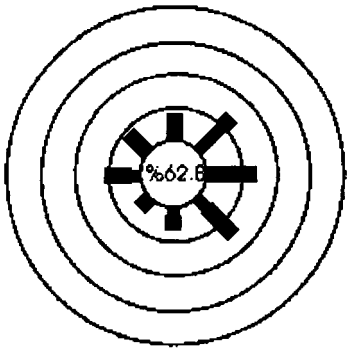

September

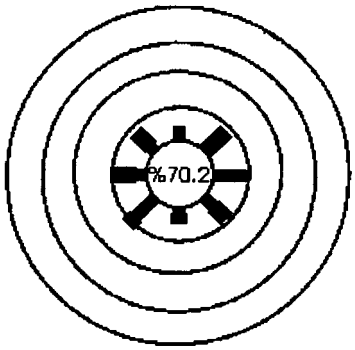

October

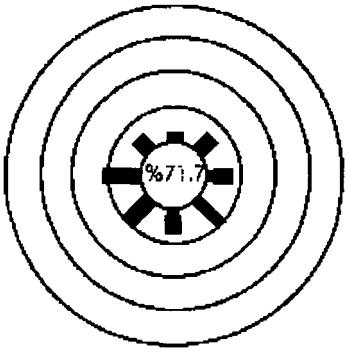

November

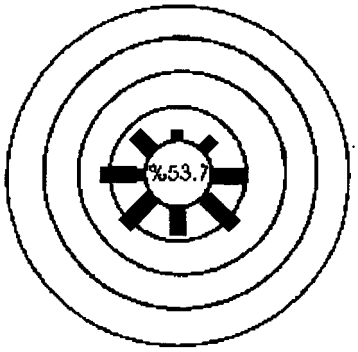

December

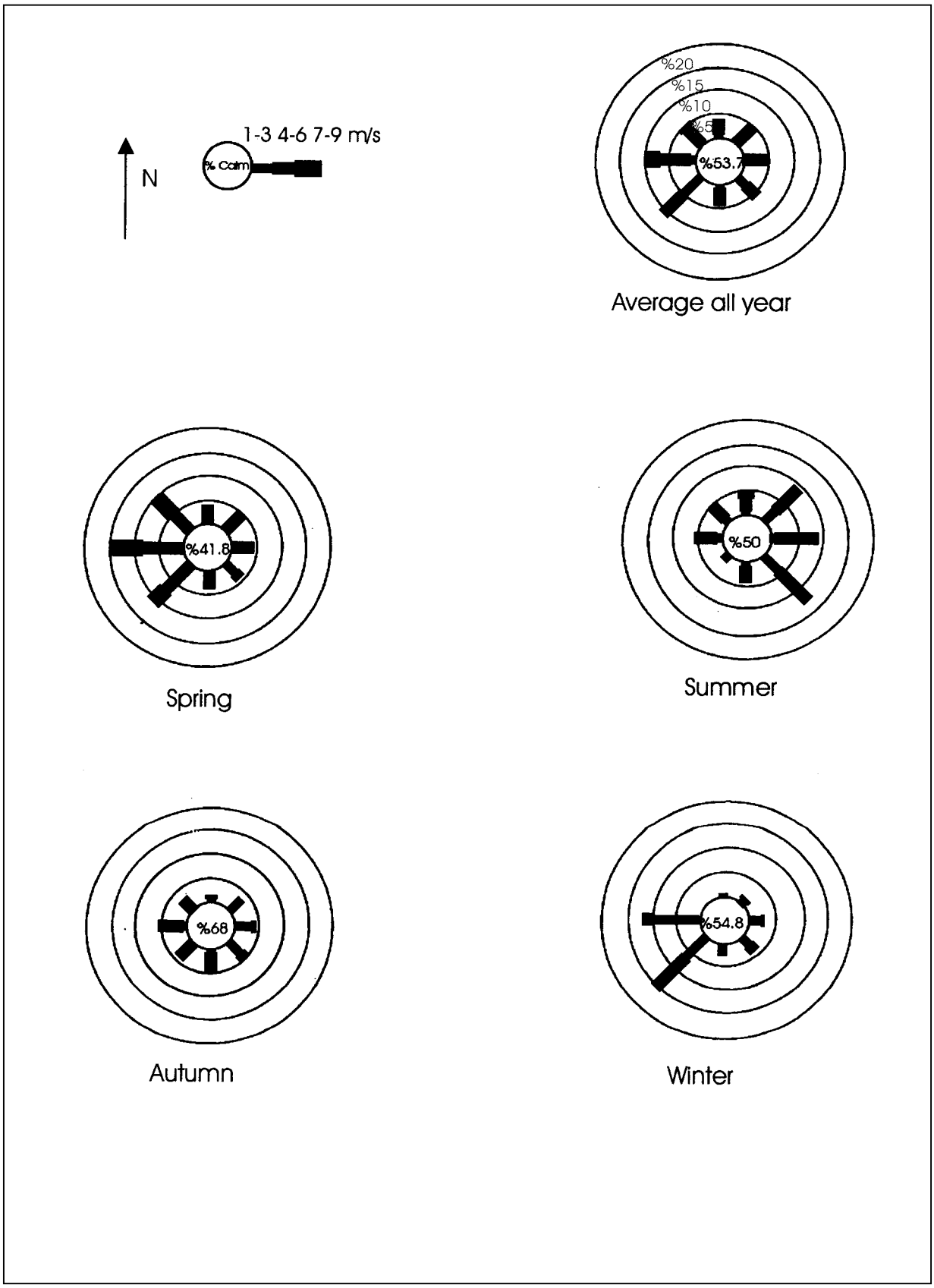

Fig. 2.5 Wind roses for monthly, seasonally and annually average in the study area from the Varzaneh observation station.

2.5 Drainage

The Gavkhoni playa lake drainage basin, which is about 39000 km^2 in area, is fed by the Zayandeh river, two ephemeral rivers and several small streams (Fig. 2.6).

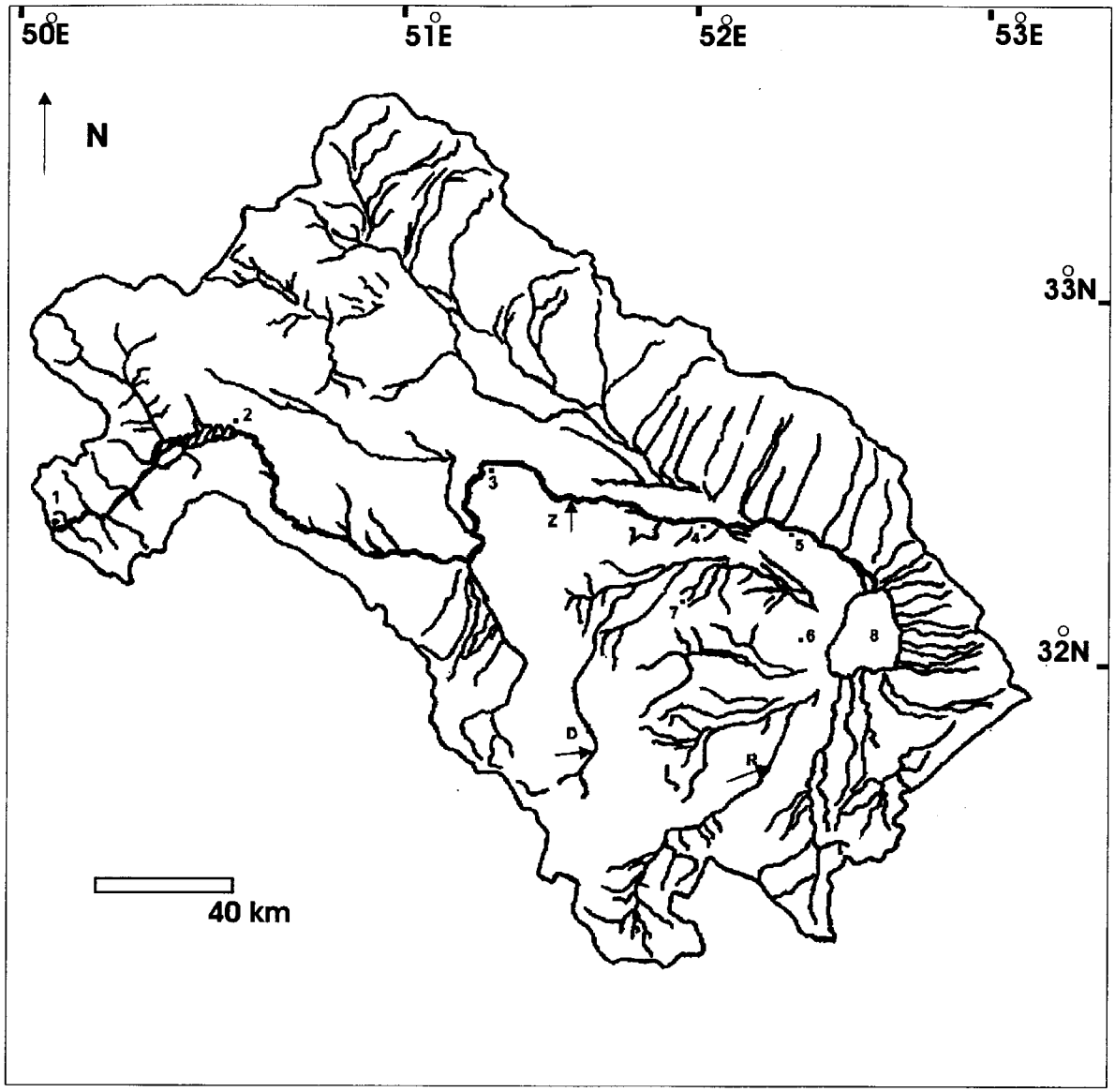

Fig. 2.6 Drainage basin of the Gavkhoni playa lake: 1. Kuhrang (3974 m elevation), Zayandeh river dam, 3. Esfahan city, 4. Ejieh, 5. Varzaneh, 6. Jarghoieh (Khara), 7. Nikabad, 8. Gavkhoni playa lake, Z. Zayandeh river, R. Rahimi river, D. Zardcheshmeh river (modified from unpublished report, Iranian Agricultural Administration, 1998).

The Zayandeh river activity forms a major part of sedimentation processes in the southeast of Esfahan sedimentary basin. It is the largest river (about 350 km long) in the center of Iran. It originates from the central part of the High Zagros mountains. Its headwater is in the Zardkuh mountain (3974 m elevation) and it terminates the Gavkhoni playa lake (1474 m elevation). The drainage basin includes the eastern part of the High Zagros zone, and most of the western part of the Sanandaj-Sirjan zone.

The Zayandeh river attains a peak discharge of 149 m^3/sec in spring. The flow of this river declines to discharge of 1 m^3/sec and annual mean discharge of 7.97 m^3/sec in the late fall (gauged in the Varzaneh station over 25 years, unpublished data, Iranian Water Organization, 1999). Floodwater is usually derived from quick snowmelt in Zardkuh (about 350 km west of Gavkhoni) and/or short periods of high precipitation in the drainage basin (unpublished report, agricultural administration, 1998). The Zayandeh river dam, constructed approximately 300 km northwest of Gavkhoni in 1971, has reduced the peak of spring flows. The Zayandeh river transports a low suspended sediment load in the lower reaches, because of drainage basin lithology (extensive deposits of carbonate, igneous, and metamorphic rocks) and the Zayandeh river dam.

The lower reaches of the Zayandeh river, according to aerial photographs and Landsat imagery, appears to be mainly meandering. Most bends are simple symmetrical, but the more sinuous ones are simple symmetrical and compound-asymmetrical (Fig. 2.7). The average slope of this river from the dam to the Gavkhoni playa lake is approximately 2 m/ 1 km but in the study reach (from about 50 km Esfahan to the Gavkhoni playa lake) is 0.3 m/ 1km along the Zayandeh river thalweg.

Other streams including Rahimi, Zardcheshmeh ephemeral rivers and small streams with steep gradient flow down into the western, the southern and the eastern part of the playa lake only in flood periods (see Fig. 2.6 for their position). Totally, 181 million m^3 water is discharged into the Gavkhoni playa lake on average annually. About 178 million m^3 belongs to the Zayandeh river and 3 million m^3 to the ephemeral streams (10 years average, unpublished data, Iranian Water Organization, 1999).

Fig. 2.7 Morphology of the Zayandeh river in a part of the study reach (from Varzaneh (indicated by circle) to about 11 km northwest) from aerial photograph.

2.6 Groundwater

Groundwater occurs by infiltration of streams in the upper fans or results from direct precipitation on alluvial fan surface. Most of the study area is composed of almost impervious to semi-previous marls and clays of Quaternary age underlying the alluvial deposits. These sediments impede recharge of water coming from mountains to aquifers. Recharge of the groundwater is high at the fan heads, which are composed of the coarsest and most permeable material. The main aquifer in the Gavkhoni playa lake basin consist of alluvial sediments with a locally thickness of 80 m (Krinsley, 1970). These coarse sediments, interbedded with fine-grained sediments (e.g. marl), are observed up to depth of 200 m (about 50 km northwest of Varzaneh) (unpublished data, Iranian Water Organization). The natural recharge of the alluvial aquifers in the basin depends mainly on run-off from the mountains, which flow onto the alluvial fans.

Except the Zayandeh river water, no run-off water usually reaches the playa, which is the local base level. The aquifers in the subsurface of the alluvial fans are phreatic, but towards the center of the basin artesian conditions develop as a result of upward confining clay layers. Evaporation through the capillary zone from the phreatic aquifer results in saturation of the water in respect to certain salts and precipitation of evaporite minerals.

2.7 Aquatic plants and algae in the Zayandeh river

The Zayandeh river provides an important part of industrial, and agricultural water of Esfahan city. Mainly in the past two decades, because of pollution sources around the Zayandeh river, the quality of water has decreased. In the past five years, because of low precipitation and a high water consumption for irrigation purposes in the Zayandeh river drainage basin, the water discharge has been reduced in the lower reaches of the Zayandeh river during summer and autumn and the ion content and organic material of the water have been increased. For this reason aquatic plants and algae, which are subjected to environmental conditions, have been affected.

From the beginning of the Zayandeh river to about 60 km southeast of Kuhrang (Zayandeh river dam) because of few villages and scarcity of farming lands, water pollution and concentration of ions is low. In this reach, aquatic plants (such as *Nasturtium officinalis* and *Ranunculus equalities*) are observed but because of gravelly bed they don't find in abundance (Fig. 2.8). Epilithic diatoms cover the surface of cobbles and pebbles. Filamentous algae such *as Batrachospermum* sp., *Cladophora* sp. and *Vaucheria* sp. are present but the variation of algae species is low (Fig. 2.9). During decrease of water quality in late summer and early autumn algae species do not change remarkable.

From the dam to 45 km east of it, water flow velocity is high and river valley is narrow and deep. In this reach of the river, because of increase of villages, population and farming lands pollution increases. In spring, diatoms grow over rocks and sometimes *Vaucheria* sp. is observed. In summer and early autumn, because of evaporation and water consumption for agriculture, river water is decreased, filamentous algae especially *Cladophora* sp. grows over bedrocks. Where the velocity of water is low (near bank), benthic algae such as *Chara* sp. and *Nitella* sp. and aquatic plants grow on the river ground and sometimes cyanobacteria (*Nostoc* sp.) are observed.

Fig. 2.8 Photograph showing aquatic plants (*Nasturtium officinalis*) in the Dimeh spring, about 22 km southeast of Kuhrang (see Fig. 2.5 for its position).

Fig. 2.9 Photograph showing filamentous algae (*Cladophora* sp.) near the Zayandeh river dam (see Fig. 2.5 for its position).

From 45 km east of the dam to Esfahan, due to entrance of the wastewater from a steel plant and polyacreal plant into the Zayandeh river and abundant water consumption, pollution of water increases. Therefore, cyanobacteria such as *Nostoc* sp., *Lyngbya* sp. *and Oscillatoria* sp., diatoms such as *Navicula* sp*., Cymbella* sp. *and Synedra* sp. and filamentous green algae (*Spirogyra* s*p.* and *Cladophora* sp.) and aquatic plants (*Typha* sp. and *Ceratophyllum* sp.) are observed on pebbles especially in dry periods.

From Esfahan to the east, caused by the increase of phosphorous, nitrates and organic material, diatoms such as *Cymbella* sp. *and Synedra* sp. *and Gomphonema* sp. increase and filamentous algae (C*ladophora* sp*.)* and red algae (*Bangia atropurpurea*) are observed on pebbles where flow velocity is high. Downstream of the wastewater refinery plant, because of entrance of abundant raw organic and chemical material (i.e. phosphorous and nitrate) into the Zayandeh river, pollution is very high. These environmental conditions are favorable for growth of filamentous algae (*Cladophora* sp*., Oedogonium* sp*. and Stigeoclonium* sp.), cyanobacteria such as *Lyngbya* sp*., Oscillatoria* sp*.* in abundance and few unicellular algae such as *Euglena* sp*.* and *Phacus sp.*.

From 20 km to 50 km east of Esfahan during wet seasons cyanobacteria (*Lyngbya* sp. and Oscillatoria sp.) and filamentous algae (*Cladophora* sp.) which are pollution indicators and aquatic plants (*Ceratophyllum* sp*. and Typha* sp.) are observed during upper flow regime. In this part of the river, because of self-cleaning capacity of the water, pollution decreases to some extent. When the river is almost dry (during dry periods) aquatic plants and algae are not present (S. Afsharzadeh, pers. com., 2000).

From 50 km to 90 km east of Esfahan, cyanobacteria (*Lyngbya* sp*., Oscillatoria* sp*. Phormidium,* sp.) and diatoms (*Navicula* sp*., Gyrosigma* sp*. and Cymbella* sp.) are observed during wet periods. Aquatic plant (*Lemna minor*), flagellates such as *Euglena* sp., *Phacus* sp. and *Chlamydomonas* sp. grow in abundance during dry periods .

From 100 km east of Esfahan to the Gavkhoni playa lake where water pollution is high cyanobacteria such as *Lyngbya* sp. and *Oscillatoria* sp. and flagellates such as *Euglena* sp. are observed. In the Zayandeh river delta district, diatoms such as *Navicula* sp., *Gyrosigma* sp. and *Cymbella* sp., cyanobacteria such as *Lyngbya* sp*., Oscillatoria* sp. and

Flagellates such as *Euglena* sp. are found (Fig. 2.10). In saline local holes halophytic algae such as *Dunaliella salina* and *D.parva* grow (S. Afsharzadeh, pers. com., 2000).

Fig. 2.10 Photograph indicating algae assemblage in a dry period (autumn 1999) near Ejieh bridge (about 75 km southeast of Esfahan). View is to the east (see Fig. 2.5 for its position).

2.8 Vegetation

The various kinds of plants, controlled by moisture, salinity and soil texture, cover locally and sparsely the study area. The plants such as *Salicornia* sp. and *Phragmites* sp. grow along the distributary channels of the Zayandeh river delta. In winter, *Salicornia* sp. in red and in summer in green color is also observed (Fig. 2.11). At the margins of the river, *Salicornia* sp., *Typha* sp. and farther *Tamarix* sp. are present. *Tamarix* sp. is found sparsely with *Phragmites* sp. where the ground water table is high. In efflorescent lands, in the west of the sand dunes, (from Jarghoieh to Varzaneh) where soil is wet, *Seidlitzia rosmarinus* and also halophytes such as *Salsola turcomanica* are present between *Phragmites* sp. (Fig. 2.12) (H. Loghman, pers. com., 1999).

Fig. 2.11 Photograph showing *Salicornia* sp. (s) and *Phragmites* sp. (f) found in the Zayandeh river delta (late summer 1999). View is to the northwest.

Fig. 2.12 Photograph showing *Seidlitzia rosmarinus* (s) and Ph*ragmites* sp. (f) in the west of the aeolian sands along the Zayandeh river (autumn 1999). View is to the east.

Erosive winds and particularly low precipitation are two factors, which have prevented growth of plants in the aeolian sand field. Generally, the aeolian sand field is bare and without vegetation, except in pits and holes of sand dunes where wind is less effective and soil humidity is enhanced. In these places, two types of plants including *Stipagrostis karelinii* and *Calligonum turkestanicum* are found. For biologic stabilization of the aeolian sands in Khara and Varzaneh, *Haloxylon ammodendron, Atriplex lentiformis* and *Atriplex canecens* have been planted (H, Loghman, pers. com.1999). Gravelly areas (mountain slopes and alluvial fans) are almost bare, and usually except *Anabasis* sp. no plant grow (S. Afsharzadeh, pers. com., 2000).

2.9 Ancient irrigation system

Five small dams were constructed over the Zayandeh river to lift water level and direct it into farmlands by some artificial channels (Fig. 2.13). They are Marvan 35 km, Goli 50 km, Jendich 64 km, Shanzdedeh 84 km, and Shakhkenar 110 km east of Esfahan city. The first four are 300-800 years old and the second one was constructed about 70 years ago.

In addition to the irrigation channels fed by the above dams, farmlands which are far from the river and where no shallow aquifers exist, very large number of subterranean passages (called ghanat or karez) make the subterranean water usable for local peoples. Each qhanat includes some wells and an underground channel, which drains and conducts groundwater onto ground surface and farmlands. The largest one is 4 km long and the deepest well (main well) is about 40 m. Qhanats water is usually brackish and is usable only for farming. The age of qhanats is not documented.

Fig. 2.13 Photograph showing artificial channels which direct water from the Zayandeh river to the Ejieh farmlands (about 75 km southeast of Esfahan) (see Fig. 2.5 for its position). View is to the northwest. Photograph provided by H. Kulke.

2.10 Quality of soil and water

The provenance of soil can be divided into three categories in the study area including: 1-Fine–grained sediments deposited in a lake basin. The soil resulted from these sediments is usually saline and consist of abundant clay and silt. 2- Sediments deposited along the Zayandeh river (from the beginning to the Gavkhoni playa lake) which are a result of inundation by the Zayandeh river (see grain size analyses of loamy silty sandy soils at Ejieh in Kulke, 1996). From the Zayandeh river toward the north and the south of the study area, these sediments gradually change to the gypsiferous debris flow deposits (particularly to the west). Soil produced from the Zayandeh river sediments consist of a mixture of sand, silt and clay and is of high quality for farming, but in some places, especially from Ejieh to Gavkhoni, because of evaporation, salinity and incorrect irrigation, it is brackish to saline. 3- Alluvial fan deposits, originated mainly from igneous rock debris to the east and northeast and carbonate rock debris to the west and southwest, are mostly products of debris flows.

The soil originated from these sediments is coarse-grained and usually contains some gypsum. Because of these properties, this type of soil is usually rather unfavorable for farming.

Ion / Station No	Na^{+}	Mg^{++}	Ca^{++}	SO_4^{--}	Cl^{-}	HCO_3^{-}
1	0.42	1.8	3.3	0.5	0.4	4.5
2	0.48	0.8	2.38	0.68	0.35	2.8
3	0.9	1	2.48	0.68	0.42	3
4	1.40	1.3	2.85	1.38	1.3	3.2
5	2.1	1.75	3.8	1.8	1.6	3.8
6	87	28.7	12.5	19.8	1.2	4.4

Table 2.1 Major content of ions (meq/l) in the Zayandeh river water from the Gavkhoni playa lake to the northwest: 1: 350 km, 2: 270 km, 3: 220 km, 4: 175 km, 5: 125 km, 6: 28 km (data after Iranian Water Organization, 1999).

The quality of water is high at the beginning of the Zayandeh river but, because of entrance of industrial domestic waste water and saline water drainage, pollution gradually increases from the west to east, so that between Varzaneh and the Gavkhoni playa lake, water is unusable for agriculture (Table 2.1). From Esfahan to about 70 km east of Esfahan, the Zayandeh river discharge is usually high, shallow groundwater is fed by the river and also the river drain waste water of the area as a natural drainage. In this reach, because of leaching of inorganic and organic material and their entrance into the river, pollution of the water increases. Despite of these conditions the water is fresh (ground and surface water) and relatively usable for farming. The Zayandeh river water and groundwater is brackish to saline from Ejieh to the Gavkhoni playa lake and is unfavorable for agriculture, except for growing resistant plants where drainage is high enough. In this region, irrigation should vary in accordance with soil type. On the other hand, correct management of irrigation and favorable drainage are important parameters in this area (unpublished data, Iranian Water Organization, 1999).

Chapter 3

The Varzaneh aeolian sand field

3.1 Introduction

The Varzaneh aeolian sand field is located in the southeast of Esfahan, between 32°,00-32°,23′N and 52°,40′-52°,47′E with an area of approximately 140 km^2. Its trend is the north-south with about 45 km long and maximum width of about 11 km in the north. Development of aeolian sands decreases from the north to the south. The Gavkhoni playa lake extends with an area of about 550 km^2 to the east of this field. The Zayandeh river, which is a permanent river, runs the north of this area and enters finally into the Gavkhoni playa lake. Coarse-grained alluvial deposits border the aeolian sand field in the west, and the south (Fig. 3.1). The land surface is of low relief with a maximum height of 1607 m (north of aeolian sand dunes) and a minimum of 1474 m (Gavkhoni playa lake) above sea level. Distribution of vegetation is variable from the north to the south of the aeolian sand field and mostly is concentrated along the Zayandeh river in the north (see Chapter 2.8 for details).

Varzaneh has a dry and hot climate with annual precipitation and evaporation average of about 80 and 3265 mm respectively. The annual average temperature ranges between +42°C (July) and –17°C (January). Wind blows from all directions but westerly winds dominate throughout the year (see Chapter 2 for details).

This chapter will represent the various types of aeolian sand forms and their dynamics in the Varzaneh aeolian sand field. It also will describe the mineralogical composition, textural characteristics, and analyze the provenance of the aeolian sands.

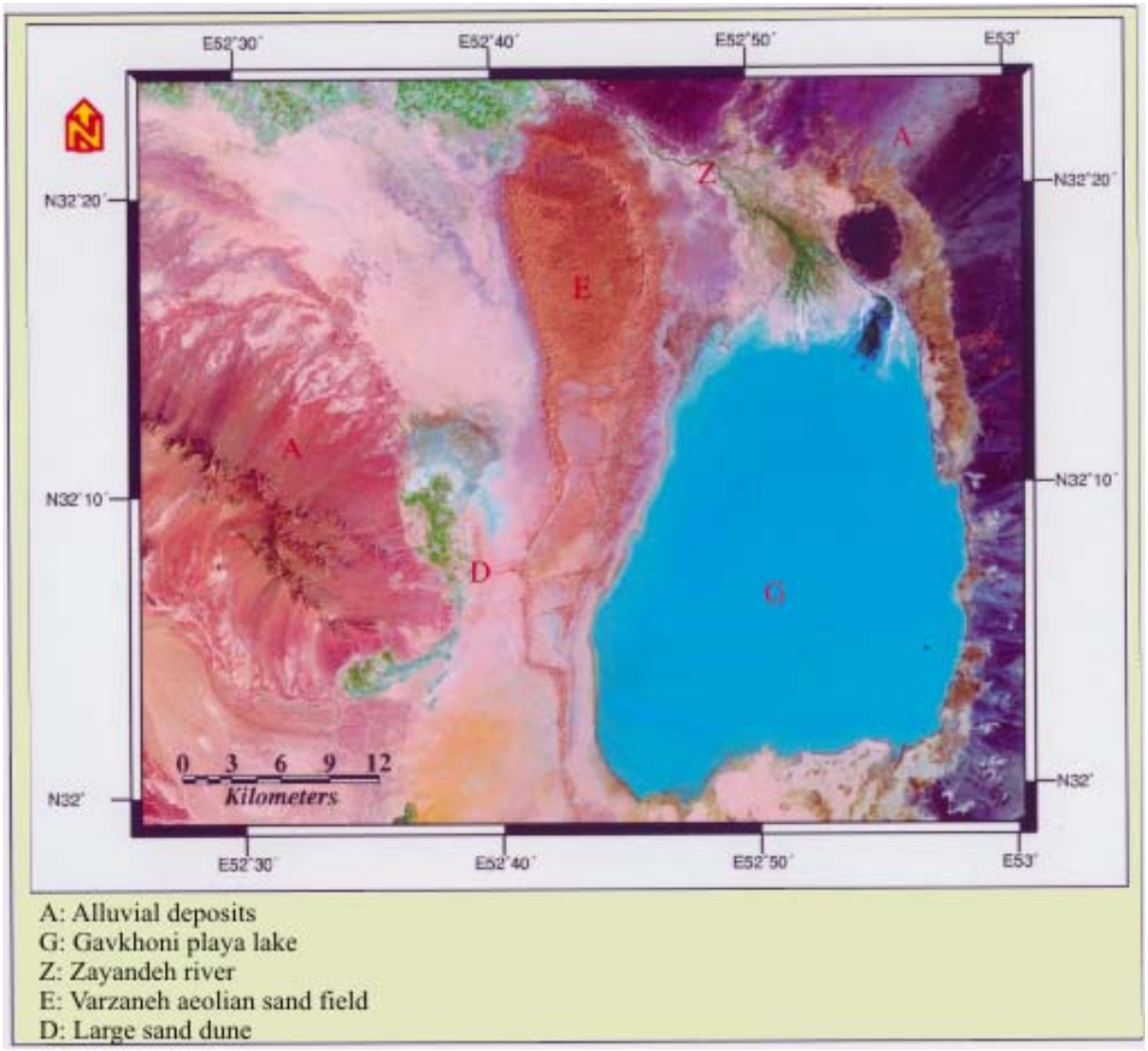

Fig. 3.1 False color-Landsat TM image of the Varzaneh aeolian sand field and its surrounding depositional environments.

.

3.2 Methodology

In order to obtaining data on the rate of the migration of aeolian sand forms and aeolian sands and also to differentiate various types of sand forms, some field and laboratory experiments were conducted. For determination of mineralogical composition, textural properties, the provenance of the aeolian sands and palaeontology studies, about 60 samples of aeolian sand and alluvial sediments were analyzed (see Chapter 1 and Appendixes A, C & D for details).

3.3 Aeolian sand forms

Based on different mode of occurrence and morphology, the Varzaneh aeolian sand field consists of three types sand forms: sand dune, sand sheet and sand drift hummock. The sand dunes usually occur in groups and also as individuals and are subdivided into four types of linear/seif barchanoid, star and dikaka. The sand sheets consist of sabkha, overbank and interdune (Fig. 3.2).

3.3.1 Sand dunes

Sand dunes are the most important feature of the Varzaneh aeolian sand field and cover an area of approximately 80 km^2. The maximum height of the sand dunes is about 130 m in the north. On the basis of their degree of complexity and activity, they are further classified into two categories, these are active sand dunes and stabilized sand dunes. The active sand dunes occur as simple and coalescend (compound and complex) dunes. The simple active sand dunes are mounds of sand that spread as separate forms. The active compound sand dunes are sand accumulations onto which smaller dunes and various slip face orientations are superimposed. The active complex sand dunes are combinations of two or more dune types (Fig. 3.3). The stabilized sand dunes (dikaka) exist only as individual simple sand dunes. They are rounded mounds with abundant plant roots (see Fig. 3.7).

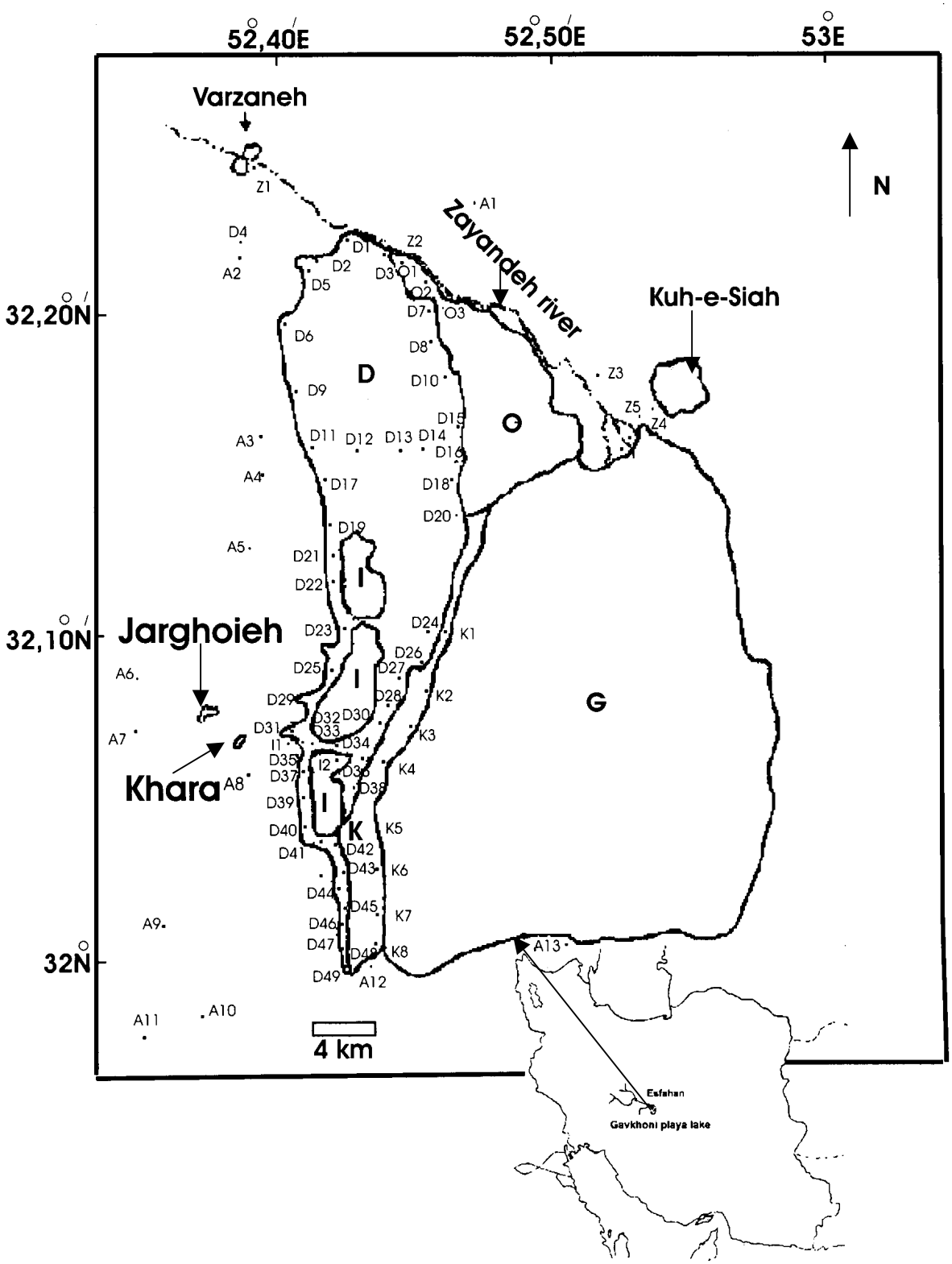

Fig. 3.2 Simplified map showing approximate locations of sampling, major representative author's sand traps and stick marks in the study area. D (sand dune), G (Gavkhoni playa lake), I (interdune sand sheet), O (overbank sand sheet), K (sabkha sand sheet).

Fig. 3.3 Field photograph showing complex sand dunes. Barchanoid ridge pattern (akle/) (B) and star dune (S). The height of star dune is about 10 m. View is to the west.

3.3.1.1 Active sand dunes

Active sand dunes are the most important and common features among the sand dunes in the study area. They can be grouped on the basis of morphology into three main types of barchanoid, linear/seif, and star dunes.

Barchanoids

Barchanoids are the simplest crescentic and most common transverse sand dunes in the Varzaneh sand dunes. Barchanoid ridges are visible as a coalescence of simple barchans with wavy ridges. Each barchanoid shows a slip face between two arms. In some cases one of the arms become extended. The crest line of barchanoides moves somewhat according to wind direction, but in general they maintain their form. Studied barchanoid dunes along the road of the salt mine of Jarghoieh and in the north of the sand dunes are usually between 5 to 10 m high and 30 to 50 m wide (Figs. 3.3 & 3.4).

Fig. 3.4 Field photograph showing barchanoid dunes (A). The slip faces are to the east. The height of the main dune is about 80 m. View is to the northwest.

Linear/seif dunes

Linear/seif dunes (simple longitudinal dunes) are mostly visible as straight crests (linear dune) and are common large features of sand dunes in the study area. They usually are asymmetrical in cross section and tend to bifurcate in the upwind direction. The end of each dune is mostly to the south. At present most linear dunes are undergoing modification to star dunes. They are 150 to 200 m long and up to 10 m high in the studied locations (west border of the Gavkhoni playa lake) (Fig. 3.5).

Star dunes

Star dunes are characterized by a pyramidal morphology, with usually three or four arms radiating from a central peak in the Varzaneh sand dunes. Some small star dunes are superimposed over the linear dunes (Figs. 3.3 & 3.5). Each arm also possesses a well-developed slip face, which is active at different times (see Fig. 3.15). The arms are developed either sharp-crested or rounded. The height of the star dunes ranges from a few meters to up to about 130 m (in the north of the sand dune field).

Fig. 3.5 Field photograph showing, linear dune (A) with development of minor star dunes (B). The linear dunes are developed southwards. The main star dune is about 10 m high. View is to the west.

3.3.1.2 Sand drift hummocks

Sand drift hummocks are temporary sand accumulations, tongue–shaped bodies, which form in the lee of the small bushes over the sand field especially in the north (near the Zayandeh river) (Fig. 3.6).

Interpretation

The barchan and barchanoid dunes, which develop in transverse unimodal wind regimes, suggest dominant wind direction (cf. El-Sayed, 1999) (see Fig 2.5 for dominant wind direction in the study area). They migrate by avalanching of sand on slip face (Reineck & Singh, 1980). They respond to essentially unidirectional winds and form more or less perpendicularly to dominant wind and at right angles to resultant sand drift direction (Nickling, 1994). They indicate compound barchanoid ridges with increased sand supply or more variable winds (cf. Thomas, 1989; Nickling, 1994).

Fig. 3.6 Field photograph indicating sand drift hummocks with small ripple marks. Dominant wind direction is toward the right hand side of the photograph (toward northwest).

Linear/seif dunes develop parallel or sub-parallel to the dominant wind or resultant of two wind directions (Einsele, 1992). Their bedforms arise under conditions of bi-directional or dispersed unimodal winds of variable strength (Galloway & Hobday, 1996). Wind velocity is generally higher for forming them (Reineck & Singh, 1980). Linear/seif dunes indicate a bimodal to wide unimodal formative wind regimes (Thomas, 1989). They are produced in the vector of two converging wind directions blowing from two quarters, about 90^0 apart. Some of them appear to develop by the extension of other dune types as a result of a change in wind direction or sand supply. Another rather popular explanation for the origin of seif/linear dunes advocates the presence of helical or roller vortices that develop in the atmosphere with horizontal axes parallel to wind direction (Nickling, 1994).

During Pleistocene glaciation, because of stronger wind, seif dunes were formed in abundance in many arid places of the world (Reineck & Singh, 1980). They change into other sand dune forms such as the star dunes, because of wind directions and velocities are not strong enough to maintain them (cf. Reineck & Singh, 1980). It is probable that an unimodal northerly paleo-wind direction was responsible for the development of the linear/seif dunes in the aeolian sand field. The star dunes are formed as a result of wind

blowing from several directions (cf. McKee, 1966; Galloway & Hobday, 1996). The degree of activity of star dunes depends on velocity and direction of wind. According to variation of wind direction the slip face changes. They, superimposing the ridges, are developed in a later stage and are formed due to multi-modal wind regimes (El-Sayed, 1999)

Four main factors control the formation of the sand drift hummocks in the aeolian sand field. They are wind, sand grain size, vegetation and sand humidity. As a result, they spread more abundantly where moisture is enough and vegetation is sparse. Such conditions are found especially in the north of the sand dunes.

3.3.1.3 Stabilized sand dunes (dikaka)

Some individual great and small dikakas extend from Varzaneh to the Gavkhoni playa lake along the southern bank of the Zayandeh river (Fig. 3.7). They form rounded mounds of sand without well-developed steep slip face. The height of some dikakas reaches up to 8 m. In some dikakas, plant growth destroyed the earlier-formed dune bedding but in some cases original bedding is still clearly visible (Fig. 3.8).

Fig. 3.7 Close-up view of a dikaka fixed by *Tamarix* sp. roots. The Varzaneh aeolian sand field is located in the background of photograph. Photograph provided by H. Kulke.

Fig. 3.8 Cross-stratification of a dikaka cut by the Varzaneh–Jarghoieh road.

Interpretation

The stabilization of aeolian sands and formation of dikaka is mainly achieved by desert plants, which possess deep penetrating root systems such as *Tamarix* sp.. The presence of enough water (non-saline water) maintains the plant growth (Reineck & Singh, 1980).

3.3.2 Sand sheets

Sand sheets are featureless sand plains, more and less flat, and usually devoid of dunes. They cover about 50 km^2 of the Varzaneh aeolian sand field. They occur to the east and within the interior of the sand dunes. According to situation and behavior, they can be grouped into three categories: sabkha sand sheet, overbank sand sheet and interdune sand sheet (see Fig. 3.2).

3.3.2.1 Sabkha sand sheet

Sabkha sand sheet is the most important type of the sand sheets in the aeolian sand field. It covers about 15 km^2 of the east of the sand dunes (see Fig. 3.2). A well developed polygonally horizontally sand layer cemented by halite covers the sabkha sand sheet a few centimeters thick. The thickness of this layer transitionally is increased towards the Gavkhoni

playa lake. During the drier months its surface is relatively hard and marked by a puffy, salty surface (Fig. 3.9). The lower sand sheet grades eastwards into the Gavkhoni salt pan. In the sabkha sand sheet, a few inactive individual small sand dunes, covered with gypsiferous muddy sediments are observed. The height of these dunes is about up to 2 m (see Fig. 4.6). Relatively hard ripple marks, cemented by gypsum and halite also occur locally in the east end of the sand sheet.

Interpretation

High groundwater table, periodic flooding and cementation by evaporites are the most important factors, which inhibit the development of sand dunes and occurrence of the sabkha sand sheet in the study area (cf. Langford, 1989). During major floods, muddy sediments were deposited over the sabkha sand sheet and gypsum minerals were formed in dry periods by evaporation. Intermittent wet and dry periods caused the formation of hardened ripple marks as a result of wind action and then cementation by evaporite minerals, especially halite.

Fig. 3.9 Field photograph showing puffy salt encrustations on the surface of the sabkha sand sheet in the east of the sand dune field. View is to the northwest.

3.3.2.2 Overbank sand sheet

A large overbank sand sheet is situated in the northern margin of the aeolian sand dunes along the Zayandeh river. It covers about 20 km^2 the northeast of the sand dune field. The overbank sand sheet is relatively flat and vegetated (Fig. 3.10). Plants, up to 2 m tall, occur along the Zayandeh river, whereas far from the river it consists of small bushes. The surface of the sand sheet is mostly covered by small gravels and sand-sized grains but a mud layer is also observed in some localities. Some observation trenches revealed interbedding of wind and water–laid deposits. Water–laid deposits consist of desiccated mud and fine to coarse-grained sand and gravel deposits. Fine sand layers exhibit climbing aqueous ripples. Wind-laid deposits consist of interbedded fine aeolian sand with coarse aeolian sand lag deposits (Fig. 3.11).

Fig. 3.10 Field photograph showing the surface of the overbank sand sheet with small bushes and mud layer on the surface (winter 1997). Sand dunes are in the background of photograph. View is to the southwest.

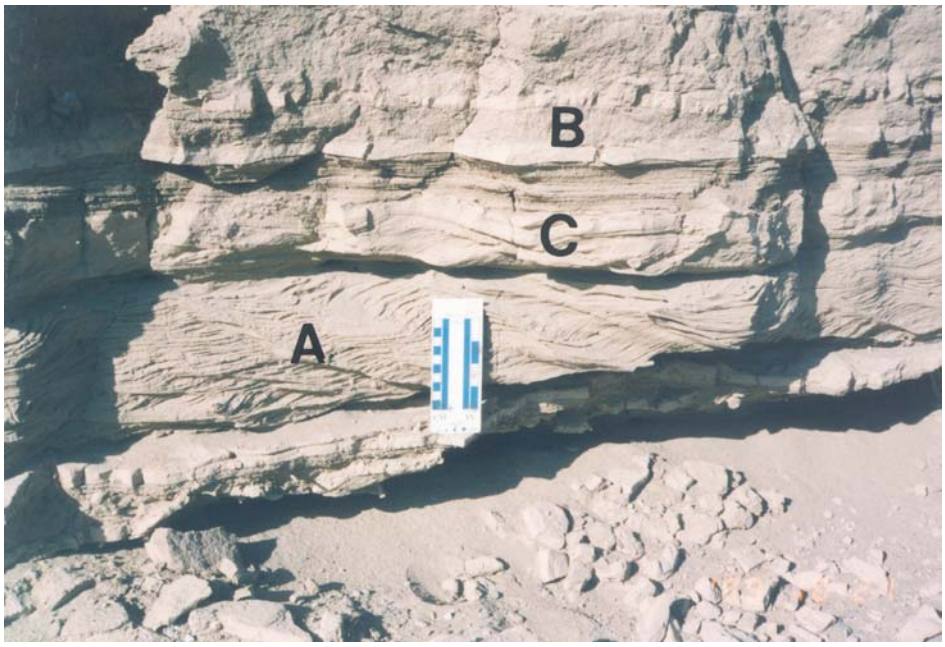

Fig. 3.11 Field photograph of a trench showing aqueous climbing-rippled fine-grained sand (A) interbedded with aeolian sands (B) and mud layers (C) in the overbank sand sheet.

Interpretation

The climbing aqueous ripples of medium to fine sand have been deposited by migration of small current ripples during strong sandy bed load transport (cf. Olsen, 1989). The mud layers result from stagnant water on the top of the overbank sand sheet. The stratigraphic sequence, the properties of sediments and their positions show that sedimentation occurred in an overbank or low gradient flood plain environment during waning flood (cf. Miall, 1992). Alternation of mud layers and aeolian sands result from fluvial-aeolian interaction.

3.3.2.3 Interdune areas

Interdunes are flat areas located between the sand dunes. They include dry, wet and evaporitic varieties and cover about 15 km^2 of the middle part of the sand dunes (see Fig. 3.2). A khaki-colored and well-sorted aeolian sand layer covers the interdune surfaces in most localities. This layer ranges in thickness from a few up to 100 cm (Fig. 3.12). In some localities a thin polygonal soft salt-sand layer, up to a few millimeters thick, covers the surface of the interdune surface. Trenches in two individual interdune areas indicate an

alternation of sand, mud to sandy mud deposits. Muddy sediments change from black to gray-white in color and contain fresh-water gastropods and ostracods in abundance, especially in the black sediments (see Chapter 4 for details). Vegetation and sand dunes are nearly absent on the interdunes surface.

Interpretation

The presence of muddy layers most probably reflects sedimentation in a very shallow fresh water perennial lake during flooding periods (cf. Benison & Goldstein, 2001). The origin of evaporite minerals, deposited in the surface layer of the interdune areas, is as a result of evaporation of capillary saline water on the surface (cf. Pye, 1980). After evaporation and desiccation, halite and gypsum were precipitated in sub-aqueous conditions followed by sub-aerial exposure (cf. Benison & Goldstein, 2001). The occurrence of the sand layers indicates sedimentation by wind in dry periods.

Fig. 3.12 Field photograph showing an interdune area located in 6 km east of Khara. View is to the northwest.

3.4 Aeolian sand dynamics

3.4.1 Introduction

In this study, dynamics and geomorphological development of the Varzaneh aeolian sand field, including sand dunes and sand sheets, are analyzed. It is attempted to assess the factors that act to maintain or move these features. Regarding dynamics, the aeolian sand field of Varzaneh can be categorized into two groups. The first group represents mobile sand accumulation, including active sand dunes and active sand sheets. The second group represents immobile ones, consisting of stabilized sand dunes and inactive sand sheets.

3.4.2 Active sand dunes

A large part of the Varzaneh aeolian sand field (about 130 km^2) consists of the active sand dunes. They are the most important landform of the study area (Fig. 3.1& 3.2). Active sand dunes are either coalscencing or individual. They consist of star, barchan, barchanoid, and linear/seif dunes. Measurements of the movement of a giant sand dune during about two years (1997-1999), presented in Fig. 3.13 (A & B) and Table 3.1, indicate that: 1-The sand dune is approximately fixed and the rate of migration is not remarkable (about few centimeter). 2-Maximum migration of the sand dune is in late winter, early spring and early autumn (see Chapter 2.4 for wind direction in the study area). 3-The rate of the movement of the sand dune is not exactly in accordance with wind direction and frequency.

Sample No	Facies	Location	
A1	Gravel plain	32°,23′,02″N	52°,47′,41″E
A4	Gravel plain	32°,15′,10″N	52°,39′,45″E
A8	Gravel plain	32°,06′,42″N	52°,37′,49″E
D33	Sand dune	32°,07′,00″N	52°,41′,03″E
I2	Interdune	32°,06′,26″N	52°,41′,57″E
K4	Sand sheet	32°,06′,04″N	52°,43′,39″E

Table 3.1 Location of measurements of groundwater table, major representative author's sand traps and stick marks in the study area.

The measurements of the gradient of the eastern and the western lee sides and stoss sides of some sand dunes (about 5 km Khara toward salt mine) indicates values between a maximum 40° on the upper parts and a minimum 15° on the lower parts. Where the slope angle of slip face is exceeded, the mass movement (avalanching) of the sands takes place. Avalanching of the aeolian sands occurs as tongue–shaped layers on the slip face of the sand dunes (Fig. 3.14).

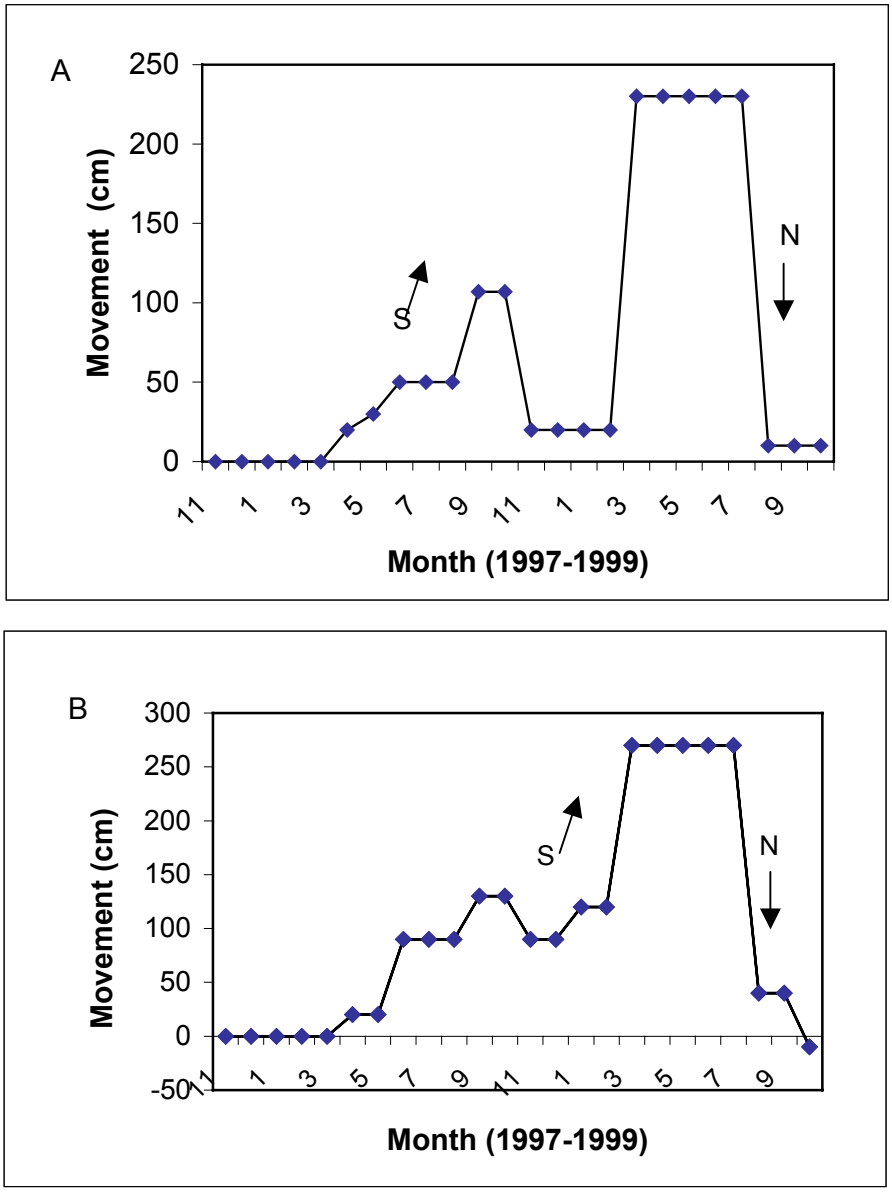

Fig. 3.13 Graph showing gradual movement of a giant sand dune in its foot in location No. D33 (about 5 km east of Khara toward salt mine in two locations (A & B) with interval of about 120 m) during more than two years (1997-1999). The height of sand dune is about 90 m (see Figs. 3.2, 3.15 and Table 3.1 for position of sites and dune morphology). S (south), N (north).

Investigation by taking photographs on a crest line of a sand dune with trends N-S shows that erosion and deposition occur and movement to the west and the east were recorded according to variations of wind directions (Fig. 3.15 A & B). Despite of migration of the crest line and the foot of the sand dune it has been approximately fixed during three years.

Fig. 3.14 Field photograph showing mass movement of aeolian sand as avalanche on the lee side of a giant dune (about 5 km east of Khara).

The amount of aeolian sands collected in the sampling traps (Fig. 3.16 & 3.17) indicates that: 1- Wind-blown sand volume or migration of sand is maximum in spring and minimum in autumn. 2- Sand content is maximum in the sampling trap No. I2 (installed in an interdune) and minimum in the sampling trap No. A8 (installed in the western alluvial fan, a few hundred meters from the sand dunes) (see Fig 3.2 and Table 3.1 for their positions). 3- The grain size accumulated in the sampling traps varies from sand to fine gravel size.

A

B

Fig. 3.15 Changes in morphology of an arm of a sand dune (about 5 km Khara, location No. D33): July 1998 (A). March 1999 (B). (see Fig. 3.2 and Table 3.1 for position of the dune). Photograph A and B is from the same sand dune. View is to the northwest. ?= no measured

Fig. 3.16 Field photograph showing a sampling trap installed in location No. A4 (see Fig. 3.2. and Table 3.1for position of sand traps). Notice gravel lag on the top of alluvial sediments resulted from wind erosion. Barometer for scale is 7 cm.

Fig. 3.17 Aeolian sand volume (in cm^3) collected in four major sampling traps No. A1, A4, A8, I2) around the sand dunes during about one year (see Fig. 3.2. and Table 3.1for position of sampling traps).

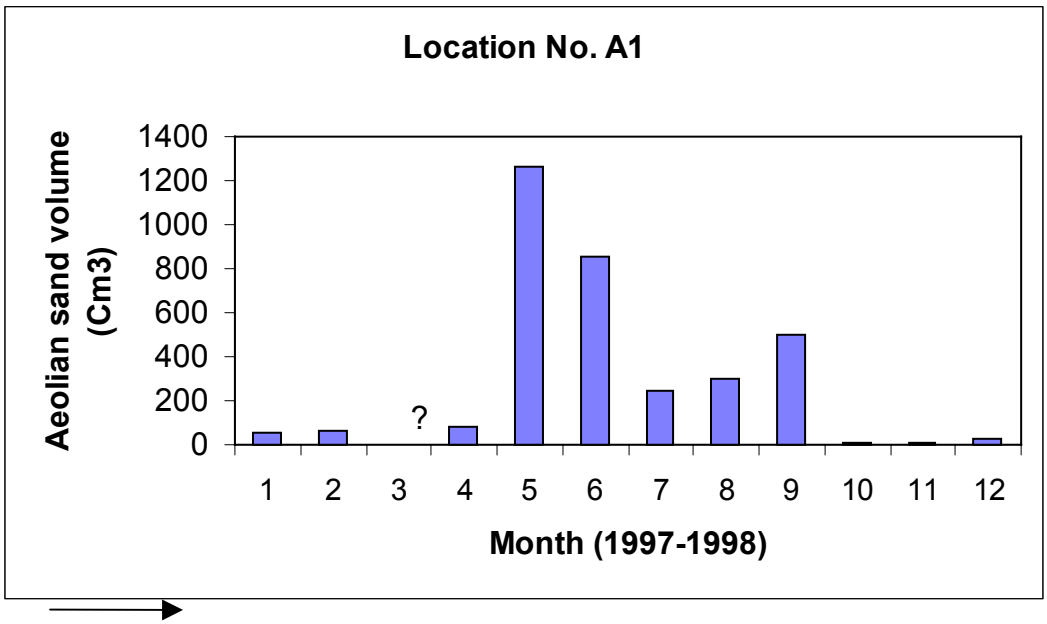

Continue

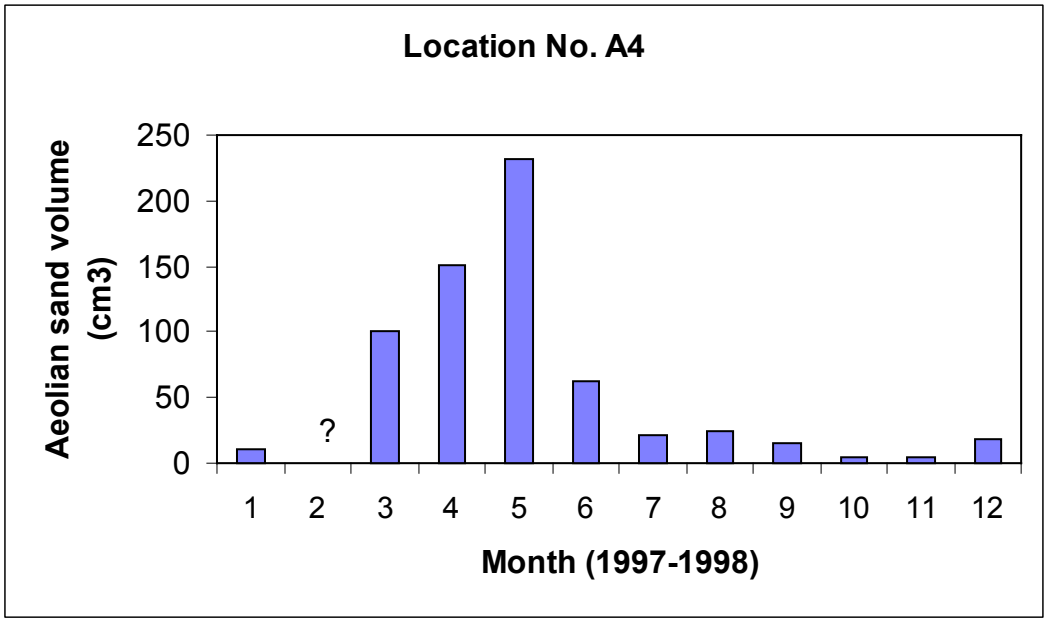
Location No. A4
Aeolian sand volume (cm3)
250
200
150
100
50
0
?
1
2
3
4
5
6
7
8
9
10
11
12
Month (1997-1998)

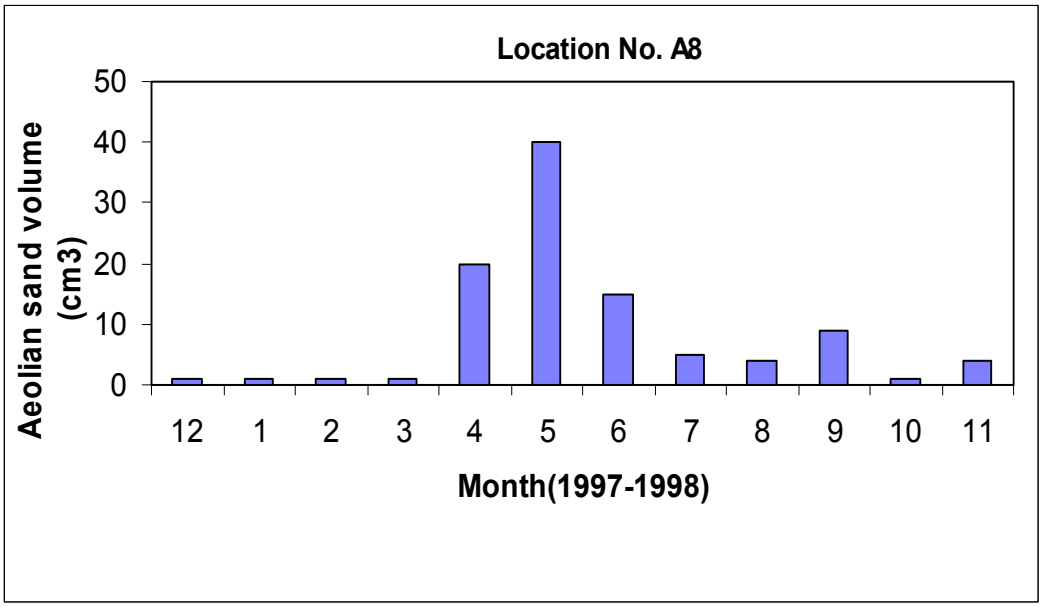
Location No. A8
Aeolian sand volume (cm3)
50
40
30
20
10
0
12
1
2
3
4
5
6
7
8
9
10
11
Month(1997-1998)

Continue

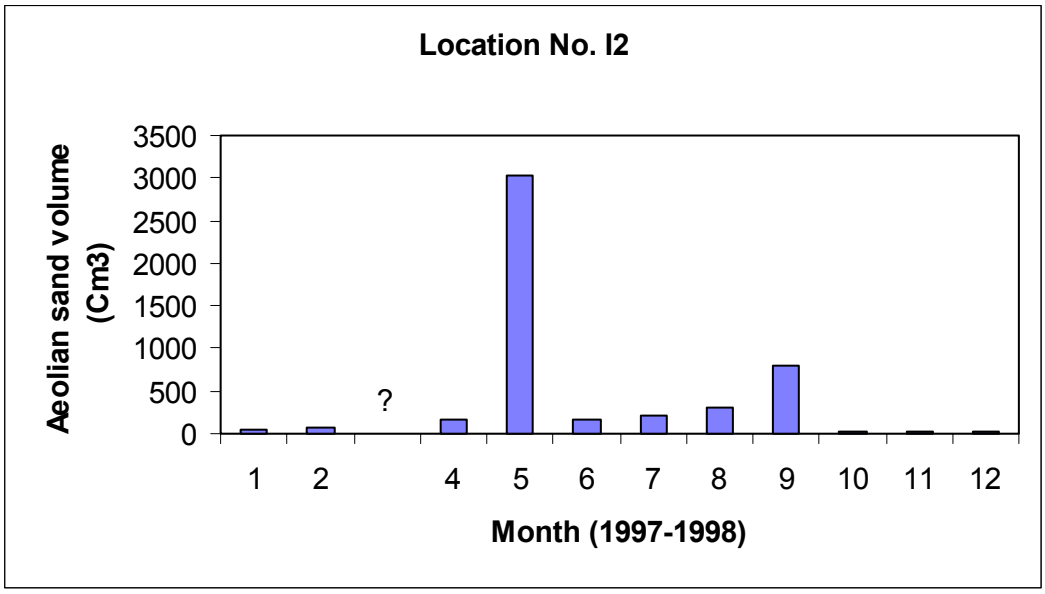

Interpretation

The result of about two years field investigation on the active sand dunes focused on the giant sand dune (about 5 km Khara toward salt mine) in the Varzaneh aeolian sand field indicate that:

1-The movement of the base of the sand dunes is very complicated and depends on wind direction, wind velocity, morphology, height, and gradient of dunes.

2-The base of the sand dunes migrates very slowly (see Fig. 3.13 for value) in different directions according to wind pattern but remain relatively fixed.

3-The upper part of the slip face advances faster than the lower part.

4-The crest line of the sand dunes moves faster than their base to different directions according to the dominant wind direction.

5-Moisture content is an important factor to control sand movement on the sand dunes but only for a short time during the wet season, because after precipitation the surface layer of sands gets dry after a few hours.

6-The result of grain size analysis of aeolian sediments accumulated in the sampling traps indicates that the wind has enough strength to transport fine gravel by rolling it on the interdune surface.

7-Sediment volume accumulated in the traps and its grain size depends on strength and frequency of the wind in each month or season and the places that the traps were installed.

8-At present, for the range of wind velocity in the study area and also regarding to grain size accumulated in the sampling traps, the wind mainly transports the grain size ranging from 0.1 to 0.3 mm.

9-Sand-sized grains move from active dunes to different directions before they are trapped within wet interdune areas or by vegetation.

3.4.3 Active sand sheets

Active sand sheets or dry interdunes are located between active sand dunes (Figs. 3.1 & 3.2). They are the sites of erosion and deposition and to some extent the areas of equilibrium between sedimentation and deflation. The land surface of the interdunes is usually dry and soft and mostly consists of fine-grained sand (Fig. 3.18) (see Chapter 3. for details).

Fig. 3.18 Field photograph showing aeolian deflation and sedimentation over an interdune (7 km from Khara toward the Jarghoieh salt mine). View is to the northwest.

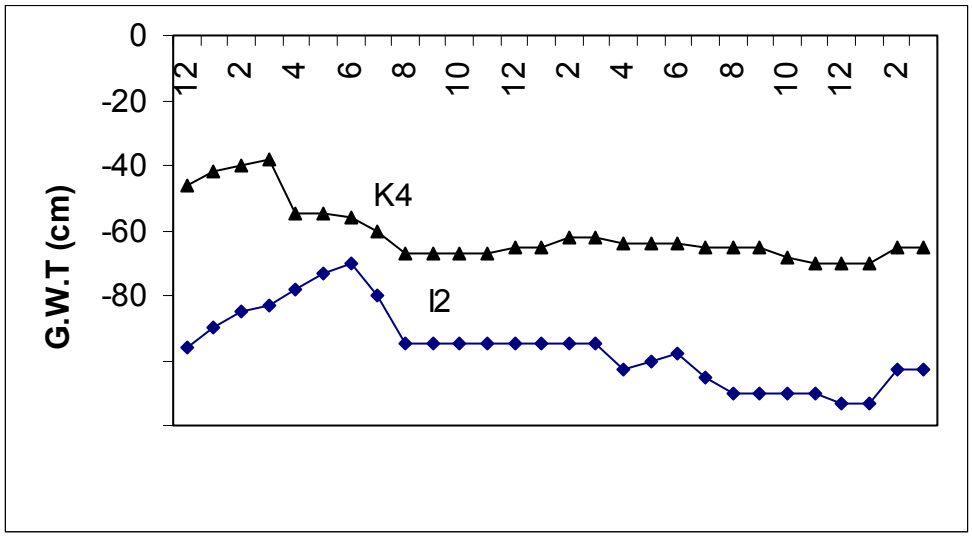

Fig. 3.19 Variation of groundwater table measured during about two years (1995-1997) in the interdune sand sheet (location No.I2) and the sabkha sand sheet (location No. K4) (see Fig. 3.2 and Table 3.1 for position of locations No).

The groundwater table is relatively low and does not play an important role to fix the aeolian sands in the active sand sheets. The measurements of the groundwater table during more than two years in two locations (sabkha and interdune sand sheets) indicate that:
1- Ground water table is higher in the sabkha sand sheet than in the interdune sand sheet. 2-It is highest in spring and lowest in winter. 3- Generally, the variation of water table is relatively low both in the sabkha and the interdune sand sheet during different seasons (Fig. 3.19).

Interpretation

Threshold velocity for transportation of wet or damp sand and of loosely cemented sediments is significantly higher than dry sand as a result of capillary water tension. (Nickling, 1984). Dry systems are characterized by non-cohesive sand above a deep water table, which has no effect on erosion or accumulation. Because of low groundwater and the lack of cementation of the surface, superficial sediments are usually soft and dry in the active sand sheet. Therefore, they usually can be eroded by wind very easily. There are also no other stabilizing factors such as vegetation to resist deflation. Therefore, accumulation is controlled by aerodynamic processes alone.

3.4.4 Stabilized sand dunes

Stabilized sand dunes are present as rounded individual sand ridges in the Varzaneh aeolian sand field (see Fig. 3.7). They develop where non-saline water table is high and inundation by the Zayandeh river takes place. Plants, which develop long roots, e. g. *Tamarisks* sp., stabilize the aeolian sand and form these features.

Interpretation

Two dominant factors control the formation of stabilized sand dunes in the Varzaneh sand dune field. These are moisture (non-saline or very poorly saline water) and vegetation.

3.4.5 Inactive sand sheets

Inactive sand sheets consist of the sabkha sand sheet, the overbank sand sheet and wet or saline interdunes. They mostly extend to the east and the northeast of the study area (see Figs. 3.1 & 3.2 for their positions). The sabkha sand sheet spread where the depth of ground water table is low and (usually less than 80 cm) and water is sucked to the surface by capillarity. Therefore, moisture content and salinity is high in comparison with the other sand sheets. The lower sabkha sand sheet is at or near water table (Fig. 3.19). The overbank sand sheet is located where the Zayandeh river occasionally floods its overbank areas. The depth of groundwater table is low in the overbank sand sheet and reaches up to about 3 m in depth. The inactive interdunes are formed where the water table is relatively high and the surface sand layer is absent or thin.

Interpretation

The inactive sand sheets may form in response to a range of factors such as a high water table, periodic or episodic flooding, slight surface cementation or coalescence of sand, effects of vegetation, limited availability of sand, and coarse-grained sand size, (Kocurek & Nielson 1986; Fryberger *et al.*, 1988).

A wet surface system involves grain cohesion where the water table or its capillary fringe attains the surface (Galloway & Hobday, 1996). Aeolian deposition and erosion are controlled by a combination of aerodynamic processes and moisture content of soil and consequently wet-interdune deposits resist deflation. High groundwater table and salinity are factors, which inhibit dune development, limit the migration of sand and promote the formation of sabkha sand sheet (Kocurek & Nielson, 1986).

In the study area, the sabkha sand sheet and wet interdunes developed as a result of the coalescence of sand by salt and moisture (see Fig. 3.9). Surface evaporation caused the formation of brines and finally the precipitation of evaporites minerals such as halite and gypsum.

Other stabilizing systems include occurrence of mud drapes or gravel lag deposits and vegetation. Frequent flooding, following formation of intermittent fine and coarse-grained sediments, caused formation of the overbank sand sheets marginal to the sand dune field.

3.5 Mineralogical/lithological composition

3.5.1 Introduction

The mineralogical/lithological composition of aeolian sands is a powerful indicator for determination of provenance of the components, but also for recognition of the tectonic setting of the source area, weathering and paleo climate history (Pettijohn *et al.*, 1987). Since the provenance determination is a main objective of this chapter, detailed description of this aspect is necessary. The aeolian sands of the Varzaneh area are composed of lithic grains (mostly sedimentary and igneous) and mineral grains. In this part of the study, the quantitative and qualitative properties of the observed grains are described.

3.5.2 Lithic grains

Lithics are the most abundant grains in the studied samples and usually decrease in frequency according to decrease in grain size. Three main types of lithics (igneous, sedimentary and metamorphic grains) are found in the studied sand grains (see Fig. 3.26). The average frequency percentage of the lithic grains and mineral grains in the representative samples are presented in Table 3.2 and Fig. 3.20.

Sample No / Lithology	A1	A2	A3	A5	A6	A7	A9	A10	A11	A13	D1	D3
I	39	50	72	52	10	11	3	4	16	41.5	55	44.5
S	39	32	18	37	70	74	95	93	72	51	30	39.7
M	11	5	2	4	0	1	0	0	0	0	3.5	3
Q	8	9.5	6	3	15	10	2	1.5	11	7	10	11
F	3	3.5	2	1	5	4	0	1.5	1	0.5	1.5	0.8
G	0	0	0	0	0	0	0	0	0	0	0	0

Sample No / Lithology	D7	D11	D13	D15	D16	D21	D27	D28	D30	D32	D35	D43
I	64	26	38	58.5	54	31	40	45	31	27	23	27
S	22.5	63	45	21	30	59	48.5	31	36	55	69	68
M	0.5	1.5	1.5	2.5	0	2	0.5	4	0.5	2	1	1
Q	12	8	13.5	15	15	7	9	15	11	15	6	4
F	1	1.5	2	3	1	1	1	5	0.8	1	1	0
G	0	0	0	0	0	0	1	0	0.7	1	0	0

Sample No / Lithology	D44	D46	I1	K1	K2	Z1	Z5
I	28	31	29	33	23	36	54
S	59	57	60	59.5	63	37	32
M	1.5	0	1.5	0.5	1.5	25	5
Q	9	10	7	5	9	1	8
F	2.5	1.5	2	1.5	0.8	1	1
G	0	0	0.5	0.5	1.5	0	0

Table 3.2 Frequency percentage of lithic and mineral grains of alluvial and aeolian sediments in the 31 representative samples in the study area. Alluvial sediments (samples No. A and Z) and aeolian sands (samples No. D, I and K) (see Fig. 3.2 and Table 3.3 for position of samples No). Igneous lithic (I), sedimentary lithic (S), metamorphic lithic (M), quartz (Q), feldspar (F), and gypsum (G). The gypsum grains (crystals) are formed in–situ, they generally were transported.

Sample No	Facies	Location		Sample No	Facies	Location	
A1	Alluvium	32°,23′,02″N	52°,47′,41″E	D21	Aeolian	32°,13′,03″N	52°,42′,12″E
A2	Alluvium	32°,21′,29″N	52°,38′,35″E	D23	Aeolian	32°,10′,32″N	52°,42′,26″E
A3	Alluvium	32°,16′,55″N	52°,39′,41″E	D24	Aeolian	32°,10′,40″N	52°,44′,02″E
A4	Alluvium	32°,15′,10″N	52°,39′,45″E	D27	Aeolian	32°,09′,20″N	52°,44′,13″E
A5	Alluvium	32°,13′,09″N	52°,40′,39″E	D28	Aeolian	32°,08′,54″N	52°,44′,10″E
A6	Alluvium	32°,09′,25″N	52°,38′,38″E	D30	Aeolian	32°,08′,03″N	52°,43′,55″E
A7	Alluvium	32°,07′,25″N	52°,38′,52″E	D31	Aeolian	32°,07′,31″N	52°,40′,33″E
A8	Alluvium	32°,06′,42″N	52°,37′,49″E	D32	Aeolian	32°,07′,11″N	52°,41′,00″E
A9	Alluvium	32°,01′,17″N	52°,34′,41″E	D33	Aeolian	32°,07′,00″N	52°,41′,03″E
A10	Alluvium	31°,55′,28″N	52°,30′,55″E	D35	Aeolian	32°,06′,50″N	52°,41′,05″E
A11	Alluvium	31°,53′,50″N	52°,30′,03″E	D37	Aeolian	32°,06′,06″N	52°,40′,59″E
A12	Alluvium	31°,59′,26″N	52°,43′,22″E	D40	Aeolian	32°,04′,41″N	52°,41′,03″E
A13	Alluvium	32°,01′,02″N	52°,51′,49″E	D41	Aeolian	32°,04′,06″N	51°,41′,24″E
D1	Aeolian	32°,21′,59″N	52°,41′,33″E	D42	Aeolian	32°,03′,48″N	52°,42′,27″E
D2	Aeolian	32°,21′,05″N	52°,41′,13″E	D43	Aeolian	32°,03′,06″N	52°,42′,28″E
D3	Aeolian	32°,21′,26″N	52°,43′,28″E	D44	Aeolian	32°,02′,23″N	52°,42′,11″E
D6	Aeolian	32°,19′,16″N	52°,40′,32″E	D46	Aeolian	32°,01′,03″N	52°,42′,15″E
D7	Aeolian	32°,19′,57″N	52°,44′,59″E	D47	Aeolian	32°,00′,21″N	52°,42′,14″E
D8	Aeolian	32°,18′,31″N	52°,45′,26″E	D49	Aeolian	31°,59′,08″N	52°,42′,51″E
D9	Aeolian	32°,17′,26″N	52°,40′,57″E	I1	Aeolian	32°,06′,40″N	52°,41′,49″E
D10	Aeolian	32°,17′,46″N	52°,45′,53″E	K1	Aeolian	32°,10′,32″N	52°,46′,44″E
D11	Aeolian	32°,16′,18″N	52°,41′,40″E	K2	Aeolian	32°,09′,25″N	52°,45′,50″E
D13	Aeolian	32°,16′,16″N	52°,43′,47″E	K4	Aeolian	32°,06′,04″N	52°,43′,39″E
D15	Aeolian	32°,16′,52″N	52°,45′,41″E	K6	Aeolian	32°,03′,10″N	52°,43′,22″E
D16	Aeolian	31°,16′,19″N	52°,45′,37″E	Z1	Alluvium	32°,24′,53″N	52°,39′,35″E
D17	Aeolian	32°,16′,19″N	51°,41′,41″E	Z2	Alluvium	32°,21′,45″N	52°,45′,55″E
D18	Aeolian	32°,16′,14″N	52°,45′,31″E	Z3	Alluvium	32°,18′,29″N	52°,51′,51″E
D19	Aeolian	32°,14′,01″N	52°,42′,08″E	Z4	Alluvium	32°,17′,51″N	52°,53′,15″E
D20	Aeolian	32°,13′,59″N	52°,45′,10″E	Z5	Alluvium	32°,17′,47″N	52°,52′,56″E

Table 3.3 Facies and location of the representative studied samples of the aeolian and alluvial sediments in the study area.

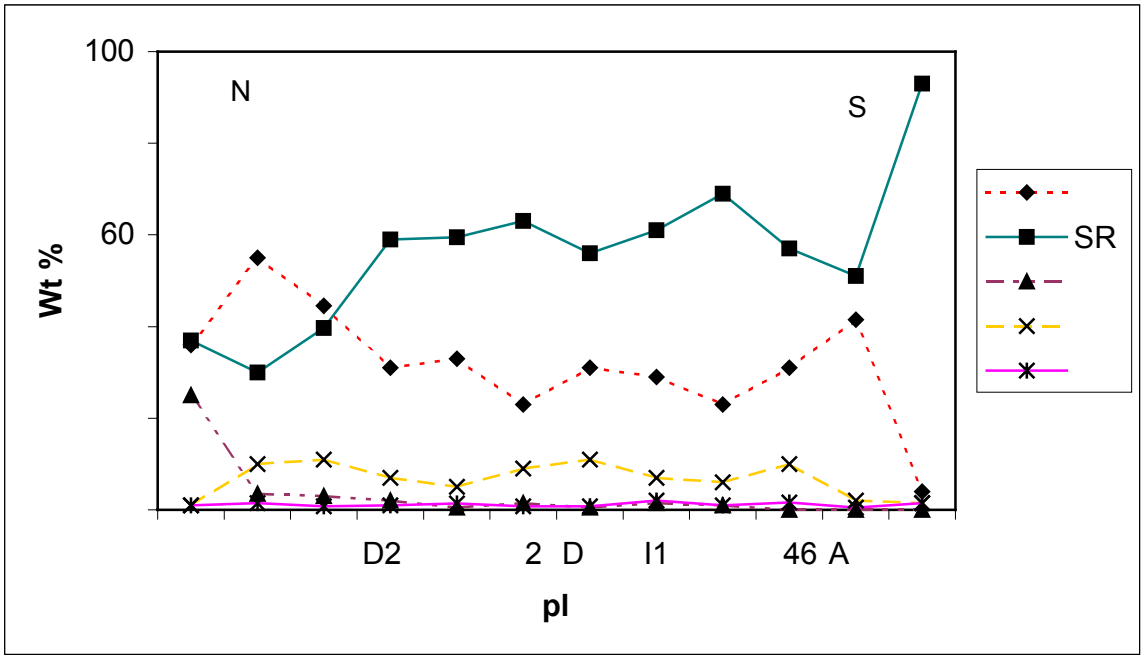

Fig. 3.20 Distribution of the various types of grains in the representative samples of aeolian sands (No D, K & I) and alluvial sediments (No A) in the study area. Igneous lithic (IR), sedimentary lithic (SR), metamorphic lithic (MR), quartz (Q), feldspar (F) (see Fig. 3.2 and Table 3.3 for position of samples No). N (north), S (south).

Igneous lithic grains

Igneous lithics consist of dacite, andesite, acidic tuff, diorite, granite, microgranite and a subordinate amount of andesite-basalt and basalt grains in the studied samples. The average frequency percentage of the igneous lithics is about 37% in the aeolian sands (Table 3.2). Their content decreases in frequency from the north to the south. Exceptionally, the amount of igneous lithic increases slightly at the end southern part of the aeolian sand field (Fig. 3.21). The composition of the volcanic lithics is identic to lithology of volcanic rocks exposed in the north and the northeast of the Varzaneh aeolian sand field.

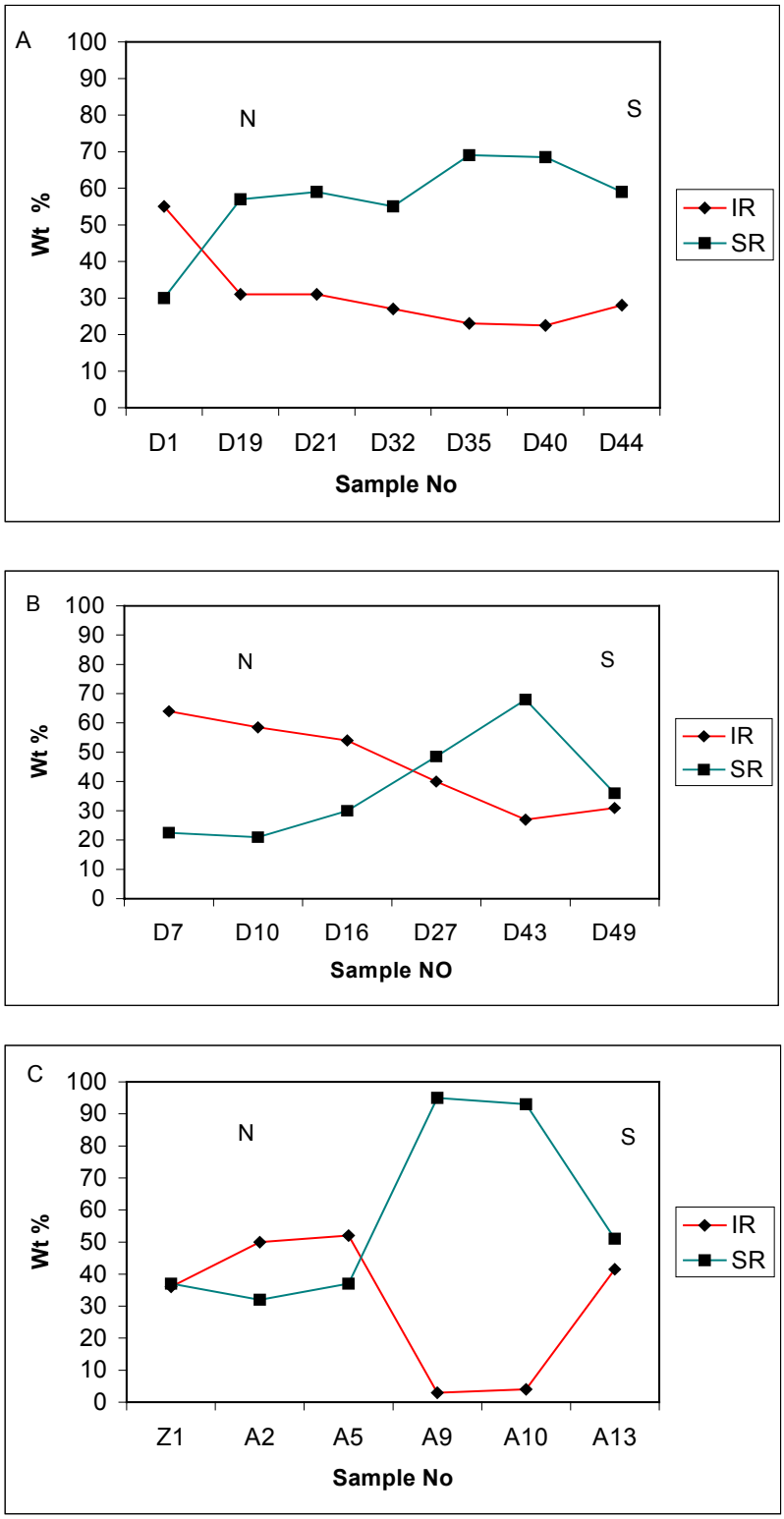

Fig. 3.21 Distribution of igneous and sedimentary lithic grains in the western (A), the eastern (B) parts of the Varzaneh sand dunes and (C) in alluvial sediments from the north to the south of the study area. Igneous lithic (IR) and sedimentary lithic (SR) (see Fig. 3.2 and Table 3.4 for position of samples No). N (north), S (south).

Sedimentary lithic grains

Sedimentary lithics mostly consist of carbonates and few sandstones, siltstones, shales and chert grains. The average frequency percentage of the sedimentary lithic grains determined by counting under polarizing microscope is about 52% (approximately 49% carbonate and 3% non-carbonate in the aeolian sand samples). The carbonate content of representative samples determined by chemical analysis ranges in turn from about 17% and 79% in aeolian and alluvial samples (Table 3.2 & Fig. 3.22).

Sample No	Facies	% Carbonate	Sample No	Facies	% Carbonate
A1	Alluvium	25	D24	Aeolian	55
A3	Alluvium	22	D27	Aeolian	55
A5	Alluvium	38	D28	Aeolian	58
A9	Alluvium	78	D30	Aeolian	58
A10	Alluvium	79	D31	Aeolian	62
A12	Alluvium	49	D35	Aeolian	64
A13	Alluvium	47	D41	Aeolian	25
D2	Aeolian	38	D42	Aeolian	54
D6	Aeolian	39	D43	Aeolian	56
D7	Aeolian	17	D44	Aeolian	67
D8	Aeolian	23	D47	Aeolian	52
D9	Aeolian	45	D49	Aeolian	51
D16	Aeolian	32	I1	Aeolian	50
D17	Aeolian	57	K5	Aeolian	43
D18	Aeolian	34	K6	Aeolian	41
D19	Aeolian	49	Z1	Alluvium	25
D21	Aeolian	48	Z3	Alluvium	23
D23	Aeolian	60	Z5	Alluvium	22

Table 3.4 Average carbonate content of the representative sand samples of the two facies (alluvial and aeolian sands) in the study area (see Fig. 3.2 and Table 3.3 for position of samples No).

The Carbonate lithic grains occur as micrit, sparite, biogenic (biosparite and biomicrite) and crystalline carbonate. Biogenic grains are composed of microfaunal shells, mostly foraminifera (*Orbitolina, Orbitoides, Heterastegina*, miliolids and ostracods), algae (red and green) and shell fragments of macrofauna include rudists, fresh water gastropods (mainly *Bithynia phialensis*) and ostracods. *Orbitolina* belongs to Aptian, *Orbitoides* to Campanian–Mastertian, algae and rudists mostly Aptian to Maastrichtian, *Heterastegina* to Oligo-Miocene, gastropods and ostracods to Quaternary. According to palaeontological studies, the carbonate grains come mostly from Cretaceous rocks, and subordinate amounts from Tertiary rocks (Oligomiocene) (H, Vaziri, pers. com., 2000).

Fig. 3.22 Variations of frequency percentage of carbonate lithic grains in the western (A), the eastern (B) parts of the Varzaneh sand dunes and (C) alluvial sediments from the north to the south of the study area (see Fig. 3.2 for position of samples No). N (north), S (south).

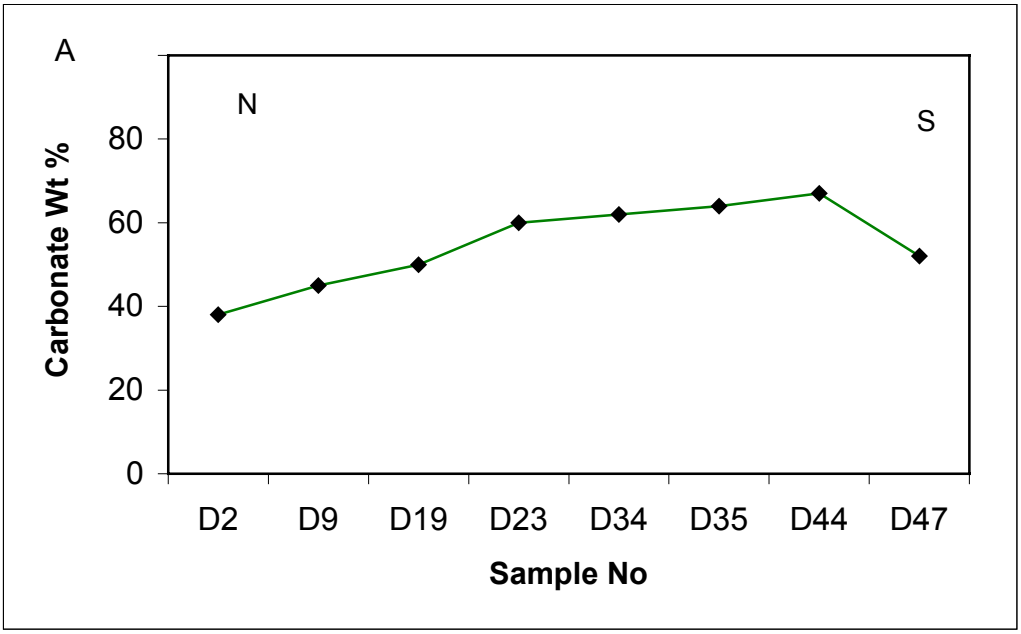

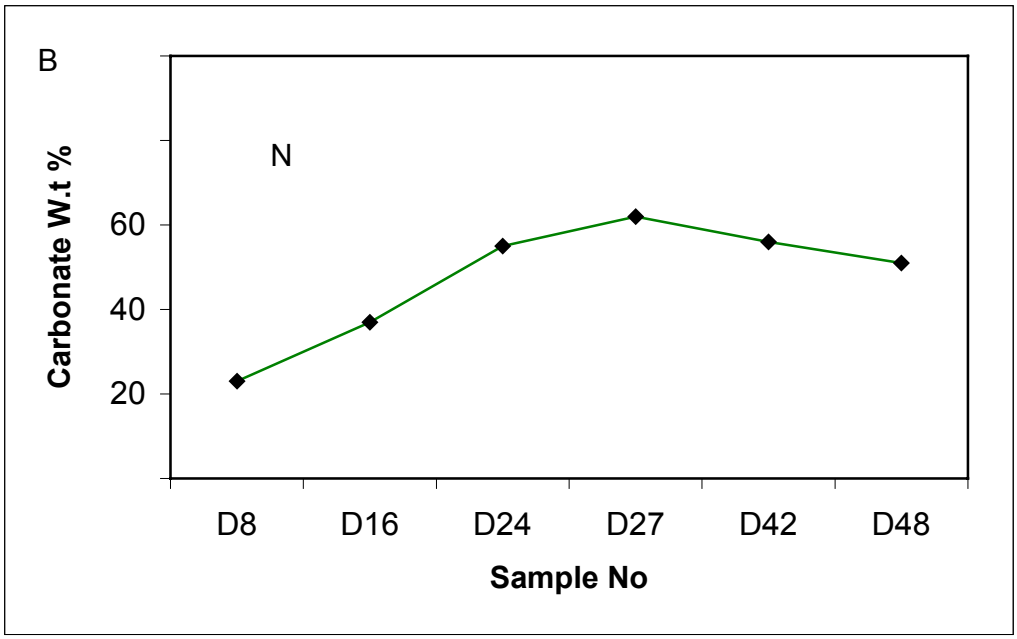

Continue

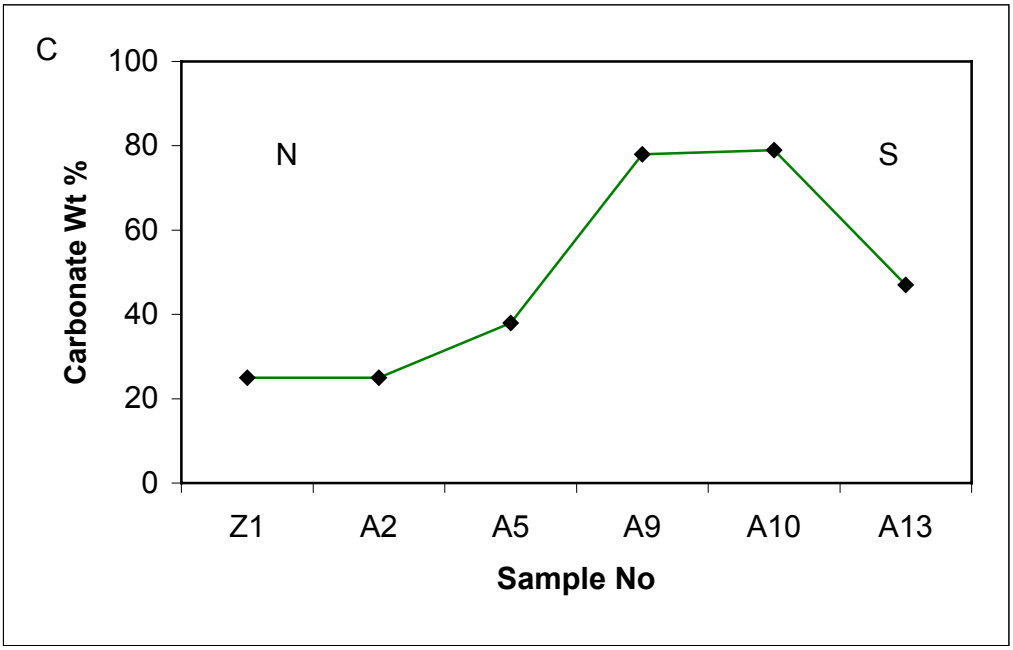

In contrast to the igneous lithics, the relative frequency of sedimentary lithics (carbonates) increases from the north to the south of the aeolian sand field, expect that they decrease slightly at the end of the southern part of the sand dunes (see Figs. 3.21 & 3.22).

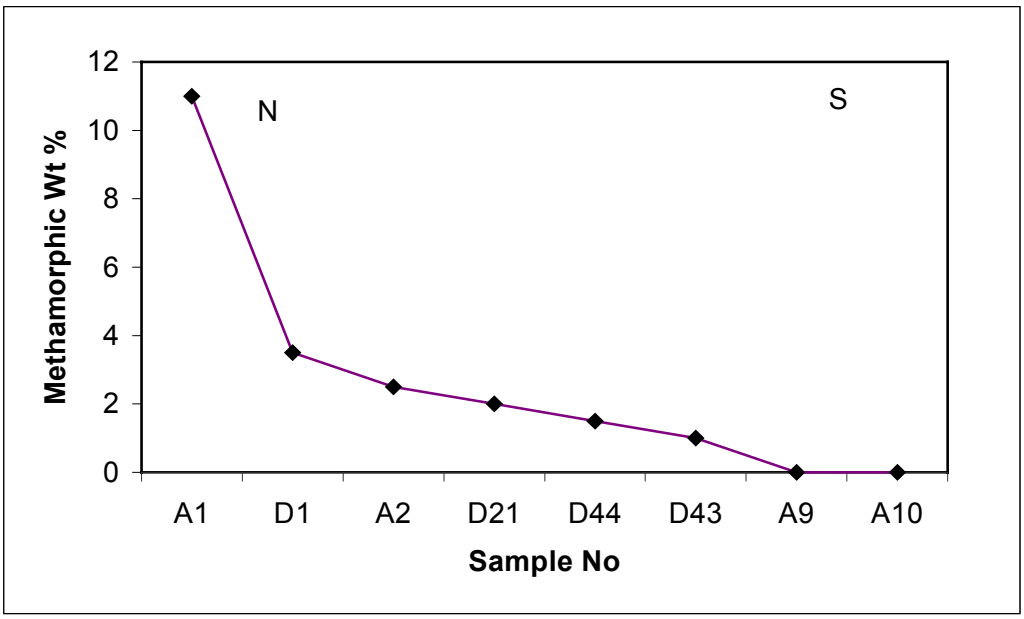

Fig 3.23 Distribution of metamorphic lithic grains in the representative samples of alluvial sediments (No. A) and aeolian sands (No. D) (see Fig. 3.2 and Table 3.3 for position of samples No). N (north), S (south).

Metamorphic lithic grains

Metamorphic lithics mostly consist of schist (chlorite, muscovite, biotite, and quartz schist), and subordinate amount of quartzite, gneiss, amphibolite schist, actinolite schist, phylite, and metagranite grains. The average frequency percentage of the metamorphic lithics is about 1.5% (Table 3.2) in the aeolian sands. The percentage of these grains decreases from the north to the south within the aeolian sands (Fig. 3.23).

3.5.3 Mineral grains

Quartz

Quartz grains are the most common mineral type in the sand size fraction (0-1, 1-2, 2-3 phi fractions) of the aeolian sands, ranging from 2% to up to 15% with an average of 10 % (see Table 3.2 & Fig. 3.24). They usually increase in frequency with decrease in grain size and therefore, are more abundant in the fine-grained sand fraction, in contrast to igneous and sedimentary lithics. Quartz grains frequency is rather irregular in the sand dunes from the north to the south (Fig. 3.24).

Feldspar

Feldspar grains are the third common mineral type in the sand size fraction of the aeolian sands. They are milky white to buff in color. Average frequency of the feldspar grains is about 1.5% (see Table 3.2 & Fig. 3.24). Distribution of the feldspar grains is irregular in the sand dunes similar that of quartz grains (Fig. 3.24). They are represented mainly by plagioclase (albite to oligoclase and andesine) with subordinate amounts of potash feldspar (microcline and orthose). The occurring major types of the feldspar grains are similar to that the intermediate and acidic volcanic igneous rocks, exposed in the northeast of the study area.

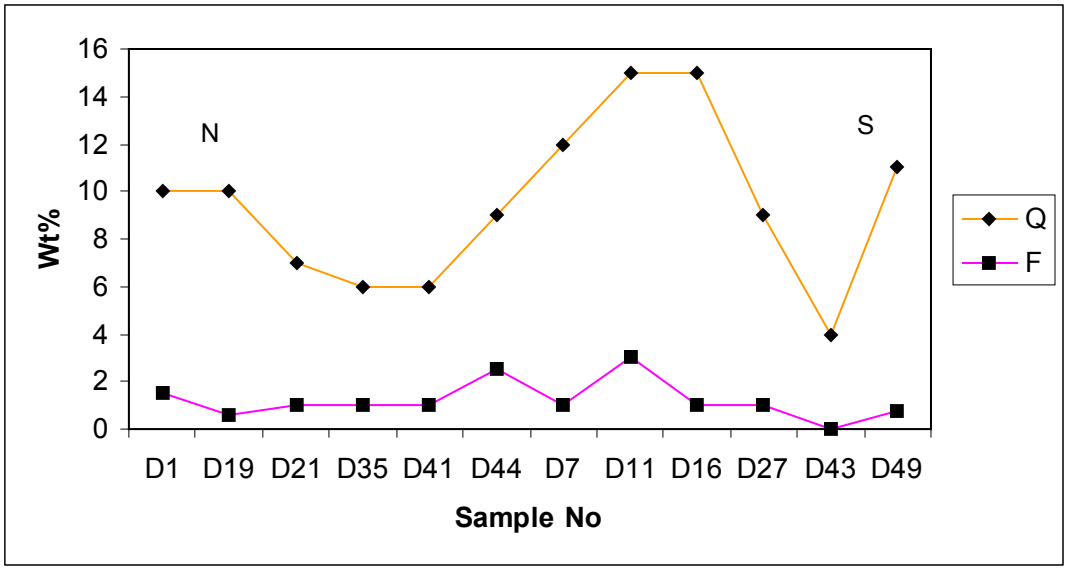

Fig. 3.24 Distribution of quartz and feldspar grains in the representative sand dune samples (see Fig. 3.2 and Table 3.3 for position of samples No). N (north), S (south).

Heavy minerals

Heavy mineral grains are the second common minerals in the fine and very fine sand fractions of the aeolian and alluvial sediments in the study area. The average frequency percentage of the heavy minerals ranges from 2 % to 3% in the fine to very fine sand fractions of the aeolian sands. Overall, the percentage of the heavy minerals decreases from the north to the south of the Varzaneh aeolian sand field (Fig. 3.25 & Table 3.5).

The occurring heavy minerals are mainly garnet, pyroxene, hematite, and, subordinately amphibole, epidote, limonite, zircon, rutile and magnetite. Mica, apatite, scheelite, pyrite (oxidized), barite, sphene, ilmenite, jarosite, glauconite, chlorite, leucoxene and celestine are also observed in traces.

Opaque minerals comprise almost one third of the heavy mineral fraction. Hematite is the most common opaque heavy mineral and its distribution is not regular from the north to the south of the aeolian sands. Garnet and pyroxene are the most abundant non-opaque heavy minerals both in fine and very fine sand.

These minerals are more frequent in the very fine sands and decrease in frequency from the north to the south of the aeolian sands.

Tow various kinds of garnet are present, i.e. colorless and dark, the later is more abundant. Augite and hyperstene are the most abundant pyroxene minerals. Amphibols are present as green and brown hornblende (Table 3.4 & Fig. 3.25)

Sample No / %Heavy mineral	A9	A10	A13	D2	D7	D20	D23
Total	0.35	0.30	2.50	2.85	2.50	2.27	1.90
Hematite	0.20	0.20	0.62	0.30	0.69	0.50	0.20
Garnet	<0.01	<0.01	<0.01	0.30	0.27	0.25	0.19
Pyroxene	0.10	0.080	0.37	1.60	1.39	1.39	1.14
Limonite	<0.01	<0.01	1.12	<0.01	<0.01	<0.01	<0.01

Sample No / %Heavy mineral	D24	D37	D47	I1	Z2
Total	1.81	1.14	0.96	1.35	7.44
Hematite	0.72	0.45	0.48	0.74	2.65
Garnet	0.09	<0.01	0.048	<0.01	0.88
Pyroxene	0.80	0.50	0.28	0.49	3.53
Limonite	0.09	<0.01	0.04	<0.01	<0.01

Table 3.5 Frequency percentage of the main heavy minerals in the representative samples of the fine to very fine sand fractions from the alluvial (sample No. A) and aeolian sediments (samples No. D & I) (see Fig. 3.2 and Table 3.3 for position of samples No).

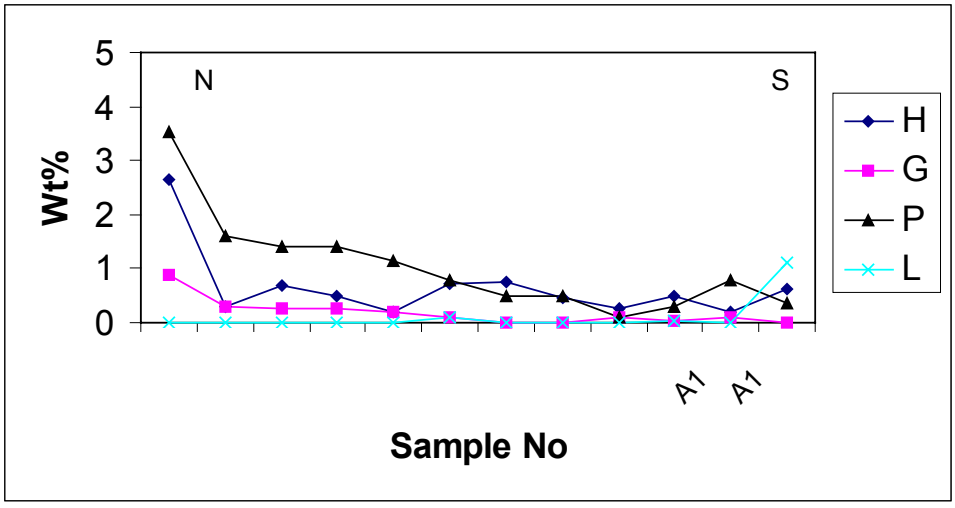

Fig. 3.25 Distribution of total heavy mineral grains in the representative samples of the aeolian and alluvial sediments sand fraction. Total (T), hematite (H), garnet (G), pyroxene (P), and limonite (L), N (north), S (south).

Fig. 3.26 Photomicrographs (crossed nicols) of the representative aeolian and alluvial sand samples. Magnification of D49, D34, A7, A1, Z3 is x23 and Z1 is x63. Aeolian (D), debris-flow deposits (A) and stream-flow deposits (Z). Biomicrite (b), fossil (f), granite (g), tuff (t), carbonate (c), quartz (q), biosparite (s), mudstone (m), metagranite (mt), siltstone (si), sandstone (sa), schist (sc) (see Table 3.3 for position of samples No).

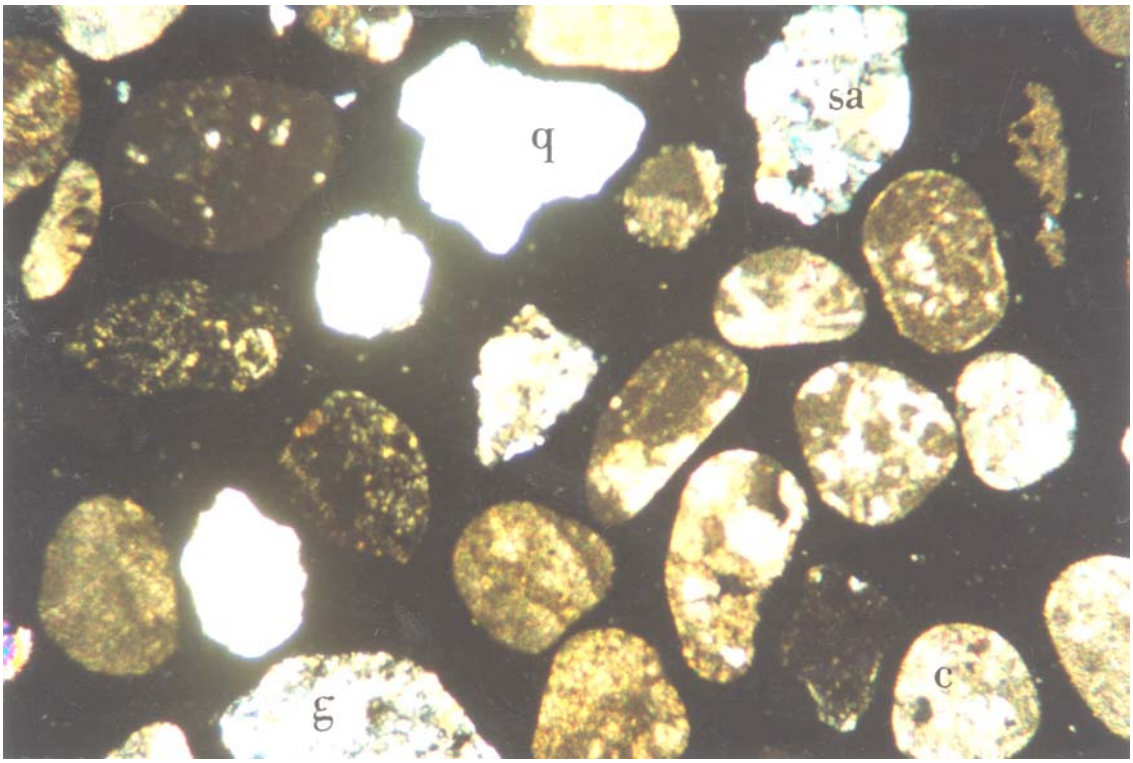

D34

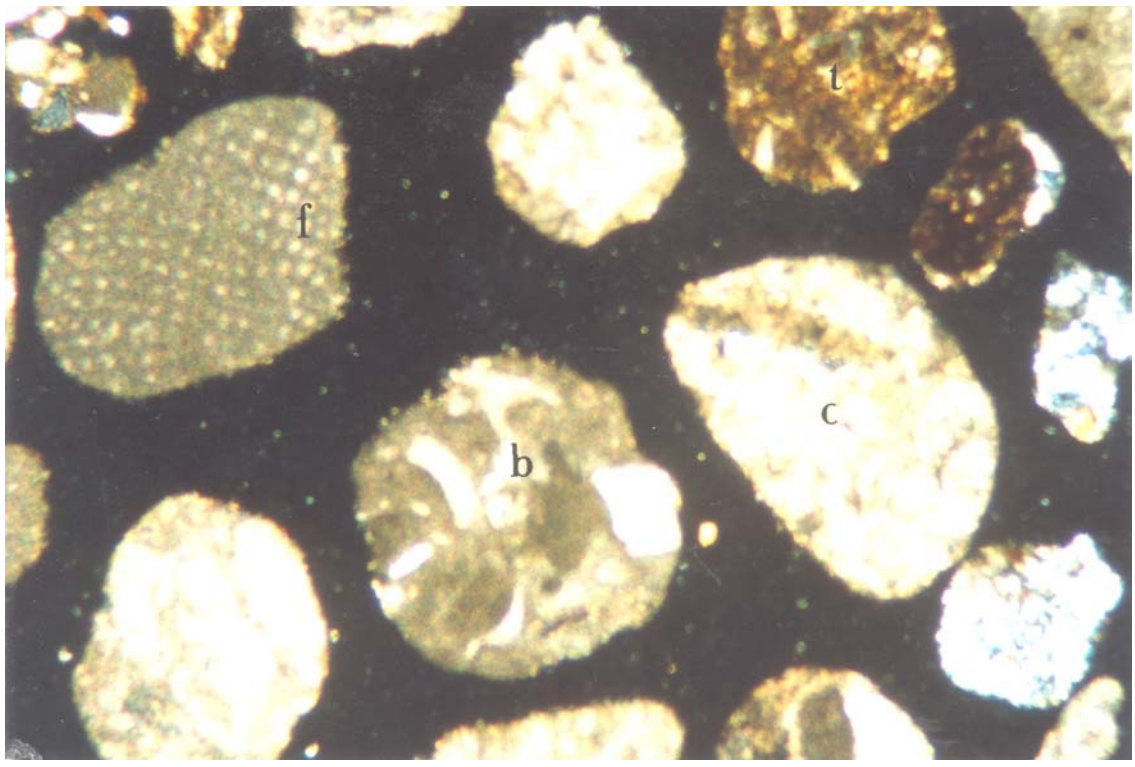

D49

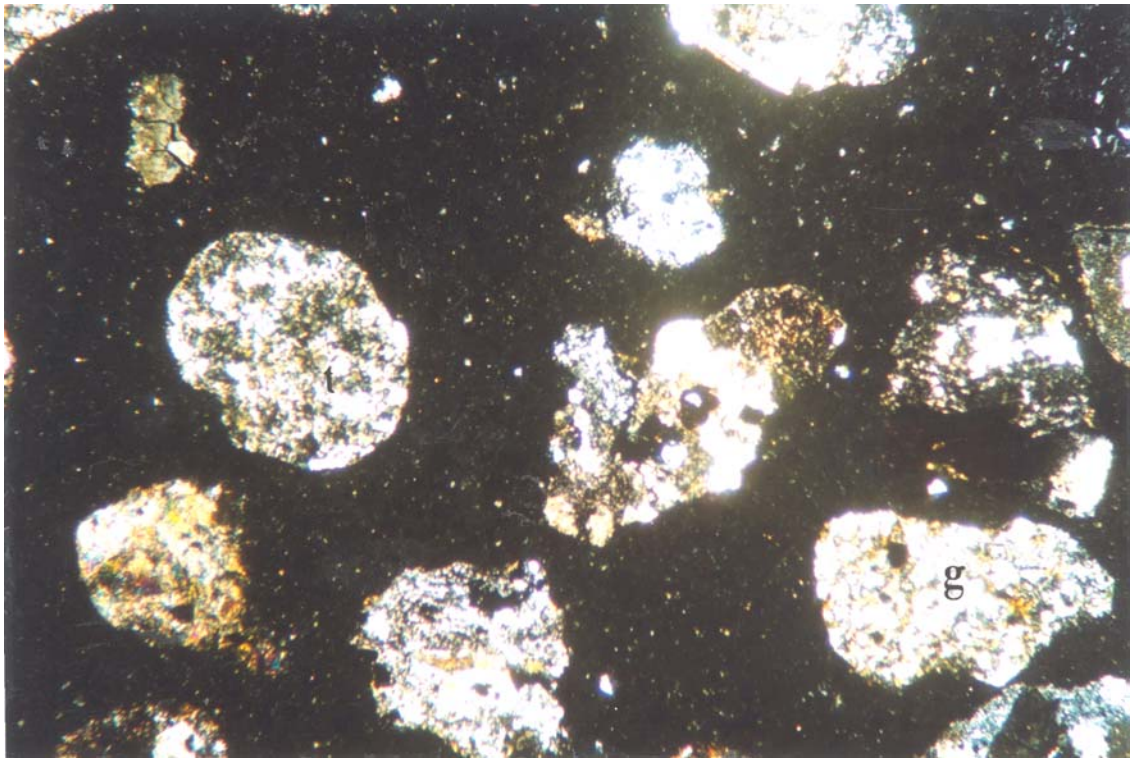

A1

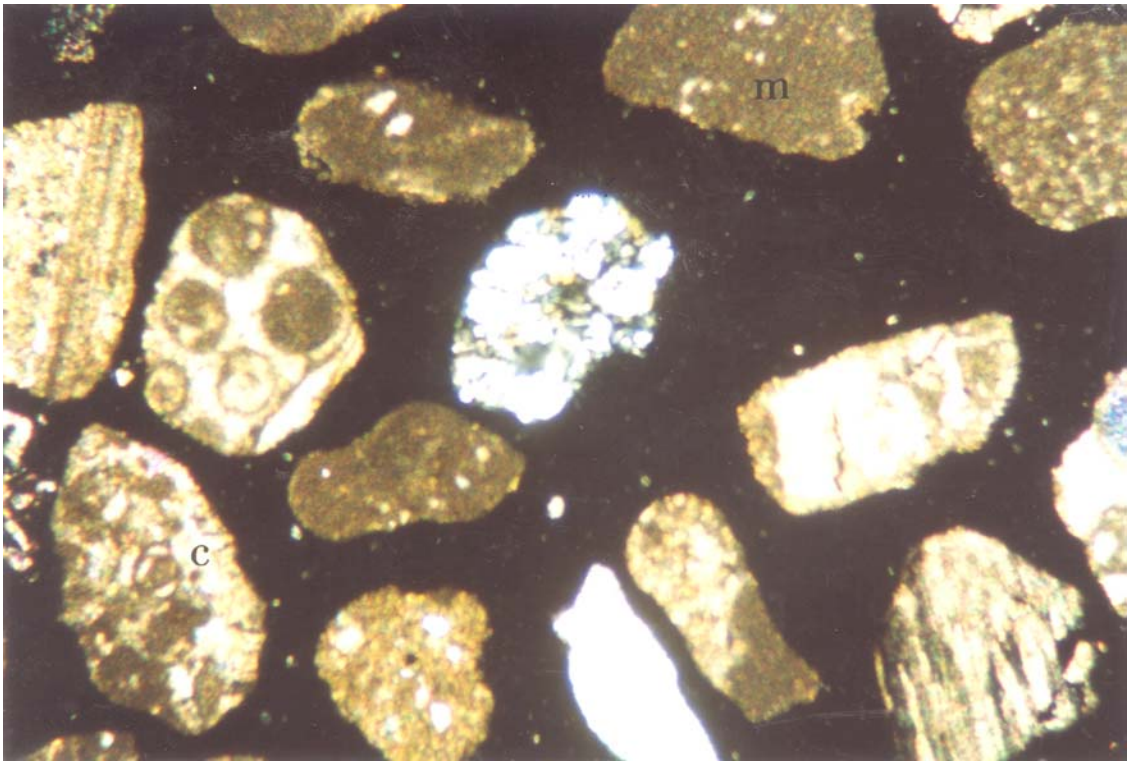

A7

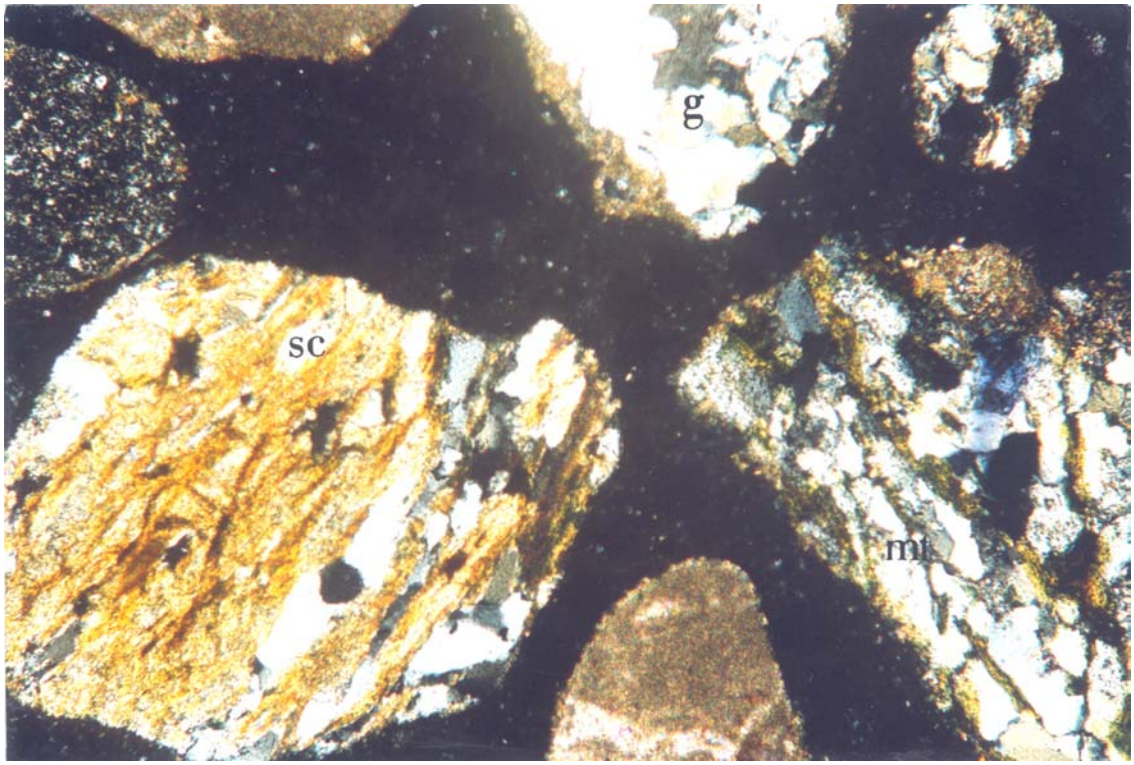

Z1

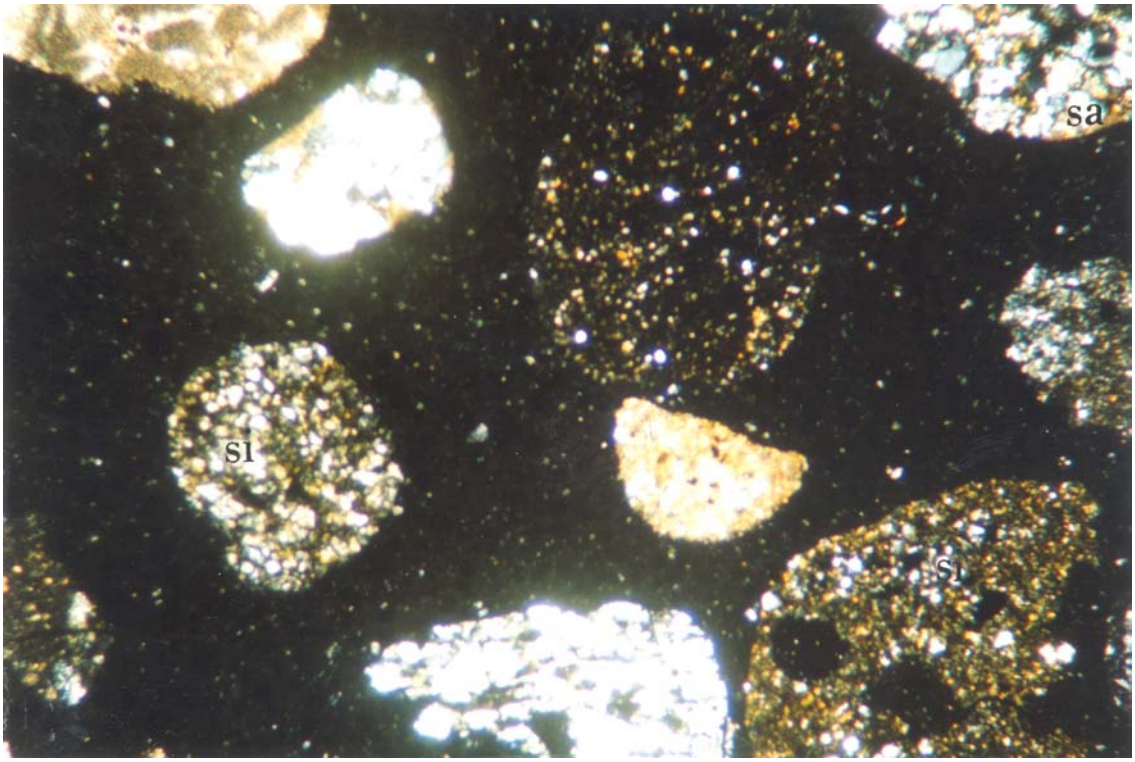

Z3

Interpretation

Mineralogical composition of the lithic grains and optical properties of mineral grains indicate that the aeolian sands are derived from igneous and sedimentary as main sources and metamorphic rocks as minor source.

The igneous lithics are mostly composed of volcanic and to a minor extent of plutonic grains. They chiefly belong to Tertiary highlands, located to the north and the northeast of the study area. The major origin of the sedimentary lithic grains (mainly carbonates) is from sedimentary rocks exposed in the west and the southwest of the study area. These rocks belong to Cretaceous and Jurassic outcrops. The main origin of the metamorphic lithic grains is from the mountain ranges located in the northwestern and the western part of the drainage basin of the Zayandeh river.

Textures and fabrics of the feldspar grains suggest that they are derived mostly from andesitic and granitic rocks. Andesitic rocks mainly outcrop in the northeast of the aeolian sands but granitic rocks are found at several locations of the drainage basin as small intrusive bodies. Garnet grains mainly are attributed to contact metamorphic rocks and pyroxenes, amphiboles, and epidotes to intermediate igneous rocks exposed in the north and the northwest of the study area. The source of zircon and rutile grains mostly could be attributed to the acidic igneous rocks outcropping in the southwest of the aeolian sands. The origin of the crystalline carbonate grains is intergranular cement from Quaternary open framework conglomeratic deposits that are exposed in the southern part of the study area.

These grains were transported and deposited mostly by the Zayandeh river to the north, and the two ephemeral streams to the south and the west margins of the aeolian sand field.

3.6 Texture

3.6.1 Introduction

In this study, general characteristics of grains such as sorting, size, roundness and surface texture of the various types of the aeolian sand forms (sand dunes and sand sheets) were determined. The study mainly concentrates on the grain size distribution of these two facies. Using the half-phi interval histograms and the simple frequency curves, the average

grain size distribution of these sediments have been studied. Statistical parameters of grain size (mean, standard deviation, skewness and kurtosis) were examined. In addition, roundness variations of grains from alluvial and aeolian deposits were investigated to some extent.

3.6.2. Grain size

Sand dunes

Sand dunes including the active and the stabilized sand dunes (dikaka) are characterized by a narrow range of grain size in which medium and fine sand fraction (mostly fine sand) form about 90% of their average grain size spectrum. The dune sands are moderately to very well sorted. The size ranges from +1 to about +5 phi (0.5 to 0.031 mm) with an average mean grain size of 2.20 phi (0.22 mm).

Sample No	Facies	Mean size	Sorting	Skewness	Kurtosis	Location	
D3	Active sand dune	2	0.43	0.21	4	32°,21′,26″N	52°,43′,28″N
D8	Active sand dune	2.43	0.31	2	9.05	32°,18′,31″N	52°,45′,26″N
D9	Active sand dune	2.19	0.31	0.37	6.89	32°,17′,26″N	52°,40′,57″N
D11	Active sand dune	2.01	0.36	1.25	5.64	32°,16′,18″N	52°,41′,40″N
D16	Active sand dune	2.39	0.33	1.14	7.49	32°,16′,19″N	52°,45′,37″N
D22	Active sand dune	2.20	0.64	-0.16	4.03	32°,12′,18″N	52°,42′,00″N
D24	Active sand dune	2.40	0.80	-1.89	7.96	32°,10′,40″N	52°,44′,02″N
D30	Active sand dune	2.30	0.48	-0.05	4.25	32°,08′,03″N	52°,43′,55″N
D31	Active sand dune	2.37	0.60	-0.25	3.25	32°,07′,31″N	52°,40′,33″N
D32	Active sand dune	2.08	0.38	0.37	4.60	32°,07′,11″N	52°,41′,00″N
D33	Active sand dune	2.32	0.49	-0.01	4.03	32°,07′,00″N	52°,41′,03″N
D34	Active sand dune	1.81	0.76	-0.06	1.78	32°,06′,30″N	52°,42′,28″N
D35	Active sand dune	2.16	0.6	-0.72	4.69	32°,06′,50″N	52°,41′,05″N
D41	Active sand dune	2.22	0.62	-0.45	3.70	32°,04′,06″N	52°,41′,24″N
D43	Active sand dune	2.20	0.64	-0.16	2.5	32°,03′,06″N	52°,42′,28″N
D49	Active sand dune	2.23	0.58	-0.79	5.62	31°,59′,08″N	52°,42′,51″N
I1	Interdune	2.36	0.59	-0.49	3.83	32°,07′,09″N	52°,40′,30″N
I2	Interdune	2.06	0.60	-0.47	4.50	32°,06′,26″N	52°,41′,57″N
O1	Overbank sand sheet	1.81	1.09	-1.23	3.8	32°,21′,39″N	52°,45′,13″N
O2	Overbank sand sheet	1.92	1.04	-1.30	3.25	32°,20′,56″N	52°,46′,05″N
O3	Overbank sand sheet	1.67	1.29	-1.40	4.40	32°,20′,32″N	52°,46′,35″N
K1	Sabkha sand sheet	2.23	0.59	-0.72	4.5	32°,10′,32″N	52°,46′,44″N
K2	Sabkha sand sheet	2.05	0.78	-0.68	3.33	32°,09′,25″N	52°,45′,50″N
K4	Sabkha sand sheet	2.23	0.62	-0.45	3.79	32°,06′,04″N	52°,43′,39″N
K5	Sabkha sand sheet	2.06	0.86	-1.01	4.11	32°,04′,53″N	52°,43′,15″N
K6	Sabkha sand sheet	2.36	0.71	-0.532	3.87	32°,03′,10″N	52°,43′,22″N
Sd	Stabilized sand dune	2.19	0.82	-0.16	1.29	32°,21′,52″N	52°,38′,45″N

Table 3.6 Statistical grain size parameters of the main types of aeolian sand samples and their positions in the Varzaneh aeolian sand field.

These deposits are generally finer than the overbank sand, sabkha and interdune sand sheets.

The dune sands are from strongly positively skewed (+1.25) to strongly negatively skewed (-0.1.89). Their kurtosis ranges between 1.78 and 9.05 (very leptokortic to extremely leptokortic) (Table 3. 6 & Fig. 3.27).

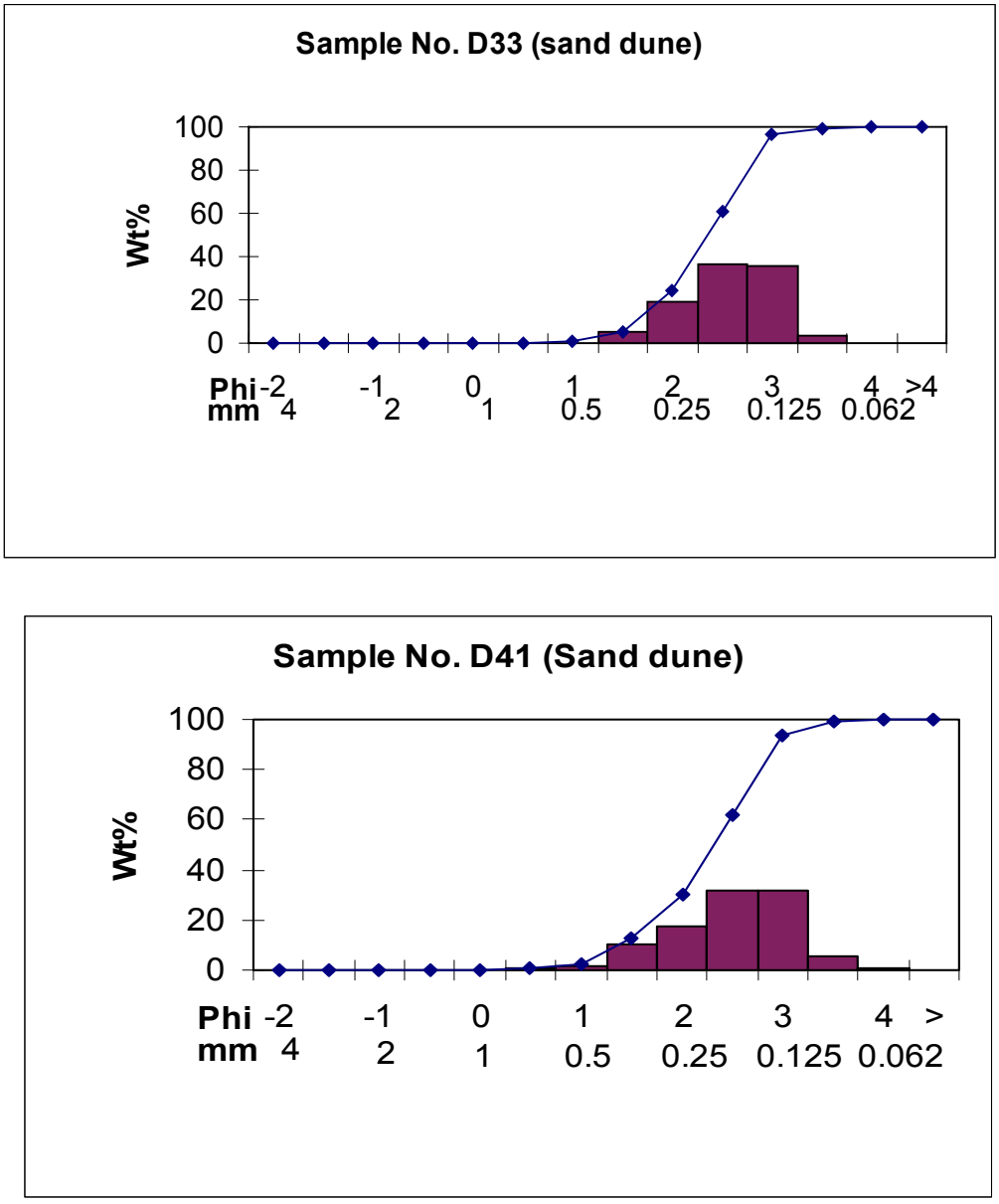

Fig. 3.27 Histograms and frequency curves of grain size distribution of the representative samples from sand dunes (samples No. D33 and D41) (see Fig. 3.2 and Table 3.6 for position of samples No).

Overbank sand sheet

Overbank sand sheet deposits have a wide range of grain size and are poorly sorted. They range between -3 and about +5 phi (8 and 0.031 mm) with an average mean of 1.8 (0.29 mm) phi in size**.** The granule size fraction comprises about 3 % of grain size distribution on average and has strongly coarse skewness. Their kurtosis ranges between 3.8 to 4.83 (extremely leptokortic) (Table 3.6 & Fig 3.28).

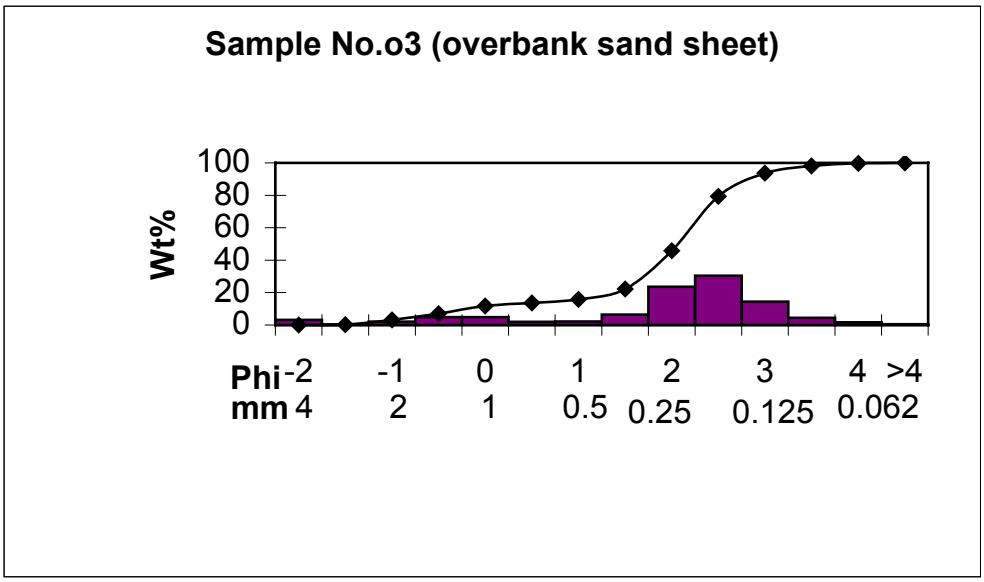

Fig. 3.28 Histogram and frequency curve of grain size distribution of the representative sample from the overbank sand sheet (see Fig. 3.2 and Table 3.6 for position of sample No).

Sabkha sand sheet and interdune

Both sabkha sand sheet and interdune sand sheet deposits have approximately a similar grain size distribution, in which medium and fine sand fractions form about 82% of grain size on average. However, fine sand is the most frequent size fraction both in the interdune sand sheet and the sabkha sand sheet deposits (Fig. 3.29). Sabkha sand sheet deposits range in size between -2 and about +5 phi (4 and 0.031 mm) with an average mean size of 2.16 phi (0.23 mm). They mostly are moderately sorted but relatively better sorted than overbank sand deposits. This sub-facies has fine skewness (+0.23) to very coarse skewness (-1.06) and mainly is coarse skewed. Interdune deposits range in size between –1 phi and about +5 phi (2 and about 0.031 mm) with an average mean size of 2.1 phi (0.235 mm). They are usually moderately well sorted to moderately sorted. These deposits are very

coarse skewed and their kurtosis range between 3.26 to 4.97 (generally extremely leptokortic) (Table 3.6 & Fig. 3.29).

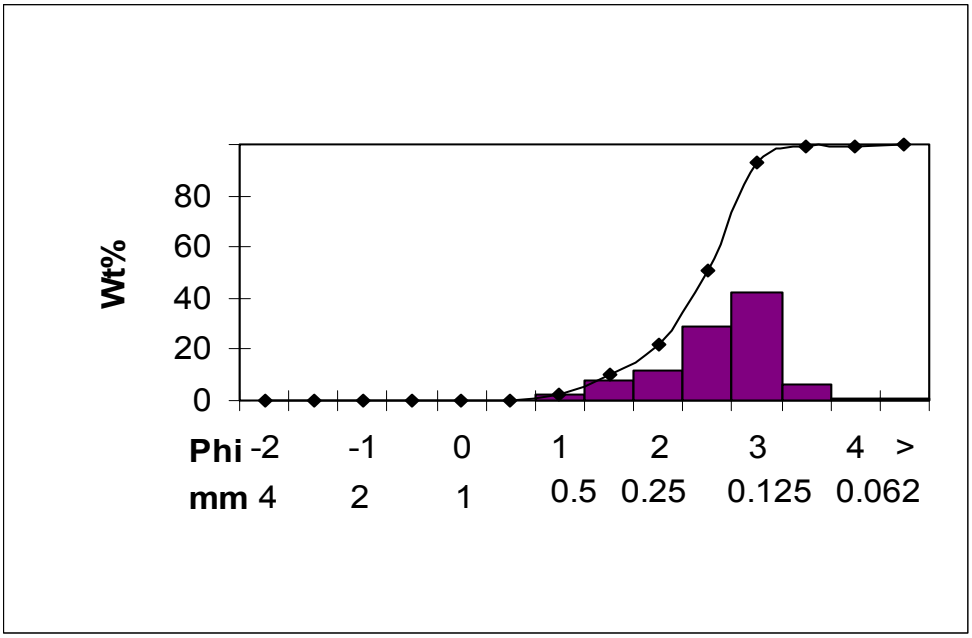

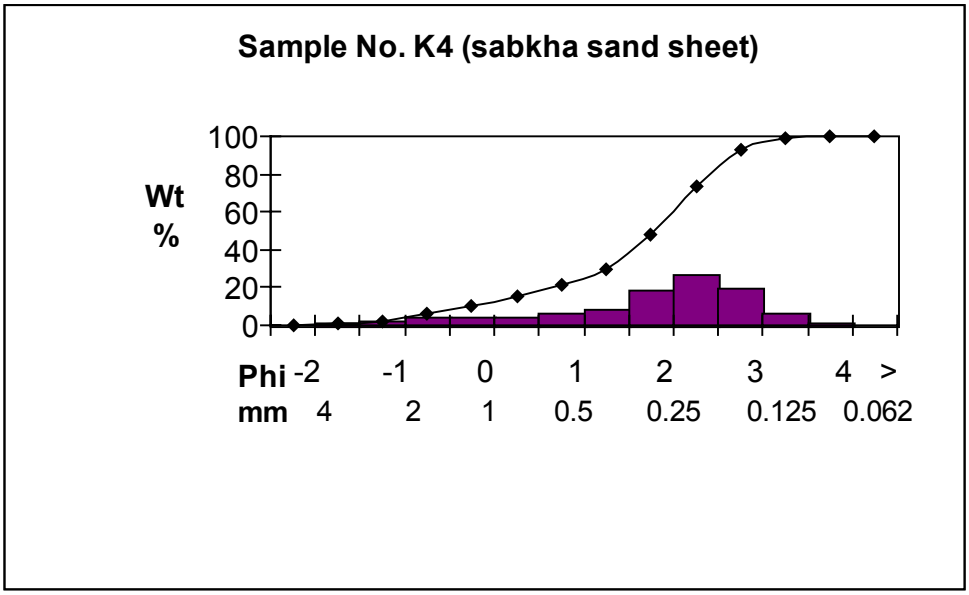

Fig. 3.29 Histograms and frequency curves of the grain size distribution of the representative samples from the sabkha sand sheet and interdune sediments (samples No. K4, I1) (see Fig. 3.2 and Table 3.6 for position of samples No).

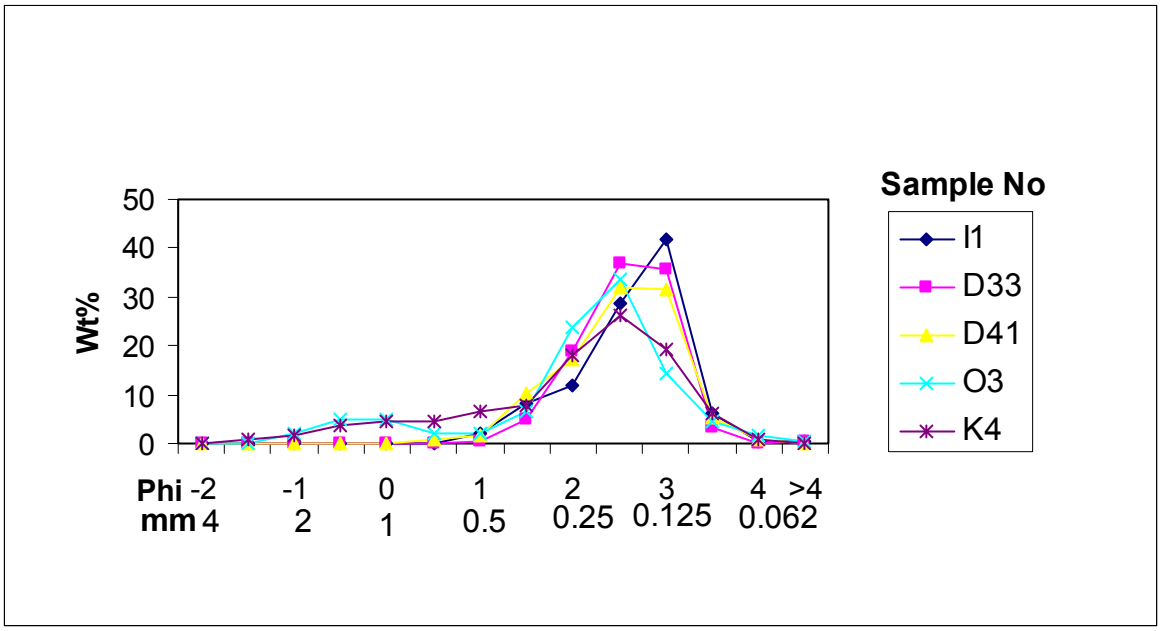

Fig. 3.30 Comparison between grain size frequency curves of representative samples from the main types of aeolian sediments in the Varzaneh sand field (see Fig. 3.2 and Table 3.5 for facies and position of samples No).

Interpretation

The capacity of wind to transport solid particles of a density similar to that of quartz (2.65 gr/cm^3) is mostly limited to fine and medium sand (0.125 to 0.5 mm). Strong storms (20-30 m/s) can slowly move pebbles by creep and sand size particles very fast. Hence wind is very effective in producing and accumulating well-sorted sands (Einsele, 1992). Excellent sorting, low content of silt and clay and sometimes the good roundness of quartz grains are the most important properties of mature aeolian sands (Reineck & Singh, 1980). An important factor that controls the sorting of the sand grains on the Varzaneh aeolian sands is the grain size distribution of source sediments (cf. Livingstone *et al.,* 1999).

Data presented here show no systematic variation of the grain–size parameters (skewness, and kurtosis) dune sands except that there is a gradual decrease in average grain size from the lower plinths toward the crest of the sand dunes. Interdune, overbank sand sheet and sabkha sand sheet sediments are moderately to poorly sorted and mostly coarse skewed (tails to the left) (Fig. 3.30). Dune sands range between very well sorted to moderately sorted and very fine (tails to the right) to very coarse skewed. Their kurtosis is generally extremely leptokortic (or good sorting in the central part of the distribution). Bimodality of the overbank

sand sheet deposits is as a result of both water and wind processes. They include the Zayandeh river (gravel and sand fractions) and aeolian sand sediments (sand fraction). Unimodality of the sediments (especially the dune sands) reflect wind activity in erosion and deposition of aeolian sands.

3.6.3 Roundness

Investigation of the various types of sand (aeolian and alluvial) shown in Fig. 3.31 represent that: 1-The quartz grains of the aeolian sands have a roundness class that varies from angular to sub-angular depending on size fraction and feldspar grains are mostly sub-angular. 2-The carbonate lithic grains of aeolian sands are rounded to well-rounded, igneous lithics sub-angular to rounded and metamorphic lithic grains angular to rounded. 3-The roundness of fluvial lithic grains is approximately similar to aeolian sand grains whereas that of debris flow carbonate lithics is angular to sub-angular. 3-The grain surface of aeolian sands displays no frosting and no small pits caused by grain impacts in the Varzaneh aeolian sand field. The roundness depends on size, composition and degree of maturity.

Interpretation

Wind is a more effective rounding medium than water. Aeolian sand grains are generally more rounded because air-transported grains are intensively subjected to pitting and become rounded faster than those transported in aqueous media (e.g. El-Sayed, 1999). Thus, wind-blown sand grains may achieve a high degree of roundness. The effectiveness of wind action as an abrasion agent is not the only factor in rounding of sand grains in desert environments (Khalaf & Gharib, 1985).

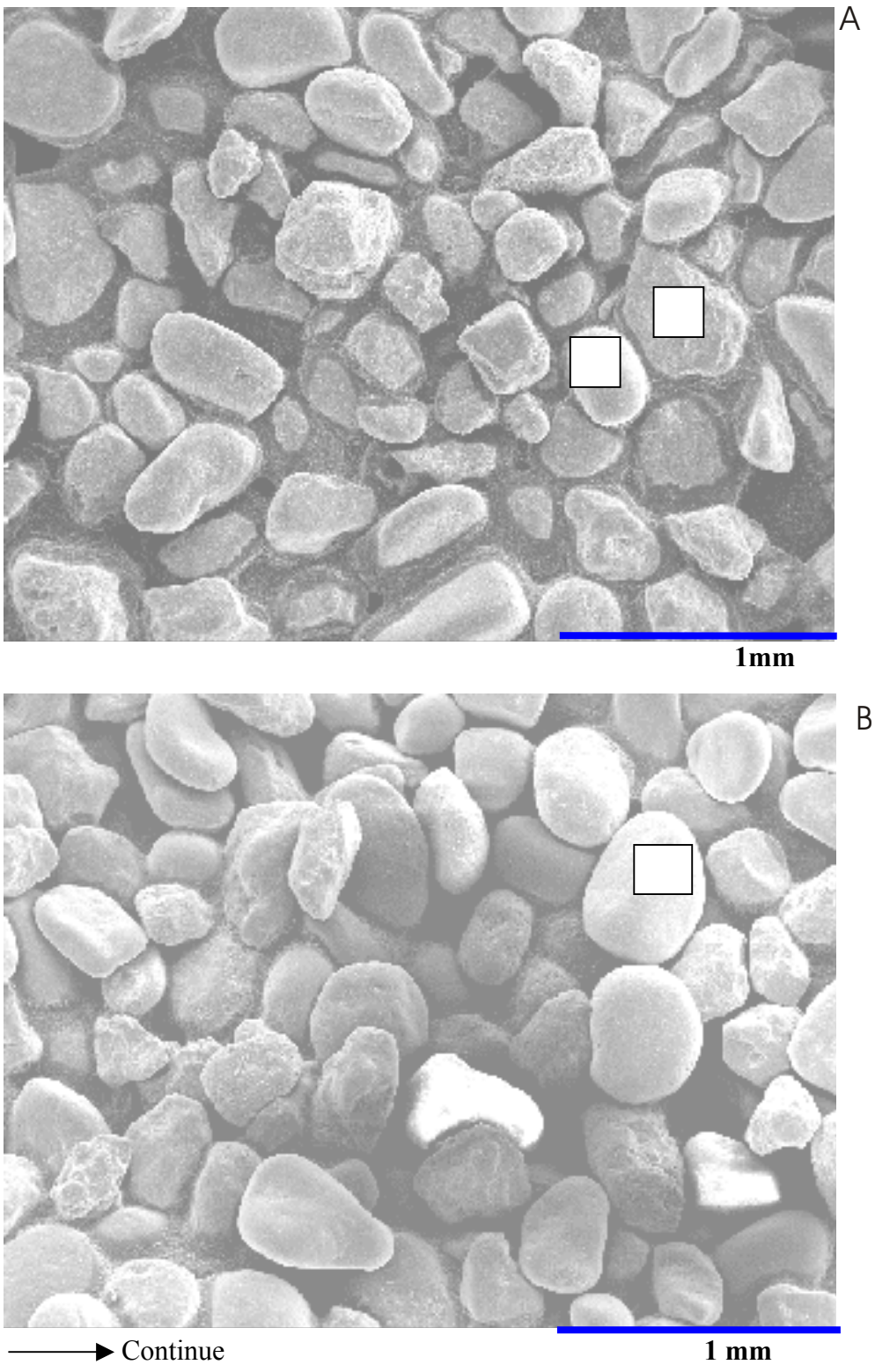

Fig. 3.31 SEM (scanning electron microscope) photomicrographs showing the textural properties of the dune sand samples. Sample from the northern part of sand dune field (A), sample from the southern part of the sand dune field (B), individual quartz grain from the aeolian sands (C). Quartz (Q), carbonate lithic grain (C), non-carbonate lithic grain (N).

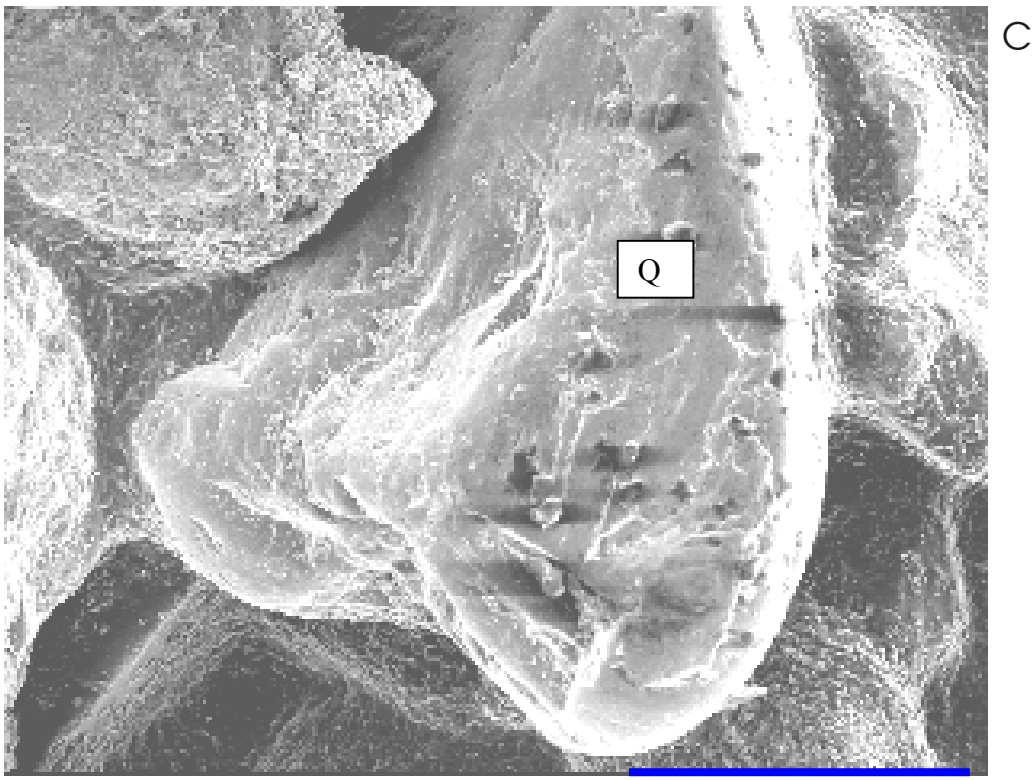

The Varzaneh aeolian sands are mostly derived from the sediments of the Zayandeh river and the two ephemeral streams (see Chapter 2.5 for position of rivers). These alluvial sediments were transported from a few to tens of kilometers. The fluvial sands show a similar roundness than do the aeolian sands. As a result, the source of sediments is considered to be the major factor controlling the roundness characteristics of the aeolian sediments and their interdunes. Hence the aeolian sands chiefly inherited the roundness characteristics from the fluvial sediments (cf. Khalaf, 1989; cf. Sagga, 1993)

3.7 Provenance

3.7.1 Introduction

The term provenance, in general, refers to a location of origin, where the sediments are derived from, and the nature of source rocks (Bates & Jackson, 1980). In provenance studies, however, it is used in a wider sense including all the factors, which influence the production and composition of sediments. These are chiefly the nature of source rocks, their

position relative to deposition site and the pathways by which sediments are transferred from source to depositional basin (Pettijohn *et al.,* 1987). In this study two important factors which control the properties of aeolian sands including source rock and transportation and sedimentation processes are described.

3.7.2 Source rocks

All aeolian and alluvial sediments accumulated on the Varzaneh aeolian sand field were originated from rocks exposed in the Gavkhoni playa lake drainage basin. They can be divided into three types of rocks: Sedimentary, igneous and metamorphic (see Chapter 2 for details). The sedimentary rocks spread mostly in the west, the southwest and the northwest of the Gavkhoni playa lake. They consist of chemical and biochemical rocks (mainly limestone, and dolomite) and detrital rocks (siltstone, sandstone, and conglomerate). The igneous rocks (mainly volcanic) outcrop in the east and northeast of the playa lake. They mainly contain andesite, dacite, granite and granodiorite. The metamorphic rocks extend mostly in the northwest of the upper reaches of the drainage basin. The main lithologies of these metamorphic rocks are schist, gneiss and amphibolite.

3.7.3 Transportation and deposition processes

The two main factors, water and wind, control transportation and sedimentation of the aeolian sands in the study area. The Zayandeh river, the largest interior river in Iran, and the two ephemeral rivers (see Chapter 2.5 for position of rivers) transport loose sediments within the study area. The fluvial sediments of the Zayandeh river mostly are concentrated in the northern part of the sand dune field (Fig. 3.32). These river sediments mainly range from coarse-grained sand to fine gravel in size. The average grain size of these sediments is considerably coarser than that of the aeolian sands. The sands are mainly composed of abundant lithic grains i.e. igneous, sedimentary, and metamorphic and mineral grains including mostly quartz and heavy minerals (see Chapter 3.3 for details). The two ephemeral streams have chiefly deposited their bed load on the western and the southern margins of the aeolian sand field (Fig. 3.1). These materials mostly consist of coarse–grained sand to gravel. The main composition of these grains is sedimentary lithics (especially carbonates). Non-carbonate sedimentary lithic grains (such as shale and sandstone), other lithic grains and mineral grains form these sediments respectively (see Chapter 3.3 for details). These streams

provided an adequate volume of loose sand–size particles for the aeolian sand field especially in favorable climate periods. These sediments (deposited from the Zayandeh river and the two ephemeral streams) are easily erodible and widely exposed so as to be accessible to aeolian erosion (Fig. 3.33).

The role of wind has been very important to distribute sediments on the Varzaneh aeolian sand field. Wind has the potential for transporting large amounts of sand (i.e. particles 60-2000 micron in diameter) (Greeley *et al.*, 1996). At present, the westerly and the southwesterly winds are dominant during winter and spring in frequency. Wind blows more often from the north and northwest during summer. Wind speed sometimes reaches 30 m/s in winter. Sandstorms blow primarily from the southwest to the northeast (see Chapter 2 for details of wind direction and velocity). The development of the linear/seif dunes (from the north to the south) indicates that paleo-winds were not exactly similar to present wind directions and at least a dominant northerly wind existed.

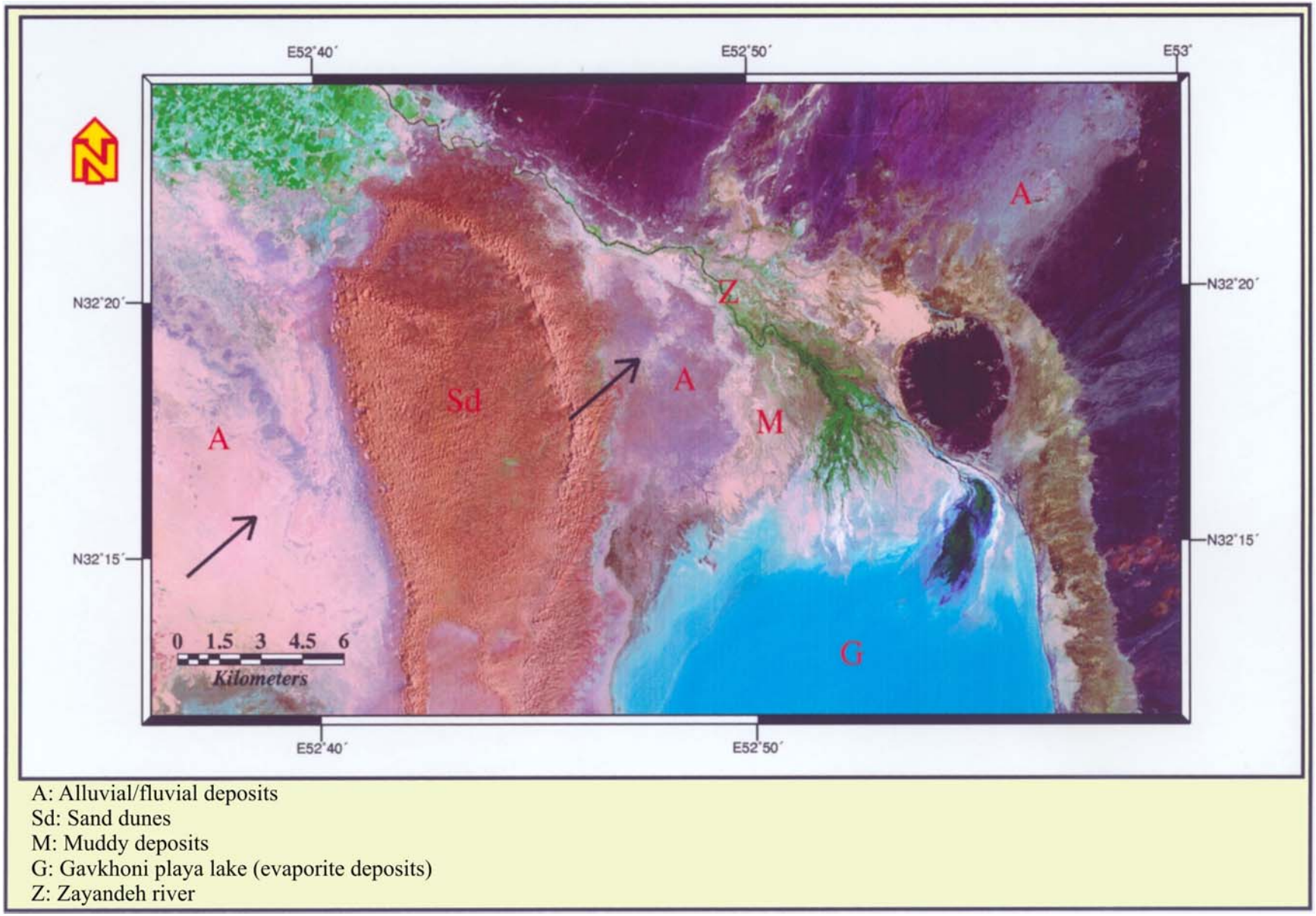

Fig. 3.32 False color-Landsat TM image showing main provenance of the aeolian sands (arrows) in the study area.

Fig. 3.33 An erosional wadi bench representing a source of alluvial clastics for the Varzaneh aeolian sands in the west of the sand dunes. The sand dunes are the background of photograph.

Interpretation

Based on the mineralogical composition of the aeolian sands and the alluvial sediments, the major supply of the sediments in the Varzaneh aeolian sand field is the Zayandeh river sediments, concentrated northward of the aeolian sands. A minor supply is from sediments deposited by the two ephemeral streams in the south and the southwest of the sand dunes. According to mineralogical studies, the first major provenance of the Varzaneh aeolian sand field (about 50%) is from sedimentary rocks, the second major one (about 40%) is from igneous rocks.

It is most probably that during interglacial periods, strong winds removed sand grains from the alluvium and concentrated them in the sand dune field. Variations of mineralogical composition from the north to the south of the sand dunes, general form of the Varzaneh sand dunes and linear dunes suggests that a large part of the sediments probably was transported from north to south by the strong northerly winds. Since the sand dune field is close enough to the supply of sand, relatively unstable heavy minerals such as epidote still are preserved in

the aeolian sands. At present, according to wind direction and wind speed, sediments move to all directions (mostly to the east) but it is not enough strength to move them in large quantities.

Many continental aeolian sand fields have developed during the late Quaternary world wide. They result from variations in climatology, vegetation cover, intensity of aeolian processes and the supply of sand (Madole, 1994 in Winspear & Pye, 1995). It is relevant also for our case that an adequate supply of loose sand with suitable size, wind capable of moving the sand and sufficient time must be available until large dunes will form. It is supposed that the sediment supply to the study area was mainly generated during the latest Pleistocene and earliest Holocene during humid periods of enhanced discharge by the streams.

3.8 Summary and conclusions

(1) The Varzaneh aeolian sand field extends the western part of the Gavkhoni playa lake and decrease from the north to the south in width, volume and height. It consists of two main sand forms: sand dunes and sand sheets.

(2) The sand dunes consist of linear/seif, barchanoid, star, and dikaka forms. The linear/seif dunes developed by wide unimodal to bimodal wind regimes. The star dunes could be initiated and developed from modification of other type dunes by multidirectional winds. The barchanoid dunes result from the latest dominant wind direction. The stabilized sand dunes (dikakas) result from enough moisture and plant roots to fix them. The morphological elements of the aeolian sand dunes indicate which paleo-winds were chiefly responsible for the overall morphology of the sand dunes and the seif dunes, and neo winds cause the barchanoids and star dunes. Therefore, according to paleo-wind direction sands mostly moved from the north to the south and neo-winds redistribute it to a certain extent toward all directions. The sand sheets occur to the east and within the interior of the sand dunes. According to situation and behavior, they can be grouped into three categories: sabkha, overbank and interdune (dry and wet) sand sheet.

(3) From consideration of dynamic behavior, the Varzaneh aeolian sand field consists of two groups. The first group represents mobile sand accumulation, including active sand

dunes i.e. barchanoids, star and seif dunes and active sand sheets i.e. dry interdune areas. The second group is characterized by immobile ones consisting of stabilized sand dunes (dikaka) and inactive sand sheets (sabkha and overbank sand sheets). The active sand dunes move according to wind directions but annual resultant migration rate is low or they are nearly fixed. The movement rate of grains gradually decrease from the sand dunes toward alluvial environments, because of relative fixation by moisture and decrease in strength of wind. Deflation occurs both on sand dunes and on interdune areas, but sabkha sand sheets and overbank sand sheets are mostly deposition sites. Therefore, main distribution and concentration pattern of the aeolian sands probably mostly took place by strong paleo-winds in this area.

(4) The Zayandeh river plays a more important role than other streams in relation to the source of the aeolian sands. The amount of the igneous and the metamorphic lithic grains of the Zayandeh river increases from Varzaneh toward the Zayandeh river delta. Therefore, the northern part of the aeolian sands, due to its proximity to the main source of the sand grains possesses more igneous and metamorphic lithic grains. The aeolian sands in the southern part of the sand dunes are mostly composed of carbonate lithic grains, because the southwestern and southern streams consist of abundant carbonate lithic grains. Abnormal increase of igneous lithic grains at the southern end of the sand dunes is attributed to the southern streams. The percentage variation of quartz and feldspar is not irregular similar to other particles. This property is attributed to disintegration of lithics especially the igneous lithics due to their mechanical instability. The amount of the heavy minerals also increases from the north to the south similar to igneous lithic grains, because they are mostly derived from the Zayandeh river. The mineralogical composition of sands in the sand dunes and the interdune areas is approximately similar, because the dune sands are the sources of the interdune sands, whereas mineralogical composition of sands in the overbank and the sabkha sand sheets change from the north to the south, because they are derived from dune sands and the fluvial sediments. The first major source of the aeolian sands belongs to sedimentary rocks located in the south, the southwest and the northwest and the second major one originates from igneous rocks exposed in the east and the northeast of the aeolian sands.

(5) The textural properties (roundness and surface texture) of the aeolian sediments are approximately the same as in the source sediments, because they are close to area of deflation and inherit them. Therefore, wind processes did not play an important role to

change the primary properties of grains. The interdune aeolian sands are better sorted than the sabkha and overbank sand sheet sands. The interdune and sabkha sands are unimodal and the overbank sands are bimodal in most localities. The sorting of sand dunes and interdune sediments is better than that of other aeolian sediments. Sorting of the aeolian sands increase from base to crest of the sand dunes.

(6) The presence of the extensive sand field with an area about 130 km^2 and 45 km in length indicates that a large amount of sediments were deposited and deflated during favorable climate conditions that lasted for a long period in this area. It is believed that present conditions could not form this sand field. It is considered that after the latest glacial period heavy rains and melting glaciers simultaneously caused strong erosion in the Zayandeh river drainage basin and much transportation of clastic to the area. These sediments were mostly deposited where aeolian sands spread at present.

Chapter 4

Sedimentology of the Gavkhoni playa lake and the Zayandeh river delta

4.1 Introduction

The study area is located between N 32°,00-32°, 23′ and E 52°,43′-52°,49′ and covers about 550 km^2. The surface of the playa lake is about 1474 m above sea level. This end lake is typical for many permanent lacustrine to saline lake basins within closed drainage basins in central Iran. Water enters to this basin via the permanent Zayandeh river, an ephemeral river, some small steams, ground water discharge and direct precipitation. The playa lake receives most of the water from the Zayandeh river in the north. The ephemeral river enters to the south of the lake and sometimes floods inundate these parts of the playa lake (see Chapter 2.5 for position of rivers). In normal years, surface water and groundwater contribution and evaporation are the largest components of hydrologic budget. For these reasons, sediments may be a sensitive indicator of any changes in the hydrological budget in this playa lake.

Alluvial fan deposits cover the north, the south and the east rim of the playa lake. These deposits, which extend from the mountains to the margins of the playa lake, derive mainly from alteration and erosion of igneous rocks. The Varzaneh aeolian sand field marks the western boundary of this playa lake. The northern shore of the lake is wetter than in other areas and is covered with abundant bushes (Figs. 4.1 & 4.2).

The study area has an arid climate. The weather is cold in winter and temperature decreases to about –17°C but in mid summer it is hot and rises to about +42°C. Evaporation exceeds precipitation and inflow. Extensive evaporation begins in May and continues till September (see Chapter 2.4 for details).

In this chapter, we will discuss the types of the sedimentary environments and facies including alluvial fan, sand flat, mud flat, saline mud flat, salt pan and delta and also geochemistry of brine and its evolution.

4.2 Methodology

For investigation of sedimentology, stratigraphy of depositional environments and the geochemistry of brine, sixteen trenches and pits were dug in the study area (Fig. 4.1). Sedimentological logs for eighth sections were drawn (see appendix F for lithostratigrafic-sedimentologic sections). Variation of groundwater table was measured and nine water samples (surface and groundwater) were analyzed. Evaporite minerals of ten representative samples from the salt pan using X-ray diffraction were detected. For determination of mineralogical composition (sand to mud fractions), paleontology studies, and the provenance of the sediments, twenty samples of sand-sized fraction and seven clay-sized fraction were analyzed. Several photographs were taken from sedimentary structures and remarkable sedimentological features (see Chapter 1 and Appendixes for details of methodology).

4.3 Depositional environments and facies

4.3.1 Introduction

Seven major facies can be easily recognized in this playa lake basin. They can be defined on the basis of texture, mineralogy, and evaporite to clastic ratio. Although the facies are distinct and can be mapped, their boundaries are usually graditional. They include, alluvial fan, aeolian sand field (sand dunes, interdunes, sand flats), sand beaches, mud flats, saline mud flats, a large salt pan and finally delta (Figs. 4.1 & 4.2). The variety of the playa lake environments and the main facies, textures and structures of the main evaporite minerals are shown in Fig. 4.3 and also compared with a coastal sabkha setting in Fig. 4.4.

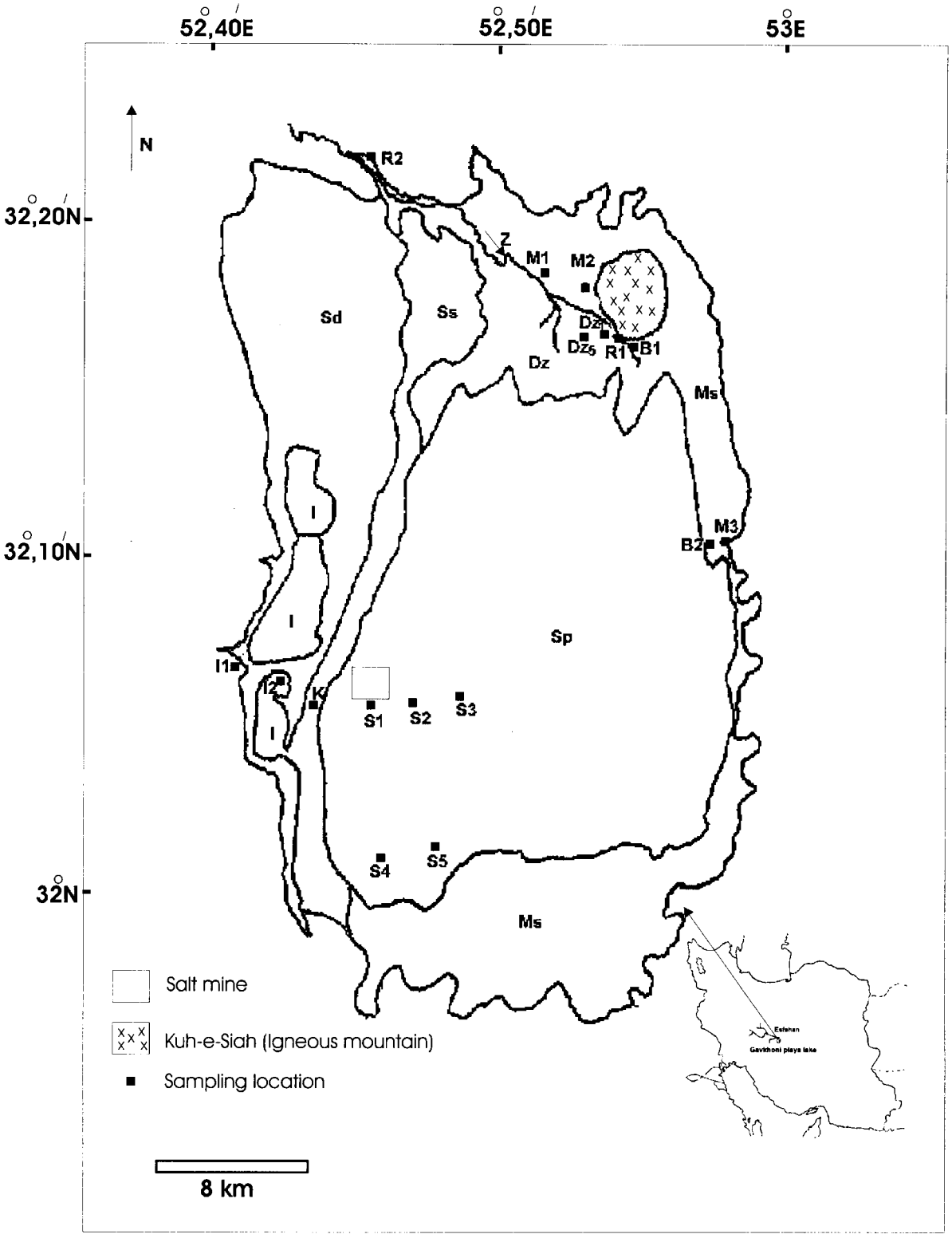

Fig. 4.1 Simplified map showing approximate location of pits, trenches and sampling localities in the study area. Sd (sand dune), Sp (salt pan), I (interdune), Ss (sand flat), Ms (mud flat/saline mud flat), Z (Zayandeh river), D (delta).

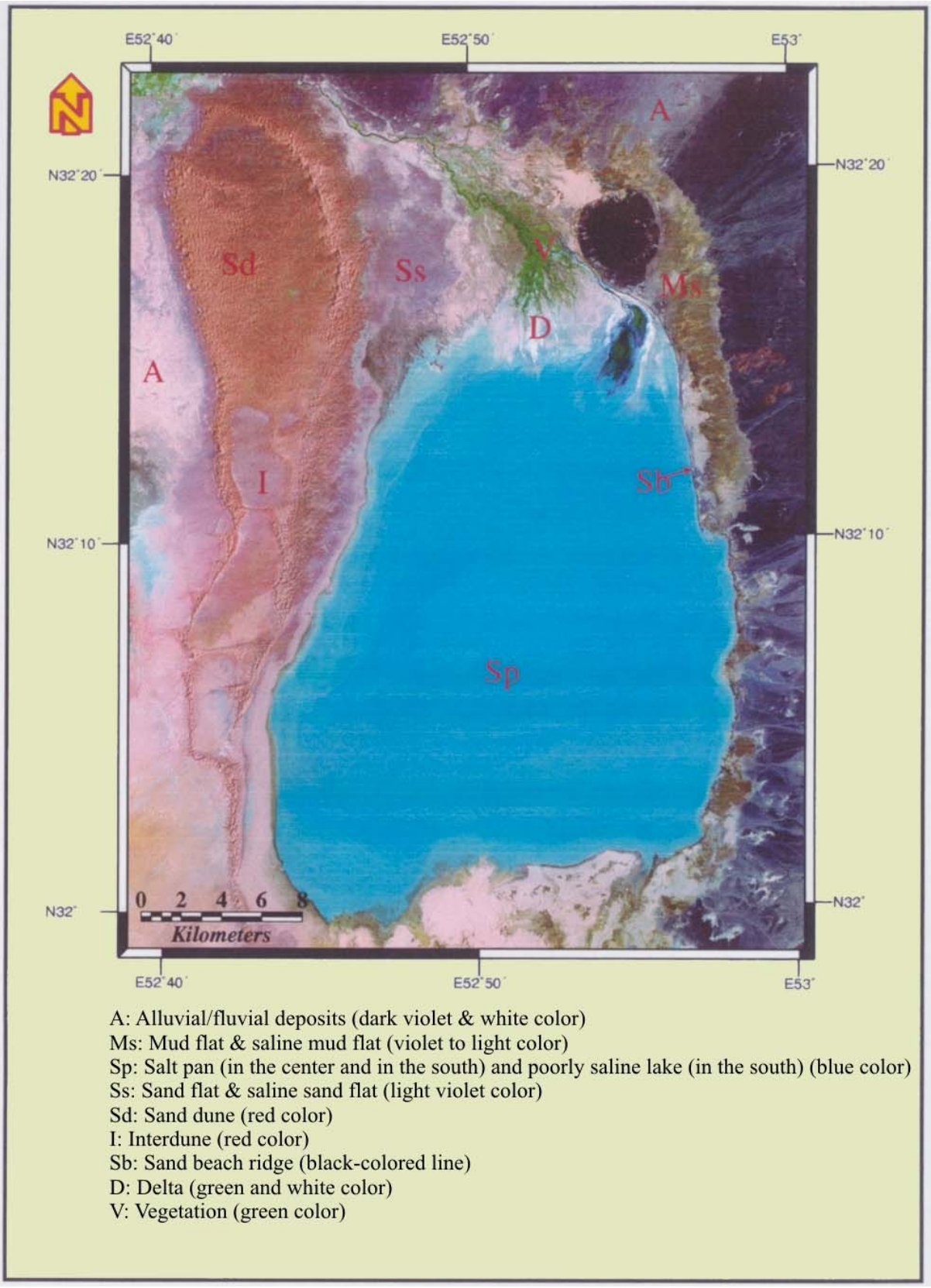

Fig. 4.2 False color-Landsat TM image showing the lowermost Zayandeh river, its lacustrine delta and evaporitic sub-environments in the Gavkhoni playa lake.

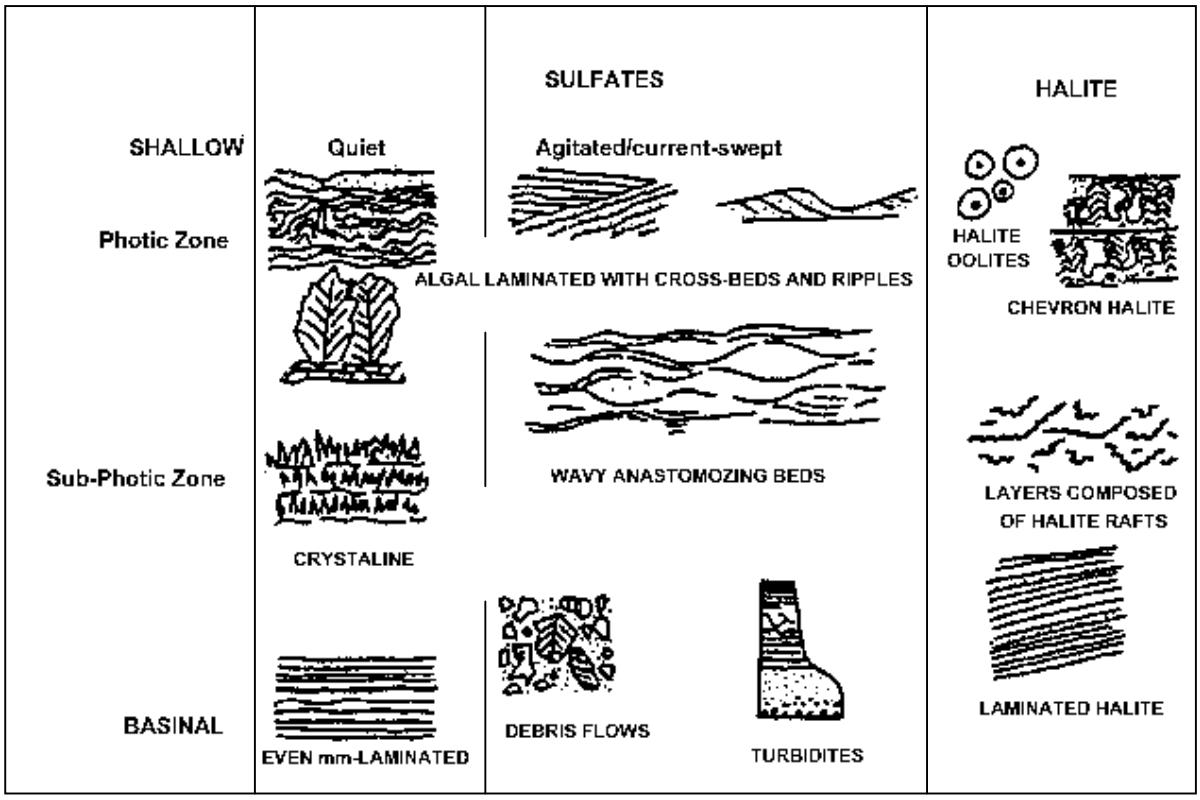

Fig. 4.3 Summary of physical environments of evaporite deposition and the main resulting sedimentary facies (after Kendall 1992, modified from Schreiber *et al.,* 1973).

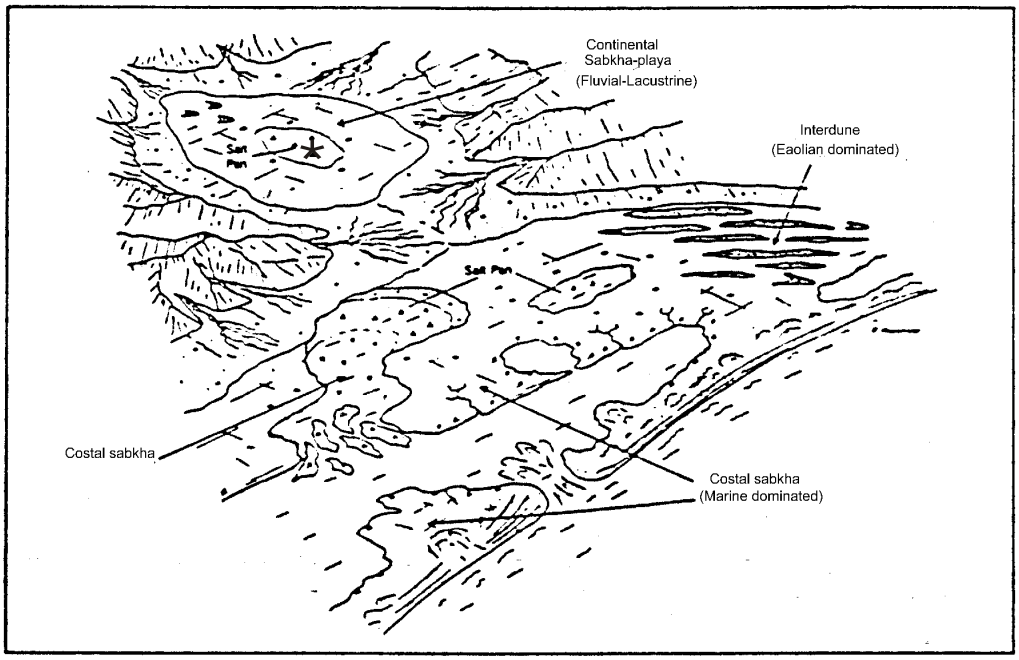

Fig. 4.4 Modern evaporite depositional environments in continental and coastal sabkha settings (after Kendall, 1992). *Gavkhoni playa lake is of that type.

4.3.2 Alluvial fans

Alluvial fan facies occurs at the base of the slopes bordering the playa lake. It grades laterally into the Varzaneh aeolian sand field to the west, and mud flat, narrow sand beach and sand flat to the north and east, and narrow sand flat, and wide mud flat to the south of the Gavkhoni playa lake. It consists of a mixture of coarse and fine clastic material that is derived from the adjacent mountains. These clastics were transported downslope by channelized flow in the upper part and dominantly by sheet flow in the lower part of the fan. Debris flows account for significant movement of sediments. The mineralogical composition of the alluvial fans in the east is dominated by igneous lithic grains, approximately similar to the northeast and the north. However, in the south and the west is mainly composed of sedimentary lithic grains (see Chapter 3 for details). Gypsum crystals are commonly found as sparsely distributed cement in the alluvial fans, especially in the western ones. They are concentrated in the surface layer and mostly are developed as fibrous and acicular to lenticular crystals. Calcite is another chemical mineral, which is present as fine–crystalline cement in this facies. Regarding development, sedimentation processes, and mineralogy, the alluvial fans will be described in detail in Chapter 5.

4.3.3 Sand dunes

Sand dunes border the Gavkhoni playa lake to the west. They grade laterally into the sand flat toward the east and alluvial fans toward the west (Fig. 4.2). The mineralogical composition of the sand grains comprises, decreasing in abundance, lithic grains (sedimentary, igneous and metamorphic lithics) and mineral grains (quartz, heavy mineral, and feldspar). Halite and gypsum crystals are also present as minor constituents. The morphology, migration, mineralogy and the source of the aeolian sands are described in detail in Chapter 3.

4.3.4 Interdune areas

Few small and large interdune areas are located between the sand dunes (Fig. 4.2). These are flat areas, where vegetation and sand dunes are nearly absent. Their surface layer consists of a very thin sand layer, weakly cemented by fine salt crystals in some localities. This layer is usually dry, soft and polygonally structured. Morphology and other characteristics of the interdune areas are also described in detail in Chapter 3.

Based on digged trenches, six facies were determined in this facies. They are aeolian sand, grey to black sandy mud, off-white sandy mud, greenish sandy mud, brown mud and sand (see Appendix F for stratigraphic logs).

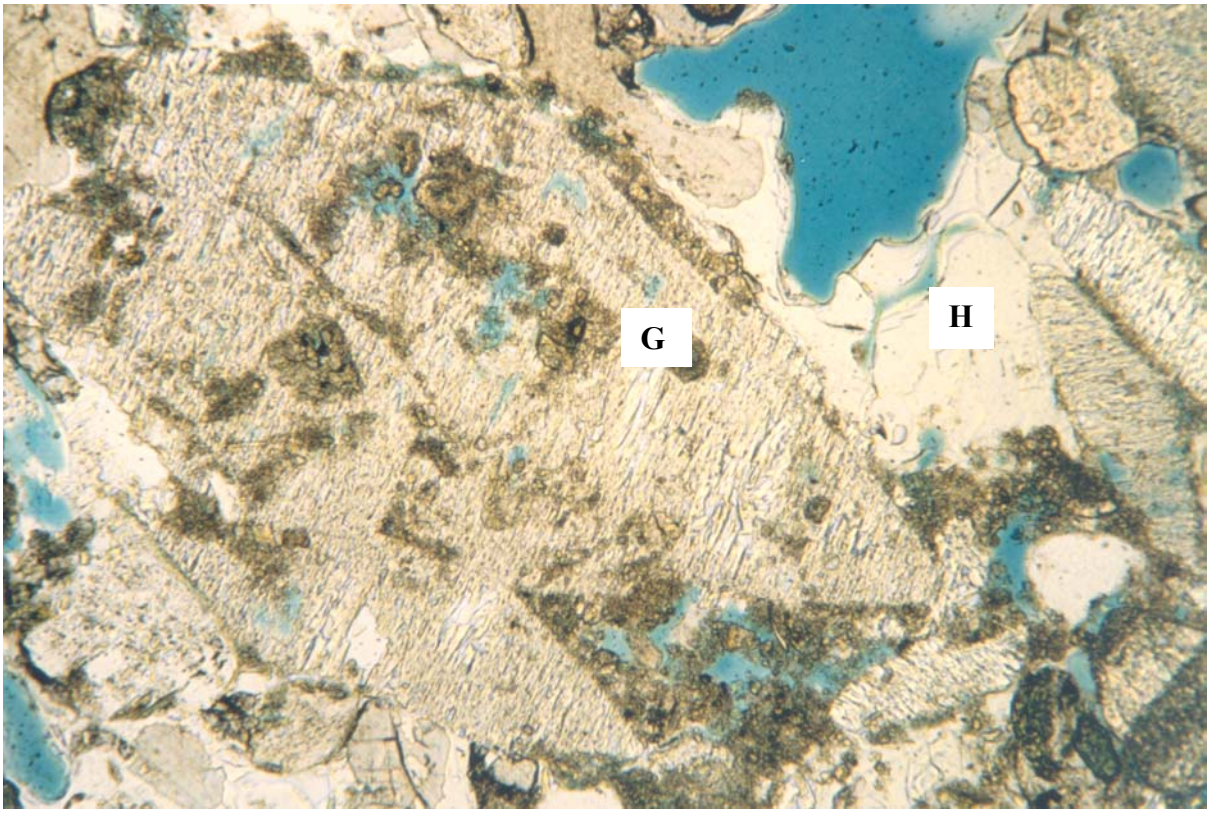

Fig. 4.5 Thin section photomicrograph showing lenticular gypsum crystals (G) and halite cement (H) from surface layer of an interdune in the Varzaneh aeolian sand field (short rim of micrograph: 0.7 mm). Photomicrograph provided by H. Kulke.

Aeolian sand

Thin-bedded fine to medium sands, tabular-shaped in geometry and with a sharp base boundary are located at the top of the interdune areas. This lithology ranges from a few to up to about 50 cm in thickness. The mineralogical composition of this sub-facies is similar to that of the sand dunes, i.e. lithic grains (sedimentary, igneous, and metamorphic) and mineral grains (quartz, feldspar and heavy mineral grains). However, it contains more gypsum and halite crystals than do the sand dunes (see Chapter 3 for mineralogical composition). Tiny halite crystals occur either as interbedded or chaotic admixture and lenticular gypsum crystals have crystallized between sand grains (Fig. 4.5).

Sample No	Facies	Location	
B1	Sand beach	32°,16′,48″N	52°,54′,14″E
B2	Sand beach	32°,10′,25″N	52°,57′,03″E
Dz1	Delta	32°,17′,12″N	52°,53′,45″E
Dz5	Delta	31°,17′,11″N	52°,53′,12″E
I1	interdune	32°,07′,09″N	52°,40′,30″E
I2	Interdune	32°,06′,26″N	52°,41′,57″E
K	Sand sheet	32°,06′,04″N	52°,43′,39″E
M1	Saline mud flat	32°,19′,10″N	52°,51′,53″E
M2	Saline mud flat	32°,18′,09″N	52°,53′,07″E
M3	Saline mud flat	32°,10′,48″N	52°,57′,56″E
R1	River	32°,16′,55″N	52°,53′,24″E
R2	River	32°,22′,54″N	52°,45′,51″E
S1	Salt pan	32°,05′,40″N	52°,45′,30″E
S2	Salt pan	32°,05′,49″N	52°,46′,57″E
S3	Salt pan	32°,06′,24″N	52°,48′,13″E
S4	Salt pan	32°,01′,33″N	52°,52′,44″E
S5	Salt pan	32°,01′,13″N	52°,48′,09″E

Table 4.1 Facies and sampling locations in the Gavkhoni playa lake and the Zayandeh river.

Grey to black sandy mud

Massive grey to black sandy mud directly underlies aeolian sands in the section No. I1 (see Fig. 4.1. and Table 4.1 for its position) and is up to 30 cm thick. It is of mixture of fine sand and black mud. The common characteristic of this sub-facies is the presence of ostracod and gastropod shells in abundance and massive bedding. In some places, gypsum crystals are scattered on the surface, where aeolian sands are absent or thin. The mineralogical composition of the sand grains is approximately similar to the of the aeolian sands. Clay minerals of this sub-facies consist of smectite, illite, kaolinite, and chlorite (Appendix B4, sheet No.17).

Off-white sandy mud

Massive off-white sandy mud with graditional borders occurs in two layers, divided by brown mud, in the section No. I1 (see Fig. 4.1. and Table 4.1 for its position). Its thickness reaches up to about 125 cm. Mineralogical composition and grain size of this sub-facies are similar to the top aeolian sand layers of this vertical section. Clay minerals and sedimentary structures are almost the same as in the dark sandy mud. There are abundant gastropod and ostracod shells in this lithotype.

Greenish sandy mud

Massive greenish fine to medium sandy mud with graditional base and top boundary occurs in two layers, divided by brown mud facies, in the section No. I2 (see Fig. 4.1 and Table 4.1 for its position) and is up to about 35 cm thick. The mineralogical composition of the sand grains is approximately similar to the aeolian sands. There are abundant ostracod and a few gastropod shells. Clay minerals determined in the mud fraction consist of smectite, illite, kaolinite, and chlorite (Appendix B4, sheet No. 19).

Brown mud

Brown to red mud with lenticular geometry occurs in the sections No. I1 and I2. The thickness of this sub-facies reaches up to 9 cm. It consists of few gastropod shells. Clay to silt ratio is high in this very fine-grained sediment. Grain size occasionally changes to sandy mud in some places. Clay minerals of this sub-facies comprise illite, kaolinite, chlorite, and smectite (Appendix B4, sheet No. 18).

Sand

Massive sandy mud with sharp top boundary forms the lowermost sub-facies in the sections No. I1 and I2 (see Fig. 4.1. and Table 4.1 for their position). It consists of mostly fine to medium sand and its mineralogical composition is similar to the uppermost layers of the aeolian sands. It contains a few gastropod and ostracod shells.

Interpretation

The properties of the sediments, black to brown color, mixture of sand and mud, presence of gypsum and halite crystals and gastropod and ostracod shells indicate which

sediments were deposited in different conditions in a shallow fresh water-brackish perennial to temporary lake and finally saline lake to sub-aerially (cf. Reineck & Singh, 1980, Benison & Goldstein, 2001). Lack of plant remains probably reflects poorly or not vegetated, semi-arid to arid conditions, high salinity of pore water and frequent flooding. Association of the sediments with gypsum in the greenish sandy mud probably reflects the evaporation of sulfate and calcium-rich pore water by capillary ascendance. A part of the gypsum crystals scattered between the aeolian sands might be derived from neighboring saline mud flats as aeolian detritus. The presence of the aeolian sands on the top of the sections keeps moisture and hinders the formation of skeletal halite at the surface. The source of the clay minerals determined in each sub-facies is most probably the same, because quantitative and qualitative characteristics of them are approximately similar. The aeolian sand layers result from wind activity in dry conditions. The sands mixed with mud are being transported by wind from the sand dunes. The fine halite crystals between aeolian sands are as a result of evaporation of brine pore water in dry periods.

4.3.5 Sand flats

Sand flats encircles the playa lake. The studied sand flat (western sand flat) extends as a wide area (about 50 km^2) in the east of the sand dunes and grades laterally to the salt pan towards the east (see Figs. 4.1 and 4.2). Mineralogical composition and texture of this part are described in chapter 3 in detail. A few small sand dunes covered by gypsiferous marl and a porous carbonate debris blanket occur in this facies (Fig. 4.6). A soft, low-relief thin efflorescence of salt crust covers its surface (Fig. 4.7). This salt crust includes a higher proportion of underlying sediment and adhesive aeolian sand and often exhibits an irregular network of puffy salt blisters. A few carbonate mounds (tufa) are found in the west of the sand dunes (2 km south of Khara) (Figs. 4.8 and 4.9).

Fig. 4.6 Field photograph indicating inactivated, subrecent individual small sand dunes, capped by gypsiferous marl, on the sand flat (8.5 km east of Khara). The elevation of hills is about 2 m. View is to the northwest.

Fig. 4.7 Field photograph showing puffy salt blisters on the sand flat, 10 km east of Khara. Geological hammer for scale is 30 cm long.

Fig. 4.8 Field photograph showing individual small tufa hills, 3 km south of Khara. Sand dunes are in the upper right part of photograph. The elevation of hills is about 2 m. Geological hammer for scale is 30 cm long. View is to the northeast.

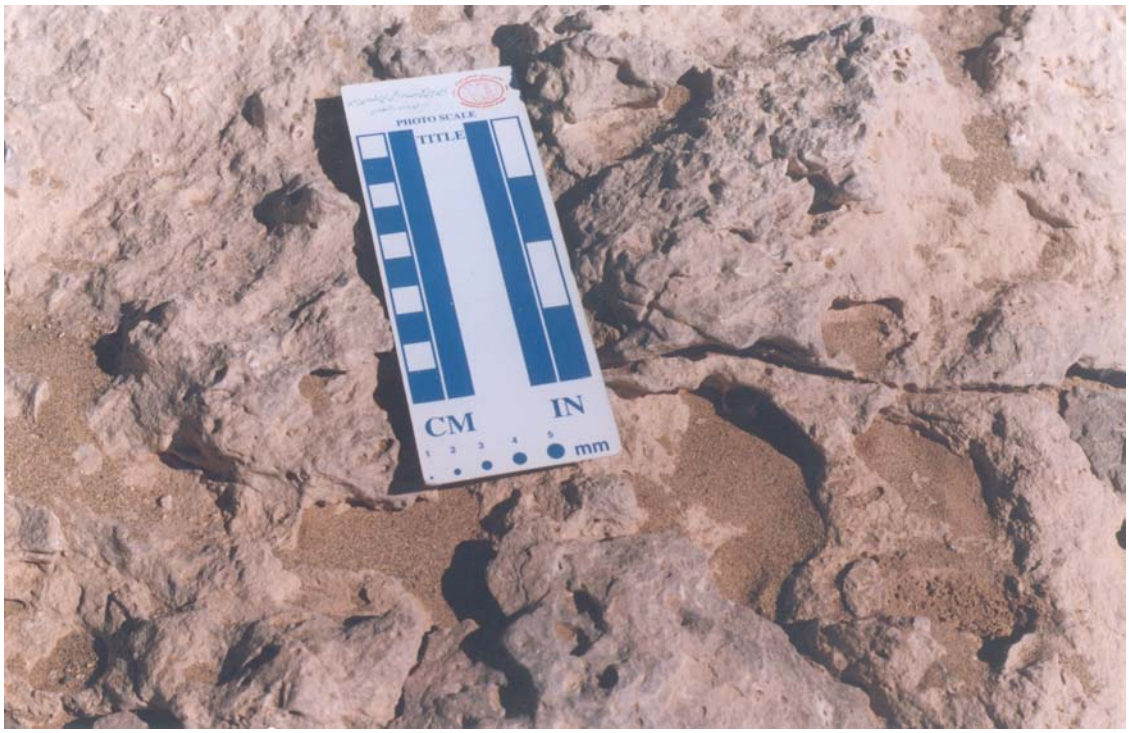

Fig. 4.9 Close-up view of photograph No. 4.8 showing hard tufa sediment.

The two types of gypsum occur in this sub-facies, acicular and zig-zag. Acicular gypsum is usually present as wavy layers, interbedded with aeolian sand layers along the western side of the sand dunes in some localities (Figs. 4.10 & 4.11). The gypsum layers are soft and friable, not more than a few centimeters thick. The zig-zag gypsum crystals are found dispersed in the marl sediments and have destroyed lamination of the sediment.

Fig. 4.10 Field photograph showing thin layers of gypsum as acicular, interbedded with the aeolian sand layers in the margin of sand dunes, 8.5 km east of Khara, 1 km north of salt mine road. Geological hammer for scale is 30 cm long. View is to the northwest.

Fig. 4.11 Close-up view of Fig 4.10 showing rippled gypsum surface layer. Photo scale is 15 cm long.

Interpretation

During desiccation periods, sand-sized clastic sediments are mostly deposited and gypsum is precipitated. The sand is transported by wind from the adjacent sand dunes and gypsum crystals formed after saturation of water (cf. Kulke, 1974). During flooding, fine-grained sediments (marl) deposited over the sand flat. Carbonate-rich springs probably built small tufa mounds and carbonate debris blanket (cf. Last, 1989). Under artesian conditions groundwater effluents may be marked by the growth of spring mounds and tufa deposits (cf. Watson, 1989 in Thomas, 1989). The flaky, thin efflorescence crust developed as the result of evaporation of saline pore water in dry periods (cf. Talbut & Allen, 1996 in Reading, 1996). Interbedded sand and gypsum layers suggest periodic flooding and desiccation and deposition of wind-blown sand.

The puffy salt blisters or pustules can be formed by two different processes, purely physical, and imitative of pre-exiting morphology. They can be produced by processes similar to those that form the polygonal ridges (crust expansion as a result of halite crystallization and thermal expansion and contraction) (cf. Warren, 1999)

4.3.6 Sand beaches

Distinct and continuos sand beach ridges occur in the east of the Zayandeh river and the Gavkhoni playa lake as a long narrow zone (Fig 4.12).

Fig. 4.12 Field photograph showing sand beach ridge in the east of the Zayandeh river delta (see Fig. 4.1 and Table 4.1 for their position). View is to the south.

They are composed of igneous, sedimentary, and metamorphic lithic grains, quartz and feldspar mineral grains. The average percentage of the igneous lithic grains (in sand fraction) is approximately 90 % in the east and 35% igneous, 53% sedimentary, and 4% metamorphic lithic grains, 6.5% quartz and 1.5 % feldspar mineral grains in the northeast (Fig. 4.13). According to the study of two pits, two lithologies were observed including gravelly sand and sand. It also contains a considerable amount of gastropod shells in the northeast of the delta (location No. B1)

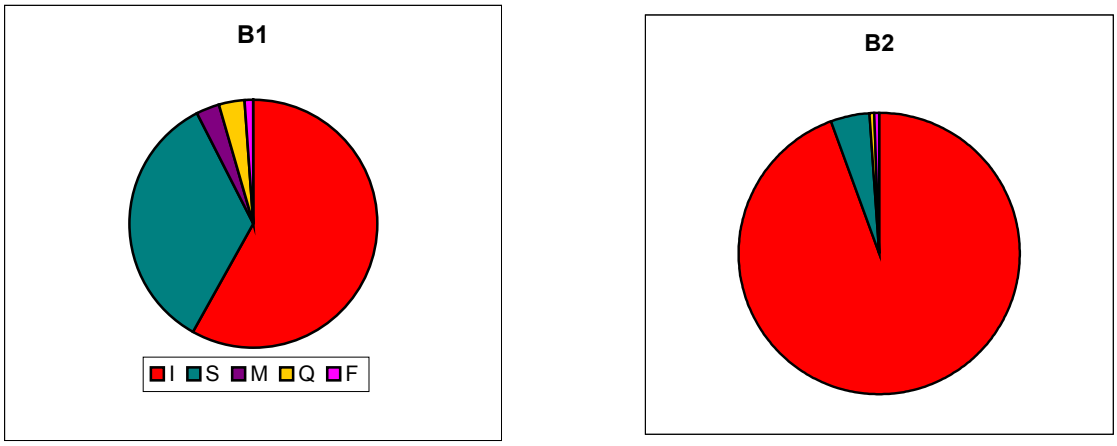

Fig. 4.13 Mineralogical composition of the sand fraction of the sand beach ridges from location No. B1 and location No. B2 (see Fig. 4.1 and Table 4.1 for their positions). Igneous (I), sedimentary (S), metamorphic (M) lithic grains, quartz (Q) and feldspar (F) mineral grains.

Gravelly sand

This lithology occurs on the top of the two studied vertical sections in the sand beach ridges. The grain size ranges from fine gravel to fine sand (mostly very coarse to coarse sand fractions) and mostly consists of igneous lithic grains in gravel size. Discoidal gypsum crystals are found with a few millimeters in diameter on the surface layer.

Sand

This sub-facies underlies graditionally the gravelly sand in the section No. B1 (see Fig. 4.1 and Table 4.1 for its position). The main grain size is fine to medium sand and

mineralogical composition is approximately similar to the gravelly sand, except that it consists of more sedimentary lithic grains.

Interpretation

The sand beach ridges usually form where the gradient of distal alluvial fan is relatively high and small streams transport coarse-grained sediments to the playa lake. They are formed by wave activity during playa lake level highstand. Distinct differences in mineral composition between the northeastern and the eastern sand beaches are related to the source of the sediments. The former originate from igneous, sedimentary and metamorphic rocks but the later mostly derive from igneous rocks. The gypsum crystals are most probably washed out from the mud flat.

4.3.7 Mud flat and saline mud flat

This sub-facies encircles the lake, except in the western part. The northern mud flat is wide, where the Zayandeh river flows into the playa lake (see Figs. 4.2 & 4.27). They are deposited mainly by sheet floods and then altered by wetting and drying. Groundwater table measurements during more than two years indicates that fluctuations are not considerable (maximum 53 cm in the section No. M1 and 41 cm in the section No. M2) (Fig. 4.14) (see Fig. 4.1 and Table 4.1 for their position).

It is characterized by polygonal mud cracks, plant roots and root casts and is not saturated by brine. The polygonal desiccation is fairly common and cracks measure up to a few centimeters across (Fig. 4.15). Calcite is found as consolidated fine mud and is dominant in the southern and the northern mud flat, where ephemeral Rahimi river and the permanent Zayandeh river enter the playa lake (see Chapter 2 for their positions). The mud flats are sites of sedimentation of silt and clay.

Saline mud flats occur between the dominant clastic environment (dry mudflat) and the evaporite-dominated environment (salt pan). In contrast to the mud flat, all depositional sedimentary structures have been destroyed in the saline mud flat. It is characterized by precipitation and preservation of evaporite minerals within the detrital sediments, including chiefly chaotic mixtures of mud, halite and gypsum.

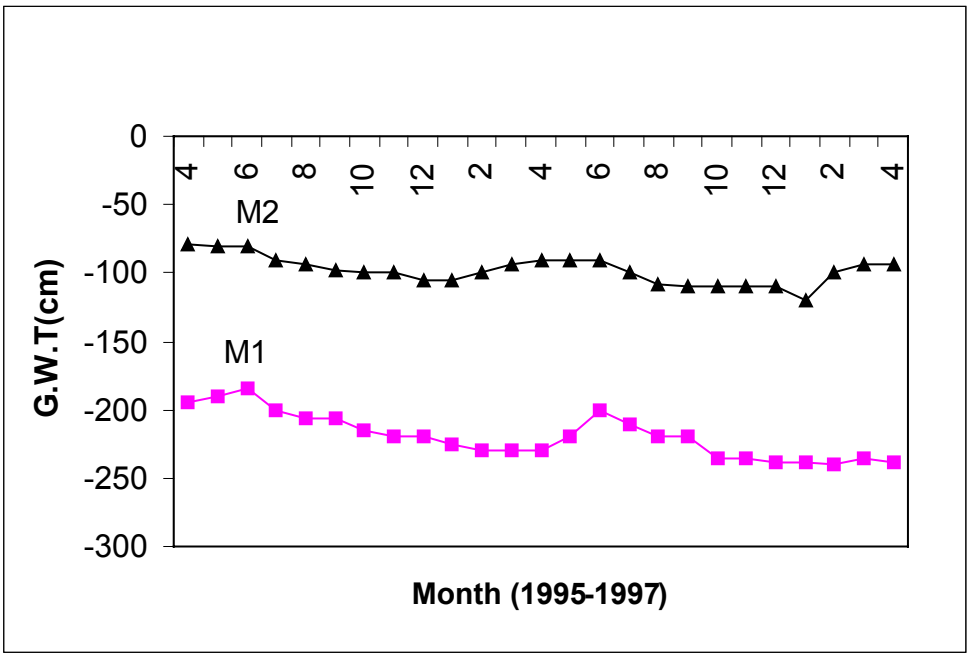

Fig. 4.14 Fluctuation of groundwater table (in cm below surface) in the saline mud flat/mud flat measured during two years (1995-97). Locations No. M1 and No. M2 (see Fig. 4.2 and Table 4.1 for their position).

Fig. 4.15 Field photograph showing small mud cracks on the mud flat, southwest of Kuh-e-Siah, near section No. Dz1 (see Fig. 4.1 and Table 4.1 for its position). Camera cap for scale is 6 cm in diameter.

A common feature of the saline mud flat is its hard and porous surface pitted by small holes which are a few centimeters wide and deep (Fig. 4.16). Displacive halite is the major chemical mineral in the saline mud flat, which forms a surface layer up to 30 cm thick. The individual halite crystals (up to few mm in diameter) show a skeletal and dendritic or pagoda form. They are found down to a few decimeters below the surface of present day's saline mud flat. Displacive gypsum is the second common mineral. Generally, gypsum is mostly found as translucent lenticular and zig-zag (twin) and acicular crystals within the mud matrix. These two minerals are found in abundance in the eastern saline mud flat. On the basis of five digged trenches and pits, five major distinctive sub-facies can be differentiated in the saline mud flat and mud flat, i.e. salt, gypsiferous mud, muddy sand, mud and sand (see Appendix F for stratigraphic sections).

Fig. 4.16 Field photograph showing hard terrain with small holes in the saline mud flat located in the northern part of the Gavkhoni playa lake (around section No. M2) (see Fig 4.1 and Table 4.1 for its position). Camera cap for scale is 6 cm in diameter.

Salt

This lithology is the uppermost one in the saline mud flat. It mostly consists of skeletal salt in the lower part and a mixture of salt and mud in the upper part (about 10 cm). Its thickness reaches up to 30 cm and is dry, hard and porous in dry seasons. The major clay minerals in mud fraction consist of illite, kaolinite, chlorite and minor smectite (Appendix B4, sheet No. 20).

Gypsiferous mud

Massive gypsiferous mud is mainly developed in the eastern saline mud flat (see Figs. 4.1 & 4.2 for position of saline mud layer). When the groundwater table is high (a few centimeters in depth) its surface is usually moist and soft whereas in dry periods the surface is dry and hard. A large number of discoidal gypsum crystals (up to 3 cm in diameter) are scattered in the sediment.

Muddy sand

Massive muddy sand occurs in the section No. M1 (see Fig. 4.1 and Table 4.1 for its position) and is divided in an upper and a lower part. It consists of mostly fine sand-sized fraction. Its mineralogical composition, comprises, decreasing in abundance, igneous, sedimentary and metamorphic lithic grains, quartz and feldspar mineral grains (Fig. 4.17). Abundant gastropod and ostracod shells are present in this lithotype.

Mud

This lithology is exposed in the section No. M2 (see Fig. 4.1 and Table 4.1 for its position). There is no evidence of the presence of bedding and plant remains in this lithology. Clay minerals of this sub-facies consist of illite, smectite, chlorite, and kaolinite (Appendix B4, sheet No. 21).

Sand

Massive fine to medium sand forms the lowermost lithology in the section No. M1 (see Fig. 4.1 and Table 4.1 for their position). Its mineralogical composition is similar to the muddy sand (Fig. 4.17). There are a large number of gastropod and ostracod shells similar to muddy sand in this lithotype. It also occurs as lenticular thin layers between mud layers.

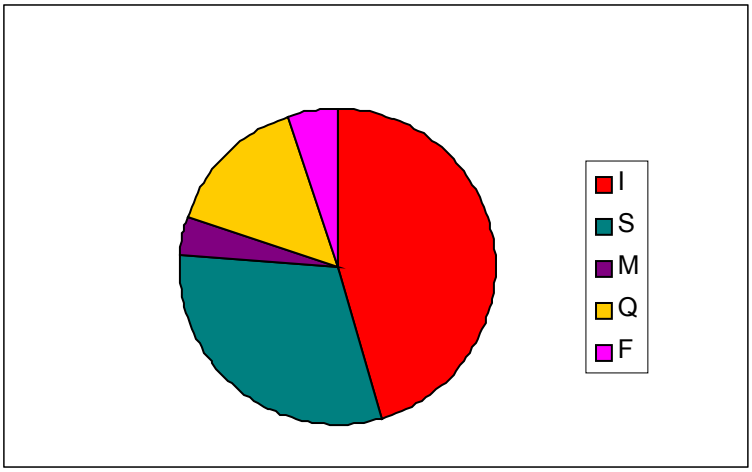

Fig. 4.17 Mineralogical composition of sand fraction in the lowermost lithology of saline mud flat in the section No. M1 (see Fig. 4.1 and Table 4.1 for its position). Igneous (I), sedimentary (S), metamorphic (M), lithic grains, quartz (Q) and feldspar (F) mineral grains.

Interpretation

The porous hard crust in the saline mud flat results from evaporation of capillary brines and pore water. Saline water moves upwards by capillarity and skeletal halite crystal (up to a few mm in diameter) form at the surface. They are a result of maintaining high moisture content in the mud flats and sand flats during the dry season. The skeletal halite is thought to grow by capillary evaporation of supersaturated pore waters in soft brine-soaked mudflat or sabkha sediments (cf. Warren, 1999). The origin of the holes may result from differential rising of the ground, caused by intersedimentary growth of salt crystals. This halite layer greatly hinders further evaporation from the underlying sediment (cf. Handford, 1982).

Lenticular gypsum crystals (up to 3 cm in diameter) occur in a seasonally vadose setting. They tend to form in the upper parts of the vadose zone of the brine pan fill where clear parallel-sided prisms are subjected to periodic dissolution and regeneration (Warren, 1999). During very early diagenesis, displacive lenticular gypsum develops within the mud matrix. They form in the Howz-e-Soltan playa lake (about 260 km northeast of Esfahan) by precipitation from pore water along the bottom of ponds in which there is dissolved organic material, particularly humid acid (Fayazi, 1991).

The scattered sand-sized sediments admixtured within some muddy layers might be interpreted as contemporaneous deposition of mud and sand by a flow with insignificant change in velocities (cf. Amini, 1997). The muddy sediments of this sequence reflect rapid deposition on a lower flood plain during wet, shortly after sheet floods (cf. Benison & Goldstein, 2001). The presence of the sand layers most probably represents deposition in the bottom of small and shallow distributary channels during upper flow regime periods.

4.3.8 Salt flat (Salt pan)

Sediments deposited in the Gavkhoni playa lake change laterally from dominantly siliciclastic (sand flat and mud flat) to dominantly evaporitic facies (salt pan). The later covers the center of the Gavkhoni playa lake as a crust that crystallized in highly saline ponds by efflorescence. It is located in the lowest area of the Gavkhoni closed basin and occupies most of the playa surface. The salt pan in turns grades outward to the mudflat or immediately to the sand flat. It is surrounded by a saline-soaked mudflat to the east and saline sand flat to the west.

The two drilled cores, up to 30 m (sections No. S4 & S5) provided by Nabian *et al*. (1991) and three shallow pits dug (see Fig. 4.1 and Table. 4.1 for their positions), record evaporitic and siliciclastic lithologies. These lithologies range from a few centimeters to up to 12 m thick. They include salt, black mud, sand, gypsiferous marl, and yellow/brown mud (see Appendix F for stratigraphic logs). Among these lithofacies only the first three ones are described in detail, because there is no sufficient data about the other facies.

Salt

This sub-facies covers the center of the playa lake as a crust, ranging from a few centimeters in thickness in the north to up to 150 cm in the south**.** Its color is usually clear and white, but black, pink and green colors also occur in some places. The surface layer consists of a mixture of mostly halite and a few sand-sized grains. The average value of the detrital sediments around the salt mine is about 3%. The most common sedimentological feature of this lithology is a polygonal halite crust (Fig. 4.18). The individual polygons usually measure up to 100 cm across. Efflorescent halite ridges popcorns (cauliflower) and hairy efflorescent surface halites are other features on the salt pan (Figs. 4.19 & 4.20). The popcorns commonly form nodular aggregates up to few cm across. The hairy efflorescent

surface halite is typically finely crystalline and has a very porous texture. Some of them also have delicate needle-like hairs of halite covering their surface.

The polygonal crust can be grouped into two categories; high relief (a few decimeters high) and low relief (a few centimeters high). The former is modified by efflorescence and occurs mostly in the southern area where the water table is high and the salt pan is susceptible to flooding after sporadic heavy rainfall. The two types of high-relief thick salt crusts have been distinguished, polygonal crusts and blocky crusts. The former is a pattern of ridges that are polygonal on their surface. The later is high-relief polygonal, thick, and saucer-shaped slabs of salt and possesses a rough blocky morphology. The small stalactites of halite are common on the undersides of the overhanging slab edges in the central part of the salt pan (1.5 km from western border of the Gavkhoni playa lake, around the Jarghoieh salt mine). The low relief salt crust is the most widespread crust type with regular and flat surface.

Fig. 4.18 Field photograph showing polygonal halite crusts, pressure ridges and spongy efflorescences at the surface of cracks, about 1.5 km from the western border of the playa lake. Form of polygons is disturbed by nearby gravel road to salt mine. Photograph, taken on 17.11.95, provided by H. Kulke. The Varzaneh aeolian sand field is in the background of photograph. View is to the northwest.

They exhibit a polygonal ridge pattern, but the polygons generally have smaller diameters than high-relief polygonals. This feature is usually widespread in the northern part of the salt pan.

Fig. 4.19 Pop-corn or cauliflower efflorescence formed on the salt pan, 1.5 km from the western border of the Gavkhoni playa lake, northern part of the Jarghoieh salt mine road. A pressure ridge in its early stage of development runs across the picture. Photograph, taken on 17.11.95, provided by H. Kulke. The small knife for scale is 8 cm long.

There are thin layers of dark mud interbedded with crystalline halite layers. The thickest mud layer is observed on the southern margin of the salt pan in close proximity to a major detrital sediment source. In contrast, the crystalline halite layers without intermittent mud layers are observed in the central portion of the salt pan.

Brine–saturated clastic sediments underlay the salt crust. The brine level (groundwater) slightly fluctuates during dry and wet seasons, ranging between –20 to +5 centimeters (Fig. 4.21).

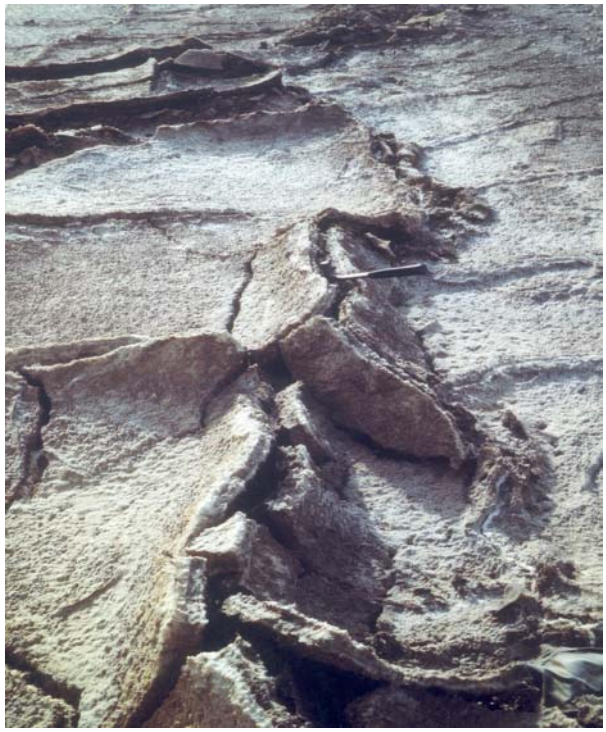

Fig. 4.20 Detail of well-developed pressure ridges near the Jarghoieh salt mine. Photograph, taken on 24.4.99, provided by H. Kulke. Geological hammer for scale is 30 cm long.

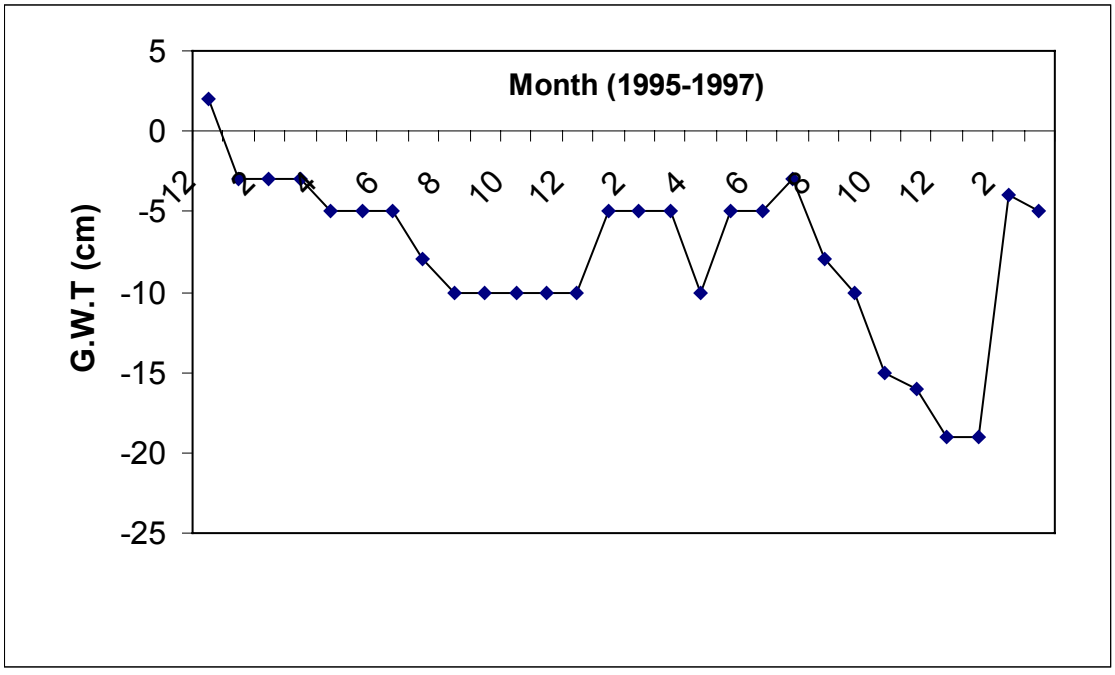

Fig. 4.21 Fluctuation of groundwater table measured in a trench (location No. S1) in the salt pan during more than two years (1995-97) (see Fig. 4.1 and Table 4.1 for its position).

Fig. 4.22 Close-up view of halite crystals from the salt crust in west-central part of salt pan. Standard scale is in cm in the left.

The voids of the salt crust and the clastic layers are filled with halite crystals and/or by saturated brine. The main evaporite mineral determined by XRD in the salt pan is halite, but other minerals including carnallite ($MgCl_2.KCl.6H_2O$), bischofite ($MgCl_2.6H_2O$) and tachyhydrite ($CaCl_2.2MgCl_2.12H_2O$) are also present locally as minor according to XRD evidence (Appendix B4, sheets No. 23 & 24). Halite crystallizes in hopper, cubic and massive form. The size of halite crystals reaches up to 2 cm (Fig. 4.22).

Black mud

Black mud underlies the salt crust in the section No. S1-S3. It also is observed as interlayering in the uppermost lithology (salt) in drilled cores in the sections No. S4 and S5 with up to 5 cm in thickness (see Fig. 4.1 and Table 4.1 for their position). Its thickness reaches up to a few centimeters in the playa lake center. The ratio of clay to silt is high (about 80% clay fraction). Clay minerals of this facies (in section No. S1) consist of illite, kaolinite, chlorite, and smectite (Appendix B3, sheet No. 22). Halite as hoppers and cubes and gypsum as acicular and discoidal crystals are scattered throughout the grey mud. The size of halite and gypsum crystals is up to 2 cm. A few gastropod and ostracod shells are present in the sediments.

Sand

nstratified well-sorted fine to medium sands underlay the above mentioned lithology in the section No. S1-S3 and occur in the drilled cores No. S4 and S5 (see Fig. 4.1 and Table 4.1 for their position). The sand grains are mostly composed of sedimentary, igneous lithic and feldspar and quartz grains (Fig. 4.23). Halite hopper and discoidal gypsum crystals are scattered between the sand grains. It also contains a few gastropod and ostracod shells.

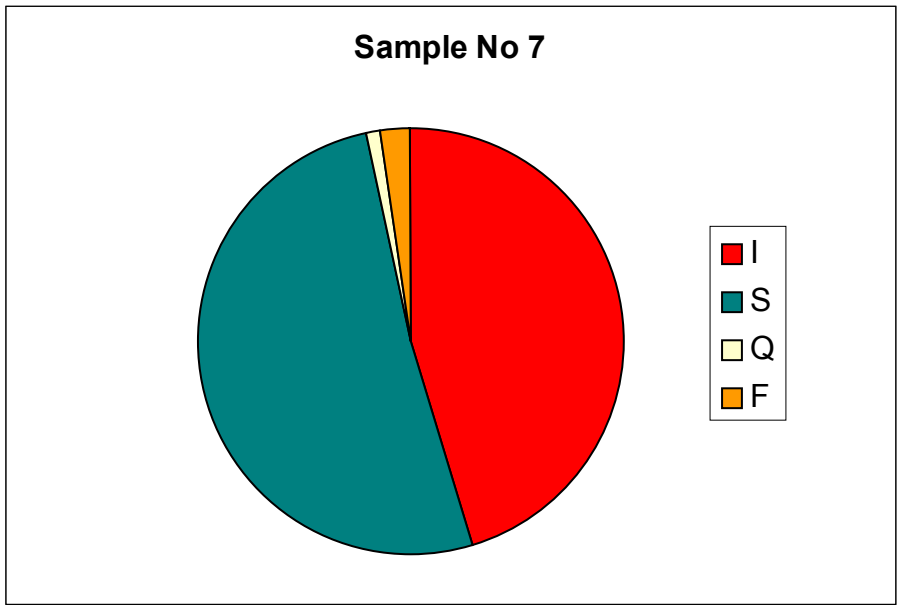

Fig. 4.23 Distribution of the various types of lithics and mineral grains of the sand sub-facies in the section No. S1 in the salt pan (see Fig. 4.1 and Table 4.1 for its position). Igneous (I), sedimentary (S), metamorphic (M) lithic grains, quartz (Q) and feldspar (F) mineral grains.

Greenish gypsiferous marl

Greenish gypsiferous marl directly overlies brown mud in the drilled core No. S4 (see Fig. 4.1 and Table 4.1 for its position). The thickness of this sub-facies is about 2 m.

Yellow to brown mud

This lithology is recognizable in the drill cores No. S4 and S5 and is divided in an upper and a lower part in drilled core No. S1 (see Fig. 4.1 and Table 4.1 for their positions). The upper one underlies immediately gypsiferous marl and the lower one is the lowermost lithology in these cores. This sub-facies ranges from 4 to more than 12 m in thickness.

Interpretation

The formation of the salt pan is as a result of three stages: flooding, evaporation and desiccation (Fig. 4.24). After flooding, when the shallow ephemeral lake becomes concentrated by evaporation, the formation of salt pan starts (cf. Lowenstein & Hardie, 1985, Benison & Goldstein 2001). In the NaCl-rich system of this lake, continuous evaporation concentrates the brines until they get saturated with halite. Crystallization starts at the brine surface as small plates and hopper crystals, which sink to the bottom. The individual floating crystals are cemented together where they touch to form rafts (Fig. 4.25).

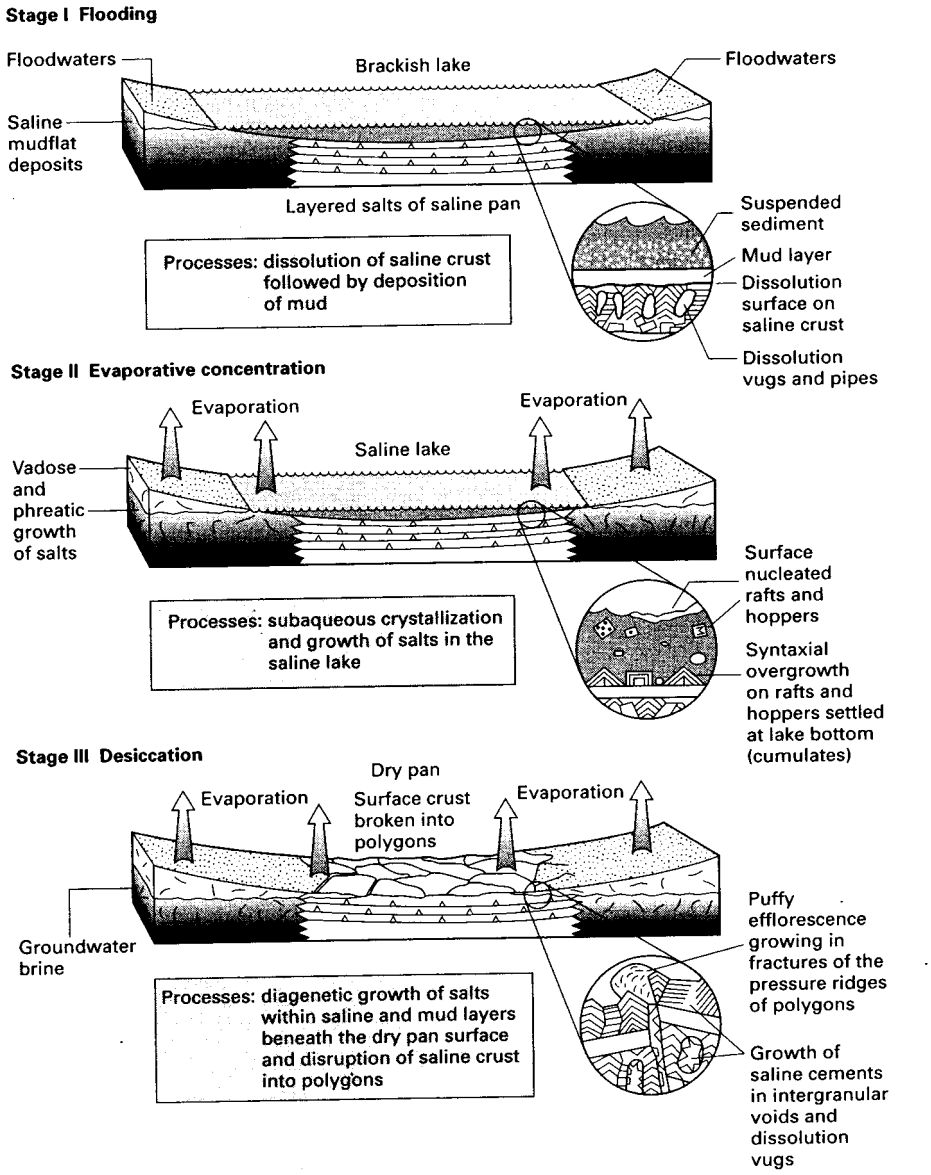

Fig. 4.24 A summary of the basic elements of the saline salt pan cycle from intramontane/ playa) (after Lowenstein & Hardie, 1985).

When surface tension is disturbed, the crystals fall to the bottom, forming an accumulation of individual halite crystals and broken rafts on the brine pool floor (cf. Hovorka, 1987, Handford, 1982) (Fig. 4.25). These serve as nuclei for further growth and widespread syntaxial overgrowth that takes place on the lake floor, ultimately resulting in the development of salt crystals and surface salt crust (cf. Lowenstein & Hardie 1985) (Fig. 4.26). In most cases, rapid evaporation does not allow halite to form as a cubic crystal at the surface of the salt crust, although in other environments hopper-shaped crystals generally record rapid growth rate (Fayazi, 1991).

Fig. 4.25 Field photograph showing raft crystals of halite floating on the top of a brine pool within the salt pan. Length of pen is 15 cm. Photograph, taken on 24.4.1999, provided by H. Kulke.

When the salt surface is exposed, the halite layers become buckled, break into a polygonal crust, and tepee structures are formed. The buckling was caused by a net volume increase due to expansion during crystallization. The continued growth of the halite crystals just beneath the dry surface of the pan causes the lateral expansion of the surface crust, and leads to disruption of the crust into large polygons rimmed, by pressure ridges that override each other like tectonic thrusts (see Fig. 4.20) (cf. Lugli *et al.*, 1999). Pumping of subsurface

brine and subsequent evaporation along the cracks between the polygons leads to precipitation of a spongy efflorescent halite (cf. Lowenstein & Hardie, 1985).

The polygonal pattern might be understood as a result of fracturing by volume reduction caused by either thermal contraction or desiccation (cf. Warren, 1999). The high-relief polygonal salt crusts were allowed to develop uninterruptedly for a number of years and eventually produced a high–relief blocky surface (cf. Eugster & Hardie, 1978).

The hairy efflorescent surface halite leaned in a downwind direction, suggest that its formation is related to the desiccating action of the wind. The wind assists in the process by drawing out surface films of brine from the crust, so forming small protuberances of efflorescent halite. Brine is continually blown to the end of the hair-like projections where it evaporates, precipitating halite and so lengthening the hairs (cf. Warren, 1999).

During spring, minor meteoric floodwaters (rainstorm runoff and snow meltwater) cover the saline pan and form a temporary shallow brackish lake. The depth of this lake is usually no more than a few tens of centimeters. The occurrence of minor flooding is much more common on saline pans than major flooding, and can create a temporarily undersaturated the saline lake without deposition of a detrital mud layer in the lake center. Repetition of such flooding can result in a sequence of partly dissolved halite crusts without detrital mud drapes in between. During a major storm flooding stage when muddy floodwaters inundate the pan, mud layers presumably are deposited in the shallow ephemeral lake. This results the formation of alternating layers of halite and mud. The presence of the hopper halite within the mud matrix results from fluctuations of brine during the wet and dry period (Figs. 4.24 & 4.26) (cf. Lowenstein & Hardie 1985; Handford, 1982)

Pink to light red color of the halite is due to impregnation by traces of iron oxides between the halite crystals (cf. Hovorka, 1987). The presence of microorganisms such as the flagellate *Dunaliella salina* can result in a striking pink coloration (cf. Watson, 1989 in Thomas, 1989). The black to greenish color of halite especially in the surface layer results from impurities of fine-grained detrital sediments.

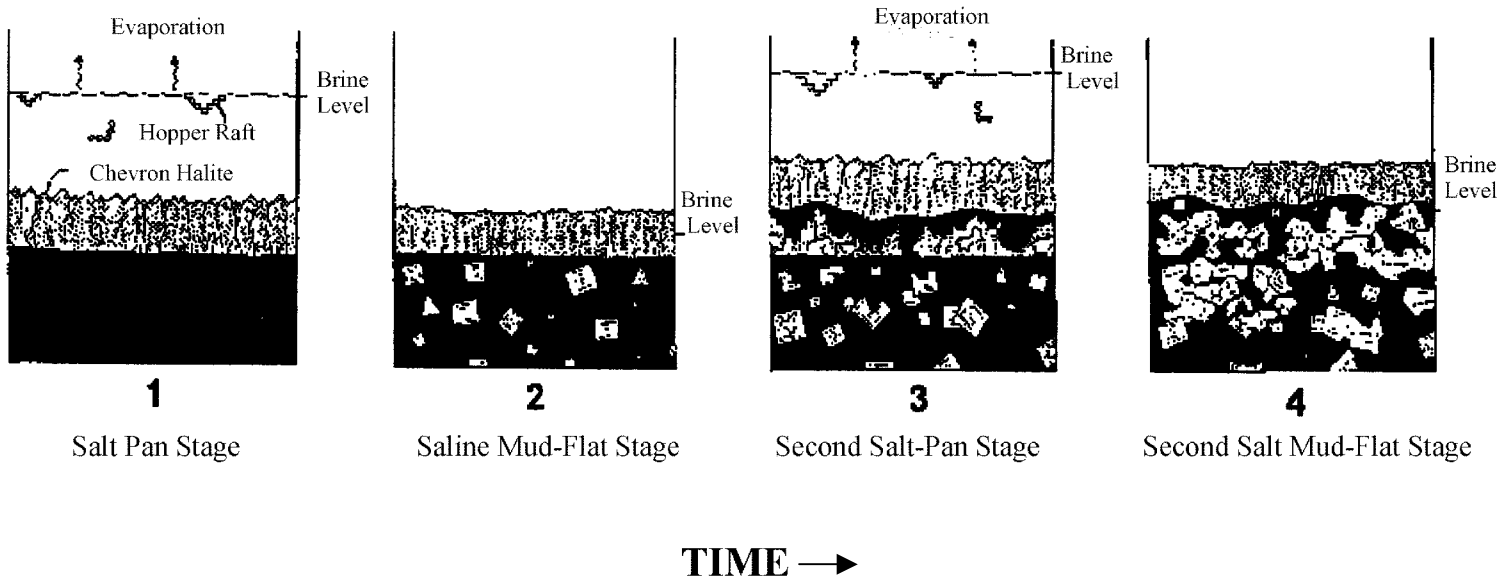

Fig. 4.26 Possible genesis of the hopper crystals within the mud sediments during four stages in a salt pan (after Handford, 1982). Stage1: Primary halite precipitate in shallow brine. Stage2: Brine level lowers and halite nucleation move down into mud sediment. Stage 3: Reflooding of salt pan, underlying halite is dissolved and mud deposited before reaching supersaturation. With evaporation, halite precipitates in salt pan brine. Stage4: Brine level drops and leads to precipitation of secondary halite and displacive halite hoppers in underlying sediment.

Clay–sized sediments are transported in two ways: 1-Clay in fresh water is suspended and can be transported over wide areas before it flocculates and slowly fall to the bottom. Floodwaters move only clay-sized material out from the shoreline; silt is deposited in deltas near the shore. 2-Aeolian dust storms are an alternative mechanism for transporting silt and clay sized material for long distances (Hovorka, 1987).

The fine to medium sand sediment intermixtured with salt crystals is derived from aeolian sands in the west of the playa lake. The sand–sized intercalations (e.g. in section No. S4) in the salt pan sediments capped by mud most likely reflect a rapid deposition of sand during thunderstorms in a shallow temporary lake or also directly as bottom load from the Zayandeh river delta. The upward change in turn from sand, black mud into the salt unit marks the transition from a sand flat, mud-dominated playa to a salt pan.

The yellow to brown mud is probably deposited in a shallow fresh water-brackish perennial lake or flood sheets in a semi-arid to arid climate (cf. Talbut & Allen, 1996 in Reading, 1996; Benison & Goldstein, 2001). The lack of plant roots in the mud flat reflects that the playa lake was poorly or not vegetated. This is indicative of high salinity of the pore water and frequent flooding.

4.3.9 The Zayandeh river delta

This deltaic environment occupies about 30 km^2 of end reach of the Zayandeh river. It gradually grades into the poorly saline lake in the south, the sand flat in the west and the sand beach ridge and the mud flat to the east of the lake (Fig. 4.27). This is an extremely shallow delta since the playa lake, into which it progrades, is a very flat and shallow geomorphic feature. Some shallow distributary channels cut up the delta into separate small islands and drain water into the Gavkhoni playa. In the immediate proximity of these channels, small ridges (point bar and levee) similar to flood plain of river banks were formed. In the development of the delta, individual branches gradually become shallower. In wet seasons vegetation develop in the small islands and distributary channels banks of the delta (see Chapter 2.7 & 2.8). The sediments are made up of alternating of sandy and muddy facies in studied trenches and have different origin and composition (see Table 4.1 for position of trenches).

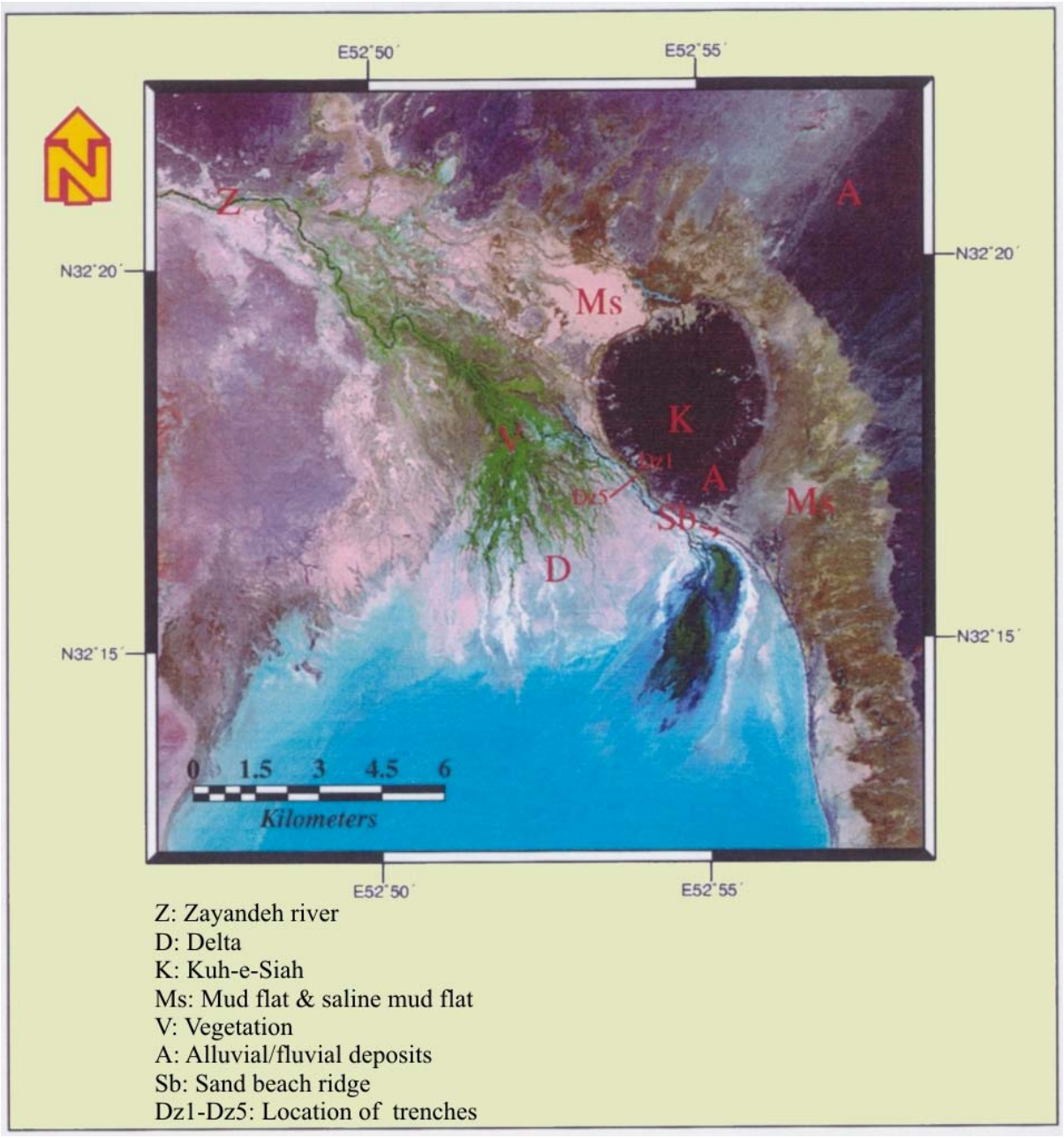

Fig. 4.27 False color-Landsat TM image showing delta and distributary channels of the Zayandeh river

They are gray to black mud, yellow to brown mud and sand. Lithology and sedimentary structures of the sections Dz1-Dz5 (see Fig. 4.1 and Table 4.1 for position of trenches) is approximately the same. Therefore, the stratigraphic sections of Dz1 and Dz5 were drawn (see Appendix F).

Grey to black mud

Gray to black massive mud, interbedded with lenticular thin sand layers, forms the uppermost lithology with sharp boundary at base in the Zayandeh river delta. Its thickness reaches up to a few centimeters. This sub-facies contains abundant vegetation, root traces, plant roots and gastropod and ostracod shells. They are found as a homogenous mixture of clay and silt with a high degree of bioturbation. The surface layer shows extensive mud cracks and algal mats (see Fig. 4.15).

Yellow to brown mud

Massive brown to yellow mud underlies the grey to black mud in the five studied vertical sections with graditional boundary at the base and top. It contains a high ratio of clay to silt. The thickness of this lithology reaches up to 85 cm. Clay minerals of this sub-facies are composed of kaolinite, illite, chlorite, and smectite (Appendix B4, sheets No. 15 & 16).

Sand

Massive fine to medium sand forms the lowermost layers in the section No. Dz5 with graditional top and base boundary. Its mineralogical composition is 45% igneous, 31% sedimentary, and 4% metamorphic lithic grains, 14% quartz and 6 % feldspar mineral grains, approximately similar to the lowermost layers in the section No. M1 (see Fig. 4.1 and Table 4.1 for its position) in saline mud flat (see Fig. 4.17). It also contains a large number of gastropod and ostracod shells.

Interpretation

The presence of the sand represents deposition in the bottom of the distributary channels during periods of stronger flow, while silt and clay are well developed on the upper parts of the point bars, swamp and levees during floods. Change of sediments both in horizontal and vertical directions is as a result of frequent shifting and migration of the channel branches. The most important factor for development of this delta is that the Zayandeh river ends in a shallow standing body of water.

Organic matter is well preserved in the greenish to black mud layer because reducing conditions occur almost immediately below the surface in this poorly drained environment. The brown mud is probably deposited in a shallow fresh water–brackish perennial lake or flood sheets in a semi–arid to arid climate (cf. Talbut & Allen, 1996 in Reading 1996; Benison & Goldstein, 2001). The lack of plant roots in the brown mud facies reflects that this depositional environment was poorly or not vegetated. The above mentioned high degree of bioturbation of mud sediments is caused by plant roots.

4.4 History and evolution of the lower reaches of the playa lake study basin

A developed system of flood-plain terraces, a rather deep morphology of valleys in the Zayandeh river and other streams (especially in the southwest of the study area), exposure of lacustrine sediments (marl) marginal to sedimentary mountains (about 100 m above the base level of the study area), cyclic sedimentation of gravel and marl in the proximal of the alluvial fans (see Chapter 5 for details) and sand and mud in the Gavkhoni playa lake indicate a repeated rise and drop of water level of the Gavkhoni playa lake in the Quaternary period. This is most probably a result of three main factors: Neotectonic movements of the High Zagros belt (southeast of the study area), subsidence of the base level of erosion (Gavkhoni playa lake) and climatic changes in the drainage basin of the Zayandeh river.

The folded and thrusted High Zagros belt, trending NNE-SSW, results from tectonic pressure, continental convergence and collision. Horizontal and vertical movements in this belt is estimated at 3.5 to 4.7 cm and more than 2 mm respectively in each year in Quaternary (Haghipour, 1983). Uplifting in the upper reaches of the rivers (specially the Zayandeh river) is connected with an increase of gradient of the longitudinal profile in the upstream reaches, resulted in increased intensity of bed erosion and deep incision of river valleys.

The Gavkhoni playa lake formed in a supposed graben and/or half graben system in response to crustal spreading along the northeastern part of the Sanandaj-Sirjan zone. This system is a result of orogenic movements and caused volcanic eruptions at the end of Cretaceous and early Eocene, and faulting which took place after the volcanism (see Chapter 2 for details). Subsidence of this base level of erosion (Gavkhoni playa lake) is most probably

due to continuing tectonic activity in Quaternary period. This probably is a major factor which is responsible for accumulation and erosion (lateral and vertical) in the drainage basin.

Changing climatic conditions took place in the Quaternary period when the vast areas of the northern hemisphere were frequently covered with thick glaciers, melting of glaciers increased the amount of water in the rivers and activated their work (Yakushova, 1986). It is supposed that this phenomenon played the most important role in relation to changing water level in the lower reaches of the study area, rise and fall in denudation and spatial distribution of Quaternary deposits in the Zayandeh river drainage basin.

To interpret the history and evolution of the lake, it may be insufficient to present a model only based on a few digged trenches. However, combined with investigation of two drill cores (up to 30 m deep) and geological cross sections (provided by NIOC), deep wells (provided by Iranian Water Organization) (see Chapters 2 & 5 for details), the late Quaternary to recent sedimentation episodes can be described to some extent in this basin. Based on these field data, a depositional model for the Gavkhoni playa lake is suggested in Figs 4. 28 & 4.29.

The material, filling the playa basin, results from a complex interplay of evaporation, precipitation, quantity and chemistry of groundwater inflow and surface runoff, and drainage basin characteristics, e.g. clastic input. The stratigraphic sequence generally indicates considerable differences in depositional and hydrological conditions and changes in water chemistry in the Gavkhoni playa lake both in time and geographic position. The deposition of intermittent sand and mud (sand flat and mud flat facies) suggest that the basin was influenced repeatedly by periods of wet and dry climate. During long wet periods it has been a shallow permanent lake possibly without considerable change in water table, resulting in deposition of fine-grained sediments in the basin. The sand-grained deposits most likely derived from aeolian sands during dry periods at the margin of the sand dunes, but also directly as bottom load from the Zayandeh river delta. With increasing aridity, the middle part of the lake gradually became shallower, resulting in a saline lake and the salt pan. The salt pan is a product of the latest dry period in this playa lake. The lack of a salt crust in studied depth, except the surface layer, implies that hypersaline conditions probably have existed only in the latest sedimentation period in the recent centuries in the Gavkhoni playa lake.

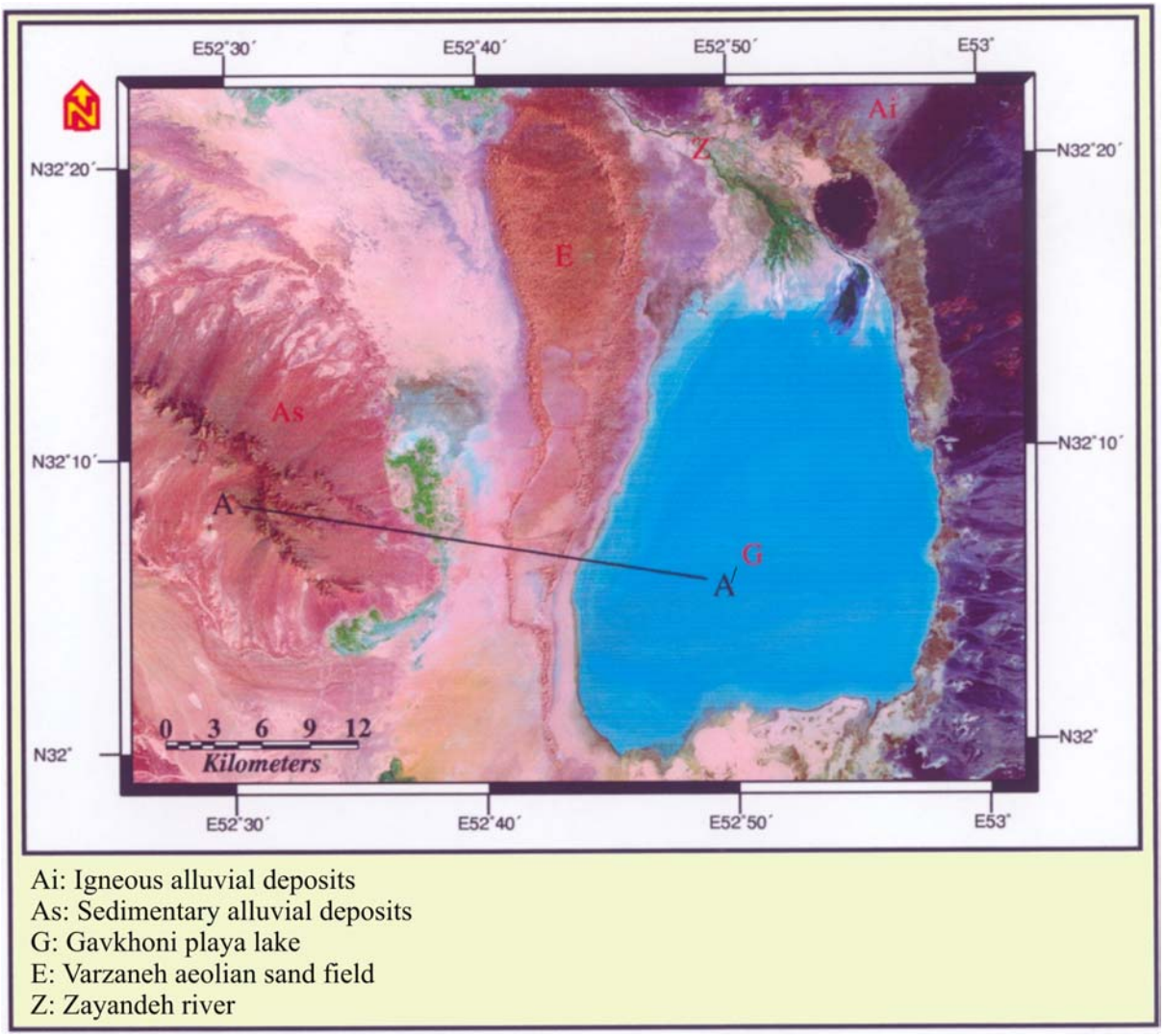

Fig. 4.28 False color-Landsat TM image showing location of hypotethic cross-section (A-A′) from northwest to southeast of the study area.

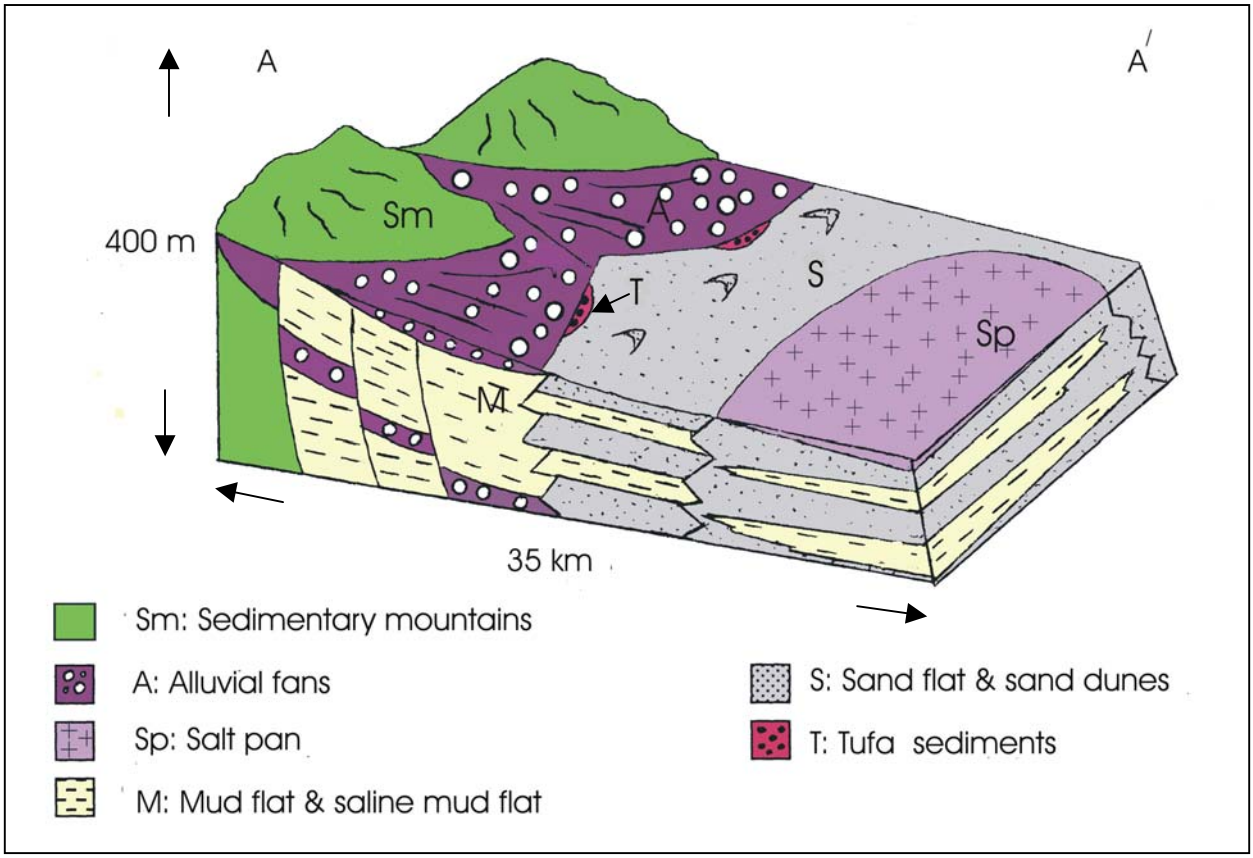

Fig. 4.29 Hypotethic model of sedimentary infill of the Gavkhoni playa lake, indicating supposed stratigraphic sequence, major geomorphic features, and sub-environments (see Fig. 4. 28 for position of cross section (A-A/).

4.5 Geochemistry of brine in relation to the deposits of the Gavkhoni playa lake drainage basin

Introduction

The composition of surface water and groundwater and ultimately of brines mainly depends on minerals and pore waters that are present in bedrocks, their relative abundance, and their chemical stability (Eugster & Hardie, 1978). Furthermore, acid waters are the most effective agents for weathering carbonates and silicates, which form the bulk of the surface rocks. Rainwater has usually a pH 5.7 (Krauskopf, 1985) which is effective for weathering carbonate rocks and also some minerals in igneous and metamorphic rocks (e.g. plagioclase, pyroxene, and amph

ibole). Chemical analysis of many salt lake environments has shown that they have a wide range of compositions. In many salt lakes Na^+ is the most abundant cation, but anion concentrations are variable (Fayazi, 1991).

The lithology of the Gavkhoni playa lake drainage basin consists of igneous, sedimentary and metamorphic rocks. Among these rocks, carbonate rocks are dominant and igneous rocks, especially andesite, are the second major rocks (see Chapter 2.3 for details).

1

Sample No	R1	R2	I1	I2	K	M1	M2	S1	S4
Location / Ion ppm	Zayandeh river (Varzaneh)	Zayandeh river (Kuh-e-Siah)	4.5 km east of Khara	7 km east of Khara	8.5 km east of Khara	23 km east of Varzaneh	28 km east of Varzaneh	10.5 km east of Khara	southwest of the playa lake
K+	78	97.5	507	1560	1950	371	936	2944	3570
Ca++	160	200	1520	1400	1800	2200	3800	1740	280
HCO_3-	414	244	146.4	73.2	73.2	195.2	73.2	512.4	500
Cl-	2095	4118	31240	143420	177500	21868	105080	183890	199254
Na+	1012	2576	57040	87200	103040	20240	52716	85100	90600
SO_4--	1512	1411	19289	13254	21950	22051	4444	9436	13280
Mg++	360	624	2088	7200	10080	1800	6600	19152	25691
NO_3-	4	5	14	5	32.5	157	307	48	n.d
Sr++	9	9	100	62	4.9	56	292	74	n.d
TDS	10900	9900	110200	295100	403700	108700	192700	359000	n.d

2

Sample No	R1	R2	I1	I2	K	M1	M2	S1	S4
Location / Ion ppm	Zayandeh river (Varzaneh)	Zayandeh river (Kuh-e-Siah)	4.5 km east of Khara	7 km east of Khara	8.5 km east of Khara	23 km east of Varzaneh	28 km east of Varzaneh	10.5 km east of Khara	southwest of the playa lake
K+	109	105	741	1638	1716	858	936	2457	n.d
Ca++	200	260	860	1400	1600	2680	3480	1500	440
HCO_3-	293	390	220	317	122	244	122	366	450
Cl-	6461	6106	88040	156910	178920	65320	101530	187440	199365
Na+	3933	3542	58420	93840	96600	36800	51520	91080	86600
SO_4--	1162	2323	17731	15872	14882	17824	5040	12864	14000
Mg++	384	702	3036	6868	9360	3084	6360	18120	24900
NO_3-	3.5	1	17	6	25.5	227	476	43	n.d
SR++	9	9	68	16.4	14.5	26.3	254	5.3	n.d
TDS	20500	19000	105200	302600	323800	91200	186500	392600	n.d

Table 4.2 Chemical analyses of the Zayandeh river water (R1 & R2) and the groundwater (I1, I2, K, M1, M, S1 & S2) of the study area taken during wet season (early spring, 1) and dry season (late summer, 2) in 1996. River (R), interdune(I), sand flat (K), saline mud flat (M) and salt pan (S) (see Fig. 4.1 and Table 4.1 for their positions). n.d= not detected.

For determination of the type of the Gavkhoni playa lake brine, the major cations and anions, i.e. sodium, magnesium, calcium, potassium, sulfate, chloride, bicarbonate, nitrate,

one of the rare elements (strontium) and total dissolved solid (TDS) have been analyzed. The water samples were collected in two periods (dry and moist season) in nine stations (Table. 4.2). In this part of the chapter, the chemical analyses of the elements and geochemistry of the water in relation to sedimentology of the drainage basin are described.

Sodium

Sodium is the most abundant cation in the brine of the salt lake and in the Zayandeh river water similar to many other ones in (semi) arid settings. It ranges between 1012 to 103040 ppm. As Fig. 4.30 shows, the content of Na^+ is maximum in sample No. K (sand flat) and minimum in samples No. R (the Zayandeh river water). This element occurs only in halite in the evaporite sediments of the playa lake.

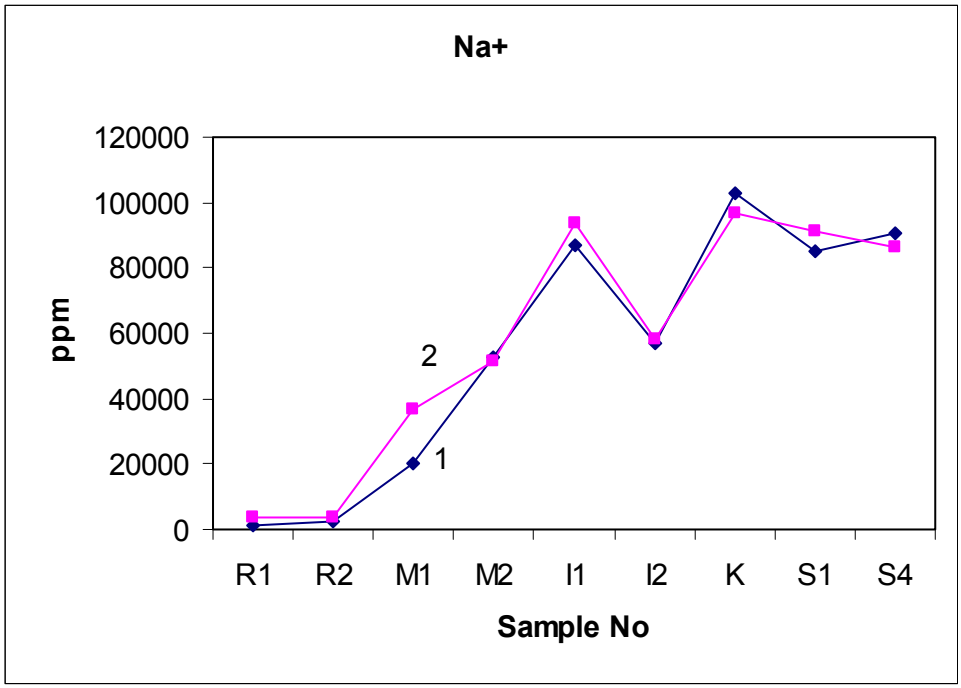

Fig. 4.30 Content of sodium in the water samples of the Zayandeh river and the groundwater of the study area taken during wet season (early spring, 1) and dry season (late summer, 2) in 1996. River (R), interdune(I), sand flat (K), saline mud flat (M) and salt pan (S) (see Fig. 4.1 and Table 4.1 for their positions).

Interpretation

Sodium is derived locally more generally from the dissolution of pre-existing halite and to a minor extent from hydrolysis of alkaline feldspars (sanidine, albite, oligoclase) and

possibly also of analcim. Halite mostly occurs in pore water of the modern marl deposits surrounding the playa lake. A major amount of Na also stems from the leaching of saline pore waters in sedimentary rocks during their erosion.

Magnesium

The magnesium content of the surface and the groundwater ranges between 360 to 25691 ppm. It increases usually toward the center and the south of the lake (Fig. 4.31). This element occurs locally in small amounts in saline minerals, i.e. carnallite ($MgCl_2.KCl.6H_2O$), tachyhydrite ($CaCl_2.2MgCl_2.12H_2O$) and bischofite ($MgCl_2.6H_2O$) in the playa lake.

Interpretation

Magnesium comes chiefly from chemical weathering of dolomite and also of Mg silicates such as amphibole, biotite, and chlorite, present in the igneous and metamorphic rocks. Locally basic rocks are a major source of magnesium (Eugster & Hardie, 1978).

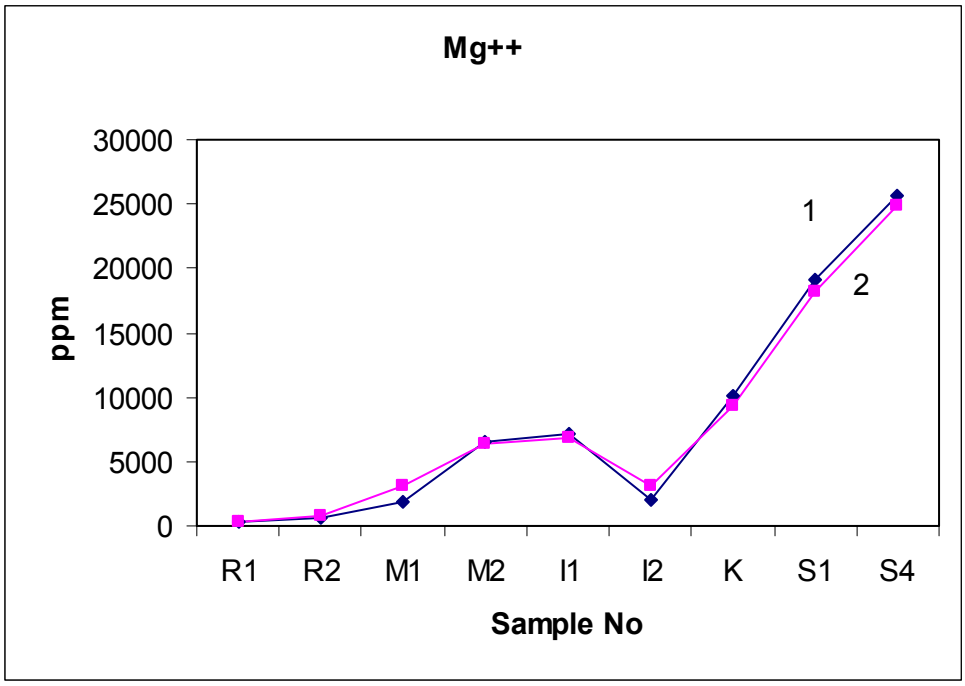

Fig. 4.31 Content of magnesium in the water samples of the Zayandeh river and the groundwater of the study area taken during wet season (early spring, 1) and dry season (late summer, 2) in 1996. River (R), interdune(I), sand flat (K), saline mud flat (M) and salt pan (S) (see Fig. 4.1 and Table 4.1 for their positions).

Dolomitic rocks are mostly found in the Permian sequence exposed in the upper reaches of the drainage basin to the west, and at the base of Cretaceous carbonate rocks in the southwest. Altered Mg silicates minerals are found mainly in the metamorphic rocks (schist, metagranite and gneiss) exposed in the upper reaches of the drainage basin in the northwest and the volcanic rocks (mainly andesite) northeast and east of the playa lake (see Chapter 2.3 for lithology of the drainage basin).

Potassium

The content of potassium in the surface and groundwater samples is low in comparison with Na^{+} and Mg^{++} (Table 4.2). It ranges from 78 in the north to 3570 ppm in the south of the playa lake (Fig. 4.32). It must be noted that during the precipitation of sodium salts in sediments, the relative amount of potassium gradually increases. Carnallite ($MgCl_2.KCl.6H_2O$) is the only potassium mineral in the salt pan.

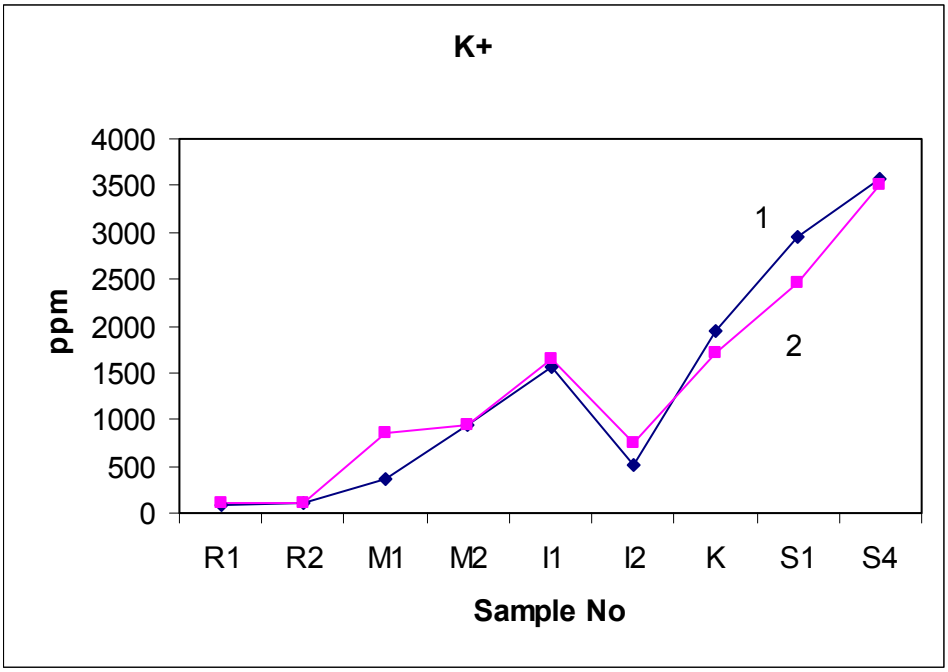

Fig. 4.32 Content of potassium in the water samples of the Zayandeh river and the groundwater of the study area taken during wet season (early spring, 1) and dry season (late summer, 2) in 1996. River (R), interdune(I), sand flat (K), saline mud flat (M) and salt pan (S) (see Fig. 4.1 and Table 4.1 for their positions).

Interpretation

Potassium comes mostly from weathering of the alkaline silicate minerals (e.g. feldspar), muscovite and biotite, which occur in the igneous, metamorphic, and sedimentary rocks similar to sodium (Eugster & Hardie, 1978).

Alkaline feldspars are found in the igneous rocks located in the east and the northeast of the lake and metamorphic rocks outcropping in the upper reaches of the drainage basin in the northwest (see Chapter 2.3 for lithology of the drainage basin).

Calcium

The content of calcium ranges from 160 in the surface water (Zayandeh river) and to 3800 ppm in the groundwater (Fig. 4.33). In contrast to Na^{+}, K^{+} and Mg^{++}. It gradually increases from the south to the north and from the center to the west of the playa lake. It occurs in two minerals, gypsum, and tachyhydrite ($CaCl_2.2MgCl_2.12H_2O$) determined in the evaporite sediments of the salt pan.

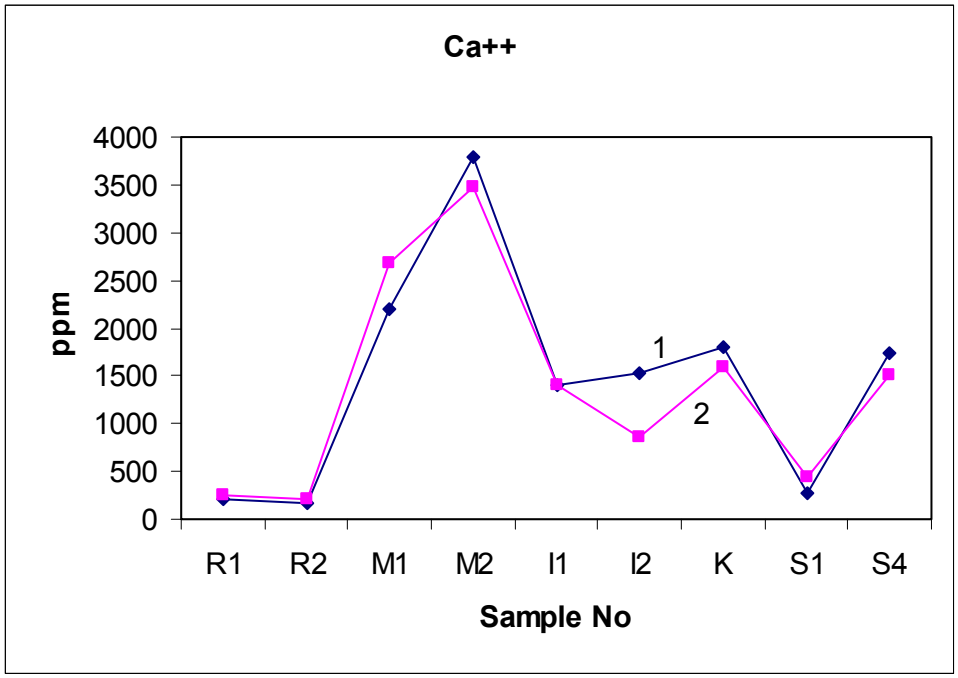

Fig. 4.33 Content of calcium in the water samples of the Zayandeh river and the groundwater of the study area taken during wet season (early spring, 1) and dry season (late summer, 2) in 1996. River (R), interdune(I), sand flat (K), saline mud flat (M) and salt pan (S) (see Fig. 4.1 and Table 4.1 for their positions).

Interpretation

Calcium comes mainly from dissolution of calcite, dolomite, gypsum, and anhydrite as well as to a minor extent from hydrolysis of silicates, such as plagioclase (andesin and Labrador), and amphibole (hornblende).

Limestone and gypsum are abundant in the sedimentary rocks surrounding the study area. The former is exposed mainly in the south and the southwest of the playa lake and as well as in other parts of the drainage basin as locally. The later is found in the recent sediment especially alluvial fans and also in the Tertiary deposits (Qom Formation). Petrographic studies of the igneous and metamorphic rocks exposed in the northeast and the east shows the presence of altered plagioclase, garnet, and amphibole.

Strontium

The content of strontium is very low in comparison to other elements analyzed in the surface water and the groundwater of the Gavkhoni playa lake. Its concentration ranges between about 5 to 292 ppm in the brines (Fig. 4.34).

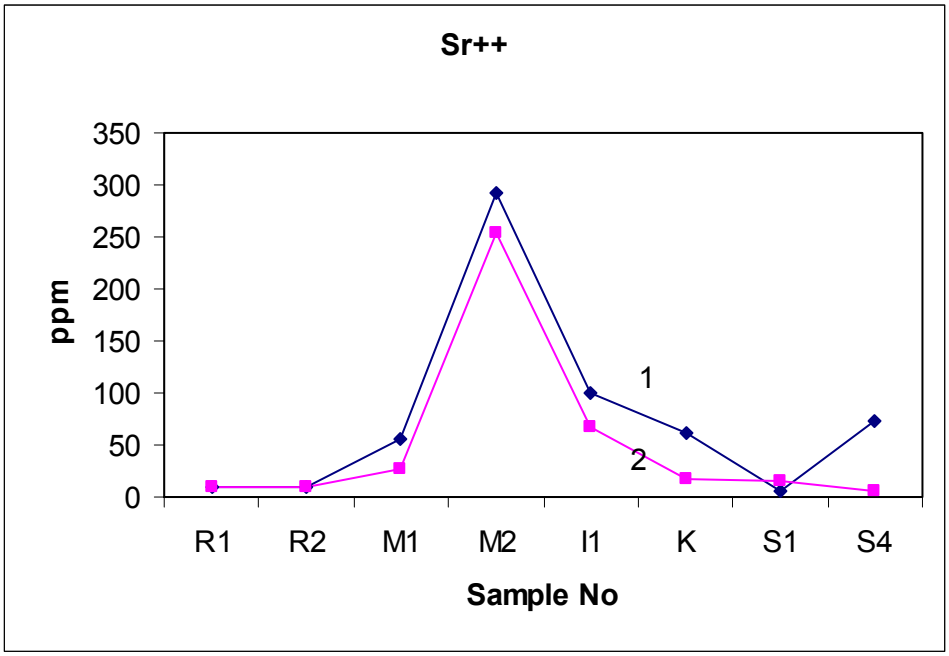

Fig. 4.34 Content of strontium in the water samples of the Zayandeh river and the groundwater of the study area taken during wet season (early spring, 1) and dry season (late summer, 2) in 1996. River (R), interdune(I), sand flat (K), saline mud flat (M) and salt pan (S) (see Fig. 4.1 and Table 4.1 for their positions).

The highest values of strontium are found in the north of the playa lake, whereas the minimum values occur in the west and in the Zayandeh river water.

Interpretation

Strontium mostly comes from gypsum, present in the recent alluvium and the Tertiary gypsiferous marl (Qom Formation) sediments, but also from limestones.

Chloride

Chloride is the major anion in the Zayandeh river water and the Gavkhoni playa lake brine. It ranges from 4118 to 199365 ppm (Fig. 4.35). The content of chloride increases from the north to the south and its concentration and distribution nearly corresponds with sodium in the playa lake. It occurs in halite (NaCl), carnallite ($MgCl_2.KCl.6H_2O$), tachyhydrite ($CaCl_2.2MgCl_2.12H_2O$) and bischofite ($MgCl_2.6H_2O$), minerals that could be determined in the evaporite sediments of the salt pan.

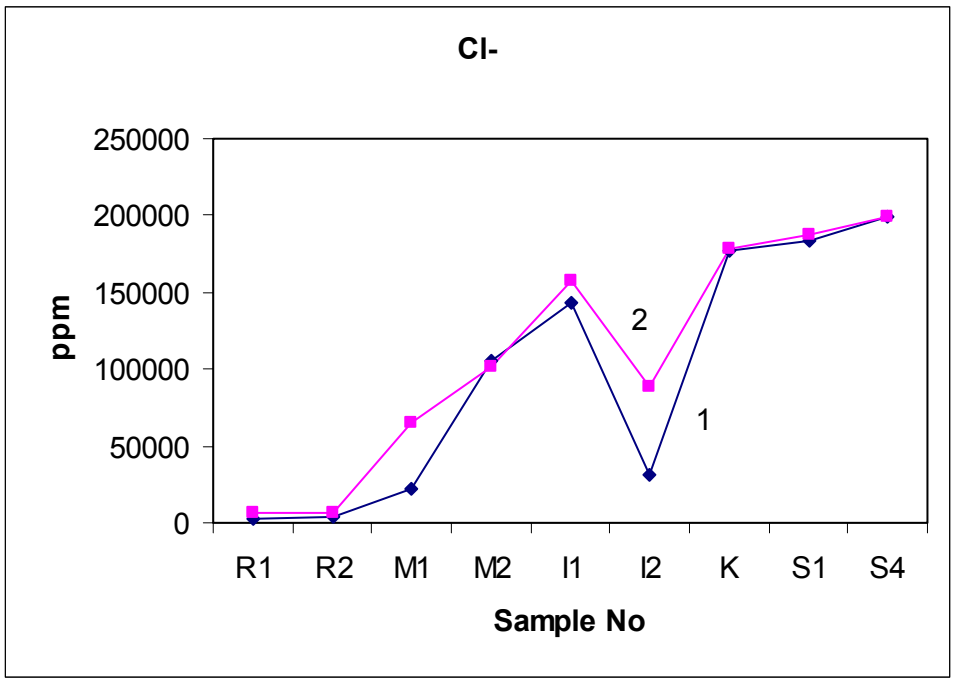

Fig. 4.35 Content of chloride in the water samples of the Zayandeh river and the groundwater of the study area taken during wet season (early spring, 1) and dry season (late summer, 2) in 1996. River (R), interdune(I), sand flat (K), saline mud flat (M) and salt pan (S) (see Fig. 4.1 and Table 4.1 for their positions).

Interpretation

Chloride comes from dissolution of halite in the modern marl deposits similar to Na^+. It also comes from pore water in the sedimentary rocks and fluid inclusions in the igneous rocks (Eugster & Hardie, 1978). Halite is mostly present in the pore water of the recent marl deposits surrounding the playa lake and the igneous rocks that are present in the north and the northeast of the study area. A major amount of Cl also stems from the leaching of saline pore waters in sedimentary rocks during their erosion.

Sulfate

After chloride it is the second most common anion in the analyzed groundwater and surface water. It precipitates to form gypsum. Chemical analyses of the brine samples show the maximum content of sulfate is 22051 ppm (Fig. 4.36). The concentration of sulfate does not change regularly in the brines from the north to the south of the lake. Its content is different in the different seasons.

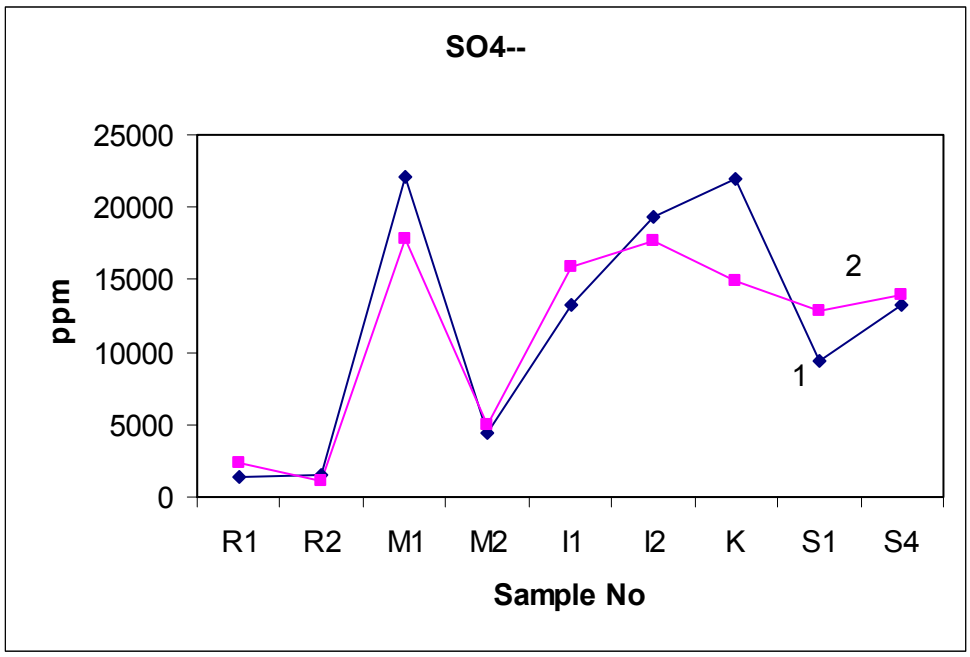

Fig. 4.36 Content of sulfate in the water samples of the Zayandeh river and the groundwater of the study area taken during wet season (early spring, 1) and dry season (late summer, 2) in 1996. River (R), interdune(I), sand flat (K), saline mud flat (M) and salt pan (S) (see Fig. 4.1 and Table 4.1 for their positions).

Interpretation

Sulfate comes predominantly from dissolution of gypsum and oxidation of sulfides. Gypsum occurs in the Tertiary Qom Formation and the recent alluvial fans. The former is locally exposed in the southwest and the northeast and the later extends around the playa lake. Another source of sulfates is produced by oxidation process of pyrite present in the Cretaceous carbonate and the Jurassic shale rocks.

Bicarbonate

Bicarbonate is the less abundant anion after nitrate measured in the Zayandeh river water and the groundwater of the playa lake. Its content ranges from 73 to 450 ppm (Fig. 4.37). The bicarbonate content is highest in the north and the west of the playa lake. It stems mostly from dissolution of carbonate. According to different seasons and locations, the content of bicarbonate changes similar to that of sulfate.

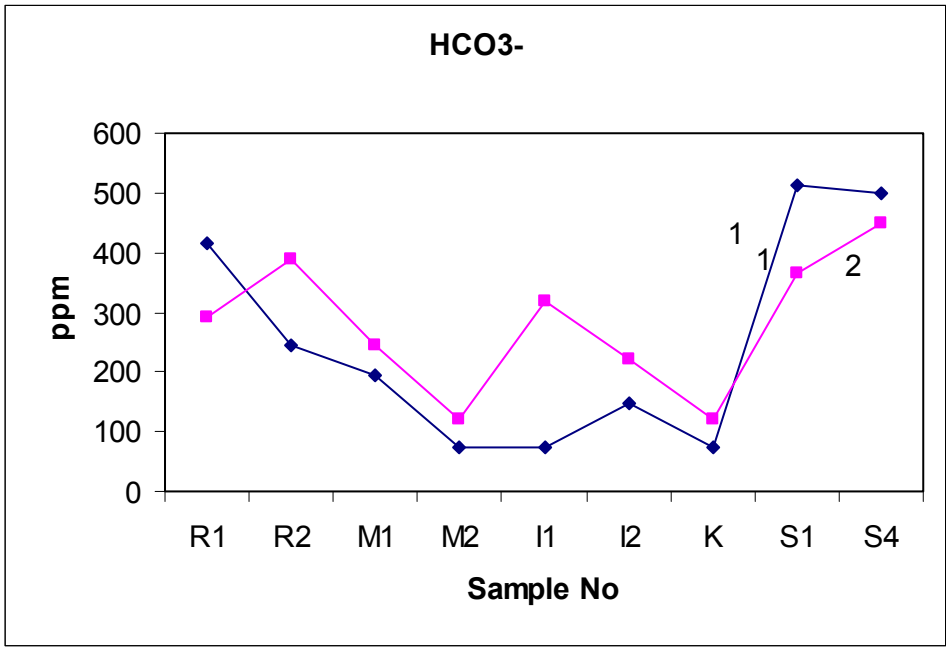

Fig. 4.37 Content of bicarbonate in the water samples of the Zayandeh river and the groundwater of the study area taken during wet season (early spring, 1) and dry season (late summer, 2) in 1996. River (R), interdune(I), sand flat (K), saline mud flat (M) and salt pan (S) (see Fig. 4.1 and Table 4.1 for their positions).

Interpretation

Bicarbonate comes from dissolution of limestone and dolomite, and also from rainwater. Limestone waters are characterized by high HCO_3^-. Dolomite waters are similar to limestone water. Waters in contact with marl also have high HCO_3^-. The weathering of igneous (acidic and basic) and metamorphic rocks produces waters rich in HCO_3^- (Eugster & Hardie, 1978). These rocks are mostly present in the drainage basin in the south and the southwestern of the study area (see Chapter 2.3 for lithology of the drainage basin).

Nitrate

Nitrate is the less frequent anion measured in the Zayandeh river water and the brines of the groundwater in the playa lake. It's content ranges less than 1 ppm to up to 476 ppm (Fig. 4.38). The nitrate content is highest in the groundwater of samples No. M1 and M2 in the north of the playa lake and lowest in the Zayandeh river water. The value of nitrate increases usually in wet season.

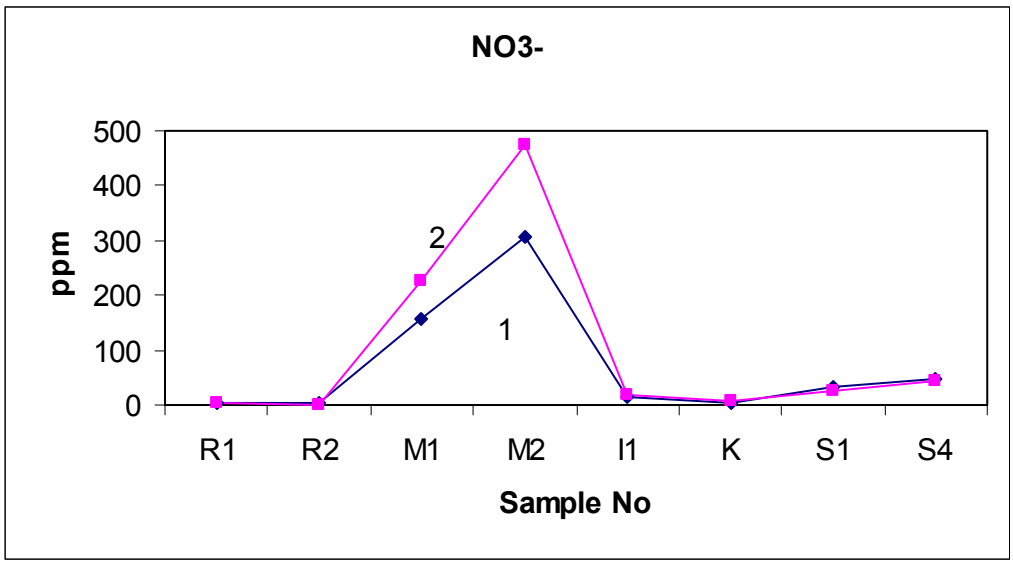

Fig. 4.38 Content of nitrate in the water samples of the Zayandeh river and the groundwater of the study area taken during wet season (early spring, 1) and dry season (late summer, 2) in 1996. River (R), interdune(I), sand flat (K), saline mud flat (M) and salt pan (S) (see Fig. 4.1 and Table 4.1 for their positions).

Interpretation

Half of the nitrogen supplied to cultivated fields is from fertilizer, followed in descending rank by root residue, biological nitrogen fixation, and rainfall (Jensen, 1986). Eroded soil, the burning of fossil fuel, and decaying organic matter can contribute to airborne nitrogen (Jensen, 1986). The cyanobacteria fix nitrogen on the surface of moist soils, in or near, ephemeral lakes and playas or in soils of areas that are moistened by frequent and heavy winter fogs (Warren, 1999). Nitrogen is also found in sedimentary deposits, e.g. organic materials in lignite and bituminous coal, clay and caliche soils, and marine shales. It is returned to the earth as nitrate precipitation. Nitrate as soluble, moves quickly through soils, and often indicates potential biological contamination (Jensen, 1986). A high content of nitrogen in the groundwater of the Gavkhoni playa lake is most probably from the leaching of organic material, fertilizers and industrial waste waters. These materials enter to the Zayandeh river and groundwater from farmlands and industrial plants. Another minor source of nitrogen is inorganic material, e.g. carbonaceous rocks, shales, and marls. Carbonaceous rocks are found in Jurassic sediments in most of drainage basin. Jurassic marine shales are present at the base of the Cretaceous carbonate rocks in the southwest of the study area. Clays are mostly present in recent marl deposits surrounding the playa lake. It is supposed that the role of inorganic material in relation to the content of nitrogen is low, because of minor contribution of organic material-bearing sediments in the drainage basin.

Total dissolved solid (TDS)

The content of total dissolved solid (TDS) of the analyzed waters (surface water and groundwater) ranges from 99000 to 403700 ppm. The lowest values are found in the Zayandeh river and the highest in the center of the saline lake (Fig. 4.39).

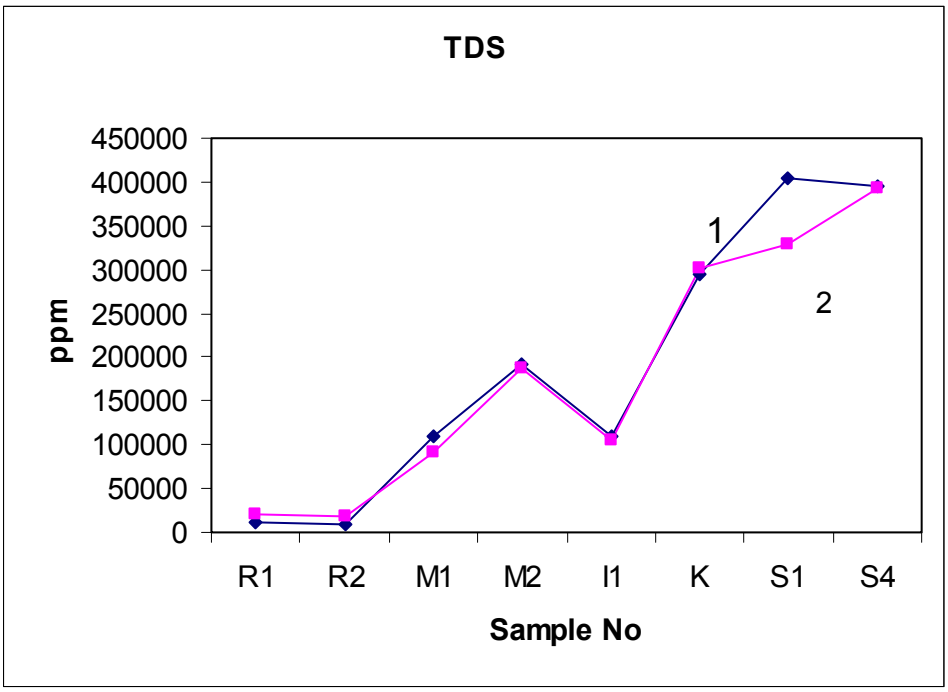

Fig. 4.39 Content of total dissolved solid (TDS) in the water samples of the Zayandeh river and the groundwater of the study area taken during wet season (early spring, 1) and dry season (late summer, 2) in 1996. River (R), interdune(I), sand flat (K), saline mud flat (M) and salt pan (S) (see Fig. 4.1 and Table 4.1 for their positions).

4.6 Evolution of brine in the Gavkhoni playa lake

As figure 4.33 shows, the percentage of Ca^{++} decreases toward the center of the playa lake after precipitation of gypsum and carbonate at the margin of the playa lake (alluvial fan, saline mud flat and mud flat). The evolution of saline waters in seawater (to some extent comparable with saline water of non-marine environments) starts with early precipitation of alkaline earth carbonate at 2 times of concentration of the seawater. After carbonate, gypsum starts to precipitate when the concentration of the brine reaches approximately 3.5 times of concentration of the seawater. Calcium thus is removed from brines at an early stage of concentration.

At the end of dry period, when the brine is concentrated many folds (to equivalent of more than ten times that of seawater) halite is precipitated, covering mostly the center of the playa lake and forming the salt pan. At this stage a large portion of Na^{+} and Cl^{-} is extracted from the brine.

As chemical analyses show (Table 4.2) magnesium content is relatively high in the brines of the Gavkhoni playa lake and increases in relative concentration after precipitation of gypsum. Where evaporation is very strong, it is used to form carnallite ($MgCl_2.KCl.6H_2O$) and then bischofite ($MgCl_2.6H_2O$) (Appendix B4, sheets No., 23 & 24).

The brine of the Gavkhoni playa lake is very poor in K^{+} because of its deficiency in the source rocks and also absorption onto active surfaces of clay minerals in the early phases of brine concentration. Therefore, potassium sulfates/chlorides which precipitate from supersaline waters at concentrations more than 70-90 times that of the original seawater can not form in Gavkhoni (cf. Fayazi, 1991; Warren, 1999).

The brine is also relatively poor in bicarbonate, carbonate and sulfate, so that evaporitic carbonate and sulfate minerals such as glauberite ($CaSO_4.Na_2SO_4$), trona ($Na_2CO_3.2H_2O$), nahcolite ($NaHCO_3$), mirabilite ($Na_2SO_4.10\ H_2O$) and thenardite (Na_2SO_4) can not form in the Gavkhoni playa lake (cf. Fayazi, 1991).

The chemical analyses of dilute water (surface water) taken from the Zayandeh river in the two locations (Varzaneh and delta samples No. R1, R2) and the groundwater from, interdune, sand flat and saline mud flat (e.g. samples No. I1, K, M1) exhibit a chemistry dominated by Na-Cl type (cf. Bryant *et al*., 1994). Based on Eugster & Hardie, 1978's terminology, major cations and anions from the surface waters reveal that they have a chemistry dominated by Na^{+}, (Mg^{++}), Cl^{-}, (SO_4^{--}) type. The chemistry of the groundwaters in the center and the south of the salt pan (e.g. samples No. S1 & S4) indicate Na^{+}, (Mg^{++}), Cl^{-} to Na^{+}, Mg^{++}, Cl^{-} types (see Fig 4.1 and Table 4.1for position of samples No).

The main cations and anions in the concentrate water of the Bristol Dry Lake, the Great Salt Lake in the USA and the Howz-e-Soltan salt lake in the center of Iran compared with the Gavkhoni playa lake shows that Mg^{++} and K^{+} values are higher and Ca^{++}, Na^{+} and SO_4^{--} is lower in the Gavkhoni playa lake than in the other lakes (Table 4.3 & Fig. 4.40).

Location Ion	Great Salt lake	Bristol Dry Lake	Howz-e-Soltan lake	Gavkhoni playa lake
Ca^{++}	300	43296	46260	2117
Mg^{++}	7190	1061	13776	32090
Na^{+}	80800	57365	275608	57129
K^{+}	4230	3294	2224	5063
SO_4^{--}	156300	223	5000	13239
Cl^{-}	138000	172933	443400	203595

Table 4.3 Comparison of the main cations and anions of the concentrated water (in ppm) in the Howz-e-Soltan salt lake (center of Iran), the Bristol Dry Lake, and the Great Salt Lake (USA) (after Fayazi, 1991) with the Gavkhoni playa lake (Sample No. S4) (see Fig. 4. 1 and Table 4.1 for its position).

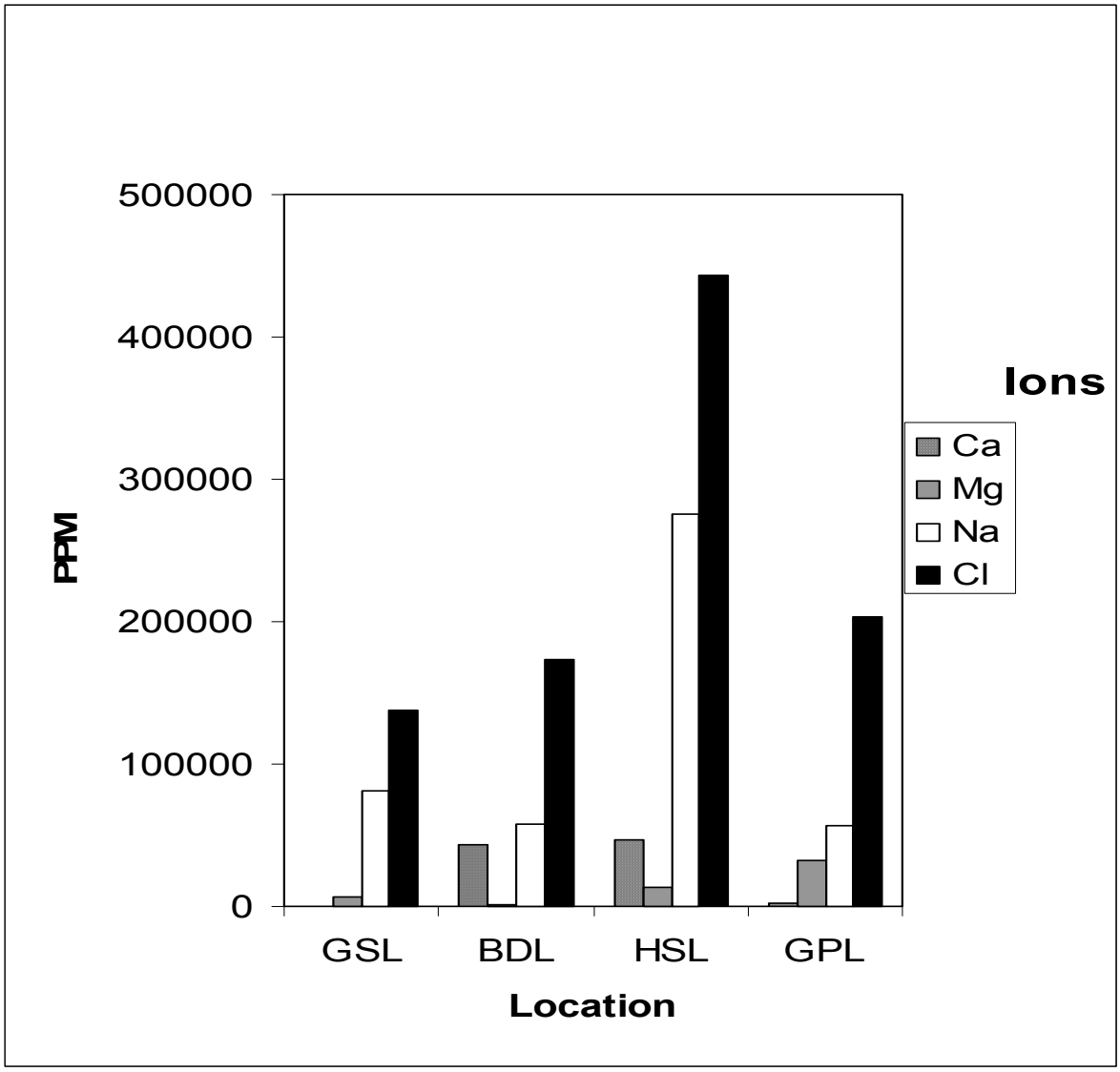

Fig. 4.40 Histograms showing the main cations and anions of the concentrated water in the Howz-e-Soltan salt lake, HSL (center of Iran), the Bristol Dry Lake (BDL), and the Great Salt Lake, GSL (USA) (after Fayazi, 1991) in comparison with the Gavkhoni playa lake, GPL (based on data of Table 4.2)

4.7 Summary and conclusions

The Gavkhoni playa lake is typical for many permanent lacustrine to saline lake basins within closed drainage basins in central Iran. Seven major facies can be easily recognized in this playa lake. They include alluvial fan, aeolian sand field (sand dune, interdune, sand flat), sand beach, mud flat, saline mud flat salt pan and delta.

The alluvial fan facies is one of the remarkable sedimentological features in the study area. Regarding distribution, lithology, stratigraphy and development it is described in details in Chapter 5.

The sand dunes border the playa lake to the west and grade laterally into the sand flat. The morphology, migration, mineralogy and the source of the aeolian sand dunes were described in detail in Chapter 3.

The interdune areas are located between the sand dunes and are covered mostly by a dry and soft aeolian sand layer. Based on digged trenches, six sub-facies, i.e. aeolian sand, grey to black sandy mud, white sandy mud, greenish sandy mud, brown mud and sand were determined in this environment. The properties of the sediments indicate deposition in a closed basin with a shallow-brackish water perennial lake to sub-aerial conditions, and semi arid to arid climate with wind activity.

The sand flat surrounds the playa lake. In the studied sand flat (western sand flat) gypsiferous marl mound, porous tufa, puffy surface and efflorescent salt crust are common features. The properties of the western sand flat suggest periodic flooding, evaporation, and desiccation in this area affected by dry climate.

The sand beach ridges occur as a long narrow band to the east of the salt pan and the Zayandeh river delta. They formed by wave action during wet seasons when the lake level stands high.

According to study of two pits, two sub-facies were observed in this facies including gravelly sand and sand.

The mud flat and saline mud flat encircle the playa lake, except in the western part. The mud flat is characterized by polygonal mud cracks, plant roots, root casts and is not saturated by brine. It is deposited mainly by sheet floods and then altered by wetting and drying. The properties of detrital sediments in the mud flat indicate periodic rather high and low flow velocities. A common feature in the saline mud flat is its hard and porous surface pitted by small holes with a few centimeters wide and deep, resulting from evaporation of capillary brines and rapid and differential rising of the sediment surface. The evaporite minerals (halite and gypsum) scattered in the sediments develop during lower water level as the result of evaporation of brine pore water in dry periods. Based on digged trenches, five sub-facies were recognized in the mud flat and saline mud flat: salt, gypsiferous mud, sandy mud, mud, and sand. The properties of these lithologies indicate that sedimentation occurred in variable conditions of chemical composition, environment and climate. They formed in fresh water to brackish perennial lake and ephemeral saline lake in semi-arid to arid conditions.

The salt pan covers the major part of the center of the playa lake as a hard crust. The thickness of this crust ranges from a few centimeters to the north and up to 150 cm to the south. The salt pan is as a result of flooding, evaporation and desiccation. The most common features of the salt pan are polygonal halite crusts, efflorescent halite ridges and popcorns (cauliflower). Halite occurs in hoppers, cubic crystals and massive form. The size of the halite crystals reaches up to 2 cm in diameter. Stratigraphic sequence, based on drilled cores to the depth of up to 30 m and digged trenches, shows sedimentation of mud–sized, interbedded with sand-sized sediments. These properties suggest that the basin was influenced repeatedly by wet and dry periods. During the floods it was a shallow fresh water to brackish permanent lake with changing level of water table, resulting in deposition of fine-grained sediments in this basin during flooding.

The sand-grained deposits are most likely derived from the aeolian sands during dry periods at the margin of the sand dunes, but also directly as bottom load from the Zayandeh river delta. With increasing aridity, the middle part of the playa lake gradually became shallower and finally the ephemeral saline lake and the salt pan developed.

The Zayandeh river delta occupies about 30 km^2 of the lower reach of the Zayandeh river. It gradually grades into the poorly saline lake in the south, the sand flat in the west and the sand beach ridge and the mud flat to the east. Based on studied trenches with depths reaching 150 cm three main sub-facies were determined. They are grey to black mud, yellow to brown mud and sand. The presence of the sand sub-facies represents deposition in the bottom of distributary channels during periods of rather high flow velocity, while silt and clay are well developed on the upper parts of point bars, swamp and levees during floods.

The chemical analyses of dilute water (surface water) and the major cations and anions reveal that it has a chemistry dominated by Na^+, (Mg^{++}), Cl^-, (SO_4^{--}) type reflecting of the nature of the catchment lithology. The evolution of the brines show that they are progressively depleted from carbonate and sulfate from the margins to the center of the playa lake and ultimately produced a Na^+, (Mg^{++}), Cl^- and Na^+, Mg^{++}, Cl^- brine type. This type of the brine is approximately similar to many other playas worldwide in (semi)-arid regions. After complete desiccation, the mineral assemblage comprises mainly halite but other minerals including gypsum ($CaSO_4$, $2H_2O$), carnallite ($MgCl_2.KCl.6H_2O$), tachyhydrite ($CaCl_2.2MgCl_2.12H_2O$) and bischofite ($MgCl_2.6H_2O$) are also determined as minor constituents in the central and the south of the saline pan. There is no relic of glauberite ($CaSO_4.Na_2SO_4$), trona ($Na_2CO_3.2H_2O$) in the sediments.

The Gavkhoni playa lake formed in a supposed graben and/or half graben system along the northeastern part of the Sanandaj-Sirjan zone. This system is a result of volcanic eruptions at the end of Cretaceous and Early Eocene, and faulting which took place after the volcanism. Subsidence of this base level of erosion (Gavkhoni playa lake) is most probably due to continuing tectonic activity in Quaternary period.

It is supposed that, changing climatic conditions in the Quaternary period played another important role in relation to changing of water level in the lower reaches of the basin (Gavkhoni playa lake), rise and fall in denudation and spatial distribution of Quaternary deposits.

Chapter 5

Sedimentology of alluvial fan and the Zayandeh river deposits

5.1 Introduction

The study area is bordered by sedimentary mountains to the south, west and northwest, and igneous mountains to the east and the north. The sedimentary mountains rise as much as 1110 m in the south, the igneous mountains 1860 and 974 m to the northeast and the east respectively above the Gavkhoni playa lake level. The most active depositional environment in this basin is the Zayandeh river (Fig. 5.1). Sedimentation occur under the hottest and driest conditions found in the Esfahan province, with annual rainfall averaging 80 mm, annual potential evaporation of 3265 mm, and with summer temperature reaching + 42^{o}C (see Chapter 2.4 for details).

The purpose of this study is to present sedimentology, development and morphostratigraphy of the Zayandeh river (channel and overbank) and modern alluvial fan deposits in the southeast of Esfahan. Sedimentology of the Zayandeh river delta was described in Chapter 4.

5.2 Methodology

Twenty-two vertical sections were selected to study stratigraphic sequence and development of the Zayandeh river and alluvial fan deposits (see Fig. 5.2 and Table 5.1for position and sections No). Sedimentological logs for twenty sections were drawn (see appendix F for lithostratigrafic-sedimentologic sections). Some photographs were provided from each facies and their sketches were drawn. For determination of mineralogical composition (gravel to mud), textural properties of grains, sedimentary structure, the provenance of the alluvial sediments and paleontology studies, about 60 samples were analyzed (see Chapter 1 and Appendixes for detailed methodology and stratigraphic sections).

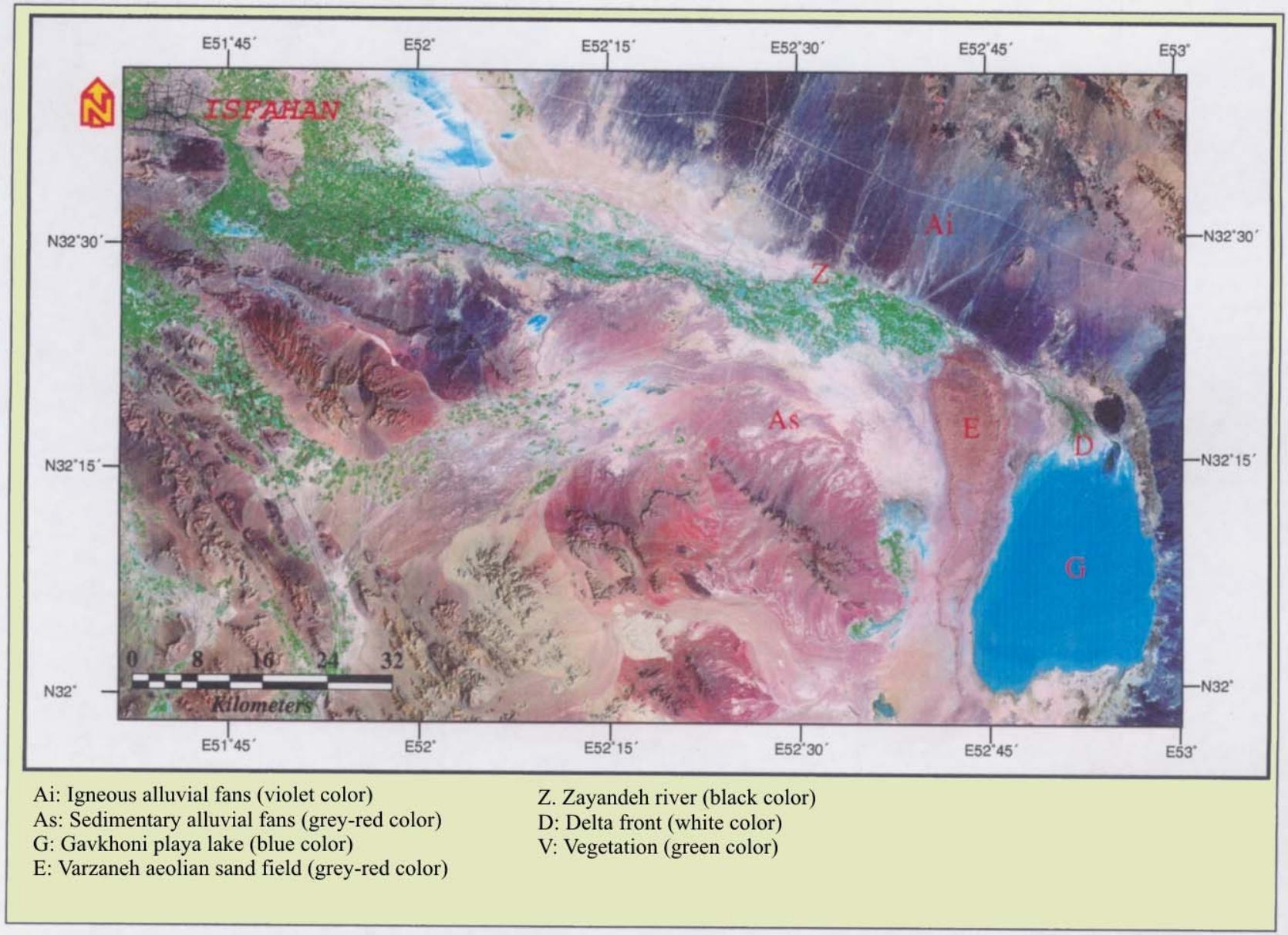

Fig. 5.1 False color-Landsat TM image showing the situation of the Zayandeh river and alluvial fan deposits in the study area.

5.3 Setting and geomorphology

The major sedimentological features of the study area include lacustrine/overbank, alluvial fan and the Zayandeh river deposits. Lacustrine/overbank sediments (mainly yellow mud), deposited during probably Quaternary period, are overlain by recent coarse-grained sediments. These deposits sometimes form cut-banks of the Zayandeh river up to 10 m in height. In the most of the study area, the Zayandeh river flows between well-defined steep banks, with channel width of 50 m on average and in its distal end (Zayandeh river delta) it is divided in many narrow channels (3-5 wide). The flood plain of the Zayandeh river is narrow at the beginning of the study area and wide to the end, bordered by overbank and alluvial fan sediments. The major channel averages about 3 m in depth below the level of adjacent levees. Minor channels reaches up to 50 cm in depth in the delta. The river carries a sediment load ranging from fine gravel through sand grains. Small gullies originating from alluvial fans dissect the floodplain to join the main channel, especially in the delta reach of the Zayandeh river.

The alluvial fan deposits, regarding lithology, can be classified into two parts, igneous and sedimentary. The igneous alluvial fan deposits occur mostly in the north of the Zayandeh river and the east of the Gavkhoni playa lake. The sedimentary alluvial fan deposits mostly extend in the south of the Zayandeh river (Fig. 5.1).

The northern fans are relatively extensive, with an area of 2000 km^2, an average radial length of 20 km and an average width of the laterally coalescing fans of 95 km. The apex elevation is about 2100 m, and the toe elevation is about 1500 m above the sea level. The alluvial fan sediments are derived from a catchment area, underlain mostly by Eocene igneous rocks, that are approximately 110 km long, 6–15 km wide, 1100 km^2 in area and maximum elevation of 3330 m. These laterally coalescing fans are drained by several shallow, ephemeral, small streams, averaging few decimeter in depth. The proximal sector has an average slope of 4.14% medial 1.38% and the distal 0.3%.

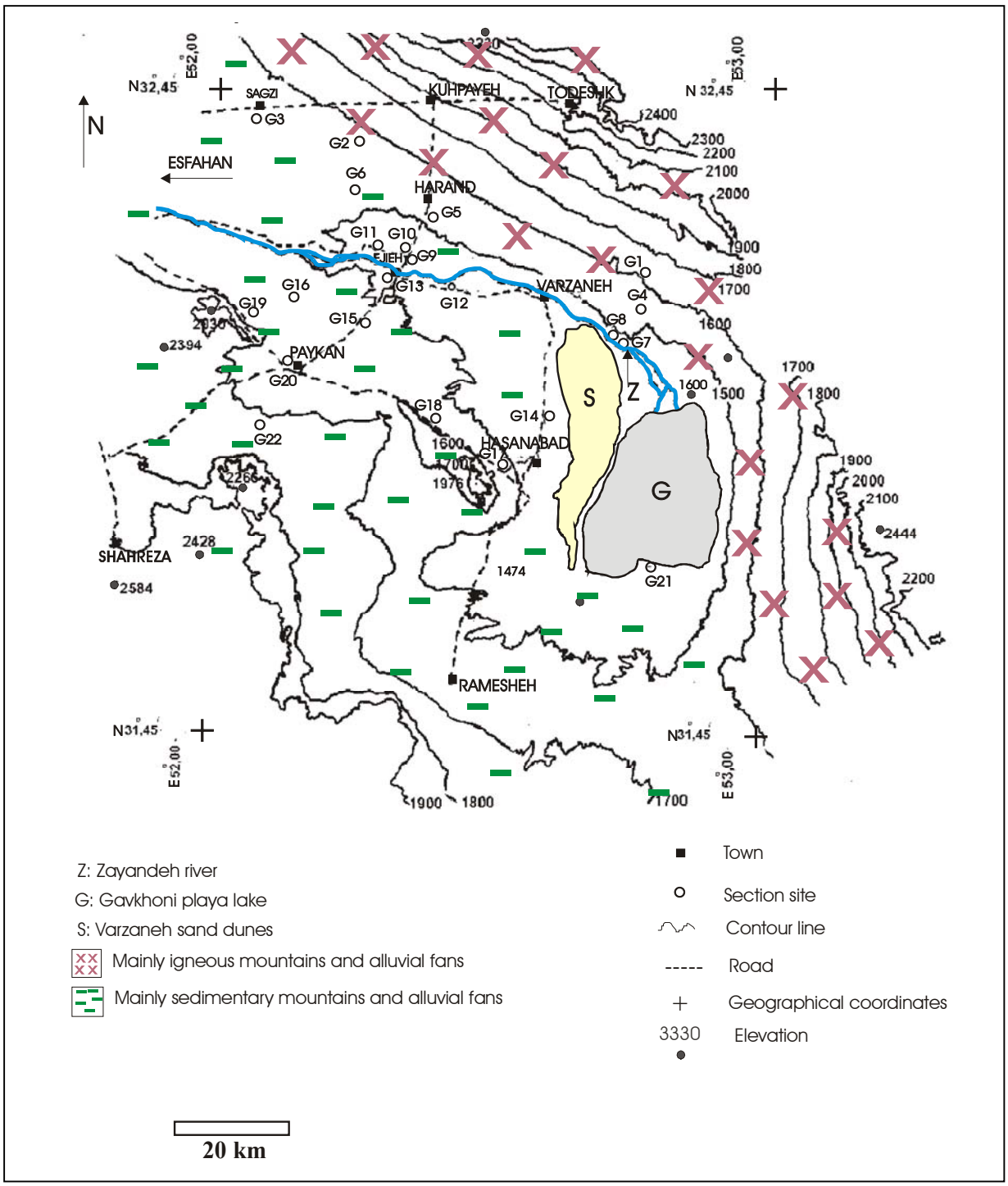

Fig. 5.2 Simplified topographic map of the lower reaches of the drainage basin of the Zayandeh river and the location of stratigraphic sections in the study area.

Section No	Geological situation	Depth (cm)	Location		Main lithology
G1	Stream cut	430	32°,27′,05″N	52°,50′,35″E	gravel
G2	Ghanat well	420	32°,40′,40″N	52°,16′,15″E	Sandstone/sand
G3	Stream cut	220	32°,41′,54″N	52°,07′,49″E	Conglomerate/gravel
G4	Irrigation channel	610	32°,23′,01″N	52°,47′,41″E	Mud
G5	Trench	500	32°,31′,58″N	52°,27′,37″E	Gravel/conglomerate
G6	Irrigation channel	380	32°,34′,31″N	52°,16′,42″E	Conglomerate/gravel
G7	Zayandeh river cut	390	32°,21′,45″N	52°,47′,55″E	Sand, coglomerate
G8	Zayandeh river cut	410	32°,22′,41″N	52°,46′,56″E	Sand, coglomerate
G9	Zayandeh river cut	130	32°,29′,44″N	52°,25′,24″E	Conglomerate, sandstone
G10	Zayandeh river cut	205	32°,30′,34″N	52°,24′,39″E	Mud
G11	Irrigation channel	125	32°,31′,11″N	52°,21′,04″E	Conglomerate/gravel
G12	Zayandeh river cut	310	32°,27′,10″N	52°,29′,10″E	Mud, conglomerate/gravel
G13	Zayandeh river cut	630	32°,26′,44″N	52°,23′,02″E	Conglomerate/
G14	Trench	340	32°,13′,09″N	52°,40′,29″E	gravel
G15	Stream cut	650	32°,24′,34″N	52°,20′,56″E	Conglomerate, mud
G16	Stream cut	630	32°,23′,25″N	52°,09′,19″E	Conglomerate, mud
G17	Trench	210	32°,32′,08″N	52°,35′,52″E	Gravel
G18	Trench	160	32°,14′,50″N	52°,25′,05″E	Gravel
G19	Ghanat well	315	32°,22′,30″N	52°,06′,45″E	Gravel, mud
G20	Stream cut	400	32°,19′,54″N	52°,08′,41″E	Gravel, mud
G21	Stream cut	410	32°,01′,02″N	52°,51′,49″E	Mud
G22	Stream cut	620	32°,12′,20″N	52°,07′,06″E	Conglomerate, mud

Table 5.1 Geological situation, depht, and location of studied sections in the study area.

The southern alluvial fan group is somewhat smaller than the northern one and covers an area of about 1500 km^2, it has an average radial length of 20 km and an average width of 75 km. The apex elevation is 1900 m, and the toe elevation is about 1500 m above sea level. It contains few relatively deeply incised channels, providing nearly continuous good quality exposures of several meters to several decimeters in height. These channels cross-cut the older proximal and medial fan deposits. The fan sediments are derived from a catchment, which is approximately 75 km long, 50 km wide, 3750 km^2 in area and maximum elevation of 2584 m. A surficial fine fraction, derived from mudflow, covers the toe of the fans. The catchment area consists mostly of Cretaceous carbonate rocks. The proximal sector has a average slope of 10.5% and the medial 2.6% and the distal 0.4% (Fig. 5.2).

The Varzaneh aeolian sand field, which cover the toe of the fan, consist of well sorted fine to medium to fine- grained sand (see Chapter 3 for details). The aeolian sand deposits are derived from the alluvial fans that interfinger with the debris-flow deposits in the distal part of the fans.

5.4 Depositional environments and facies

5.4.1. Introduction

The measured vertical sections can be grouped into four major depositional facies associations (see Appendix F for stratigraphic logs). They are debris-flow-dominated alluvial fan, stream-flow-dominated alluvial fan, lake and overbank. Based on Folk (1974) and Tucker (1991)'s terminology, deposits can be divided into three main groups including gravel/conglomerates, sand/sandstone and mud. According to Miall (1985) in Miall 1992's terminology eleven sedimentary facies are identified in this study area. They are unstratified matrix-supported gravel (Gms), massive to crudely stratified clast-supported gravel/conglomerate (Gm), planar cross-stratified, clast-supported gravel/conglomerate (Gp), trough cross–stratified, clast-supported gravel/conglomerate (Gt), massive sand/sandstone (Sm), massive mud-supported sand (muddy sand) (Sms), trough cross-stratified sand/sandstone (St), planar cross-stratified sand/sandstone (Sp), massive red mud (Fm), massive yellow mud (Fsc), laminated-khaki mud (Fl). The main characteristics of each facies are briefly described and interpreted as follows (see Table 5.3).

5.4.2 Gravel/conglomerate deposits

According to texture and induration these deposits can be divided into matrix-supported gravel and clast-supported gravel/conglomerate deposits.

5.4.2.1 Matrix-supported gravel deposits

These deposits include igneous and sedimentary lithology and consist of only one facies namely unstratified matrix-supported gravel (Gms). This facies is observed in five sections (No. G4, G5, G17, G18, G19) in the study area (see Fig. 5.2 and Table 5.1for position of sections No).

Unstratified matrix-supported gravel (facies Gms)

Facies Gms is characterized by unstratified, matrix-supported gravel, locally clast-supported, a disorganized nature of grains, typically ungraded, chaotic pebble fabric and broad lenticular geometry (Fig. 5.3). The deposits are cohesive and non-cohesive, depending on the amount of fine-grained sediments. This facies extends both in the southern and the northern part of the Zayandeh river but wider distribution is in the northern part. It is sharply

underlain by muddy deposits throughout the study area. Its maximum thickness recorded in six sections is about 4 m.

The clasts are typically angular to sub-angular and vary in shape from bladed to equant. The deposits consist of dominantly brown, yellow to purple limestone, green to olive sandstone and shale in the southern alluvial and violet andesite, white tuff and black andesite-basalt in the northern alluvial fan.

The grain size analysis of five representative samples from the studied sections shows that all samples have poor sorting and contain the full range of grain classes from clay to fine cobble. The granule, pebble and fine cobble sizes together make up 31-58%, sand 40-50% mud 5-18%. Average size of ten largest and maximum size of clasts was measured in sections No. G1, G5, G17, G18, G19 (Table. 5.2)(see Fig. 5.2 and Table 5.1 for position of sections No).

Section No	A	B	Section No	A	B
G2	20	45	G13	36	180
G3	71	118	G14	10	20
G4	90	140	G15	35	110
G5	49	100	G16	130	260
G6	20	40	G17	29	35
G7	20	40	G18	19	40
G9	36	180	G19	30	37
G11	52	77	G21	42	52
G12	20	40	G22	75	118

Table 5.2 Average size (in mm) of the ten largest (A) and maximum size (B) of clasts in the study alluvial sediments.

A high degree of desert varnish is mostly observed on the surface of sandstone and igneous lithics. Both normal and inverse grading of coarse clasts are observed locally. The winnowing of fine-grained sediments from the exposed debris flows is present in some localities. A lustrous appearance often characterizes rock fragments. Bubble sand structure is a common feature in the upper layer of this facies, if recently deposited. It shows a spongy structure in the sand sediments. Upper part of this facies (from depth of 20 to 100 cm) contains abundant fibrous displacive gypsum especially in the southern alluvial fans. In some places the gypsum content reaches up to 30%.

The framework clasts consist of abundant igneous particles in the northern part and sedimentary clastic in the southern part. The sediments consist of about 90-95% carbonate lithic grains in sections No. G17, G18, G19 in the gravel fraction and 75-80% sedimentary (mostly carbonate), 7%-10% igneous and 1% metamorphic lithic grains, 5%-13% quartz, and 1-4% feldspar mineral grains in the sand fraction. Composition of grains both in gravel and sand fractions is about 95% igneous lithics in the sections No. G1 and G5 (see Fig. 5.2 and Table 5.1 for position of sections No).

Fig. 5.3 Field photograph (section No. G18) showing massive to crudely stratified-matrix-supported gravel facies (Gms) developed in the southern alluvial fan group (see Fig. 5.2 and Table 5.1 for position of sections).

Interpretation

Matrix-supported, unsorted, muddy, sandy, cobble to pebble-sized gravel and to a certain extent inversely graded textures are suggestive of a debris flow origin (Pierson, 1980; Blair & McPherson, 1999; Blair, 1999). Such facies is generally regarded as a product of cohesive debris flow (cf. Deck *et al.*, 1996). The presence of the intervening layers of clast-supported fabric indicate reworking by stream-flood flows (cf. Ryang & Chough, 1997). Inverse graded bedding indicates that dispersive pressure operated (Lowe, 1988). Debris flow deposits are restricted to the proximal fan, or mixed with water-laid deposits in the medial fan and are dominant throughout the stratigraphic sequence of the fans. The winnowing of fines

from the exposed debris flows probably resulted from the washing of the surficial deposits by runoff that commonly follows debris flow deposition or by overland flow generated by heavy rainfall. Wind may also account for partial winnowing of fine fraction of these deposits (Blair & McPherson, 1992). Bubble structure, which is very unstable and, therefore, generally only exists immediately after depositions, is produced from the entrapment of air bubbles (Reineck & Singh, 1980). Dominance of debris flow deposits indicates semi-arid paleo-climate (Blair & McPherson, 1995).

Abundant angular siliciclastic particles in the northern debris-flow deposits indicate that sediments were derived largely from a drainage network of the igneous rocks. Abundant angular carbonate lithics in the southern debris-flow deposits suggest that sediments were originated largely from a drainage network of the sedimentary rocks exposed along the southern part of the basin.

Phreatic desert gypsum precipitates from evaporation of ground water where water table is within 1 to 2 m of the land surface (Kulke, 1974, Watson, 1989 in Thomas, 1989). Acicular and fibrous gypsum crystals form probably as a result of migration of Ca^{++} and SO_4^{--} rich water to surface by capillarity and precipitation after saturation. Most probably the origin of these ions is in the pore waters of the marl that underlie the matrix–supported deposits.

5.4.2.2 Clast-supported gravel /conglomerate deposits

These deposits are observed in eighteen vertical studied sections. The size of average ten largest and maximum size of clasts in these sections were measured (Fig. 5.2) (see Table 5.1 for position of sections No).

Clast–supported gravel/conglomerate deposits consist of about 80-95% carbonate and 20-15% siliciclastic lithic grains in the sections No. G9, G13, G15, G16, G22 and of about 95% igneous lithic grains in the sections No. A2, A3, A5,. Lithology in the sections No. G6, G7, G11, G12, G14 include carbonate, siliciclastic, igneous and metamorphic lithic grains in order of decreasing frequency. The sections No. G4 and G21 consist of 50% igneous and 50% sedimentary lithic grains.

Based on texture and sedimentary structure these deposits can be divided into three facies including massive to crudely stratified clast-supported gravel/conglomerate (facies

Gm), planar cross-stratified, clast supported gravel/conglomerate (facies Gp), and trough cross–stratified, clast–supported gravel/conglomerate (facies Gt).

Massive to crudely stratified, clast-supported gravel/conglomerate (facies Gm)

It is represented by massive to crudely stratified sandy gravel to conglomerate, mostly pebble-sized framework clasts, normal grading, wide variation in texture and grain composition. This facies consist of a few decimeters to few meters of gravel/sandy conglomerate to openwork gravel/conglomerate (Fig. 5.4). Its geometry mostly is broad lenticular, wedge–shaped and channel-shaped with erosional base and sheet-like in some places in the northern alluvial fan. The lower boundary surface is erosive, locally scoured (such as gutter casts, rarely also flute cast) mainly undulatory, slightly inclined in the southern alluvial fan (5th order boundary surface of Miall, 1988). Mud rip-up clasts, ranging from few to few ten centimeters are common in the conglomeratic deposits. The open framework deposits are indurated by intergranular calcite cement in some places. In the southern alluvial fan, the framework grains include mainly cabonate lithics in composition and rounded to well rounded in shape whereas in the northern alluvial fan, they mostly consist of igneous lithics and angular to sub-rounded in shape.

Interpretation

Clast-supported gravels and conglomerates record bedload deposition from stream flows. Openwork fabric and textural segregation of gravel and sand indicates deposition in gravel-bed streams during waning floods (Collinson, 1996 in Reading, 1996).

Such a facies originates from high energy flow, transporting and accumulating coarse bedload and keeping sand and finer material in suspension (cf. Reineck & Singh, 1980). The remaining pore space between the gravel is usually infiltered later by sand when the velocity has increased (cf. Rhee & Chough, 1993).

Gravel is transported only if the current reaches a certain critical velocity (around 1m/s) and in slower currents it may occur as lag deposits. They are deposited by steep gradients, high width/depth ratio and low sinuosity braided rivers. The erosional base, cut and fill structures, discontinuous lenticular geometry and the nature of boundary surfaces are suggestive of deposition in a stream channel of alluvial fan (c.f. e.g. Reineck & Singh, 1980)

or as longitudinal bars (cf. e.g. Einsele, 1992). Sheet like geometry is indicative of unconfined ephemeral flows (Ryang & Chough, 1997).

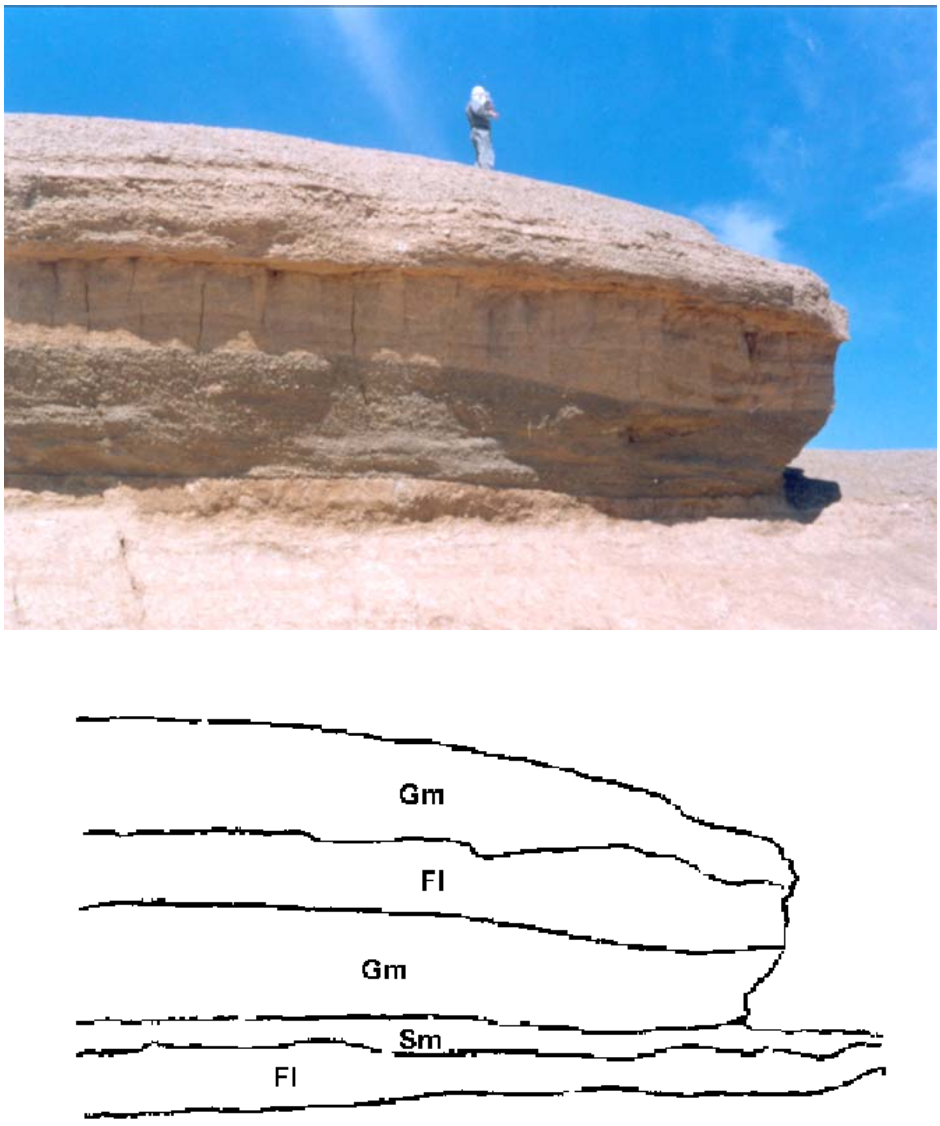

Fig. 5.4 Sketch and photograph (section No. G22) showing representative sample of massive to crudely stratified gravel/conglomerate facies (Gm). Laminated khaki mud (Fl), Massive sand/sandstone (Sm) (see Fig. 5.2 and Table 5.1 for position of section No).

Sheet flooding (unchannelized flow) and stream flooding (broad, poorly channelized) flows within ephemeral channels following intense thunderstorms. Sharp bases, distinct lower boundaries, poor sorting and limited extent of the beds are suggestive of erosion, short distance transportation, and deposition by ephemeral flows rather than perennial flow (Bridge, 1984) in semi-arid regions or steep slopes on proximal fans (Postma, 1983) or in distributary

channels of the proximal zone of alluvial fans (Salder & Kelly, 1993). Abundance of mud rip-up clasts might be related to strong erosion of the underlying mud layers or to failure of channel banks during flood events.

Position of the lithofacies within the successions and its occurrence on the top of mud sediments and its characteristics represent deposition in shallow channels which were periodically active in distributary channels of alluvial fans (cf. Kelly & Olsen, 1993). Presence of this facies is an indicator of at least occasional periods with strong rains during deposition by a longer episodic, periodic or even a perennial discharge (cf. Amini, 1997).

Planar cross-stratified, clast-supported gravel/conglomerate (Facies Gp)

This facies is marked by planar cross-stratified, clast–supported sandy gravel /conglomerate, mostly granule to pebble framework clasts and a wide range variation in texture (Fig. 5.5). The size of the ten largest clasts is similar to facies Gm, except for gravels deposited by the Zayandeh river, occurring in outcrops along this river. Mud rip-up clasts are observed along the Zayandeh river with decimeter down to few centimeters in size. The thickness of the facies recorded at six sections (No. G1, G5, 7, G13, G15, G16) ranges from 60 to 160 cm (see Fig. 5.2 and Table 5.1 for position of sections). The external geometry is usually lenticular, wedge-shaped with a scoured erosional base. In some places, set boundary is undulatory with a convex top. Individual forests are parallel and in some localities laterally tangential. The foresets are sometimes graded and show changes in grain size along the sets. The slope of these foresets ranges from 25^{o} to 40^{o}.

Interpretation

This facies was deposited under high-energy flow conditions similar to the facies Gm (cf. e.g. Ryang & Chough, 1997). Tabular cross-bedding, in which the foresets are graded and show changes in grain-size along the set, probably reflect stage fluctuations over the crest of the bar which possess active slip faces (Collinson, 1996 in Reading, 1996) in braided streams. Local high-angle dipping planar cross-bedding is related to migration of high bars with steep slip faces (Reineck & Singh, 1980).

Some authors represent mid-channel or channel-confluence bars, formed in deep sectors of a channel (Steel & Thompson, 1983) while others compare this feature with the large bedforms developed on the flanks of bedrock valleys as a result of catastrophic floods (Talbut

& Allen, 1996 in Reading, 1996).This facies is interpreted as result of migration of longitudinal and lingoid bar (Einsele, 1992) in ephemeral rivers in semi-arid regions (Miall, 1992).

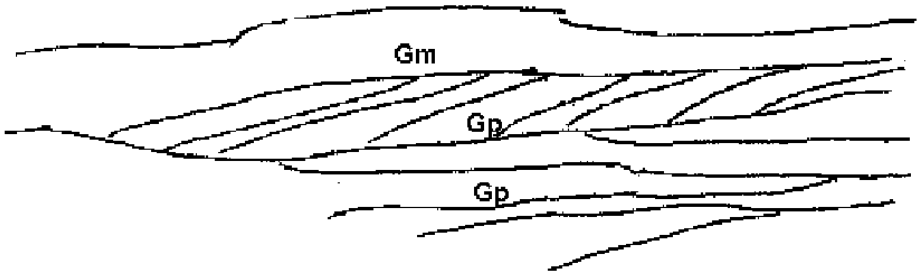

Fig. 5.5 Sketch and photograph (section No. G16) showing an example of facies planar cross-stratified conglomerate (Gp) overlain by crudely stratified to massive conglomerate (Gm) (see Fig. 5.2 and Table 5.1 for position of section No)

Situation, lithology and overlaying lower part of fining–up sequence of point bars of the Zayandeh river suggest that this facies is ,in some places, a product of a meandering river. (Reineck & Singh, 1980).

Trough cross-stratified, clast-supported gravel/conglomerate (facies Gt)

This facies is marked by cross-stratified, clast–supported gravel/conglomerate, granule-sized framework grains, and shows a wide variation in texture, composition and thickness. This is a very common facies along the Zayandeh river. Mud rip-up clasts reach up to 10 cm in length. The base is concave, channel-shaped, lenticular, and asymmetrical in shape (Fig. 5.6). The upper boundary is mainly undulatory flat to slightly inclined.

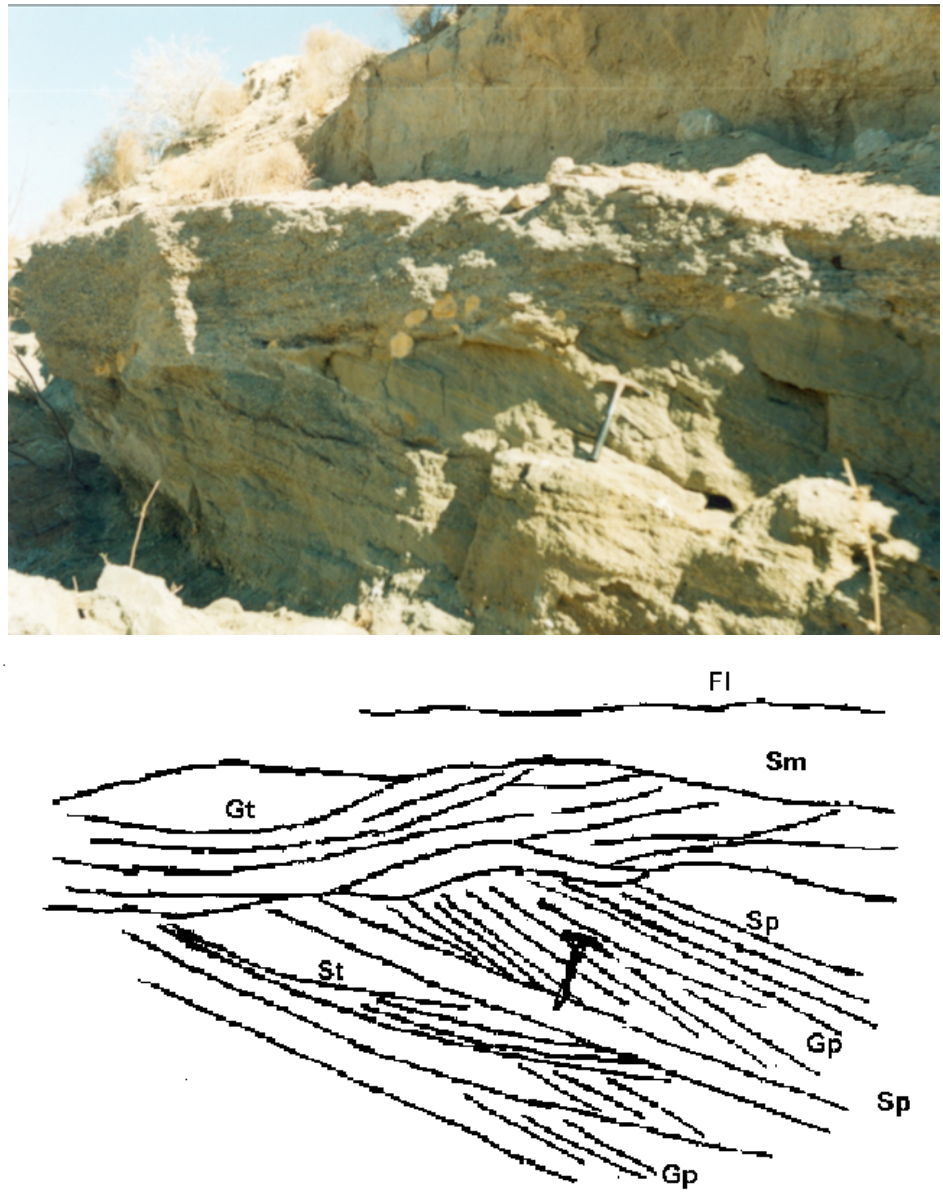

Fig. 5.6 Sketch and photograph (section No. G7) illustrating of facies trough cross-stratified grave/conglomerate (Gt) with erosional base. Massive sand (Sm), planar cross-stratified, gravel/conglomerate (Gp), trough cross-stratified sand/sandstone (St), Planar cross-stratified sand/sandstone (Sp) (see Fig. 5.2 and Table 5.1 for position of section No).

Maximum thickness of this facies placed in the central part is about 50 cm. Horizontal bedding with thickness of a few centimeters and normal graded bedding is observed in some localities. The slope of isolated layers ranges from slightly inclined to up to 20^{o}. The ten largest clasts of gravel/granules along the Zayandeh river is between 2 to 6 mm recorded in three sections (No. G7, G8, G9) (see Fig. 5.2 and Table 5.1for position of sections No).

Interpretation

This facies is deposited during high-energy flow conditions (e.g. Reineck & Singh, 1980; Ryang & Chough, 1997) similar to the facies Gm and Gp. Channel cross-beds may be produced in the filling-up of small alluvial or erosional channels (e.g. Reineck & Singh, 1980). Similar restricted (narrow) channel conglomerates occur in proximal parts of distributary alluvial systems (Postma, 1983). Flat-bedded gravels form by vertical accretion on longitudinal bars (Rust, 1984). In some localities along the Zayandeh river, this facies may result from the activity of a meandering river and it was deposited at the base of its point bar. An erosional scoured base and presence of mud rip-up clasts mainly in the lower part are indicative of scouring and subsequent filling in coarse-grained meandering or in braided rivers.

5.4.3 Sand/sandstone deposits

According to texture and induration they can be divided into mud-supported sand and clast-supported sand/sandstone deposits.

5.4.3.1 Mud-supported sand deposits

These deposits can be classified into two groups: igneous and sedimentary lithology and consist of only one facies namely unstratified mud-supported sand (facies Gms). This facies is observed in two sections (No. G1, G5) in the study area (see Fig. 5.2 and Table 5.1 for position of sections No) .

Massive mud-supported sand (facies Sms)

This facies can be compared with facies Gms in Miall (1977 & 1992) terminology. It is characterized by khaki to yellow massive muddy very fine to coarse sand (matrix-support sand), alternating with gravelly muddy sand and rich in calcrete nodules in some localities. It shows a lenticular, wedge-shaped geometry and an erosional upper boundary (Fig. 5.7). This

unit is observed only in the northern alluvial fan group and changes laterally and vertically into the facies Gms in most localities. It consists of approximately 95% igneous lithics in composition. Maximum thickness of this facies recorded in two sections (No. G1, G5 is about 150 cm (see Fig. 5.2 and Table 5.1 for position of sections No).

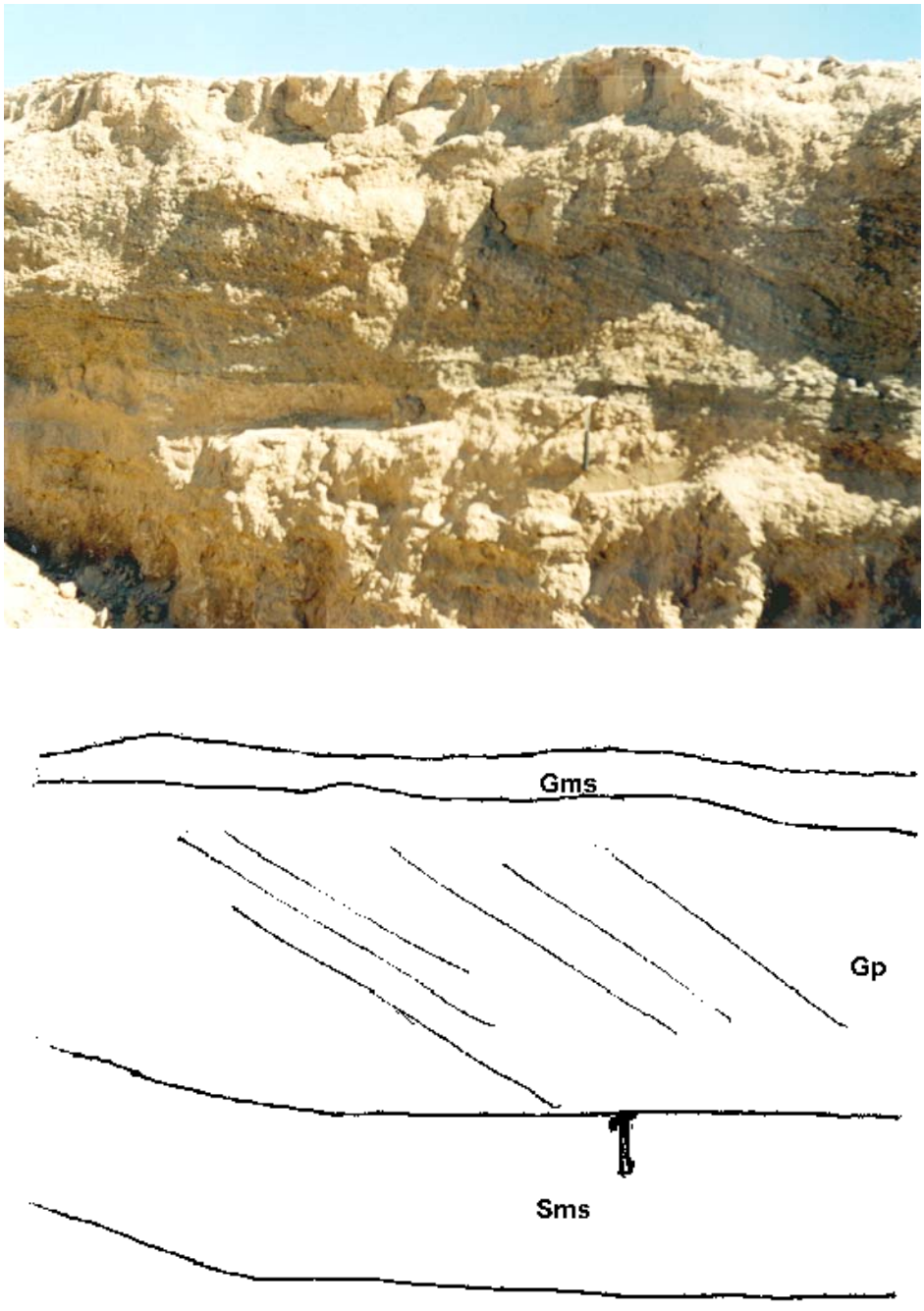

Fig. 5.7 Sketch and photograph (section No. G5) showing example of facies muddy sand (Sms). Planar cross-stratified conglomerate (Gp), Unstratified matrix-supported gravel (Gms) (see Fig. 5.2 and Table 5.1 for position of section No).

Interpretation

Matrix-supported, unsorted gravelly sand bodies might suggest deposition from visco-plastic sand flows. It is generally considered to be intermediate between debris flow and normal stream flows and was termed hyper-concentrated flood flow. Such flood flows have been related to sand-sized debris flows that take up water as they move down stream (Smith, 1986) or developed by adding sediments to fast flowing stream flows (Turner & Monro, 1987). Well-developed calcrete nodules indicate long subaerial exposure under semi-aridic climate before deposition of the following unit (c.f. Kulke, 1974).

5.4.3.2 Clast-supported sand/sandstone deposits

These deposits are observed in the seven vertical studied sections (No. G7, G8, G9, G12, G13, G15, G22) in the study area (see Fig. 5.2 and Table 5.1 for position of. It consists of 35-63% sedimentary lithic (mostly carbonate), 19-45% igneous lithic, 3-7% metamorphic lithic grains, 7-13% quartz and about 1% feldspar mineral grains in the sections (No. G9, G13, G15). Lithology in the sections (No. G7, G8, G12), include 16-20% sedimentary lithic (siliciclastic and carbonate), 50-70% igneous and 10-15%metamorphic lithic grains 2-13% quartz and about 1% feldspar mineral grains in order of decreasing frequency. Section A21 consist of 55%, sedimentary lithic (mostly carbonate), 40% igneous lithic, 5% quartz (see Fig. 5.2 and Table 5.1 for position of sections).

Based on texture and sedimentary structure these deposits can be divided into three facies including massive sand/sandstone (facies Sm), trough cross-stratified sandstone (facies St), and planar cross-stratified sand/sandstone (facies Sp).

Massive sand/sandstone (facies Sm)

This facies found in sections No. G9 and G13, is represented by structuresless, mature sand/sandstone with slight gravel admixture in some localities and abundant gastropod and ostracod shells. It is mostly broad lenticular, tabular, locally wedge shaped, and shows flat boundaries. Contact with underlying and overlaying units is usually graditional and relatively flat. Its maximum thickness recorded in the two studied sections (No. G7, G12) is about 50 cm (Fig. 5.8). The facies usually occurs on the top of a channel shaped conglomerate with mud rip-up clast along the Zayandeh river (see Fig. 5.2 and Table 5.1 for position of sections No).

Interpretation

Mature massive sand bodies are attributed to rapid deposition from suspension during floods (Collinson, 1996 in Reading, 1996). Gravel size clasts have been supported by combined effects of fluid turbulence and matrix (sand) buoyancy (Rhee & Cough, 1993)

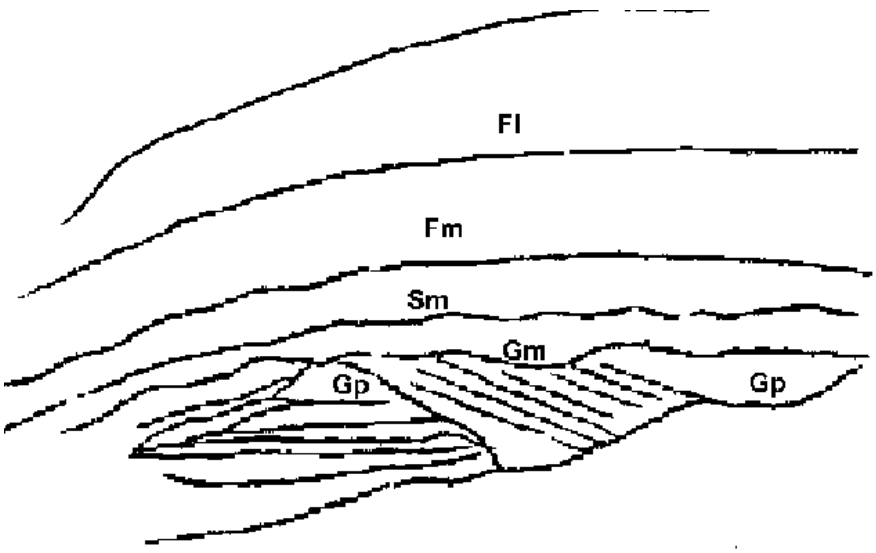

Fig. 5.8 Sketch and photograph (section No. G12) showing example of facies massive sand (Sm). Facies massive red mud (Fm), massive to crudely stratified gravel (Gm), planar cross-bedded gravel (Gp), laminated khaki mud (Fl) (see Fig. 5.2 and Table 5.1 for position of section No).

Trough cross-stratified sand/sandstone (facies St)

This facies, observed in sections (No. G9 and G13) is marked by trough cross-bedding, fine to coarse-grained, khaki sand/sandstone. Its geometry is mainly lenticular, wedge and channel–shaped, concave downward, and asymmetrical. It is mainly underlain by crudely stratified to massive conglomerate and shows a lower and upper sharp boundary (Fig. 5.9). In some places, this facies is underlain by muddy deposits (facies Fsc). Individual laminations range from few to a few tens of millimeters in thickness. Lateral accretion of sets locally is observed. The facies shows high variation in thickness and its maximum thickness reaches up to 60 cm in the central part. It laterally passes into gravelly sandstone and massive to crudely stratified conglomerate. The gradients of laminations change from slightly inclined to up to 30^0 and dip direction is also variable from the west to the east. At the base of some set laminations, lag gravel is present.

Interpretation

The main characteristics of the facies: erosional base, lateral accretion, channel-shaped and lenticular geometry is indicative of deposition in a channel and/or at subaqueous channel dunes under lower regime (Miall, 1992) in ephemeral rivers in a semi arid region (Parkash *et al*, 1983). It can be interpreted as a result of scouring channels in high flood stage and subsequent filling in waning stages (Miall, 1992). Lateral changes from sandstone to gravelly sandstone and conglomerate indicates changes in velocity, variable dip direction of cross bedding and vertical and lateral variation of the facies probably result from high variability of discharge and/or rapid shifting of the channels, characteristic of ephemeral braided rivers (Amini, 1997). Occurrence of the facies on the top of lag type gravel and facies Gm most likely suggest its development as a result of migration of three-dimensional dunes in channels under the conditions of the upper part of the lower flow regime (Hjellbakk, 1997). Local lag type deposits within the unit can be considered as deposition in minor channels cut in the sediments due to change in discharge values or shifting in channel position, typical of periodically active channels (Amini, 1997)

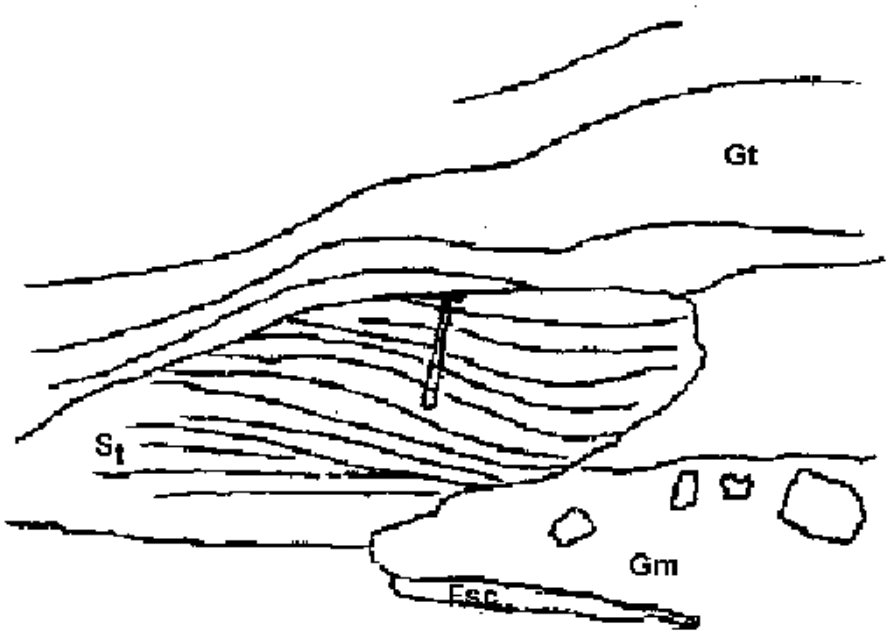

Fig. 5.9 Sketch and photograph (section No. G9) showing facies trough cross-stratified sandstone (St). Gt (trough cross-stratified conglomerate), Gm (Massive to crudely stratified conglomerate), Fsc (massive yellow mud). Hammer length is 30 cm (see Fig. 5.2 and Table 5.1 for position of section No).

Planar cross-stratified sand / sandstone (facies Sp)

Facies Sp, observed in sections (No. G8 and G15), is characterized by fine to coarse planar cross-bedded sand/sandstone with minor gravel, ranging from few to 60 cm in thickness. It shows mainly flat boundary, tabular, locally wedge-shape and lenticular geometry (Fig. 5.10).

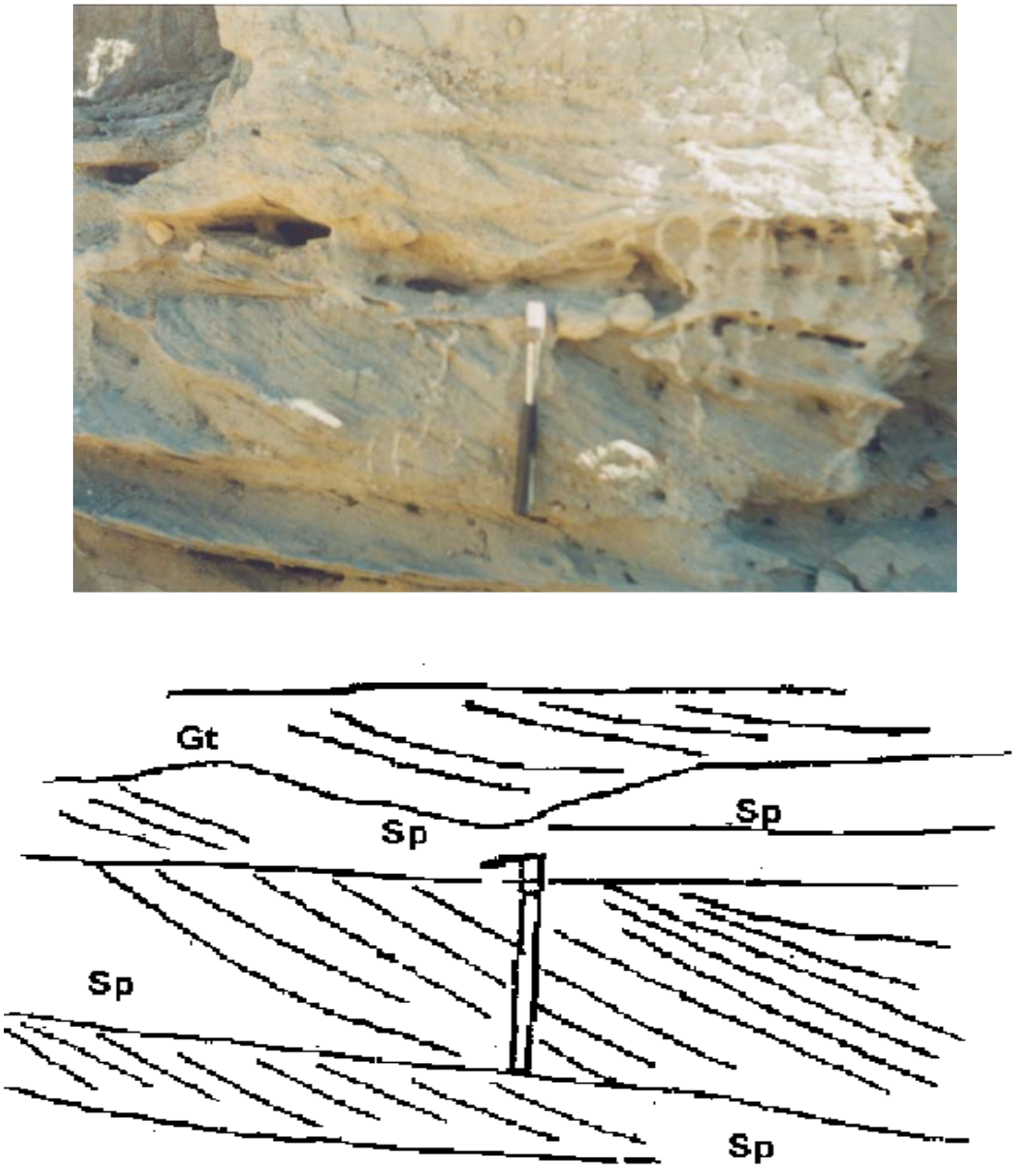

Fig. 5.10 Sketch and photograph (section No. G8) showing example of facies planar cross-stratified sand/sandstone (Sp) with lenticular geometry overlain by facies trough cross-stratified gravel (Gt) (see Fig. 5.2 and Table 5.1 for position of section No).

Foresets are parallel to slightly tangential locally, with slopes of 15^{o}-40^{o}. The maximum set thickness is up to 40 cm. Large amounts of mud rip up clasts with up to 4 cm in diameter are observed at the top of this facies in some localities. Contact with underlying and overlaying units is usually sharp. It changes upward to channel–fill conglomerate and massive sand respectively in most localities.

Interpretation

The sedimentary structures and grain size of this facies indicate formation by processes operating in the lower to middle part of the lower flow regime, either deposition in areas on the floodplain, or deposition during periods of low water level or waning flow in channels (cf. Hjellbakk, 1997). Planar stratification, grain size (fine to coarse sand and minor gravel), large amounts of mud rip-up clasts and the position of the facies are also indicative of deposition by sand waves or transverse bars of lingoids (cf. Abdullative, 1989). Smaller tabular sets suggest that sets are produced by straight–crested subaqueous dunes and, less commonly, scour bars and chute bars. (McCabe, 1977). They result from migration of simple foreset bars and sand waves (Miall, 1992), bar top deposits (Amini, 1997), and dunes with straight crest (Wizevich, 1992). Some sets (up to 30 cm) were probably formed by large transverse or lingoid bars, which may have been bank attached, or of mid-channel origin (cf. McCabe, 1977)

5.4.4 Mud deposits

Mud deposits indicate a wide range of variation in thickness, sedimentary structure color and narrow composition in the studied sections. They are dominated by massive to laminated types of yellow, khaki and red in color. They are interbedded with sandy and gravelly layers in some places. Based on color, texture, geometry and sedimentary structure three major facies including massive red mud (facies Fm), massive yellow mud (facies Fsc), and laminated khaki mud (facies Fl) were determined in the study area.

5.4.4.1 Massive red mud (Facies Fm)

This facies is represented by a red to purple mud, well-developed calcrete nodules and relatively high clay/silt ratio. It ranges from 50 to 200 cm in thickness in three found sections (No. G4, G5, G12) and is overlain by facies Fl in the Zayandeh river cut bank (Fig. 5.11). It is only observed in the northern part and along the Zayandeh river. The external geometry is mainly broad tabular with graditional boundary. The average carbonate is about 15% and

average clay-sized content is %60 in three sections. The clay minerals consist of smectite, illite, chlorite, and kaolinite (Appendix B4, sheets No. 2 & 3).

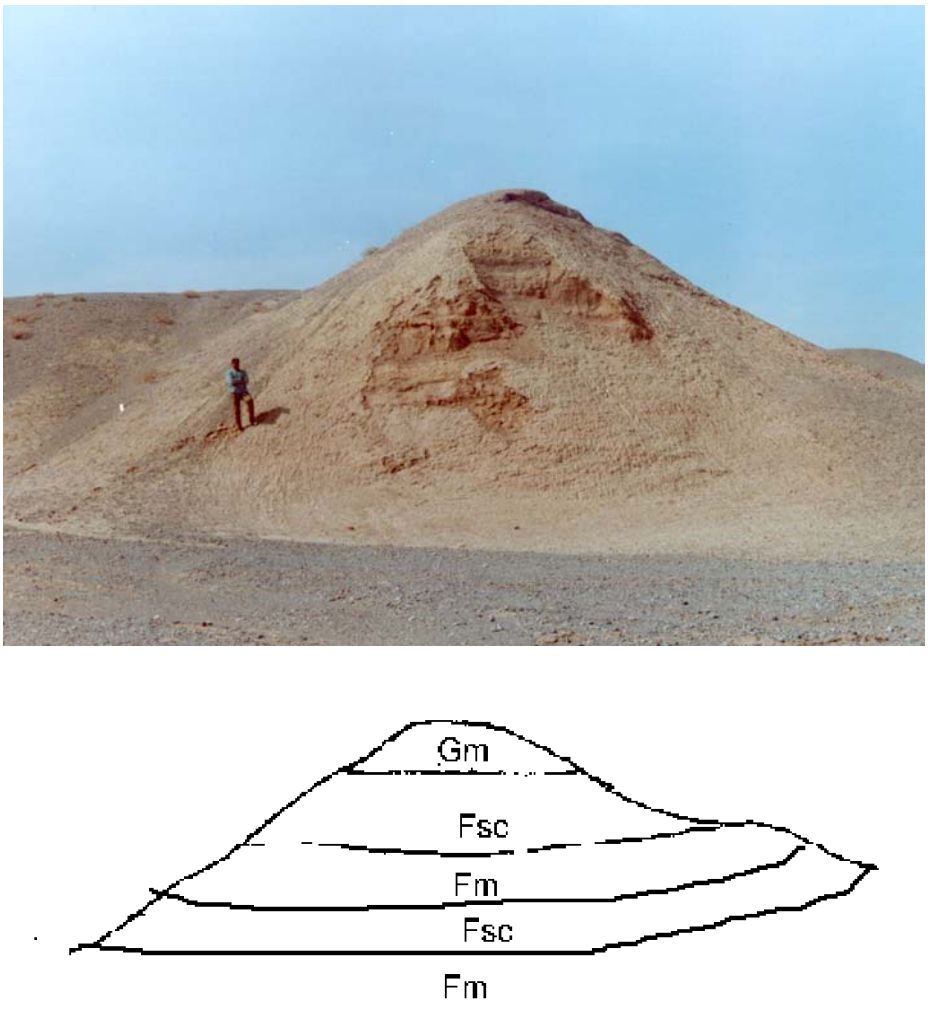

Fig. 5.11 Sketches and photograph (section No. G4) showing example of facies massive red mud (Fm) overlain by facies (Gm) at top with an erosional boundary (see Fig. 5.2 for position of stratigraphic section No). Gm (Massive to crudely stratified gravel), Fsc (massive yellow mud), Fm (facies massive red mud) (see Fig. 5.2 and Table 5.1 for position of sections).

Interpretation

The major characteristics of this facies may indicate rapid settling of suspended grains (silt and clay fractions) below water level in pond or lake, oxidizing condition during and after deposition (cf. Ryang & Chough, 1997). The relatively minor content of carbonate, color and the type of the clay minerals indicate that the provenance of these sediments is most probably from deeply weathered igneous rocks located in the northeast of the area. Lack of

plant remains probably reflect non-development of shallow lacustrine and back swamp environments in wet climate (Shanley & McCabe 1993) and indicative of a semi-arid and ephemeral conditions of deposition. Well-developed calcrete nodules indicate long subaerial exposure before deposition of the following unit in origin (Hjellbakk, 1997). In semi-arid zone most of the calcretes are pedogenic in origin (Kulke, 1974). Calcretes develop by crystallization of calcium carbonate from ascending ground water. This facies could also be deposited on the distal part of the northern alluvial fan.

5.4.4.2 Massive yellow mud (facies Fsc)

This facies is characterized by mainly massive, locally laminated, yellow to green mud, interbedded with sand layers up to a few centimeters thick in some places (Fig. 5.12). Its thickness ranges from 150 to 700 cm in the studied sections (No. G2, G4, G6, G9, G10, G13, G14, G15, G16, G17, G19) (see Fig. 5.2 and Table 5.1for position of sections). It is mostly broad lenticular, and of wedge-shaped geometry. In most localities it contains few gastropod and ostracod shells. The average carbonate content ranges between 14% (section No. G2) to 40% (section No. G13). The clay minerals consist of smectite, illite, kaolinite, chlorite and rectorite? (Appendix B4, sheets No. 1, 4, 6,7, 8, 9, 10, 11, 12,).

Interpretation

The sediments of this facies formed in a sub-aqueous lacustrine environment when a possibly small-scale lake was formed or base level rose toward the basin margin (cf. Ryang & Chough, 1997). The dominant sedimentary process was settling from suspension, accompanied by periodic input of current-transported sands. Interlayering of thin-laminated fine sand may be as a result of vertical accretion in channels especially where the deposits display a channel-shaped geometry (Amini, 1997). Lack of bedding results from rapid deposition by flood. Homogenization by bioturbation can almost be excluded due to color, indicating absence of organic matter.

Fig. 5.12 Sketch and photograph (section No. G13) illustrating an example of facies massive yellow mud (Fsc) overlain by facies massive to crudely stratified gravel (Gm) along an erosional scoured base(see Fig. 5.2 and Table 5.1 for position of section No).

5.4.4.3 Laminated khaki (cream) mud (facies Fl)

This facies is represented by mostly well-laminated to locally massive khaki-colored mud, often with a blocky fracture pattern and interbedded by gravel and sand layers in some studied sections (Fig. 5.13). It is located in the fining-up sequence of the study area. The external geometry is mainly wedge-shaped, channel-shaped, irregular flat top and base and

sheet–like in some places. Horizontal and vertical burrows and root traces are relatively abundant in the upper part of this facies (Fig. 5.14). It ranges between 50 to 150 cm in thickness in six the studied sections (No. G7, G8, G12, G20, G21, G22) (see Fig. 5.2 and Table 5.1 for position of sections No).

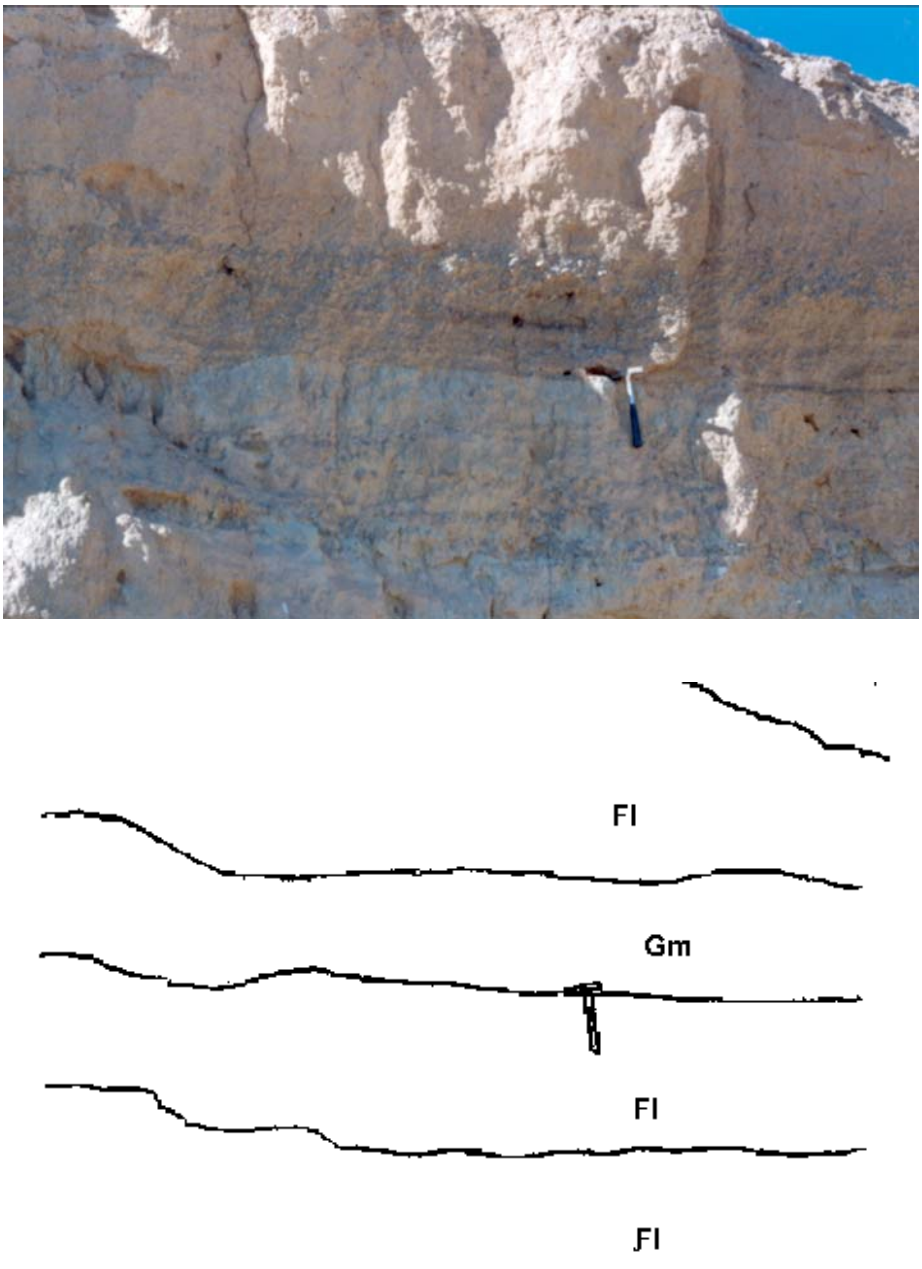

Fig. 5.13 Sketch and photograph (section No. G20) representative of facies laminated khaki mud (Fl), interbedded with facies massive to crudely stratified gravel (Gm), located at the bank of an ephemeral river in the southern alluvial fan (see Fig. 5.2 and Table 5.1 for position of section No).

The average carbonate content ranges between 15% (section No. G12) to 37% (section No. G21). The clay minerals consist of smectite, illite, kaolinite, and chlorite (Appendix B4, sheets No. 14, 13, 5).

Fig. 5.14 Field photograph indicating borrows and/or root traces in the facies Fl.

Interpretation

General characteristics of the facies (Fl) and its position in the fining-up sequence shows that it was deposited in low energy conditions in overbank or low gradient flood plain environments during varying flood stages (cf. Miall 1977; Hjellbakk, 1997). Such facies were deposited either on the floodplain or in abandoned channels such as ox-bow lakes (Hjellbakk, 1997). Sand layers, interbedded with mud layers, may reflect subsequent flooding and new channeling into these fine-grained deposits (Bridge, 1984). Relatively thick layers of massive mud probably represent deposition by sheet flooding during major flood events (Collinson, 1996 in Reading, 1996).

5.5 Facies associations

Based on the studied vertical sections, four major facies associations can be suggested. They are debris-flow-dominated alluvial fan, stream-flow-dominated alluvial fan, lake and overbank, representing four depositional environments (Table 5.3)

5.5.1 Facies association I: Debris-flow-dominated alluvial fan

This facies association, the most common sedimentary facies in the study area, is characterized by matrix-supported gravel (facies Gms) and muddy sand or matrix supported sand (facies Sms). The former extends both in the northern and the southern alluvial fans and the later is found only in the northern alluvial fans. Regarding lithology, the matrix-supported gravel can be divided into two groups, including igneous and sedimentary lithic grains but the facies Sms includes only igneous lithic grains. They are generally a product of cohesive debris flows. Debris flow sediments are restricted to the proximal fan, or mixed with water-laid deposits in the medial fan and indicate deposition in semi-arid (paleo-)climate conditions.

5.5.2 Facies association II: Stream-flow-dominated alluvial fan

It consists of five facies including massive to crudely stratified (facies Gm), planar cross-stratified (facies Gp), trough cross-stratified (facies Gt) clast supported gravel/conglomerate, and, trough cross-stratified (facies St), planar cross-stratified (facies Sp) sand/sandstone. The first three facies (Gm, Gp, Gt) are mostly deposited under high energy flow, steep gradients in ephemeral braided or meandering rivers of alluvial fan environment in semi-arid region. Sandy conglomerates can be interpreted as a result of scouring channels in high flood stage and subsequent filling in waning stages of rivers. The second two facies (St, Sp) are attributed to deposition in a channel and/or at sub-aqueous channel dunes under lower to middle parts of lower flow regime in ephemeral rivers in a semi-arid region.

Asso. facies	Facies	Description	Interpretation, depositional environment
I	Gms	Pebble/cobble sized, matrix-supported, unstratified gravel with broad lenticular shape.	Deposition by cohesive mass debris flow with slight fluctuation in flow stage in proximal fan.
I	Sms	Massive muddy sand, rich in calcrete nodules, lenticular shaped.	Deposition in proximal alluvial fan by very fine-grained debris flow.
II	Gm	Pebble/cobble sized, clast-supported, massive to crudely stratified, wedge-shaped gravel/conglomerate.	Deposition in shallow channel with periodic activity. Result of rapid deposition in ephemeral system in semi-arid region on rather steep slopes.
II	Gp	Pebble/cobble sized, clast-supported, planar cross-bedded, lenticular to wedge-shaped gravel/conglomerate.	Deposition in high energy flow in deep sectors of a channel.
II	Gt	Pebble/cobble sized, clast-supported, trough cross-bedded, lenticular channel-shaped gravel/conglomerate.	Filling up of small alluvial or erosional channel. Indicative scouring and subsequent sedimentation in braided or meandering river.
II	Sp	Planar cross-bedded, lenticular, wedge-shaped sand/sandstone	Deposition by lingoid or transverse bars. A product of small scale, straight crested dunes, scour bars, chute bars.
II	St	Trough cross-bedded, wedge-shaped sand/sandstone.	A product of three-dimensional dunes migrating in channel under the lower flow regimes.
III	Fm	Massive, calcrete-rich red mud.	Rapid settling of suspended grains below water table in short-lived pond or lake. Sheet floods on distal flood plains.
III	Fsc	Massive yellow mud, broad lenticular, wedge-shaped geometry.	Formation in lacustrine environment.
IV	Sm	Massive sand/sandstone, broad lenticular, tabular in shape, graditional boundary.	Rapid deposition during floods.
IV	Fl	Laminated khaki mud, channel-shaped, irregular flat top and base.	Deposition in low energy conditions in overbank or low gradient flood plain environment.

Table 5.3 Major facies of alluvial fans and the Zayandeh river deposits, their brief description and depositional sub-environments in the study area.

5.5.3 Facies association III: Lake/lacustrine

This facies association includes two facies of yellow to light green (facies Fsc) and red mud (facies Fm). The former is commonly characterized by massive or to some extent stratified mud with lenses of sand. It is observed throughout the study area from the north to the south. The later is mostly developed in the northern alluvial fans. It is characterized by massive mud and well-developed calcrete nodules. The properties of the two facies, e.g. interlayering of thin-laminated fine sand, lack of root traces, broad lenticular geometry, thickness, most probably indicate rapid settling of suspended grains in local pond or lake in semi-arid and ephemeral conditions. Lenticular sand layers may be a result of vertical accretion in channels. Lack of bedding results either from rapid deposition or less probable of homogenization by bioturbation. The presence of calcrete nodules suggests long-term subaerial exposure before deposition of the following units.

5.5.4 Facies association IV: Overbank

Facies association overbank consist of two facies: Laminated khaki mud, interbedded with sand and gravel layers (facies Fl), and matrix-free massive sand (facies Sm). They extend along the Zayandeh river and main ephemeral streams in the southern alluvial fans. Some properties such as texture, fining-up sequence, external geometry (e.g. wedge-shaped, channel-shaped), burrows and root traces and interlayering of sand and gravel most probably reflect flooding and new channeling in overbank system. Matrix-free massive sand bodies are attributed to rapid deposition from suspension during floods.

5.6 Summary and conclusions

The major sedimentological environments of the study area consist of alluvial fans, the Zayandeh river deposits, a large dune field and the Gavkhoni playa lake. The alluvial fan deposits, regarding lithology, can be classified into two parts, igneous and sedimentary. The igneous alluvial fan deposits occur in the north of the Zayandeh river and the east of the Gavkhoni playa lake. The sedimentary alluvial fan deposits mostly extend in the south of the Zayandeh river (Fig. 5.1).

Based on the study of twenty one vertical sections in the lower reaches of the sedimentary basin of the Zayandeh river drainage basin in the southeast of Esfahan four association of facies, i.e. debris-flow-dominated alluvial fan, stream flow dominated alluvial fan, lake and overbank and eleven major facies were differentiated.

Facies association (I) includes two facies: matrix–supported gravel (facies Gms) and massive muddy sand (facies Sms). The former is characterized by unstratified, matrix-supported gravel and extends both in the southern, and the northern alluvial fans. The later is characterized by massive muddy sand (matrix-support sand) with abundant calcrete nodules and only occurs on the northern alluvial fans. They were deposited on the proximal fan, or with water-laid deposits in the medial fan as a result of cohesive debris respectively sand flows.

Facies association (II) includes five facies: unstratified to crudely stratified (facies Gm), planar cross-bedded (facies Gp), through cross-bedded (facies Gt), and clast-supported gravel/conglomerate, trough cross-bedded (facies St), and planar cross-bedded (facies Sp) sand/sandstone. The first three facies are represented by gravel to conglomerate, mostly pebble-sized framework grains, local normal grading, variable texture and grain composition. They originate from high-energy flow, transport and accumulation as coarse bedload and keeping sand and finer material in suspension. The remaining pore space between the gravel is usually infiltered later by sand when the velocity has decreased. Facies Gm is deposited in a stream channel on an alluvial fan. Facies Gp formed in deep sectors of mid-channel bars or bedforms developed on the flanks of bedrock valleys as a result of catastrophic floods. Facies Gt might represent the filling of small alluvial or erosional channels. The second two facies

are characterized by sand/sandstone to gravelly sand/sandstone bodies with a relatively wide variation in thickness, texture, grain composition, matrix content and cement. Facies St is a product of migration of three-dimensional subaqueous dunes on channel floors. Facies Sp suggests deposition by sand waves or transverse bars might be deposited in scour bars, chute bars, sand waves, transverse bars or straight crested subaqueous dunes.

Facies association (III) includes two facies: red to purple massive mud (facies Fm) and yellow to greenish mud, interlayering with sand layers (facies Fsc). The properties of these two facies are supposed to result from deposition from suspension of silt and clay-sized particles in a sub-aqueous lacustrine environment when a lake was formed or base level of the Gavkhoni playa lake rose toward the basin margin and deposition of sand –sized material may reflect subsequent flooding and new channeling into these fine-grained deposits.

Facies association (IV) includes two facies. These are massive sand/sandstone (facies Sm) and laminated khaki mud (facies Fl). Facies Sm is attributed to rapid deposition from suspension of sand-sized material during floods in a probable overbank situation. Facies Fl was deposited either on low gradient flood plain or on overbank of meandering rivers.

The sharp boundary between mud and debris-flow or stream-flow indicates that the alluvial system developed progressively from margin to the center. The quantitative summary of these facies emphasizes a periodic deposition in a semi-arid setting and ephemeral rainy conditions of deposition with dominance of low energy. Fluctuation in rainfall caused periodic change of the base level, which are reflected both in lacustrine deposits and in the deposits produced by the alluvial systems, particularly in the distal fan.

Chapter 6

Summary and conclusions

6.1 Introduction

The main sedimentary environments of the studied area (lower reaches of the Gavkhoni playa lake drainage basin) include the Varzaneh aeolian sand field, the Gavkhoni playa lake, and alluvial fans. In this chapter, the main significant aspects, results of these three major components of the study and the evolution of the studied basin, which have been described and discussed in foregoing chapters, are outlined separately.

6.2 Evolution of the study basin

In this intramontane basin, sedimentation has occurred in a supposed graben or half-graben system. This structural basin is a result of orogenic movements, volcanic eruptions at the end of Cretaceous and Early Eocene, and faulting which took place after the volcanism in some central parts of Iran, and also in the study area. Controlling mechanisms in fluctuation of water level reflected in sedimentation of alluvial fans (particularly in the distal fan) and lacustrine sediments are most likely a result of combination of three main factors. These are: neotectonic movements of the High Zagros belt, subsidence of the base level of erosion (Gavkhoni playa lake) and climatic changes in the drainage basin of the Zayandeh river.

6.3 Aeolian sand field

1) The Varzaneh aeolian sand field consists of two main sand forms, sand dunes and sand sheets. The sand dunes comprise linear (seif), barchanoid, star, sand drift and dikaka dune forms. The sand sheets can be grouped into three types: sabkha, overbank and interdune.

2) In the term of dynamic behavior, the sand dunes and sand sheets can be divided into two groups, mobile and immobile. The mobile sand dunes move according to wind directions, but the rate of resultant migration is low annually or they are almost fixed. Deflation occurs over the sand dunes and the dry interdunes but sabkha and overbank sand sheets are immobile on most sites. The rate of movement of sand grains gradually decreases from the sand dunes towards alluvial fan and the playa lake environments, because of relative fixation of these sediments by stabilizing factors such as moisture and vegetation. The overall form of the aeolian sand field and the various forms of sand dunes indicate that ancient winds were chiefly responsible for the linear/seif and modern winds for the barchanoid and star dune

forms. Therefore, according to ancient wind direction, sand dunes mostly moved from the north to the south and to recent winds towards all directions.

3) Mineralogical investigations indicate that the main provenance of the aeolian sands is from sedimentary rocks extended in the south, the southwest and the northwest and also from igneous rocks exposed in the east and the northeast of the aeolian sand field. The metamorphic rocks, exposed mostly at the upper reaches of the drainage basin, are a minor source. The concentration place of the aeolian sands, mineralogical composition, textural properties, and dominant wind direction indicate that the water laid sediments of the Zayandeh river, widespread to the north of the aeolian sands, are the main supply of the aeolian sands.

4) The morphology of the aeolian sand grains (i.e. roundness and sphericity) indicates that they are similar to the Zayandeh river sediments. This results that wind processes did not play an important role in changing the primary form of the grains in this case.

5) Immobile sand sheets deposits (i.e. sabkha sand sheet) are less well-sorted than the active sand dunes (i.e. star dune) and active sand sheets (i.e. dry interdune). This mainly results from the fact that the mobile sand deposits became better sorted by wind deflation processes than the immobile sand deposits. Interdune, overbank sand sheet and sabkha sand sheet sediments are mostly coarse skewed and dune sands range between very fine to very coarse skewed because this statistical parameter depends on variety of factors such as the nature of source, availability of fine fractions, wind regime and mechanism of deposition. All aeolian facies have the highest kurtosis index and are mainly very leptokortic, indicating high sorting of their center of size populations.

6) The presence of the extensive sand field with an area of about 130 km^2 (45 km long and maximum of 11 km wide) indicates that a large amount of sediments were deposited and deflated under favorable climate conditions for a long period of time. It is believed that present conditions are not favorable to form this sand field. It is supposed that after the latest glacial period, heavy rains and melting glaciers simultaneously caused severe erosion in the Zayandeh river drainage basin followed by transportation and deposition of great amounts of fluvial sediments close to the recent aeolian sand accumulation. Deflation of the fluvial sediments, affected by strong winds in dry periods, has formed this aeolian sand field.

6.4 Gavkhoni playa lake

1) The Gavkhoni playa lake comprises six main facies of sand flat, sand beach, mud flat, saline mud flat, salt pan and delta.

2) The sand flat covers mostly the west of the playa lake. The remarkable characteristics of this facies are gypsiferous marl mounds, porous tufa, gypsum layers, puffy surface and efflorescent salt crusts. These properties suggest that sedimentation occurred under periodic flooding and desiccation conditions.

3) The long narrow sand beach ridges that extend to the east and the north of the playa lake, were formed mostly by wave action during flood periods by reworking sand from the Zayandeh delta.

4) Saline mud flats and mud flats surround the playa lake, except in the western part. The most common characteristic of the saline mud flat is a hard surface pitted by small holes with a few centimeters wide and deep and displacive gypsum and halite crystals, resulting from evaporation of capillary brines and rapid and differential rising of the sedimentary surface. The mud flat is characterized by polygonal mud cracks, plant roots and root casts. It is deposited mainly by sheet floods and then altered almost syndepositionally by wetting and drying. Based on digged trenches in the mud flat and saline mud flat, five units of salt, gypsiferous mud, muddy sand, massive mud, and sand were recognized.

5) The salt pan covers the most central part of the playa lake as an efflorescent crust. The thickness of the salt crust varies from a few centimeters to the north and up to one meter to the south. The most common features of the salt pan are polygonal halite crusts, efflorescent cauliflower and halite pressure ridge. The lithostratigraphic sequence, up to 30 m deep in drill holes in the salt pan, shows intermittent sedimentation of mud–sized and sand-sized sediments followed by a salt crust on the surface. The formation of the salt pan is as a result of three stages: flooding, evaporation and desiccation.

6) The Zayandeh river delta occupies about 30 km^2 of the end reach of the Zayandeh river. Its sediments are made up of alternating sandy and muddy facies in studied trenches. Based on five digged trenches, three main sub-facies were determined in the delta. They are gray to black mud, yellow to brown mud and sand. Change of sediments both in horizontal and vertical directions is as a result of frequent shifting and migration of the channel branches. The most important factor for the development of this shallow, fast prograding delta is a large supply of sediments by the Zayandeh river.

7) The chemical analyses of the dilute water (surface water) and the amount of major cations and anions indicate a brine type of Na^+, (Mg^{++}), Cl^-, (SO_4^{--}). The evolution of concentrated waters (groundwater) show that brines are progressively depleted from carbonate and sulfate from margins to the center. This ultimately produced the Na^+, (Mg^{++}), Cl^- and Na^+, Mg^{++}, Cl^- brine type. The later is comparable to the composition of many saline

playa brines. After complete desiccation, the mineral assemblage comprises halite, bischofite, carnallite, and tachyhydrite in the central and the south of the salt pan. There is no relic of sylvite, thenardite, glauberite, and trona in this facies, because of insufficient bicarbonate, sulfate and potassium ions.

8) Stratigraphic sequence in the playa lake suggest that sedimentation occurred under variable conditions regarding chemical, compositional, hydrologic environment and climate. They were formed in a fresh to saline water in a semi-arid to arid climate with rather strong wind activity. During the flash floods the playa was a shallow fresh water to brackish perennial lake with resulting deposition of fine-grained sediments. During the latest dry period the middle part of the lake gradually became shallower and more restricted and the salt crust formed. Sand-grained deposits were derived from aeolian sands in most sites during dry periods.

6.5 Alluvial fans

1) Based on facies analysis of studied sections 4 facies associations including, debris-flow-dominated alluvial fan (I), stream-flow dominated alluvial fan (II), lake/lacustrine (III) and overbank (IV) were recognized.

2) Facies association (I) is dominated by gypsiferous matrix-supported conglomerate/ gravel. This facies association is restricted to the proximal fan, or mixed with water-laid deposits in the medial fan, resulting from cohesive debris flows.

3) Facies association (II) mainly consists of clast-supported conglomerate/gravel originated from high-energy flow, transported and accumulating in erosional channels, channel bars in braided (or meandering) rivers.

4) Facies association (III) is dominated by yellow mud indicating deposition from suspension in a lacustrine environment.

5) Facies association (IV) includes mud-dominated sediments alternating with gravel and sand lenticles. They are attributed to rapid deposition on overbank environments during floods.

6) Sharp boundary between the facies association (III) and the facies association (II) most probably is as a result of a strong variation of local climatic conditions especially in the south of the study area.

REFERENCES

Abdullative, O.M., 1989, Channel fill and sheet flood facies sequences in the ephemeral terminal River Gash, Kassala, Sudan. Sedimentary Geology. v. **63**: 171-184.

Alavi, M., 1994, Tectonics of the Zagros orogenic belt of Iran: new data and interpretations. Tectonophysics. v. **229**: 211-238.

Amini, A., 1997, Provenance and depositional environment of the Upper Red Formation, Central Zone, Iran. Unpublished Ph.D. thesis. University of Manchester.

Bates, R.L. and Jackson, J.A., 1980, Glossary of Geology. 2nd ed, American Geological Institute, Virginia, 751 pp.

Benison, K.C., & Goldstein, R.H., 2001, Evaporites and siliciclastics of the Permian Nippewalla Group of Kansas USA: a case for non-marine deposition in saline lakes and saline pans. Sedimentology. v. **48**: 165-188

Berberian, M., 1983, Continental deformation in the Iranian plateau, Geological Survey of Iran, Report No. 52. 625 pp.

Blair, T.C., & McPherson, J.G., 1992, The Trollheim alluvial fan and facies model revisited. Geological Society of America Bulletin. v. **104**: 762-769.

Blair, T.C., & McPherson, J.G., 1995, Quaternary alluvial fans in southwestern Crete: sedimentation processes and geomorphic evolution. Sedimentology. v. **42**: 531-549.

Blair, T.C., 1999, Sedimentology of the debris-flow-dominated Warm Spring Canyon alluvial fan, Death Valley, California. Sedimentology. v. **46**: 941-965.

Blair, T.C., & McPherson., J.G., 1999, Grain size and textural classification of coarse sedimentary particles. Journal of Sedimentary Research. v. **69**: 6-19.

Bridge, J.S., 1984, Large-scale facies sequences in alluvial overbank environments. Journal of Sedimentary Petrology. v. **54**. 583-588.

Bryant, G.B., Sellwood, B.w., Millington, A.C., & Drake, N.A., 1994, Marine- like potash evaporite formation on a continental playa: case study from Chott el Djerid, southern Tunisia. Sedimentary Geology. v. **90**: 269-291.

Carver, R.E., 1971, Procedure in Sedimentary Petrology. John & Wiley, 663 pp.

Collinson, J.D., 1996, Alluvial Sediments. In: Reading, H.G. (ed.) Sedimentary Environments and Facies. 3rd ed., Blackwell, Oxford, 37-82 pp.

Deck, T., Hein, F.J., & Trotter, R., 1996, Granite wash alluvial fans, fan deltas and tidal environments, northwestern Alberta: implication for controls on distribution of Devonian clastic wedges associated with the Peace River Arch. Bulletin of Canadian Petroleum Geology. v. **44**(3): 541-565.

Einsele, G., 1992, Sedimentology of Basins: Evolution, Facies and Sediment Budget. Springer–Verlag, 628 pp.

El-Sayed, M.I., 1999, Sedimetological characteristics and morphology of the aeolian sand dunes in the eastern part of the UAE: a case study from Ar Rub, Al Khali. Sedimentary Geology. v. **123**: 219- 238.

Eugster, H.O., & Hardie, L A., 1978, Saline Lake. In: Lerman, A., (ed): Lakes: Chemistry, Geology, Physics. New York, Springer-Verlag, pp. 237-293.

Fayazi, F., 1991, Sedimentological studies in the Qom area, Central Iran. Unpublished Ph.D. thesis. University of East Anglia, England.

Folk, R.L., 1974, Petrology of Sedimentary Rocks. Hemphill, Austin, 182 pp.

Foroghi, H., 1983, Genesis of saline soils and role of topography and source material on their formation around the Gavkhoni playa lake. Unpublished. Ms thesis. Technical University of Esfahan, Iran.

Fryberger, S. G *et al.,* 1988, Stokes surfaces and the effects of near surface groundwater table on aeolian deposition. Sedimentary geology. v. **55**: 21-41.

Galloway, W.E., & Hobday, D.K., 1996, Terrigenous clastic depositional systems: An Application to Fossil Fuel and Groundwater Resources. Springer-Verlag. 489 pp.

Greeley, R, Blumbery, D.G, & Williams, S.T., 1996, Field measurement of the flux and speed of wind-blown sand. Sedimentology. v. **43:** 41-52.

Haghipour, A., 1983, Geological and seismological of the Hana region (Semirom), unpublished report, Iranian Water Organization.

Handford, R.H., 1982, Sedimentology and evaporite genesis in a Holocene continental-sabkha playa basin, Bristol Dry Lake. California, Sedimentology. v. **29**: 239-253.

Hardy, R., & Tucker, M., 1988, X-ray powder diffraction of sediments. In: Tucker, M., (ed): *Techniques in Sedimentology*. Blackwell, pp. 191-228.

Hjellbakk, A., 1997, Facies and fluvial architecture of a high energy braided river: the Upper Proterozoic Seglodden Member, Varanger Peninsula, northern Norway. Sedimentary Geology. v. **114**: 131-161.

Honarjo, N., 1982, They study of evolution and variation of clay minerals in the Zayandeh river terraces soils. Unpublished. Ms thesis. Technical University of Esfahan, Iran.

Hovorka, S., 1987, Depositional environment of marine-dominated bedded halite, Permian San Andres Formation, Texas. Sedimentology, v. **34**: 1029-1054.

Jensen, R., 1986, Threats to ground water quality. Texas Water Resources Institute, v. **12**, No. 1.

Kelly, S.B. and Olsen, H., 1993, Terminal fans-a review with reference to Devonian examples. Sedimentary Geology. v. **85**, 339-374.

Kendall, A.C., 1992, Evaporites. In: Walker, R.G., & James, N.P., (eds): *Facies Models: Response to See Level Change*. Geological Association of Canada. pp. 375-409.

Khademi, H., 1985, The study of evolution and recognition of clay minerals in Rodasht region soils. Unpublished. Ms thesis. Technical University of Esfahan, Iran.

Khalaf, F., 1989, Textural characteristics and genesis of the aeolian sediments in the kuwaiti desert. Sedimentology. v. **36**: 253-271.

Khalaf, F.I., & Gharib, I.M., 1985, Roundness parameters of quartz grains of recent aeolian sand deposits in Kuwait. Sedimentary Geology. v. **45**: 147-158

Kocurek, G., & Nielson, J., 1986, Conditions favorable for the formation of warm-climate aeolian sand sheets. Sedimentology. v. **33**: 795-816.

Krauskopf, K.B., 1985, Introduction to Geochemistry. McGraw-Hill, London, 613 pp.

Krinsley, D.B., 1970, A geomorphological and paleoclimatological study of the playa of Iran. U. S. Government Printing Office, Washington, D. C. 20, 402 pp.

Kulke, H., 1974, Zur Geologie und Mineralogie der Kalk-und Gipskrusten Algeriens. Geol. Rundschau. v. **63**(3): 970-998

Kulke, H., 1996, Large pigeon towers in the Province of Esfahan (Iran). Trialog, Karstruhe. v. **4** 30-35

Langford, R.R,. 1989, Fluvial-aeolian interactions: Part1, modern systems. Sedimentology. v. **36**: 1023-1035.

Last, W.M., 1989, Sedimentology of a saline playa in the northern Great Plains, Canada. Sedimentology. v. **36**: 109-123.

Lewis, D.W., 1983, Practical Sedimentology, Van Nostrand Reinhold Company, 229 pp.

Lindholm, R.C., 1987, A Practical Approach to Sedimentology. Allen & Unwin. London. 278 pp.

Livingstone, I., Bullard, J.E., Wiggs, G.F.S., & Thomas, D.S.G., 1999, Grain–size variation on dunes in the southwest of Kalahari, Southern Africa. Journal of Sedimentary Research. v. **69**: 546-552.

Lowe, D.R., 1988, Suspended-load fallout rate as an independent variable in the analysis of current structures. Sedimentology. v. **35**: 765-776.

Lowenstein, T.K., and Hardie, L.A., 1985, Criteria for the recognition of salt pan evaporites. Sedimentology. v. **32**: 627-644.

Lugli, S., Schreiber, B.C., & Triberti, B., 1999, Giant polygonals in the Realmonte Mine (Agrigento, Sicily): evidence for the desiccation of a Messinian halite basin. Journal of Sedimentary Research. v. **69** (3): 764-771.

Madole, R.F., 1994, Stratigraphic evidence of desertification in the west-central Great Plains within the past 1000 year. Geology. v. **22**: 483-486.

Mange, M.A., & Maurer, H.F.W., 1992, Heavy Minerals in Color. Chapman & Hall. 147 pp.

McCabe, P.J., 1977, Deep distributary channels and giant bedforms in the Upper Carboniferous of the Central Pennies northern England. Sedimentology. v. **24**: 271-290.

McKee, E.D., 1966, Structures of dunes at White Sands National Monument, New Mexico (and a comparison with structures of dunes from other selected areas). Sedimentology. v.**7**: 1-69.

Miall, A.D., 1977, A review of the braided river depositional environment: Earth Science Reviews. v. **13**: 1-62.

Miall, A.D., 1985, Architectural-element analysis: a new method of facies analysis applied to fluvial deposits. Earth Science Reviews. v. **22**: 261-308.

Miall, A.D., 1988, Architectural elements and bounding surfaces in fluvial deposits: anatomy of the Kayenta Formation (Lower Jurassic), southeast Colorado. Sedimentary Geology. v. **55**: 233-262.

Miall, A.D., 1992. Alluvial deposits. In: Walker, R.G., & James, N.P., (eds): *Facies Models: Response to Sea Level Change*. Geological Association of Canada, Toronto, pp. 119-142.

Nabian, A., *et al* 1991, Exploration project of potash in the Gavkhoni playa lake brine. Geological Survey of Iran, unpublished report. pp. 33.

National Iranian Oil Company (NIOC), 1975, Geological Cross Sections of South-Central Iran, scale 1: 500 000.

National Iranian Oil Company (NIOC), 1977, Geological map of Iran, sheets No. 2 and 5, scale 1:1 000 000.

National Iranian Oil Company (NIOC), 1978, Geological map of Iran, sheet No. 4, scale 1:1 000 000.

Nickling, W.G., 1984, The stabilizing role of bonding agents on the entertainment of sediment by wind. Sedimentology. v. **31**:111-117.

Nickling, W. G., 1994, Aeolian Sediment Transport and Deposition. In: Pye, K. (ed): *Sediment Transport and Depositional Processes*. Blackwell, pp. 293-350.

Olsen, H., 1989, Sandstone-body structures and ephemeral stream processes in the Dinosaur Canyon Member, Moenave Formation (Lower Jurassic), Utah, USA. Sedimentary Geology. v. **61**: 207-221.

Parkash, B., Awasthi, A.K., and Gohain, K., 1983, Lithofacies of the Mrkanda terminal fan, Kurukshetra district, Haryana, India. In: Collinson, J.D. and Lewin, J. (eds) Modern and ancient fluvial systems. International Association of Sedimentology, Special Publication, No. **6**, 337-344.

Pettijohn, F.G., Potter, P.E., & Siever, R., 1987, Sand and Sandstone, 3rd ed, Springer-Verlag, New York, 553 pp.

Pierson, T.C., 1980, Erosion and deposition by debris flows at Mt.Thomas, North Canterbury, New Zealand. Sedimentology. v. **5**: 227-247.

Postma, G., 1983, Water escape structures in the context of a depositional model of a mass flow dominated conglomeratic fan-delta (Abrioja Formation, Pliocene, Almeria Basin, SE Spain). Sedimentology. v. **30**: 91-103.

Pye, K., 1980, Beach salcrete and aeolian sand transport: evidence from North Queensland. Journal of Sedimentary Petrology. v. **50**: 257-261

Ramesht, M., 1992, The study of Zayandeh river terraces and their effect on special landscape of Esfahan. Unpublished. Ph.D. thesis. University of Shahid Beheshti, Iran.

Reineck, H.E., and Singh., I.B., 1980, Depositional Sedimentary Environments. Springer-Verlag, Berlin, 551pp.

Rhee, C.W. & Chough, S.K., 1993, The Cretaceous Pyonghae sequence, southeast Korea: terminal fan facies. Palaeogeography, Palaeoclimatology, Palaeoecology, v. **105**. 139-156.

Rust, B.R., 1984, Proximal braid plain deposits in the Middle Devonian Malbaie Formation of Eastern Gaspe , Quebec, Canada. Sedimentology. v. **31**: 675-695.

Ryang, W. H., & Chough, S.K., 1997, Sequential development of alluvial/lacustrin system: southern Eumusung Basin (Cretaceous), Korea. Journal of Sedimentary Research. v. **67**(2): 274-285.

Sagga, A.M.S., 1993, Roundness of sand grains of longitudinal dunes in Saudi Arabia. Sedimentary Geology. v. **87**: 63-68.

Salder, S.P. and Kelly, S.B., 1993, Fluvial processes and cyclicity in terminal fan deposits: an example from the Late Devonian of southwest Ireland. Sedimentary Geology. v. **85**: 375-386.

Schreiber, B.C., Friedman, G.M., Desima, A & Schreiber, E., 1973, Depositional environments of Upper Miocene (Messinian) evaporite deposits of the Sisilian basin. Sedimentology. v. **23**: 729-760.

Shanley, K.W. and McCabe, P.J., 1993, Predicting facies architecture through sequence stratigraphy-an example from the Kaiparowits Plateau, Utah. Geology. v. **19**: 742-745.

Smith, G.A,. 1986, Coarse-grained non-marine volcaniclastic sediment: terminology and depositional process. Bulletin Geological Society of America. v. **97**: 1-10.

Steel, R.J., & Thompson, D.B., 1983, Structures and textures in Triassic braided stream conglomerates (Bunter Pebble Beds) in the Sherwood Sandstone Group, North Staffordshire, England. Sedimentology. v. **30**: 341-367.

Stoecklin, J., 1968b, Structural history and tectonics of Iran; a review. America Association of Petroleum Geology Bulletin. v. **52**(7), 1229-1285.

Tabatabaei, J., 1996, The study of the source of aeolian sands in the Varzaneh region, Unpublished. Ms thesis. Azad University, Iran.

Tabatabaei, N., & Makoui., T.N., 1994, The structural map of the Nikabad area (east of Esfahan). National Iranian Oil Company (NIOC), scale 1:500,000, Tehran.

Talbot, M.R., & Allen, P.A., 1996, Lakes. In: Reading, H.G., (ed.) Sedimentary Environment and Facies, 3rd ed, Blackwell, Oxford, pp. 83-124.

Thomas, D.S.G., 1989, Arid zone geomorphology. Belhaven Press, London, 327 pp.

Trewin, N., 1988, Use of the Scanning Electron Microscope in Sedimentology. In: tucker, M., (ed): Techniques in Sedimentology. Blackwell, pp. 229-273

Tucker, M 1991, Sedimentary Petrology: An Introduction to the Origin of Sedimentary Rocks. Blackwell, 260 pp.

Turner, B.R., & Monro, M., 1987, Channel formation and migration by mass flow processes in the Lower Carboniferous fluviatile Fell Sandstone Group, northeast England. Sedimentology. v. **34**: 1107-1122.

Vogel, A.T., 1971, *A* Text Book of Quantitative Inorganic Analysis Including Instrumental Analysis, Longman 1216 pp.

Warren, J., 1999, Evaporites: Their Evolution and Economics, Blackwell, pp. 438.

Watson, A., 1989, Desert Crusts and Rock Varnish. In: Thomas, D.S.G., (*ed*): *Arid Zone Geomorphology.* Belhaven Press, London, pp.25-55.

Winspear, N. R., & Pye, K., 1995, Sand supply to the Algodones dunefield, south-eastern California, USA. Sedimentology. v. **42**: 875-891.

Wizevich, M.C., 1992, Sedimentology of Pennsylvanian quartzose sandstone of the Lee Formation, central Appalachian: fluvial inter-pretation based on lateral profile analysis. Sedimentary Geology. v. **78**, 1-47.

Yakushova, A.F., 1986, Geology with the elements of geomorphology. Mir, Moscow, 400 pp.

Appendixes

Appendix A: Chemical analysis

A1: Procedure of chemical analysis of brines conducted in Chemistry Department of Esfahan University:

1. For determination of Na^{+}, Ca^{++}, Mg^{++}, K^{+}, by AAS (atomic absorption spectrophotometer), 20 ml of representative sub-samples was taken from each water sample, for some cations high concentration 10, 100, 1000 and 2000 times dilutions were used.
2. For determination of Sr^{++}, 20 ml of main solution was transferred to a 25 ml volumetric flask, and 1 ml nitric acid (10%) added. Then 1. 25 ml sodium base solution was added and the solution diluted to 25 ml for AAS measurement of Sr^{++}.
3. For determination of Cl^{-}, 5 ml of main solution was transferred into 250 ml of volumetric flask and 20 ml of standard Ag solution added, plus 1 ml concentric nitric acid. The solution was diluted to 250 ml, mixed and allowed to stand overnight in darkness. The precipitate was then separated by centrifuging, and the solution diluted 10 times in order to measure excess Ag by AAS.
4. For determination of sulfate, 25 ml of main solution was transferred into a 250 ml beaker (plus two empty beakers for blanks). In each beaker 100 ml of 10% HCl, was added, covered and then beaker were boiled for one hour. They were then filtered (using 542 filter paper) into 400 ml conical beakers, together with 20 ml hot water washing four times. The solutions were neutralized with 50% (v/v) ammonium hydroxide solution using a methyl red indicator. 1 ml concentrate hydrochloride acid, was then added, and solution diluted to 200 ml with water. 25 ml potassium sulfate solution (2g/l) was then added, the solution was boiled, then 10 ml barium chloride solution (10%) was added and boiling kept for half an hour. The precipitate was filtered using 542 paper, and washed with hot water until the washing was chloride-free. The filter paper was ignited with the precipitate in silica crucibles at 800^{0}C for 15 minutes. It was then allowed to cool in a desiccator, and then weighed. Later the precipitate was removed and the crucible weighed.
5. For determination of bicarbonate, a portion of the cold brine was slowly titrated with standard 0.1 N- hydrochloric acid, using phenolphthalein. This (*M* ml) corresponds to half the carbonate (CO_3^{--} $+H^{+} = HCO_3^{-}$). Another sample of equal volume was then titrated

with the same standard acid using methyl orange as indicator. The volume of acid used (*m* ml) corresponds to carbonate = bicarbonate. Hence 2=carbonate, and *m-2M*= bicarbonate.

6. For determination of NO_3^-, standard solutions of potassium nitrate (0.01-0.5 ppm) were transferred into backers . 2 ml of sodium salisilate ($C_8H_5O_3Na_2$) was added into each beaker and were dried in water boil. The residues were heated at 100^oC for two hours. After cooling, 2 ml concentric sulfuric acid was added into the solutions and to be allowed to stand for 10 min. Then 15 ml alkaline tartarate ($C_4H_4O_6KNa.4H_2O$) was added into the solutions and dilute them to 100 ml. These processes were also treated for water sub-samples and then absorption value was measured by spectrophotometer (Vogel, 1971).

A2: Procedure of carbonate content determination:

1. Approximately 5 gr samples was transferred to a pre-weighed tall-form 250 ml beaker, and covered with watch glass.

2. 5ml of 0.1 N HCl was added into 10 ml of distilled water and stirred to promote reaction. After initial reaction ceased, additional 2 ml 0.1 N HCl was added and continued until no further reaction was observed or until the solution will be showed strongly acidic with pH indicator paper.

3. Excess acid was decanted and sample carefully washed in distilled water until all $CaCl_2$ being removed.

4. Remaining sample was heated to 110^oC before transferring to desiccator to be dryness and cool 5. Weight loss was weighed and calculated.

5. Results may be calculated and reported as follow (Carver, 1971).

$$\%CaCO_3 = 100 \times \text{weight loss/ initial dry weight of samples}$$

Appendix B: XRD analysis

B1: Procedure of clay minerals analysis:

Carbonate was removed by buffered sodium acetate (Lewis, 1983) and clay-sized fraction extracted by pipette, at the required depth of the measuring cylinder (Hardy &Tucker, 1988 in Tucker, 1988).

For identification of clay minerals involved making oriented samples, standard pretreatment of ethylene glycol, air drying at 60^{o}C, chloride acid (6N) and heating at 550^{o}C. For this reason, suction onto ceramic disc under a vacuum and also sedimentation of suspension onto a slide method was used for the preparation of oriented clay samples. The oriented slides were introduced into desiccator containing half a pint (0.25 liter) of ethylene glycol, and then placing the desiccator in an oven at 60^{o}C for about 4 hours. Further treatment involved heating the samples at 550^{o}C in a furnace. Another treatment was resolving the samples by HCl (6N at 60^{o}C for 16h) (Hardy & Tucker, 1988 in Tucker, 1988). After the samples were air-dried, they were prepared for XRD analysis as an oriented mount. X-ray diffraction was accomplished using copper radiation and Phillips pw automated diffractometer.

The semi–quantitative estimates of the relative amounts of clay minerals were calculated. The absolute peak area under the characteristic lattice spacing (d-spacing) of the identified minerals was used as a measure of the relative abundance of minerals in bulk samples (Hardy & Tucker, 1988 in Tucker, 1988).

B2: Procedure of XRD analysis for determination of evaporite minerals:
In this method samples were crushed with electrical machine to prepare powder mixed with water and was mounted on a glass slide. The analyses were worked out with a philips X-ray diffraction unit using Ge filter, Cu K radiation.

B3: Symbols used in XRD analysis sheets, sheet No., section No., size fraction, lithology, facies and semi- quantitative of clay and evaporite minerals types (in turn of decreasing in abundance) determined in the study area.

k	kaolinite	ca	calcite	H	heat	t	tachyhydrite
i	illite	g	gypsum	N	air dried	cr	carnallite
ch	chlorite	h	halite	G	ethylene glycol		
s	smectite	b	bischofite	HCl	chloride acid		

Sheet No.	Section No.	Clay & evaporite mineral types	Lithology	Size	Sedimentary environment & facies	Location	
1	Dz1	Sm, I, K, Cl	Brown mud	<6	Delta, mud flat	32°,17′,12″N	52°,53′,45″E
2	Dz5	I, K, Cl, Sm	Brown mud	<6	Delta, mud flat	32°,17′,11″N	52°,53′,12″E
3	G2	Sm, I, Cl, K	Yellow mud	<2	Lake/lacustrine, mud flat	32°,40′,40″N	52°,16′,15″E
4	G4	Sm, I, K, Cl	Red mud	<2	Lake/lacustrine, mud flat	32°,23′,01″N	52°,47′,41″E
5	G5	Sm, I, Cl, K	Red mud	<2	Lake/lacustrine, mud flat	32°,31′,58″N	52°,27′,37″E
6	G6	Sm, I, Cl, K	Yellow mud	<2	Lake/lacustrine, mud flat	32°,34′,31″N	52°,16′,42″E
7	G7	I, Sm, Cl, K	Khaki mud	<6	Lake (Overbank), mud flat	32°,21′,45″N	52°,47′,55″E
8	G9	Sm, I, K, Cl	Yellow mud	<2	Lake/lacustrine, mud flat	32°,29′,44″N	52°,25′,24″E
9	G10	I, Sm, Cl, K	Yellow mud	<2	Lake/lacustrine, mud flat	32°,30′,34″N	52°,24′,39″E
10	G13	Sm, I, K, Cl	Yellow mud	<6	Lake/lacustrine, mud flat	32°,26′,44″N	52°,23′,02″E
11	G14	Sm, I, K, Cl	Yellow mud	<2	Lake/lacustrine, mud flat	32°,01′,13″N	52°,48′,09″E
12	G15	I, K, Cl, Sm	Yellow mud	<6	Lake/lacustrine, mud flat	32°,24′,40″N	52°,20′,53″E
13	G16	I, Sm, Cl, K	Yellow mud	<2	Lake/lacustrine, mud flat	32°,23′,25″N	52°,09′,19″E
14	G19	Sm, I, K, Cl	Yellow mud	<2	Lake/lacustrine, mud flat	32°,13′,09″N	52°,40′,29″E
15	G21	Sm, I, K, Cl	Khaki mud	<2	Overbank, mud flat	32°,01′,02″N	52°,51′,49″E
16	G22	I, Sm, Cl, K	Khaki mud	<2	Overbank, mud flat	32°,12′,20″N	52°,07′,06″E
17	I1-1	Sm, I, K, Cl	Black sandy mud	<6	Lake, mud flat	32°,07′,09″N	52°,40′,30″E
18	I1-2	I, K, Cl, Sm	Brown mud	<2	Interdune, mud flat	32°,07′,09″N	52°,40′,30″E
19	I2	I, Sm, K, Cl	White sandy mud	<6	Interdune, mud flat	32°,06′,26″N	52°,41′,57″E
20	M2-1	I, K, Cl, Sm	Khaki mud-salt	<6	Flood plain, saline mud flat	32°,18′,09″N	52°,53′,07″E
21	M2-2	Sm, I, K, Cl	Khaki mud	<2	Flood plain, mud flat	32°,18′,09″N	52°,53′,07″E
22	S1	I, K, Cl, Sm	Black mud	<6	Salt lake, saline mud flat	32°,05′,40″N	52°,45′,30″E
23	S3	b, cr, t, h, ca, g	White salt	Powder	Salt pan	32°,06′,24″N	52°,48′,13″E
24	S4	h, b	White salt	Powder	Salt pan	32°,01′,33″N	52°,52′,44″E

B4: XRD analysis sheets (No. 1-24)

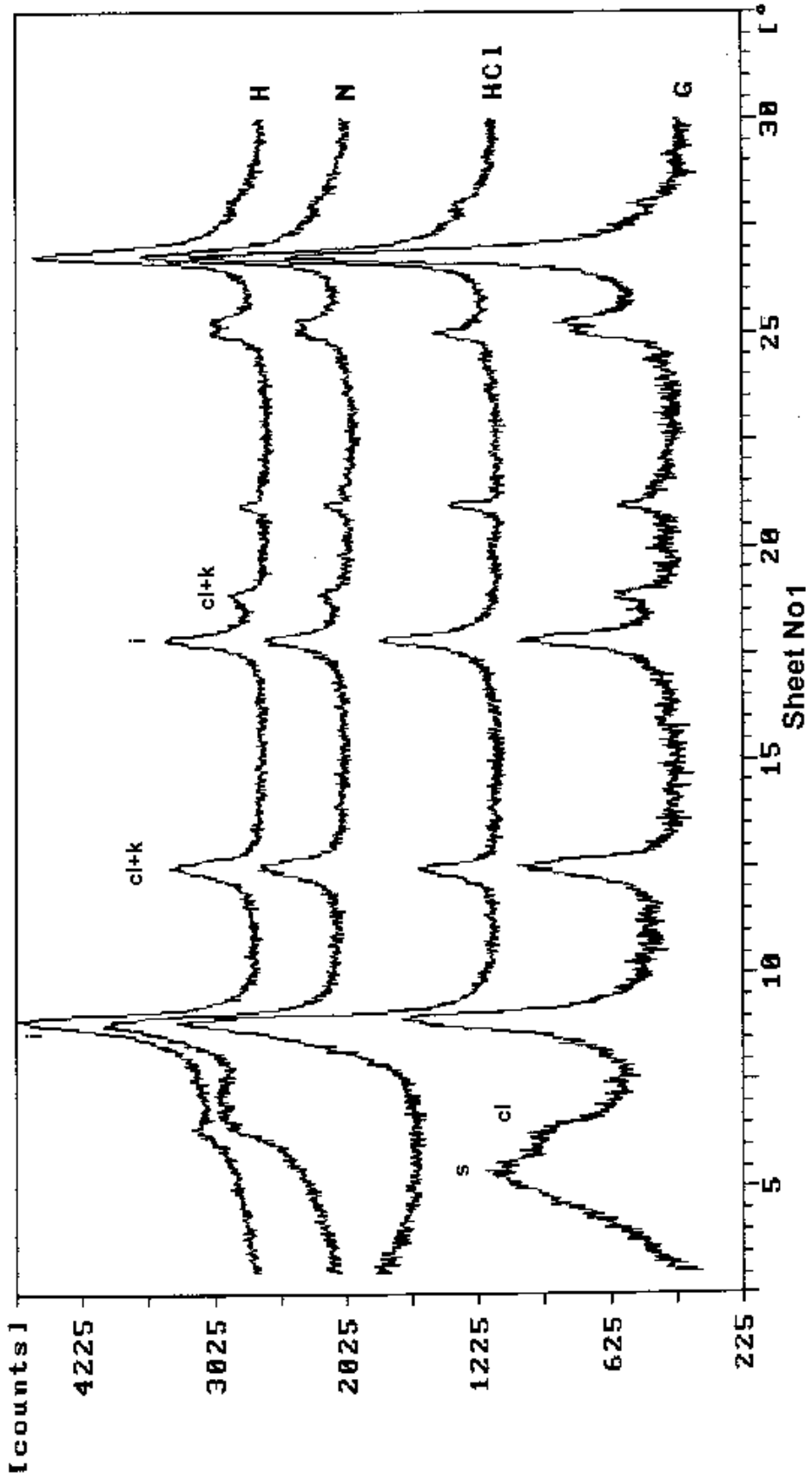
[counts]
4225
3025
2025
1225
625
225
5
10
15
20
25
30
[°
Sheet No1
H
N
HCl
G
i
cl+k
i
cl+k
s
cl

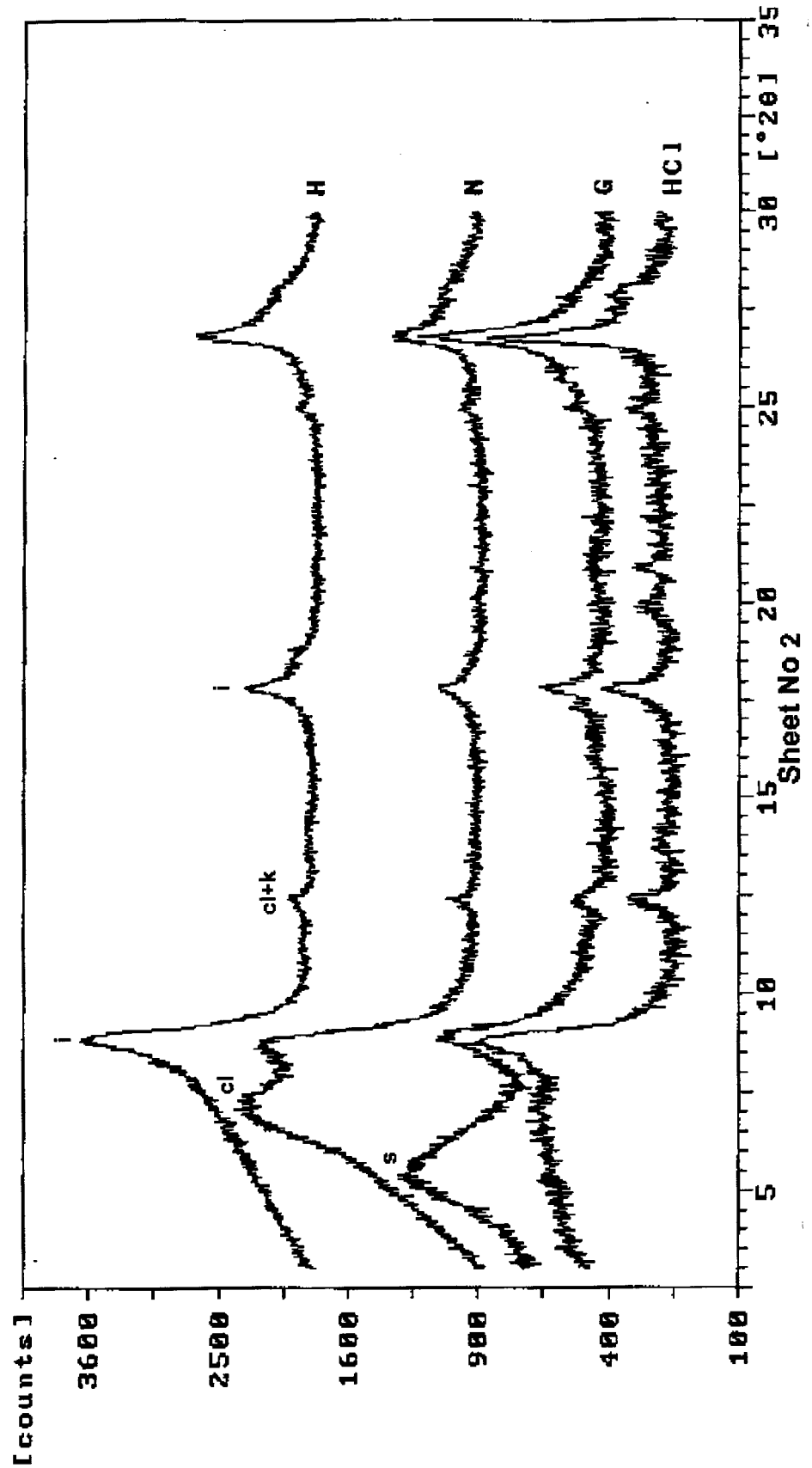
[counts]
3600
2500
1600
900
400
100
5
10
15
20
25
30
35
[°2θ]
Sheet No 2
i
cl
cl+k
s
i
H
N
G
HCl

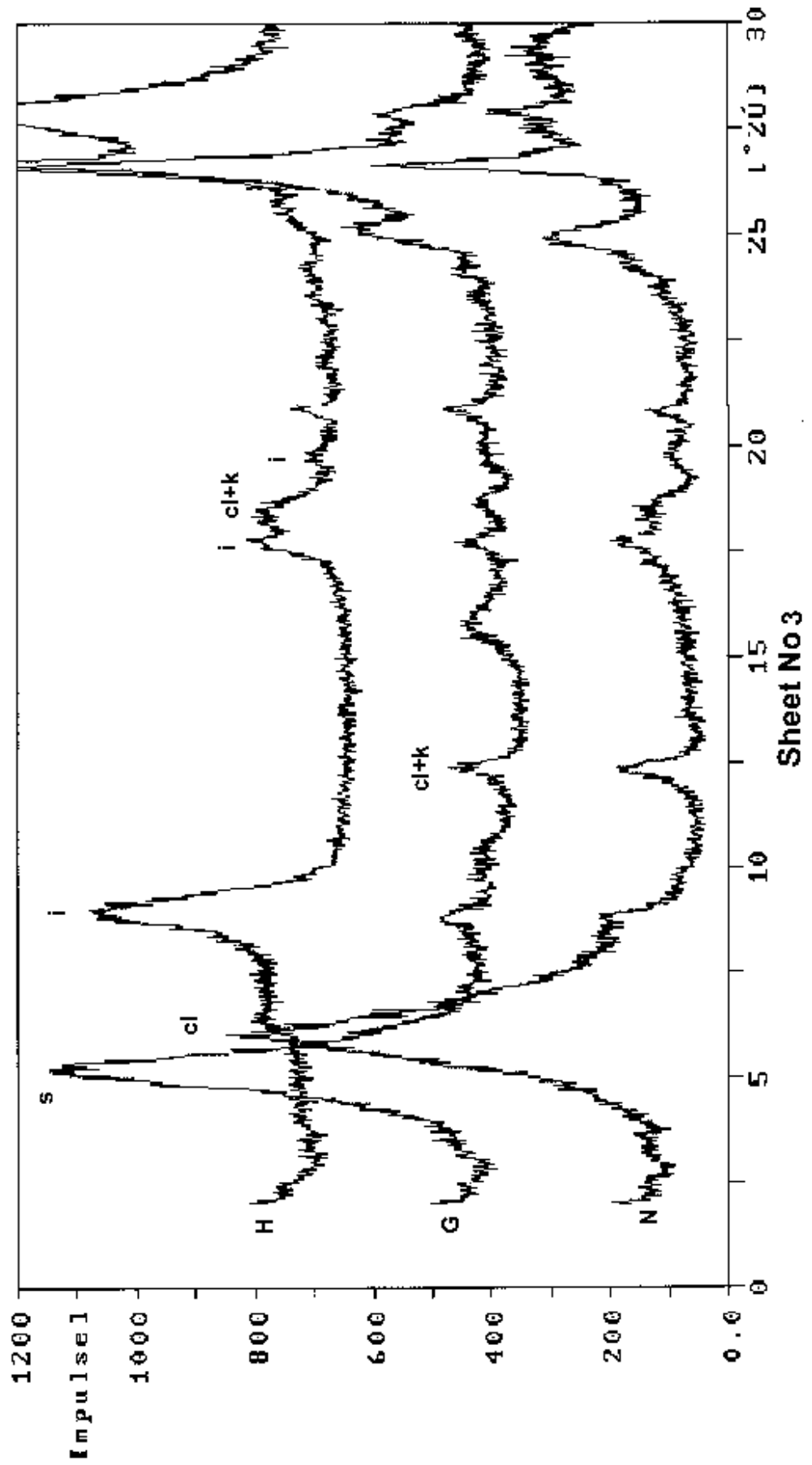
Impulsel
1200
1000
800
600
400
200
0.0
0
5
10
15
20
25
30
°2Θ
Sheet No 3
s
cl
i
i cl+k
i
cl+k
H
G
N

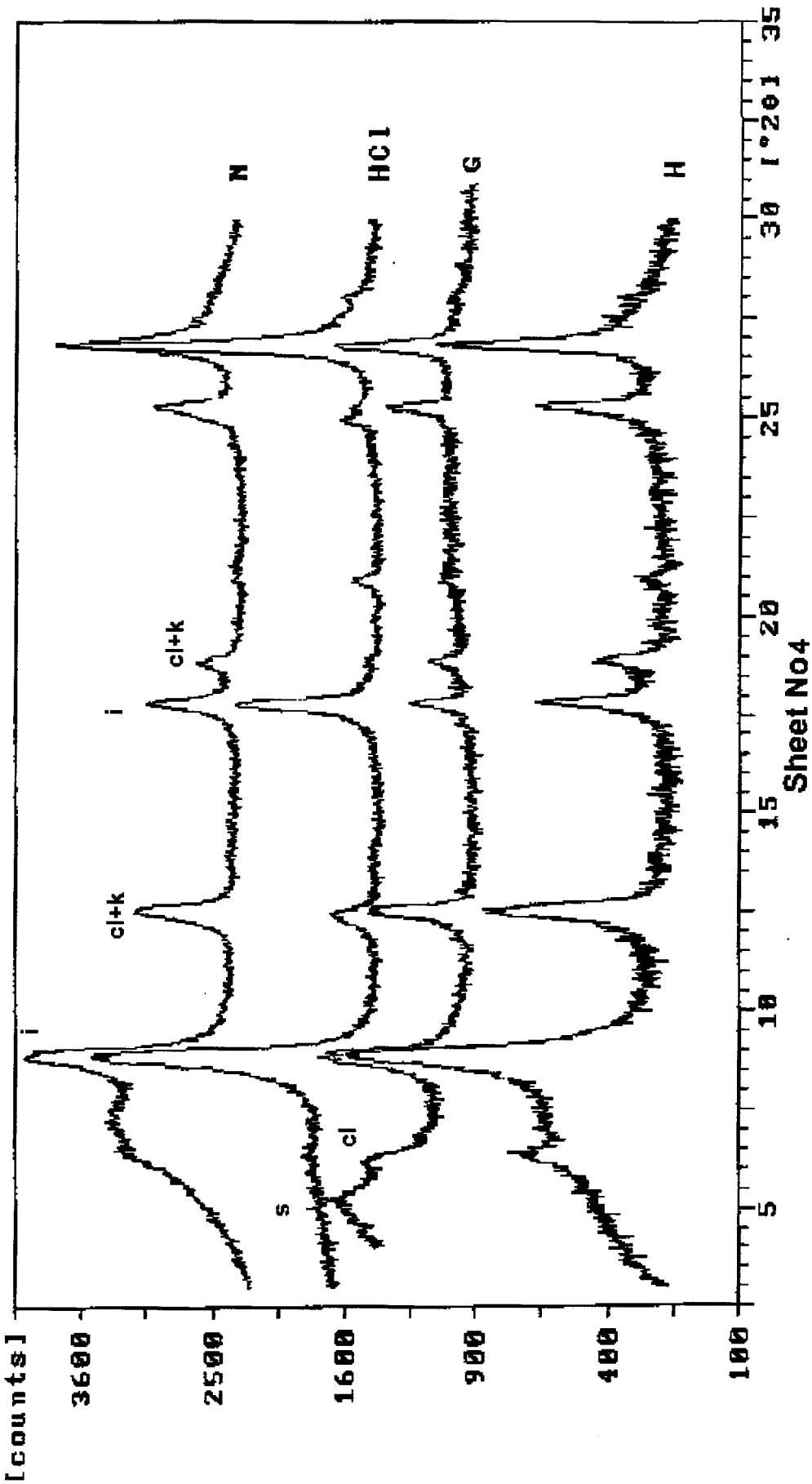
[counts]
3600
2500
1600
900
400
100
5
10
15
20
25
30
35
I°2θ1
Sheet No4
i
cl+k
i
cl+k
s
cl
N
HCl
G
H

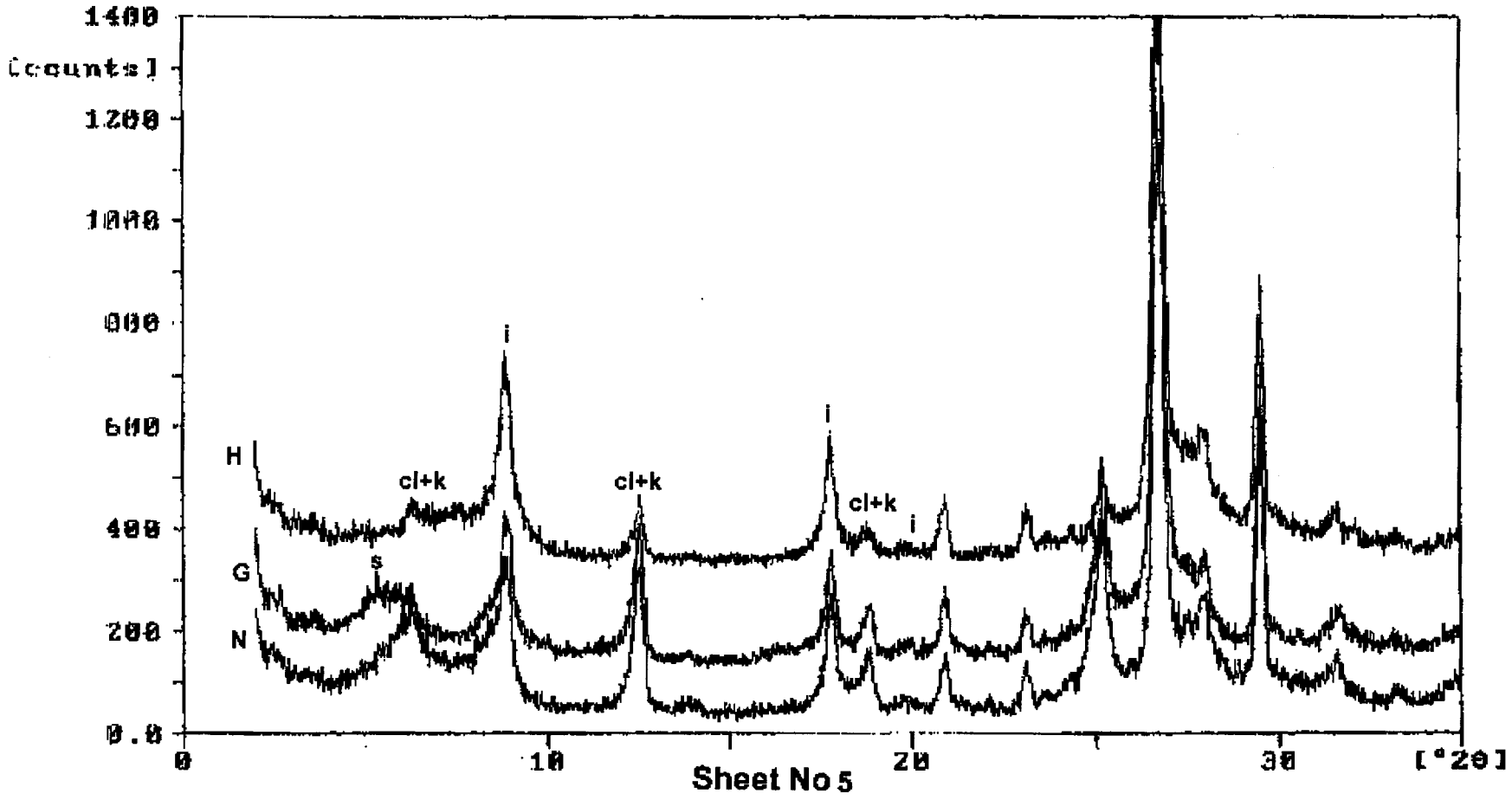
1400
[counts]
1200
1000
800
600
400
200
0.0
H
G
N
cl+k
cl+k
cl+k
i
i
i
s
0
10
20
30
[°2θ]
Sheet No 5

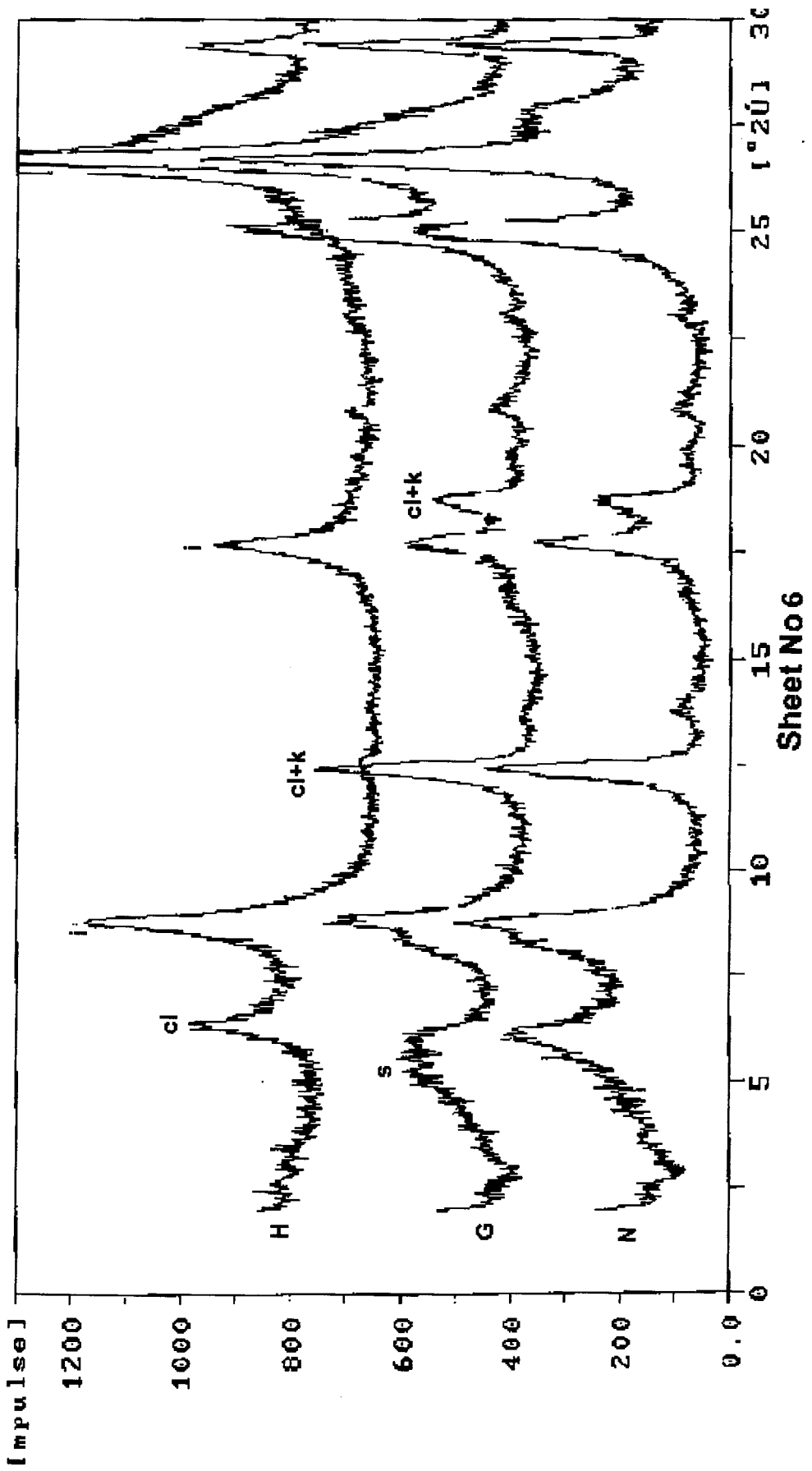
[mpulse]
1200
1000
800
600
400
200
0.0
0
5
10
15
20
25
Sheet No 6
H
cl
i
cl+k
s
G
N
cl+k
i

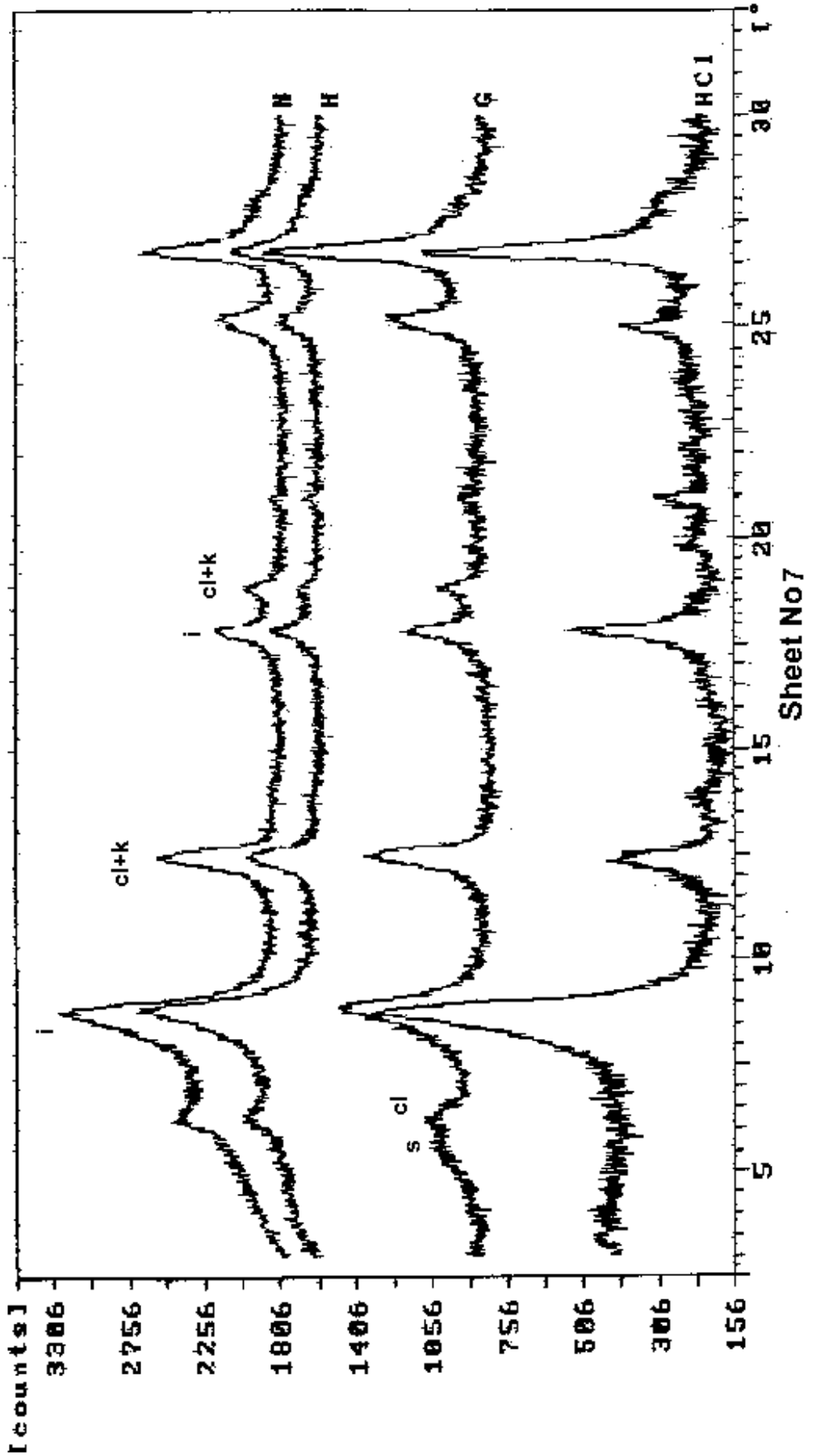
[counts]
3306
2756
2256
1806
1406
1056
756
506
306
156
5
10
15
20
25
30
t°
Sheet No7
i
cl+k
i
cl+k
s
cl
N
H
G
HCl

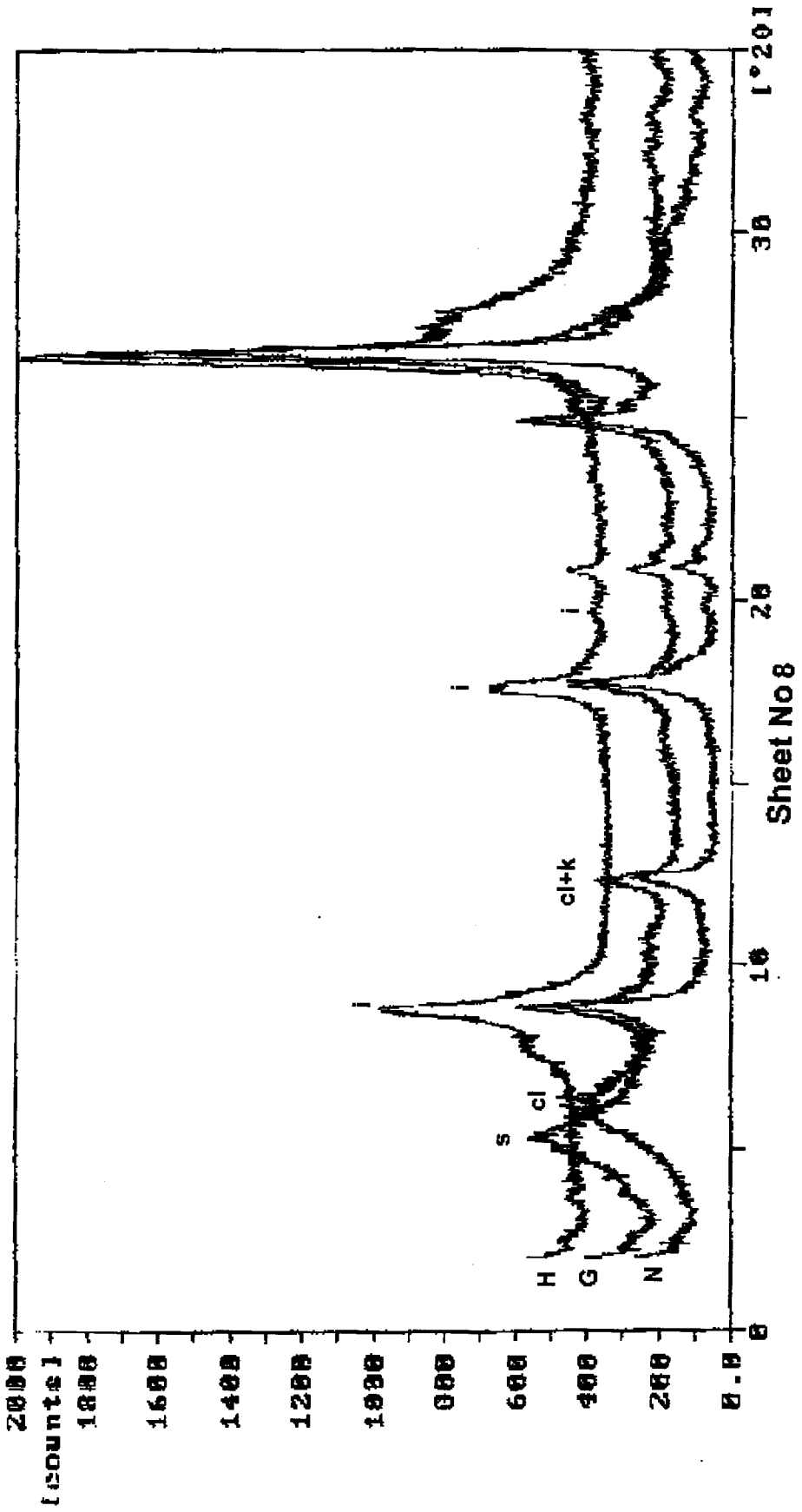
Sheet No 8
[counts]
2000
1800
1600
1400
1200
1000
800
600
400
200
0.0
0
10
20
30
[°2θ]
H
G
N
s
cl
i
cl+k
i
i

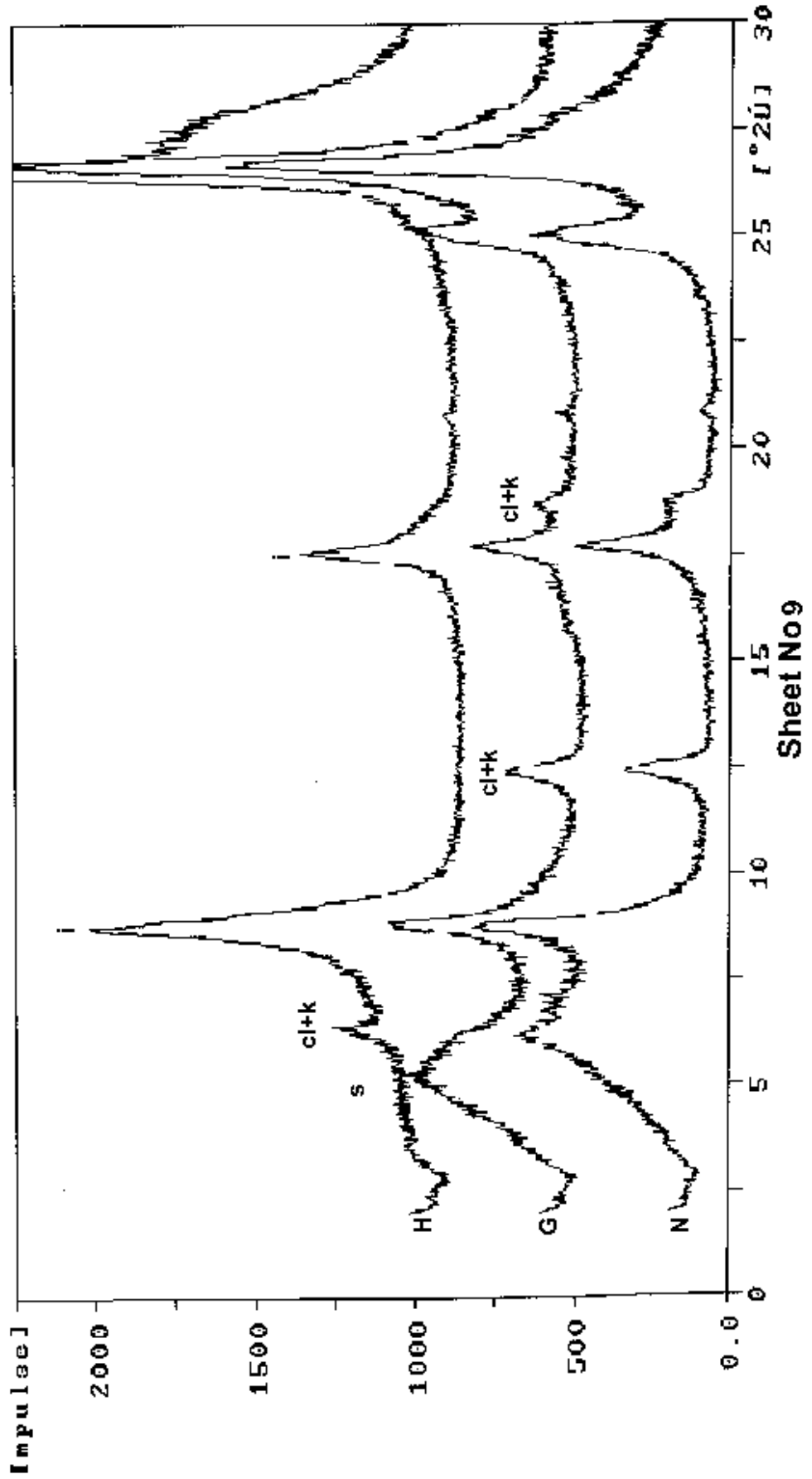
[Impulse]
2000
1500
1000
500
0.0
0
5
10
15
20
25
30
[°2Θ]
Sheet No 9
i
cl+k
s
H
cl+k
G
cl+k
N

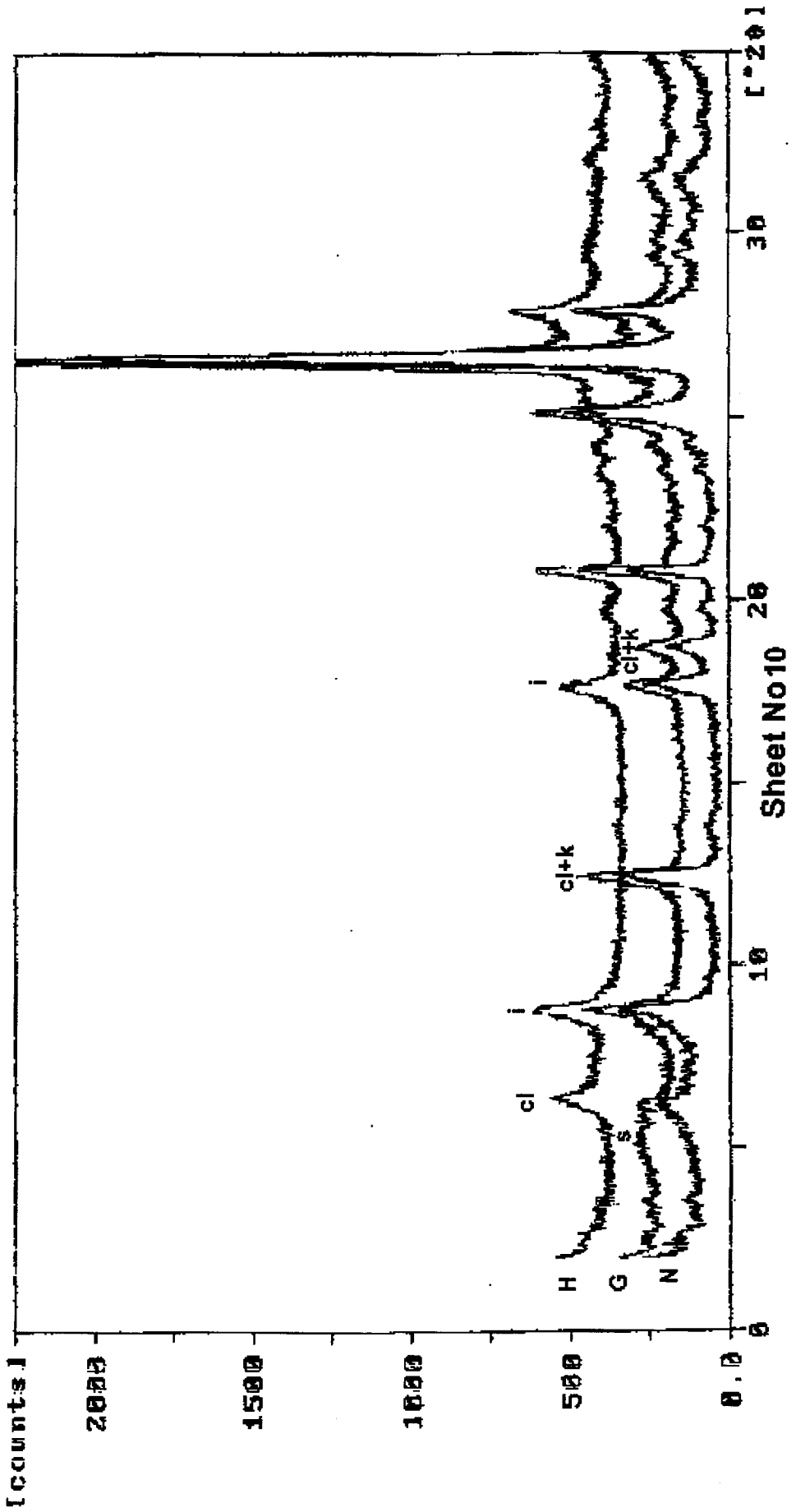
[counts]
2000
1500
1000
500
0.0
0
10
20
30
[°2θ]
Sheet No10
H
G
N
S
cl
i
cl+k
i
cl+k

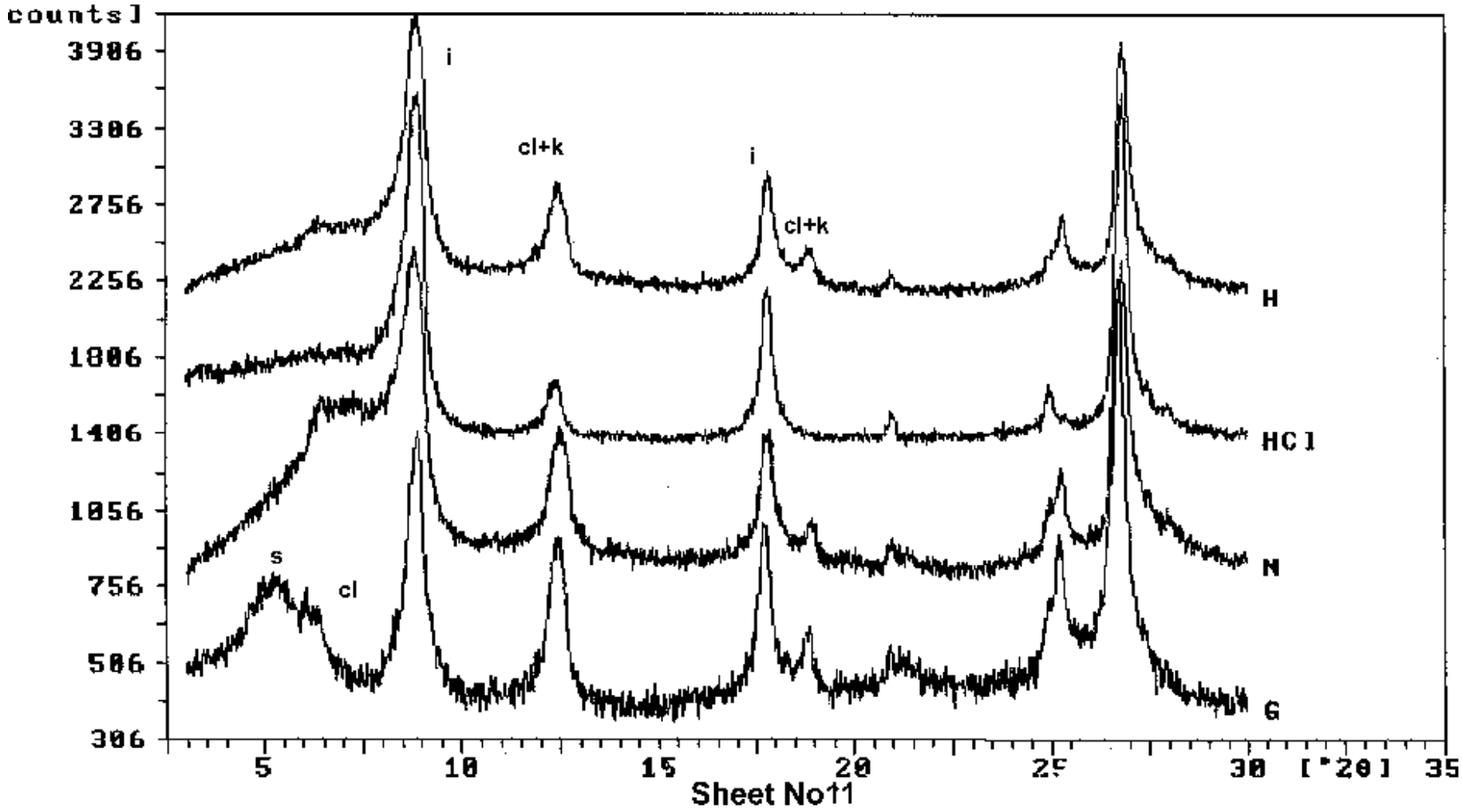
counts]
3986
3306
2756
2256
1806
1406
1056
756
506
306
i
cl+k
i
cl+k
H
HCl
N
G
s
cl
5
10
15
20
25
30
[°2θ]
35
Sheet No11

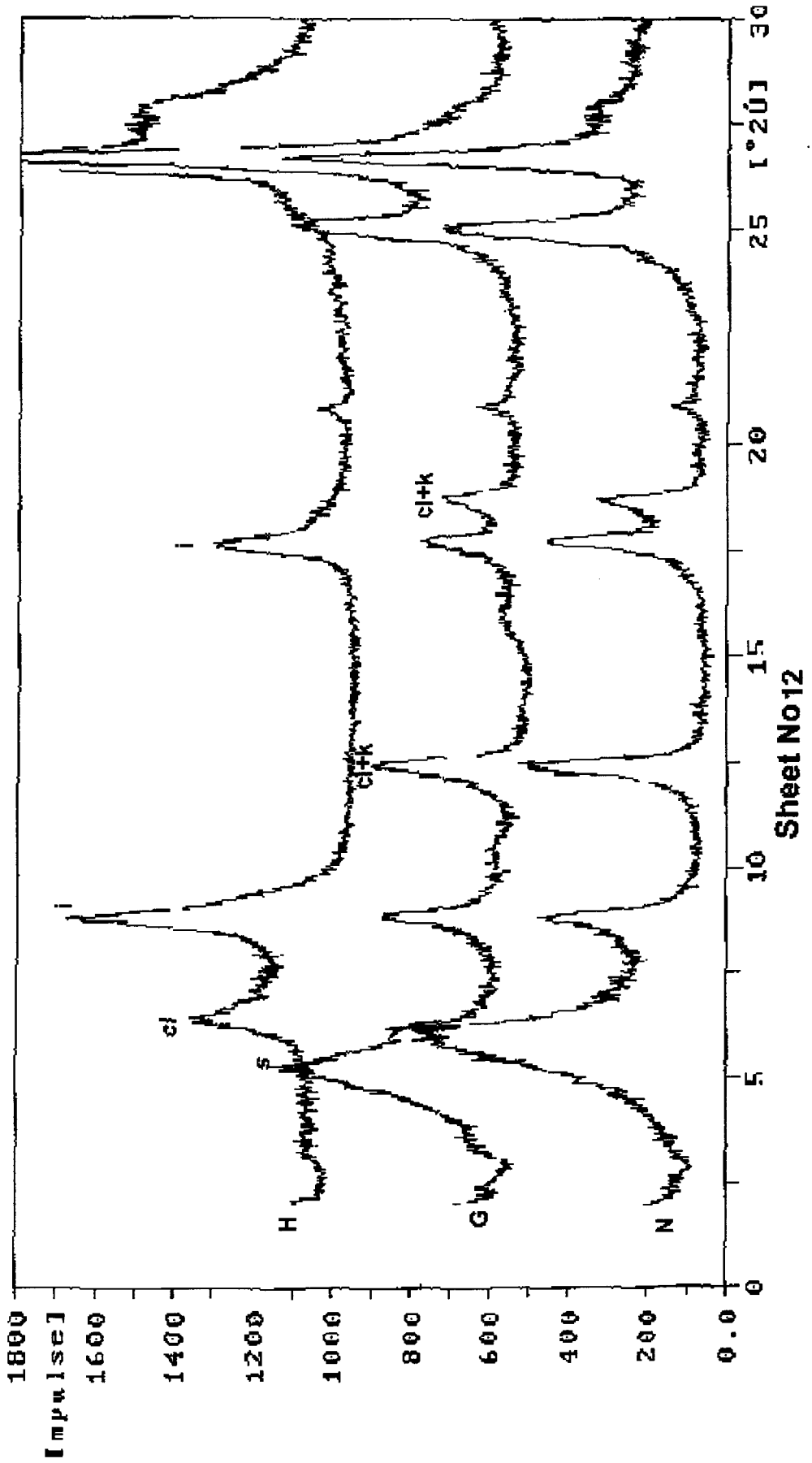
Sheet No12
[°2Ü]
[mpulse]
H
G
N
cl
cl+k
i
s

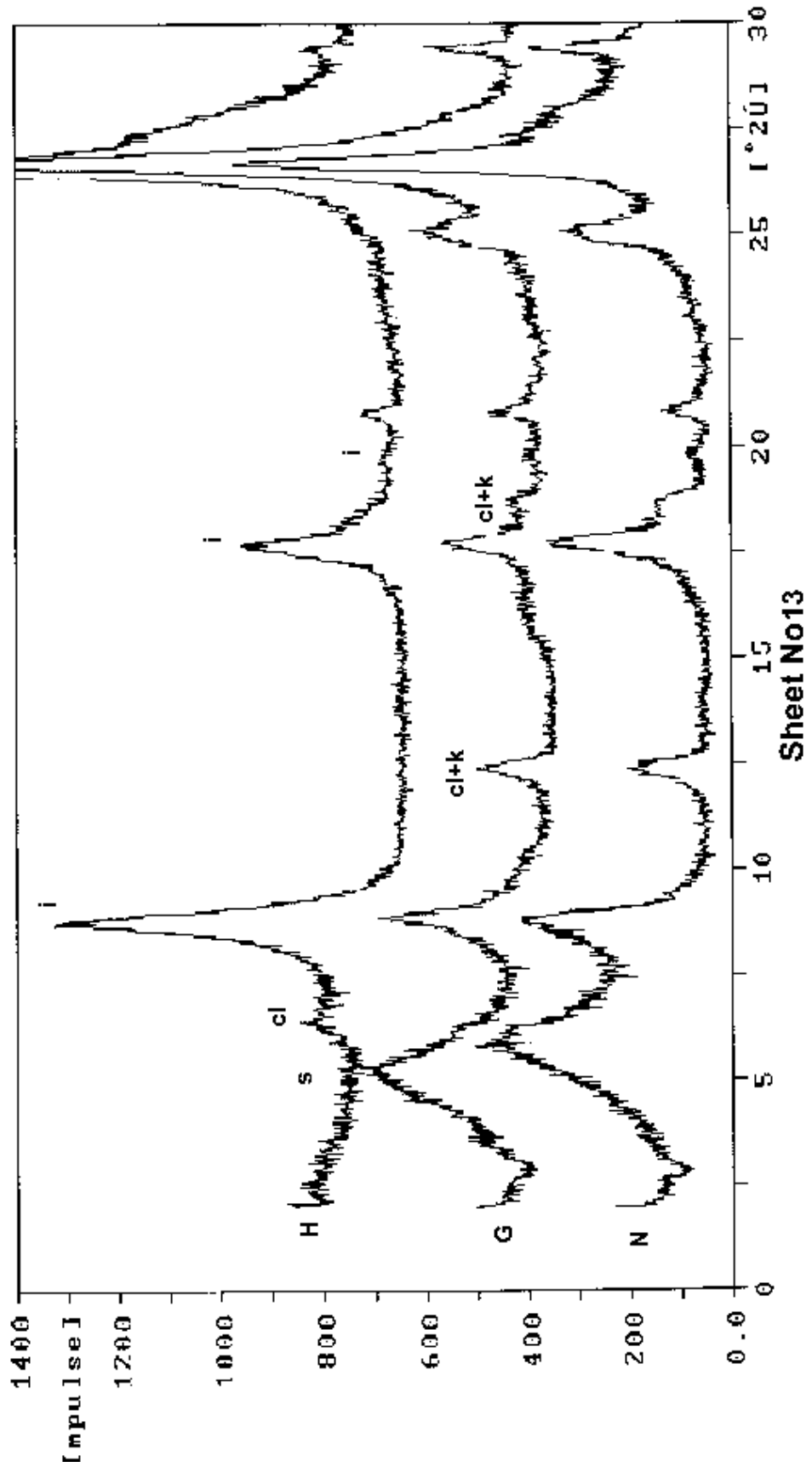
1400
[mpulse]
1200
1000
800
600
400
200
0.0
0
5
10
15
20
25
30
[°2Θ]
Sheet No13
H
G
N
cl
s
i
cl+k

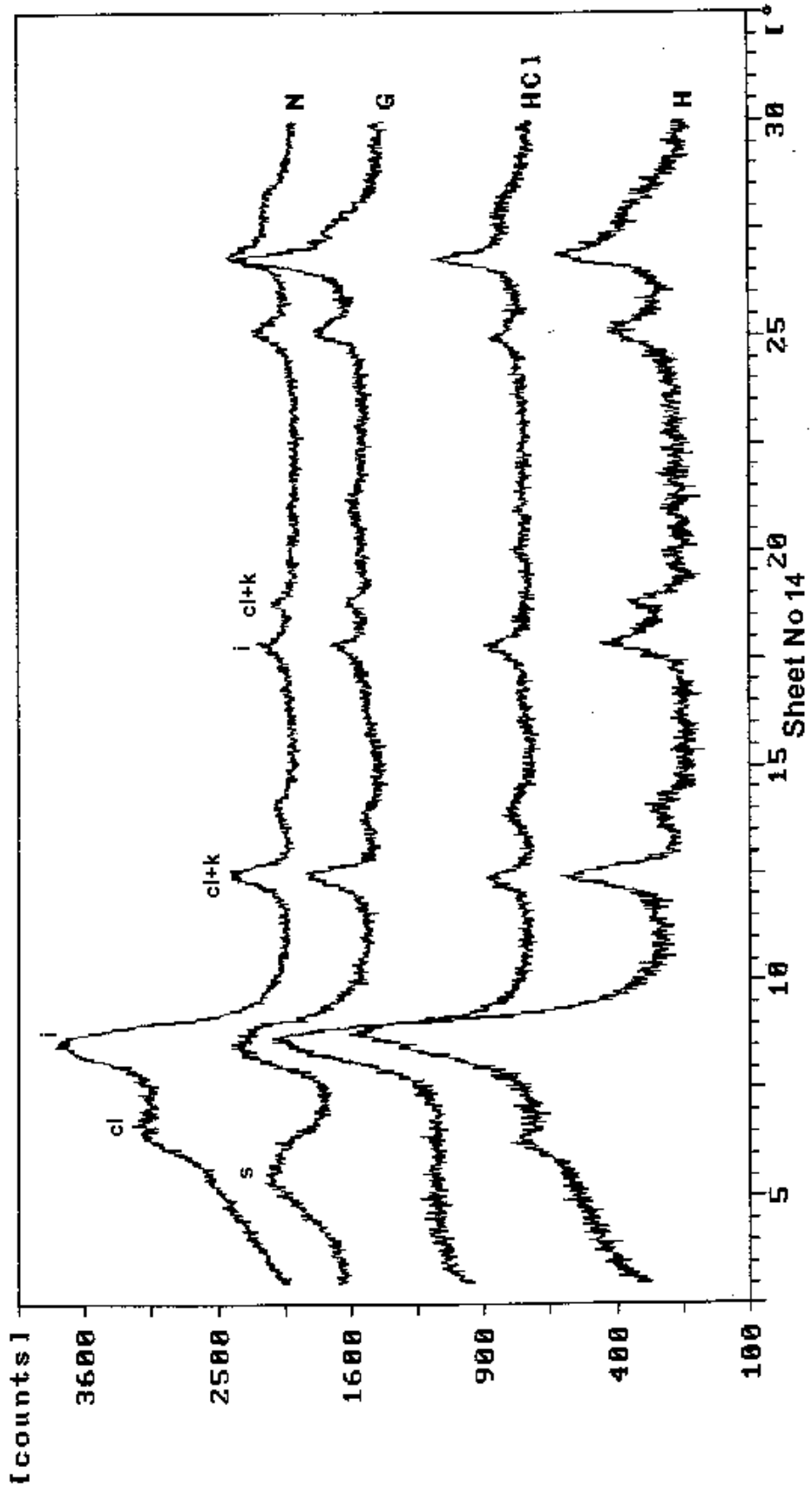
[counts]
3600
2500
1600
900
400
100
5
10
15
20
25
30
Sheet No 14
i
cl
s
cl+k
i
cl+k
N
G
HCl
H

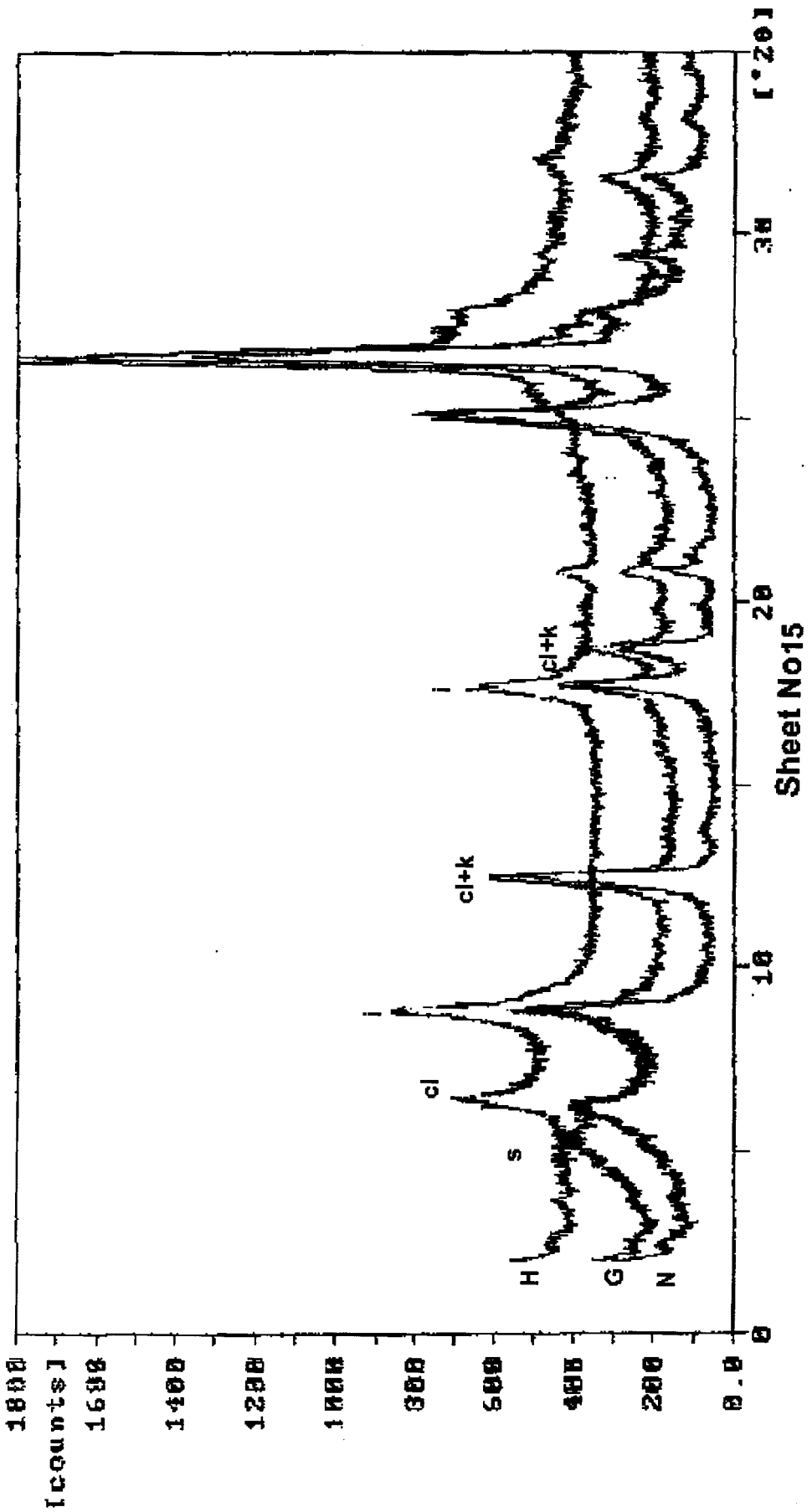
1800
[counts]
1600
1400
1200
1000
800
600
400
200
0.0
0
10
20
30
[°2θ]
Sheet No15
H
G
N
S
cl
cl+k
cl+k

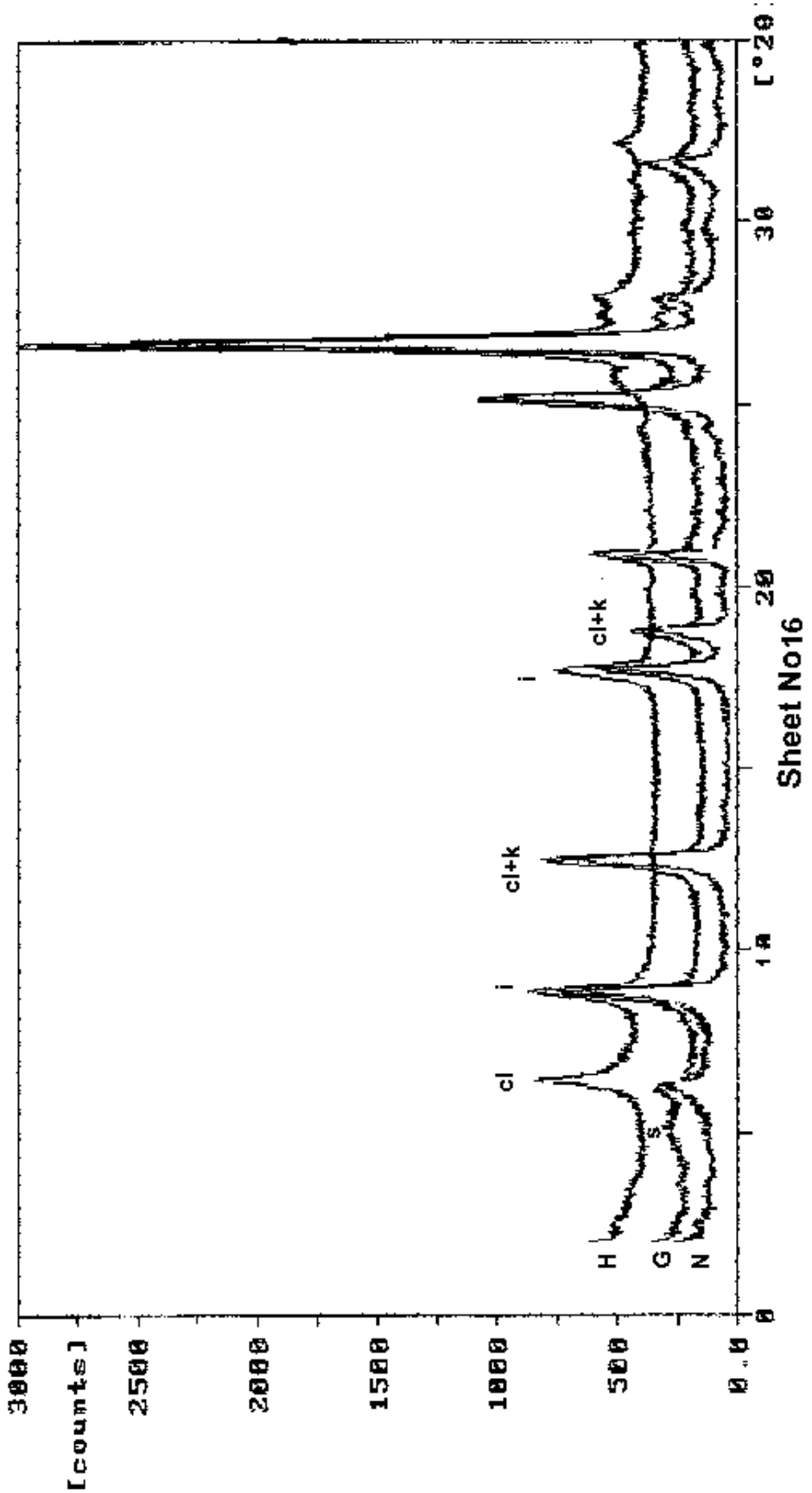
3000
[counts]
2500
2000
1500
1000
500
0
0.0
H
G
N
S
cl
i
cl+k
i
cl+k
10
20
30
[°2θ]
Sheet No16

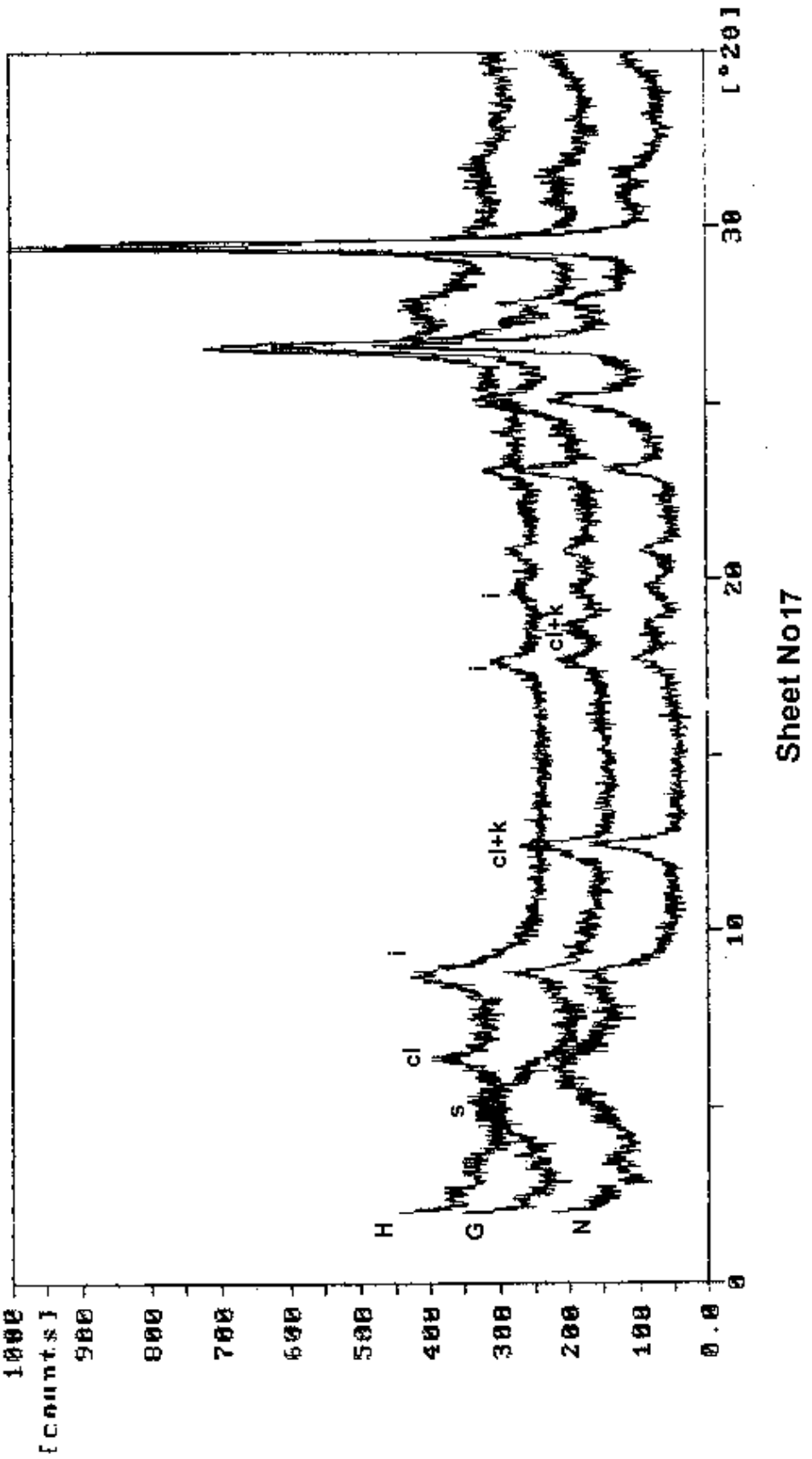
1000
[counts]
900
800
700
600
500
400
300
200
100
0.0
0
10
20
30
[°2θ]
H
G
N
s
cl
i
cl+k
i
i
cl+k
Sheet No17

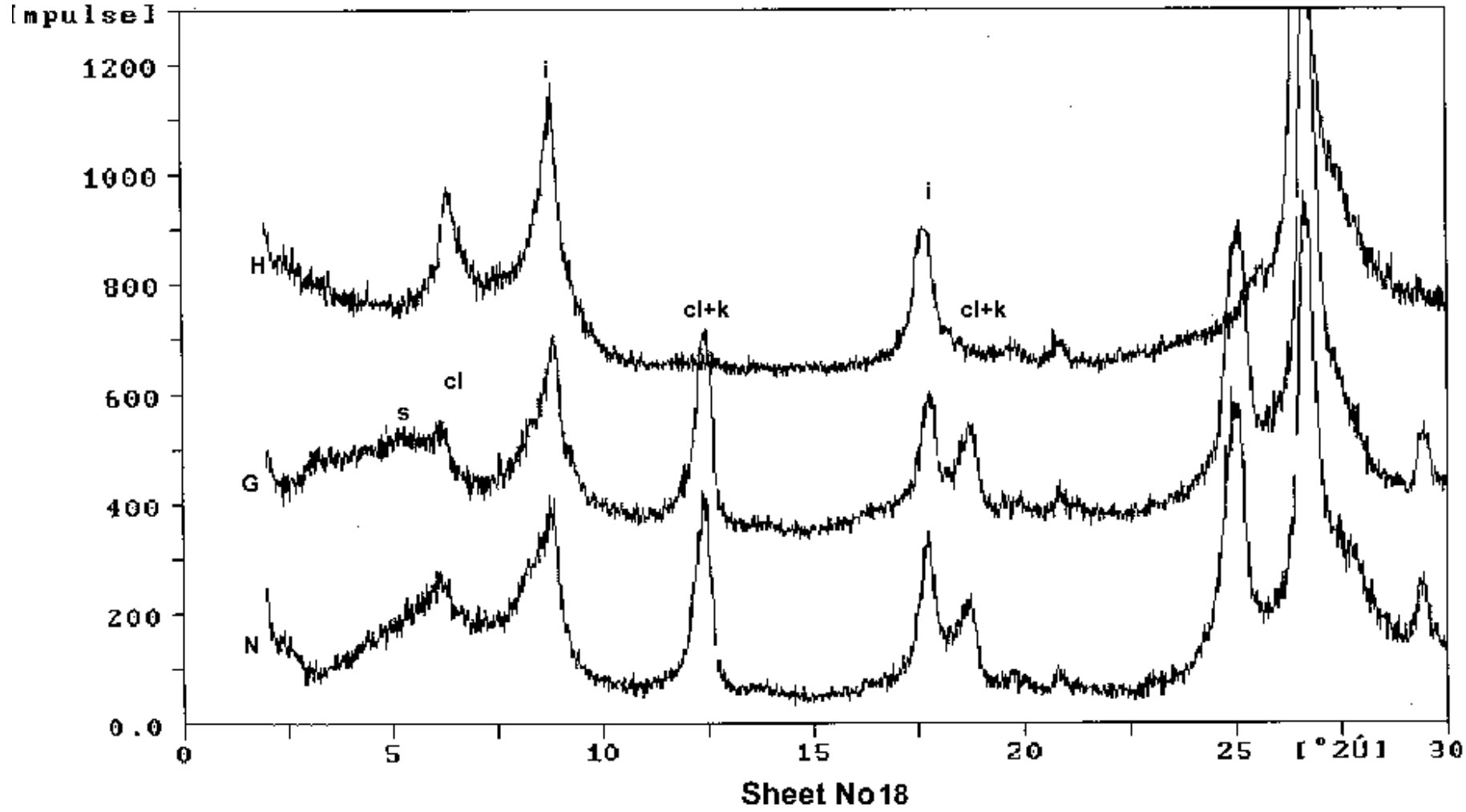
[mpulse]
1200
1000
800
600
400
200
0.0
H
G
N
i
i
cl+k
cl+k
cl
s
0
5
10
15
20
25
[°2Θ]
30
Sheet No18

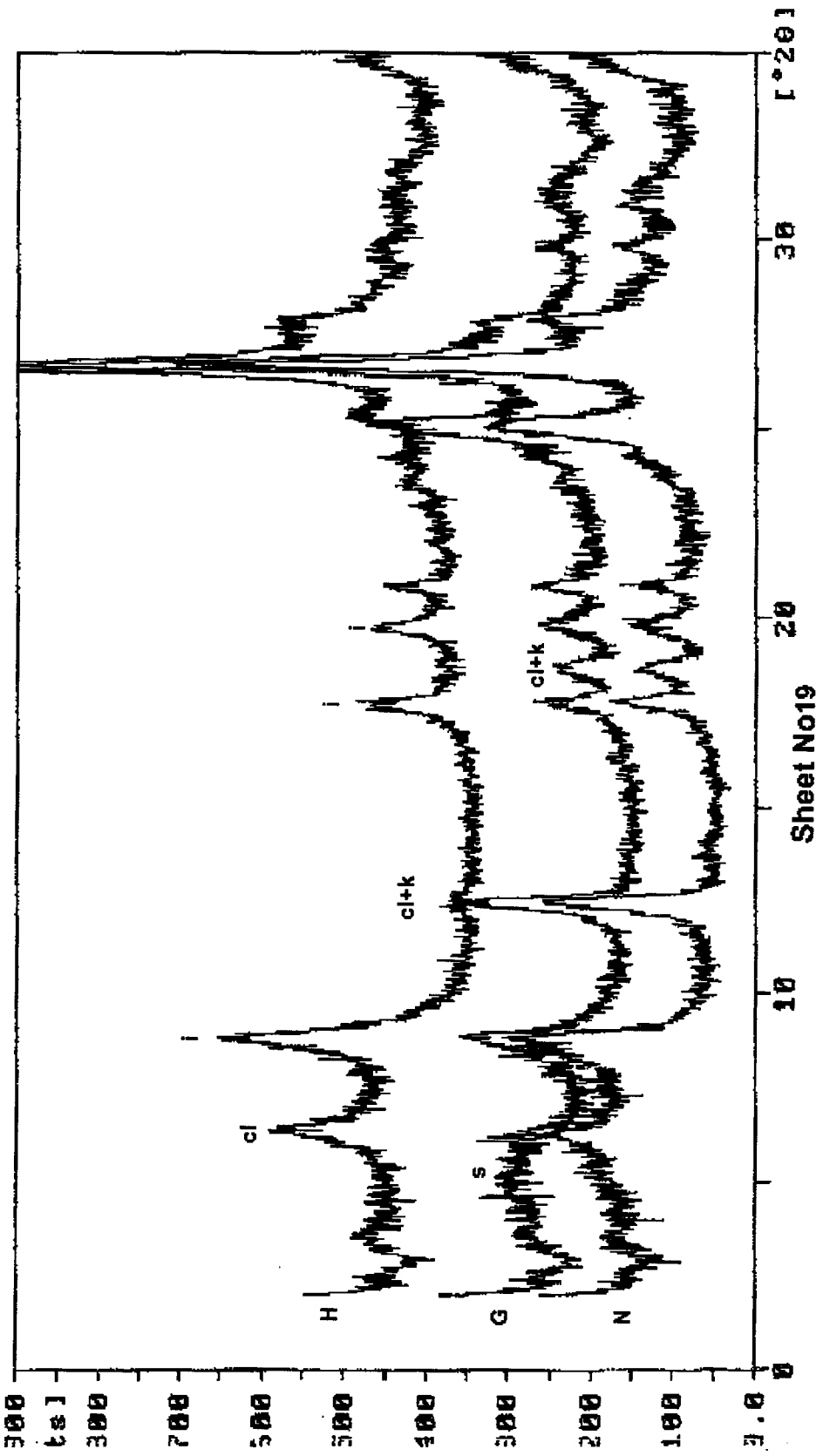
[cps]
[°2θ]
Sheet No19
H
G
N
cl
s
i
cl+k
i
cl+k
i

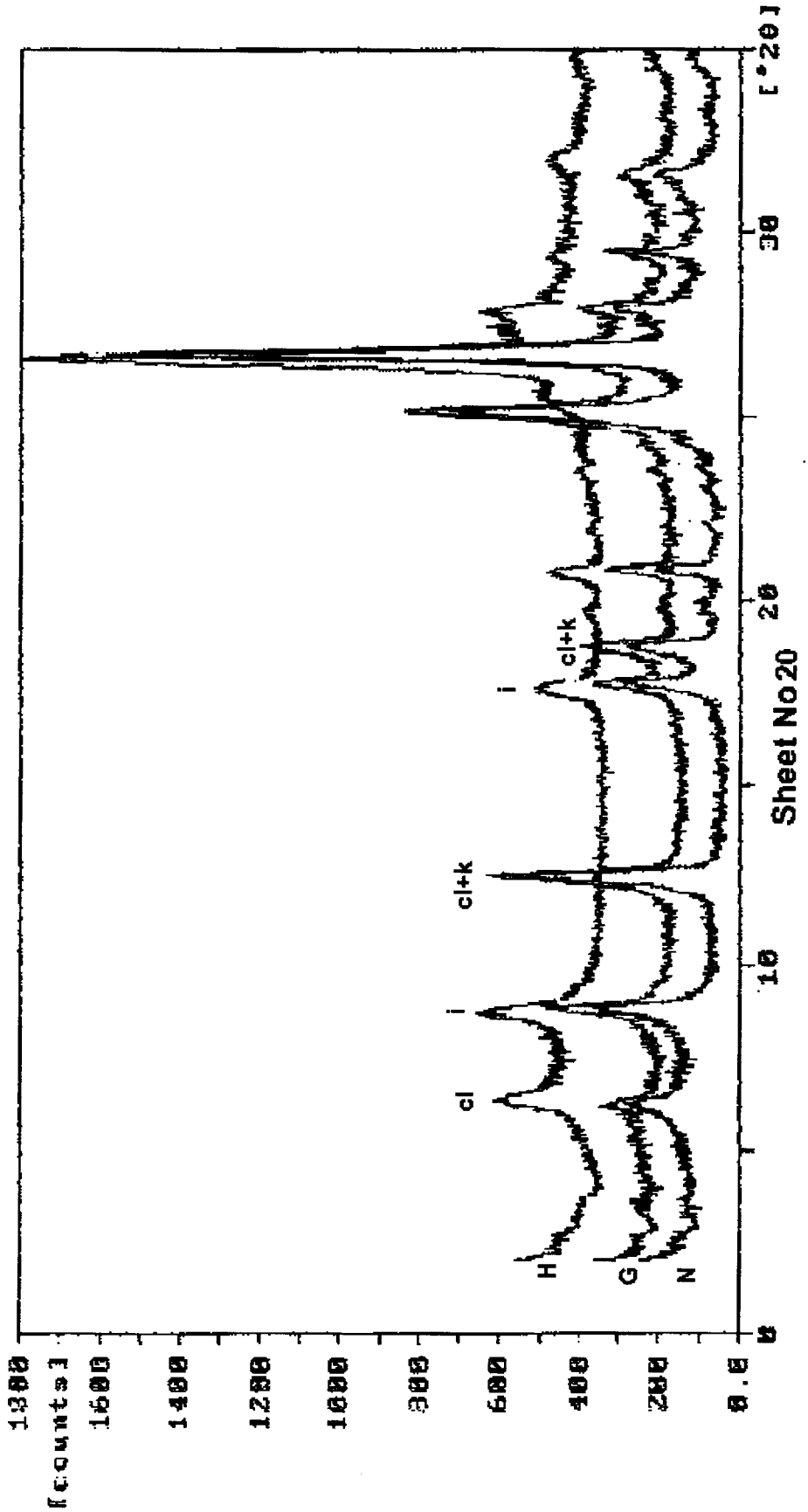
Sheet No 20
cl
i
cl+k
i
cl+k
H
G
N
[counts]
[°2θ]

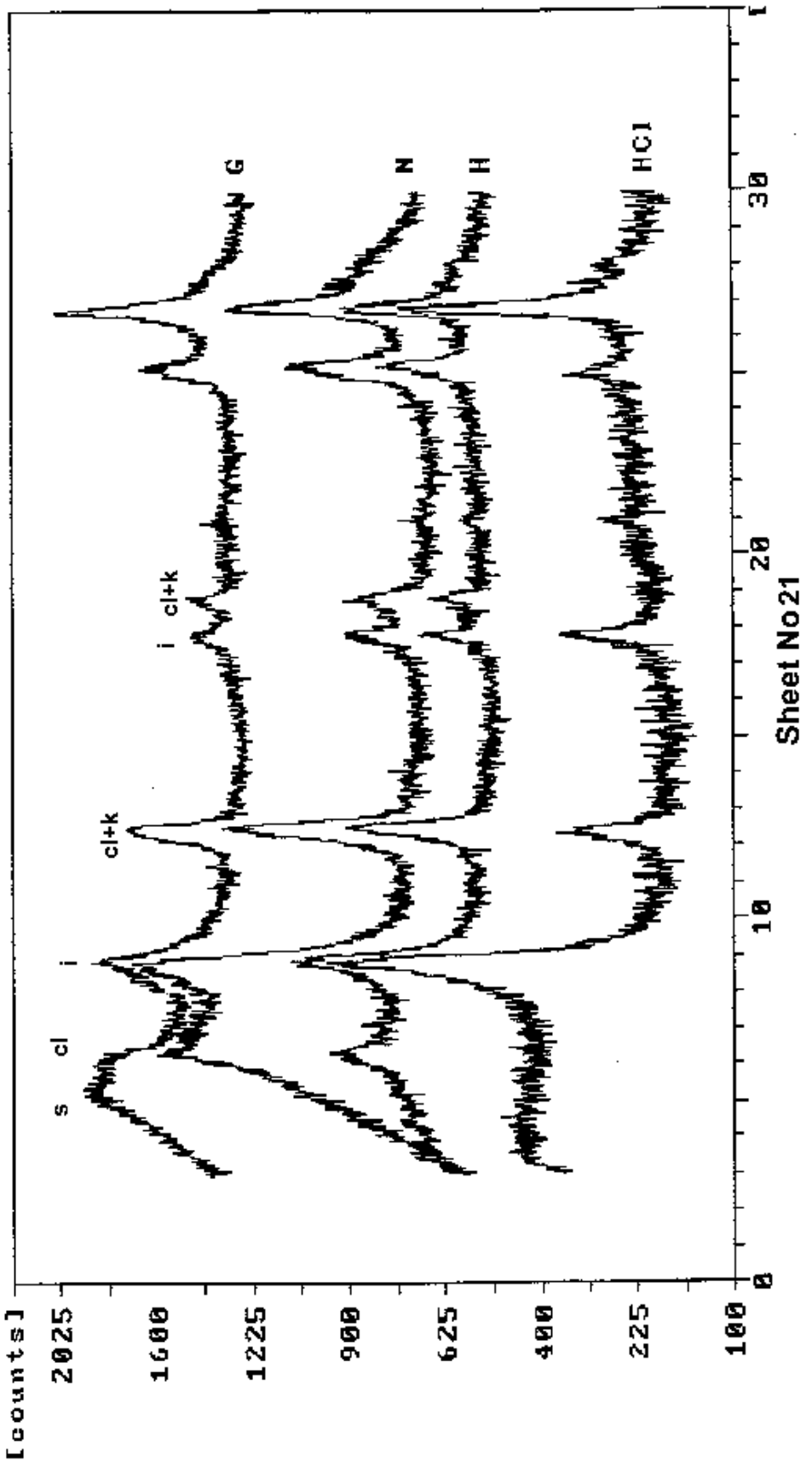
[counts]
2025
1600
1225
900
625
400
225
100
0
10
20
30
Sheet No21
s
cl
i
cl+k
i
cl+k
G
N
H
HCl

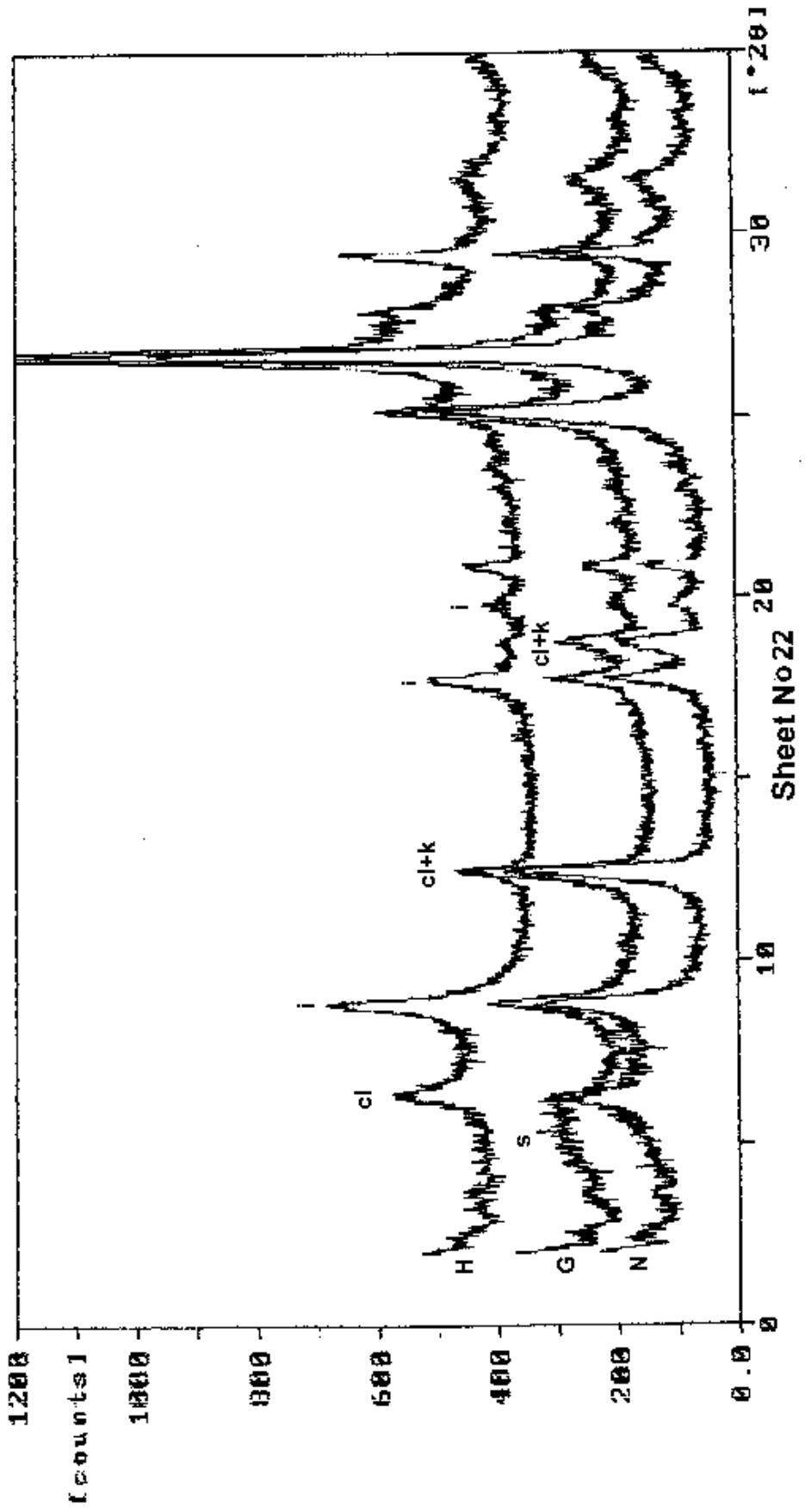
1200
[counts]
1000
800
600
400
200
0.0
0
10
20
30
[°2θ]
Sheet No 22
cl
i
cl+k
i
i
cl+k
H
S
G
N

Intensity (ADS)
400
200
0
10.0
20.0
30.0
40.0
50.0
60.0
70.0
2Theta
Sheet No 23
h
h
h
h
h
b

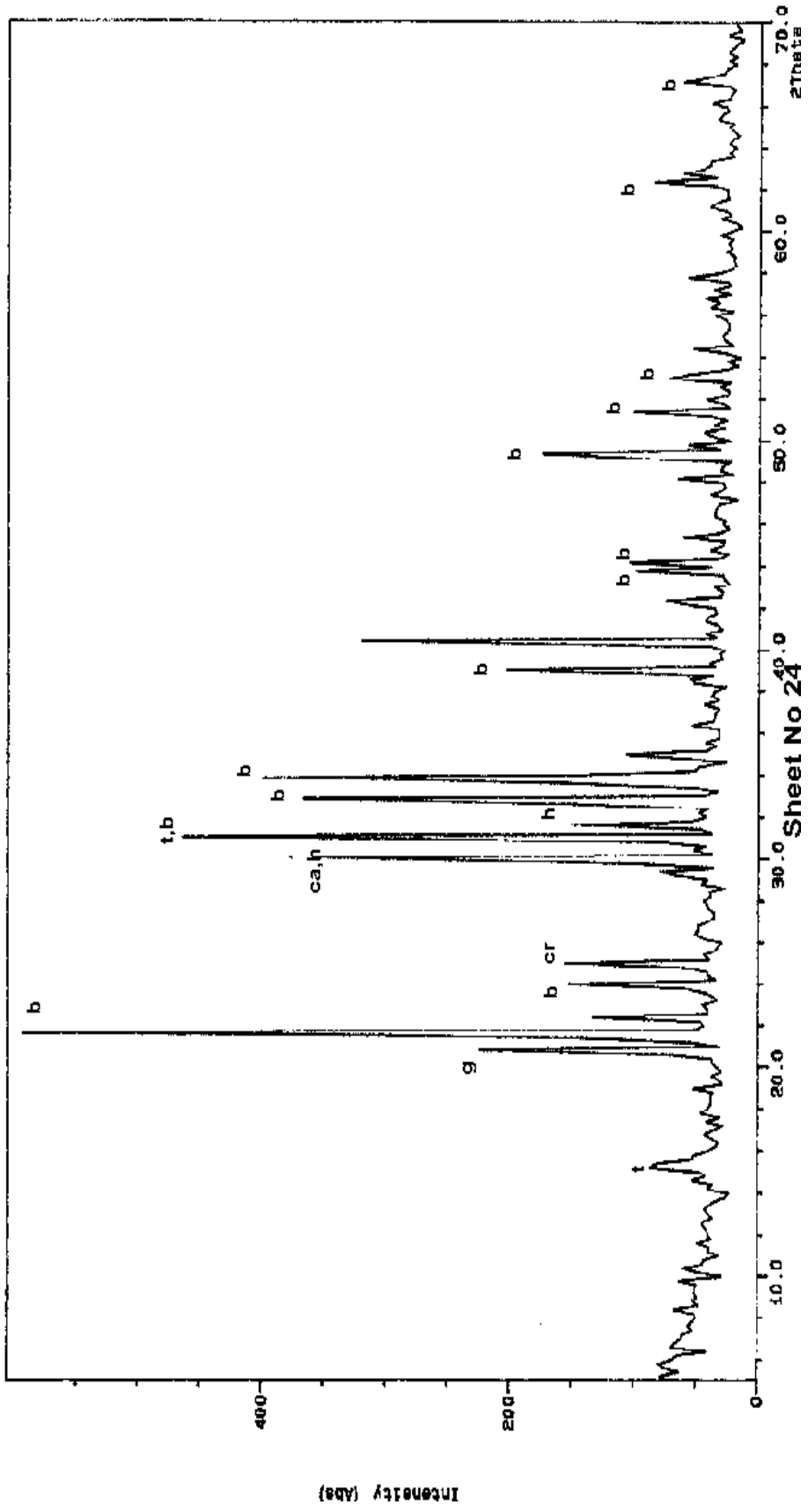
Intensity (Abs)
400
200
0
10.0
20.0
30.0
40.0
50.0
60.0
70.0
2Theta
Sheet No 24
b
g
t
b cr
ca,h
t,b
h
b
b
b
b
b
b
b
b
b
b

Appendix C: Procedure of separating heavy minerals

Fine and very fine sand fractions (0.125-0.062 mm) of samples were selected by dry-sieving method. Heavy minerals of these fractions were separated using special apparatus and standard bromoform method. The magnetic fractions were removed by hand magnet and electromagnetic method. The magnetic fractions determined by reflected polarizing microscope and X-ray diffraction where was necessary. After this stage enough light heavy mineral grains were obtained to be made one slide for each sample. A glass microscope slide was heated on a hot plate and was melted enough entellan to be covered the slide. The sample was poured on the slide and the grains were spread using a wire probe. A flame (match or Bunsen burner) applied briefly to the surface of the entellan will be destroyed any bubble. A cover glass was put on the slide and an eraser end of a pencil was used to position the cover glass and remove any bubbles. The relative frequency percentage of heavy minerals was then determined by counting at least 100 grains in each mount using by transmitted light binocular and polarizing microscope (Lewis, 1984; Lindholm , 1987; Mange & Maurer, 1992).

Appendix D: Thin Section–making process of unconsolidated sediments:

Two hundred ml of resin (Araldite) for 10 samples (a total of about 200 thin sections were prepared for this study) were mixed with a level teaspoon of waxoline blue dye and placed in an oven at 60^{o}C and gently stirred at 5 min intervals until the dye was dissolved (30 min approx.). Twenty ml of hardener was added and well mixed for 1 min. The resin was then immediately poured into the 10 labeled moulds and the samples dropped in (don't put the samples in first as a flat based samples may not be wetted or may adhere to grease). The mould plus samples was put in the desiccator and the vacuum was applied. Then the moulds were removed and allowed to be hardened for 24 hours at room temperature. Finally the impregnated samples were released from the moulds and were cut in suitable sections for examination by polarizing microscope (Trewin, 1988).

Appendix E: Procedure of installation of sampling traps:

Sediment collector traps were established in very slightly elevated places. At least two, optimum three, 10 l buckets were buried. The opening of the trap was favorably covered by a net (e.g. curtain meshwork, to prevent aeolian erosion and unwanted trapping of larger animals). The rim of the traps should be slightly above the sediment surface. Sediments, deposited in the traps, were removed every month by a kind of blade.

Appendix F: Lithostratigraphic- Sedimentologic sections of alluvial deposits

F1: Legend to stratigraphic sections

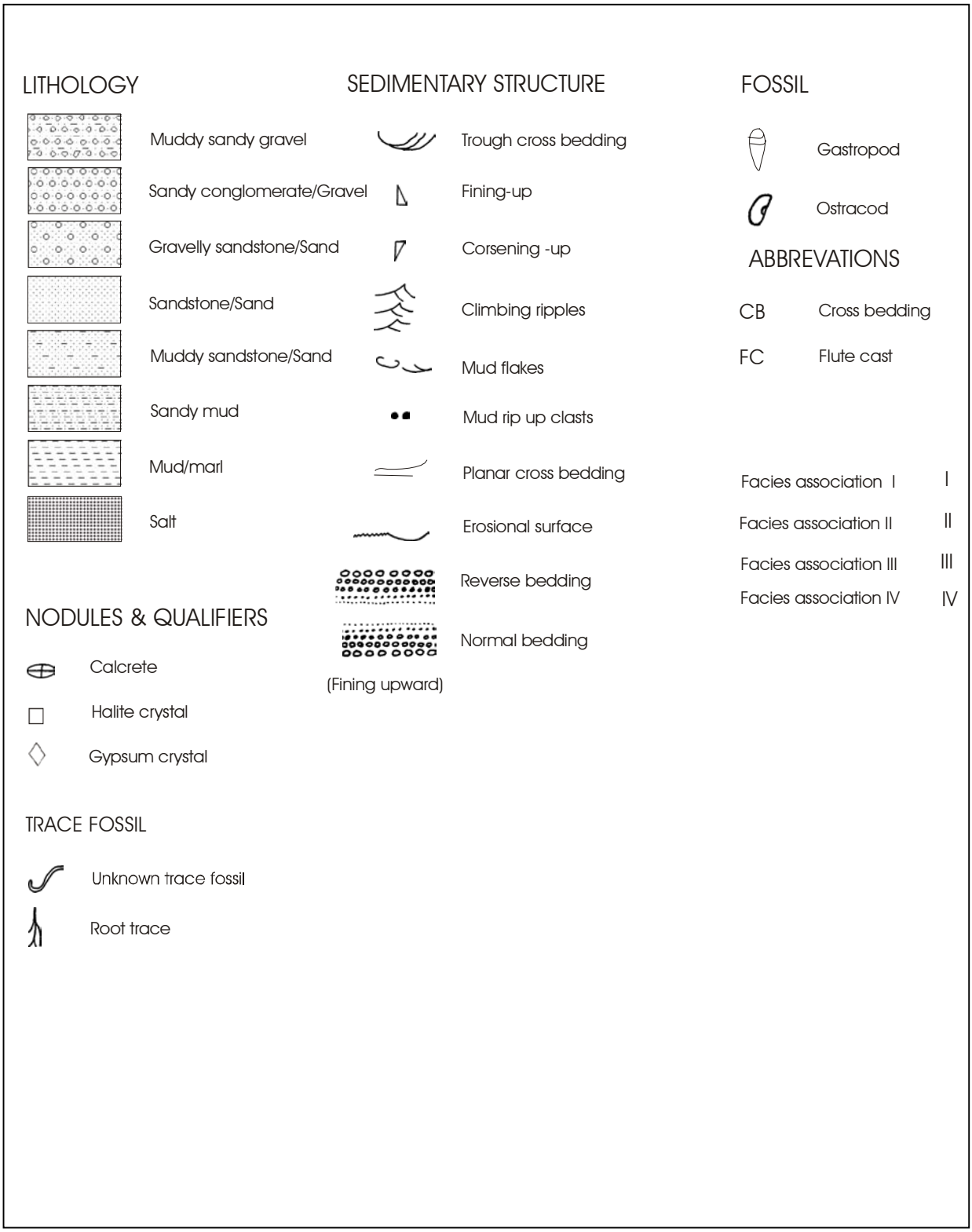

F2: Stratigraphic sections sheets (No. 1-28)

SECTION NO: Dz1
GEOLOGICAL SITUATION: Trench
SCALE 1:15

LOCATION: 32⁰,17′,12″N 52⁰,53′,45″E
NAME: Kuh-e-Siah (3o km east of Varzaneh)
SHEET 1 OF 28

DEPTH (cm)	GRAPHIC LITHOLOGY	TEXTURE AND GRAIN SIZE	Color	REMARKS AND ENVIRONMENTAL INTERPRETATION
30	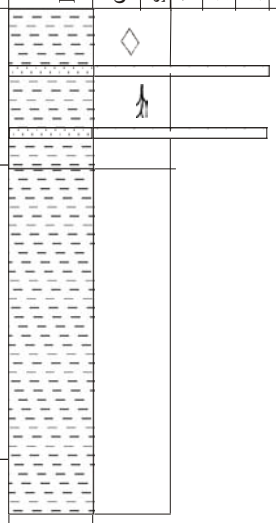	MUD: clay, silt; SAND: vfs, fs, ms, cs, vcs; GRAVEL: granule, pebble, cobble	Grey to black	Massive mud interbedded with lenticular sand layers, frequent plants, root traces and plant roots, a few gypsum crystals and sharp boundary at base. A product of deposition in shallow distributary channels and upper parts of point bars in the Zayandeh river delta.
90			Yellow to brown	Massive mud, high ratio of clay to silt. Deposition on the upper parts of point bars, swamps and levees of the Zayandeh river delta.

SECTION NO: Dz5
GEOLOGICAL SITUATION: Trench
SCALE 1:15

LOCATION: 32⁰,17′,11″N 52⁰,53′,12″E
NAME: Kuh-e-Siah (30 km east of Varzaneh)
SHEET 2 OF 28

DEPTH (cm)	GRAPHIC LITHOLOGY	TEXTURE AND GRAIN SIZE	Color	REMARKS AND ENVIRONMENTAL INTERPRETATION
30	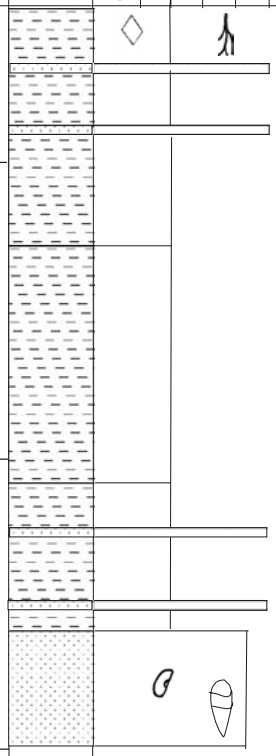	MUD: clay, silt; SAND: vfs, fs, ms, cs, vcs; GRAVEL: granule, pebble, cobble	Grey to black	Massive mud interbedded with lenticular sand layers, frequent plants, root traces and plant roots, a few gypsum crystals, sharp boundary at base. Deposition in shallow distributary channels and upper parts of levees in the Zayandeh river delta
				Massive mud, high ratio of clay to silt. A product of rapid deposition in a shallow fresh water-brackish lake or flood sheets.
90			Yellow to brown	
				Intermittent of sand and brown mud layers, graditional boundary at base and top. Deposition on the various parts of the Zayandeh river delta.
150			Khaki	Massive fine to medium sand with gastropod and ostracod shells. Deposition in the bottom of small shallow distributary channels during upper flow regime periods.

SECTION NO: G1
GEOLOGICAL SITUATION: Stream cut
SCALE 1:30

LOCATION: 32⁰,27′,05″N 52⁰,50′,35″E
NAME: Siahkuh (15 km northeast of Ejieh)
SHEET 3 OF 28

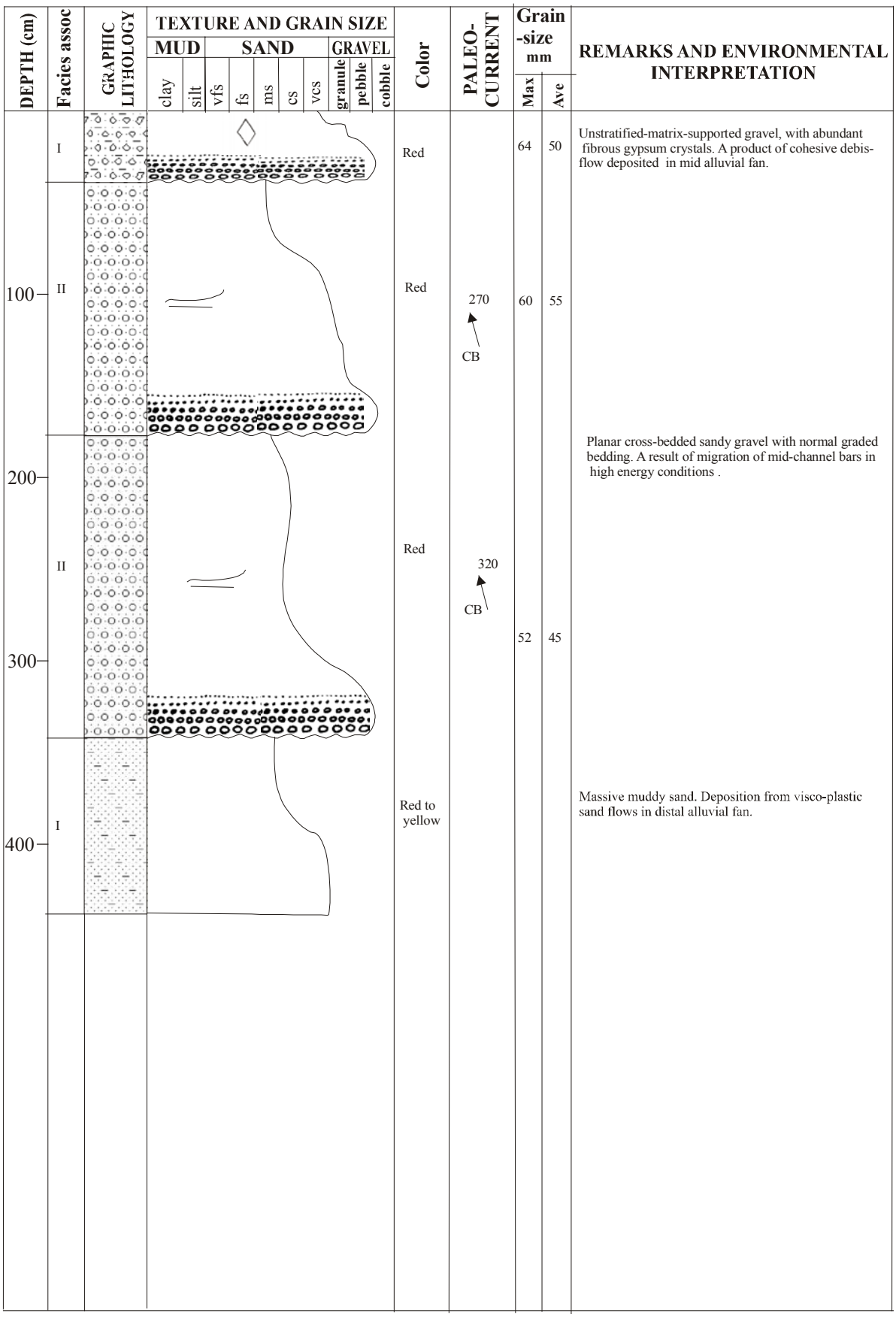

SECTION NO: G2
GEOLOGICAL SITUATION: Qnat well
SCALE 1:30

LOCATION: 32⁰,40′,40″N 52⁰,16′,15″E
NAME:Ghehi (16 km northeast of Ejieh)
SHEET 4 OF 28

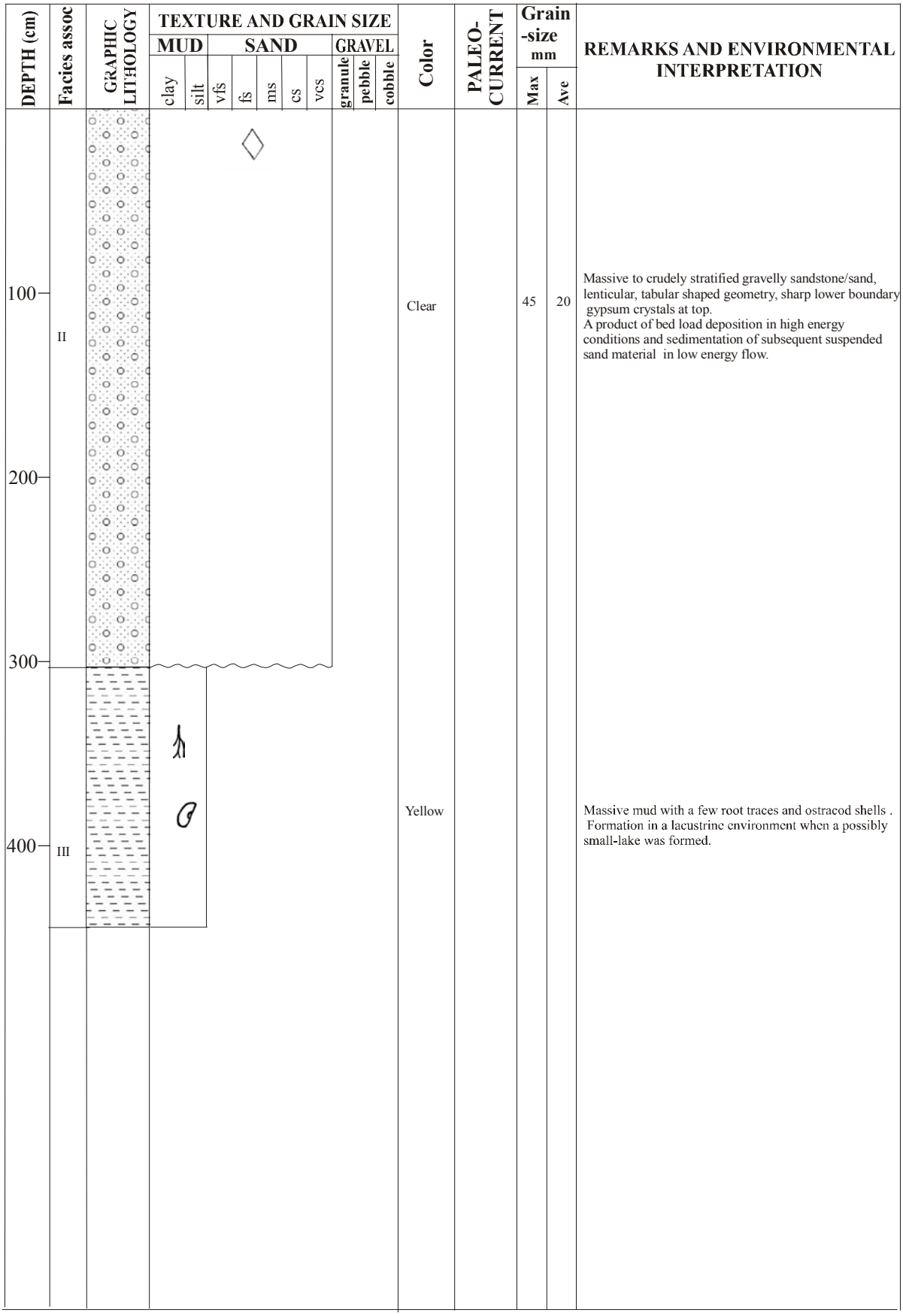

SECTION NO: G3
GEOLOGICAL SITUATION: Stream cut
SCALE: 1:30

LOCATION: 32⁰,41/,54//N 52⁰,07/,49//E
NAME: Segzi (15 km north of Shahkaram)
SHEET 5 OF 28

DEPTH (cm)	Facies assoc	GRAPHIC LITHOLOGY	TEXTURE AND GRAIN SIZE	Color	PALEO-CURRENT	Grain-size mm		REMARKS AND ENVIRONMENTAL INTERPRETATION
			MUD: clay, silt; SAND: vfs, fs, ms, cs, vcs; GRAVEL: granule, pebble, cobble			Max	Ave	
100	II	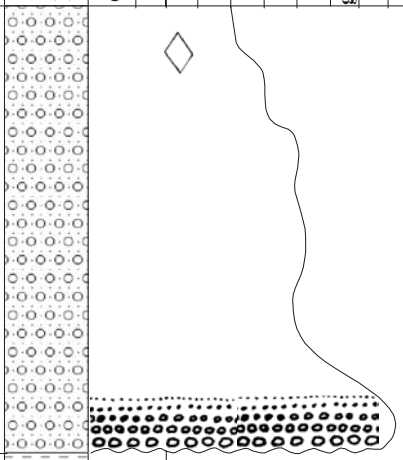		Clear		118	71	Unstratified-sandy conglomerate/gravel with abundant gypsum crystals, normal graded bedding structure, broad lenticular sheet like geometry with erosional base. Deposition from high energy flow , transporting and accumulating coarse bed load and keeping sand material in suspension.
200	III			Yellow				Massive mud with a few root traces and ostracod shells . Formation in a lacustrine environment when a possibly small-lake was formed.

SECTION NO: G4
GEOLOGICAL SITUATION: Irrigation channel
SCALE: 1:30

LOCATION: 32⁰,23′,01″N 52⁰,47′,41″E
NAME: Siahkuh (13.5 km southeast of Varzaneh)
SHEET 6 OF 28

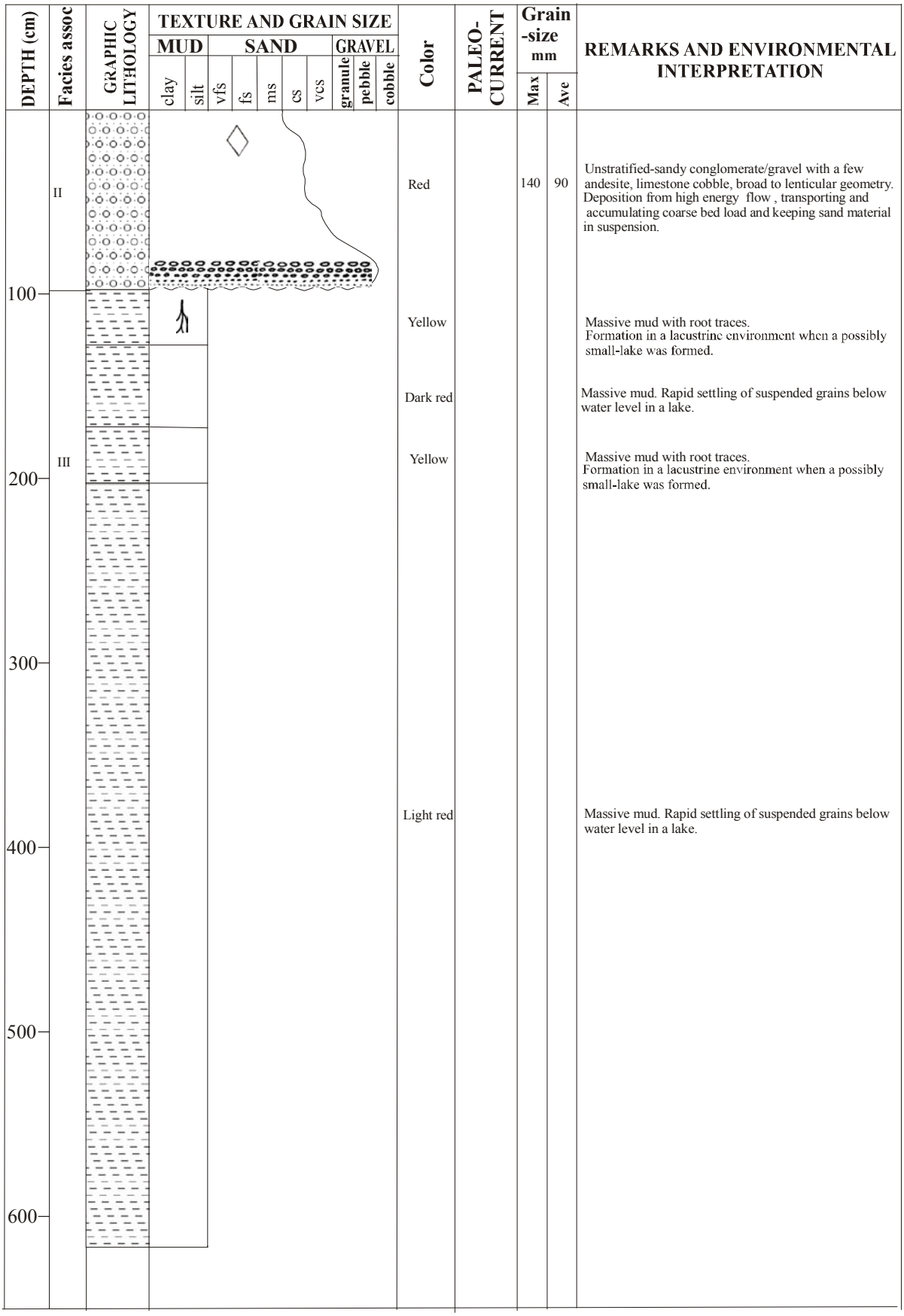

SECTION NO: G5
GEOLOGICAL SITUATION: Trench
SCALE 1:30

LOCATION: 32⁰,31′,58″N 52⁰,27′,37″E
NAME: Harand (12.5 km northeast of Ejieh)
SHEET 7 OF 28

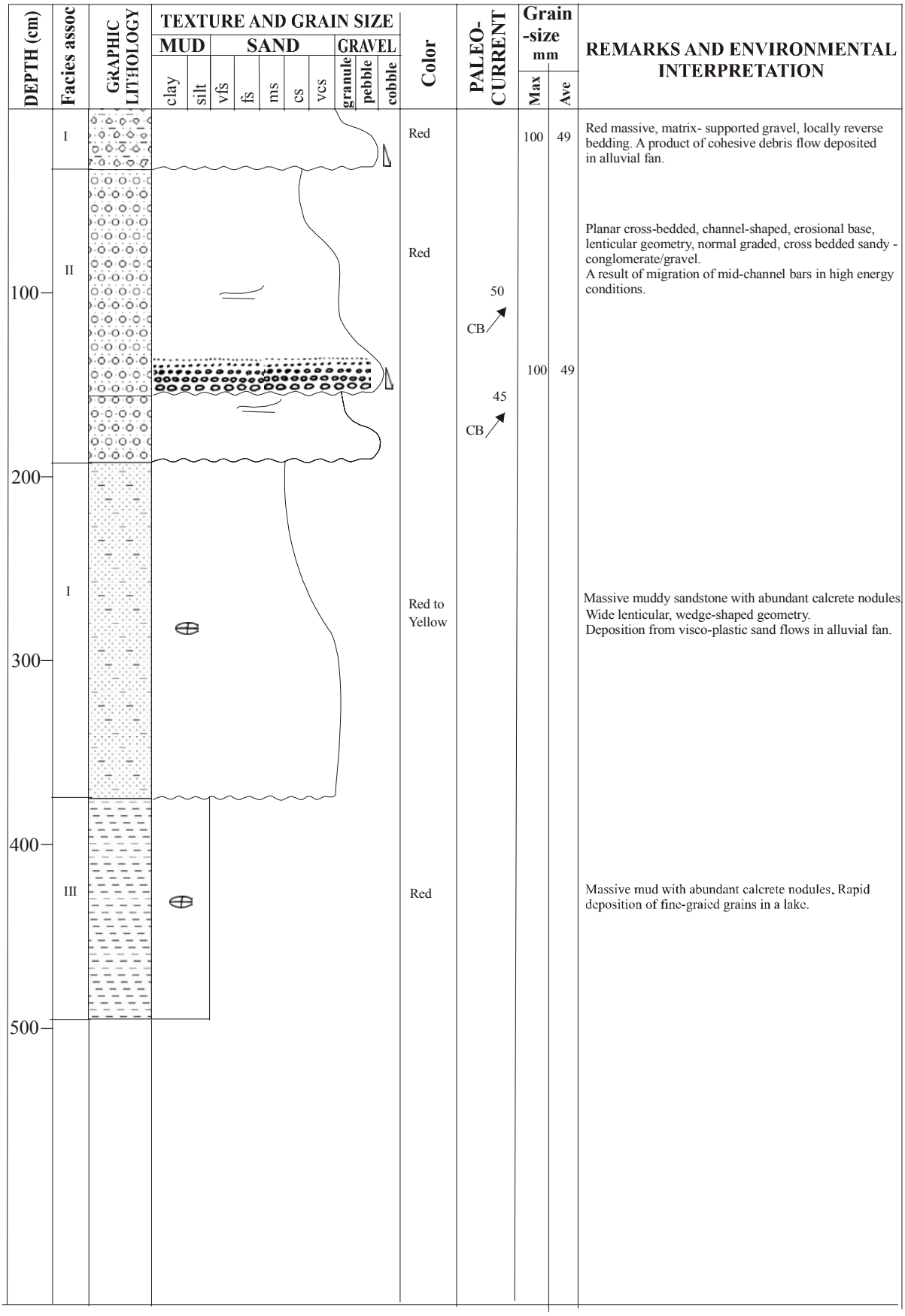

SECTION NO: G6
GEOLOGICAL SITUATION: Irrigation channel
SCALE: 1:30

LOCATION: 32⁰,34′,31″N 52⁰,16′,42″E
NAME: Serian (10 km northeast of Shahkaram)
SHEET 8 OF 28

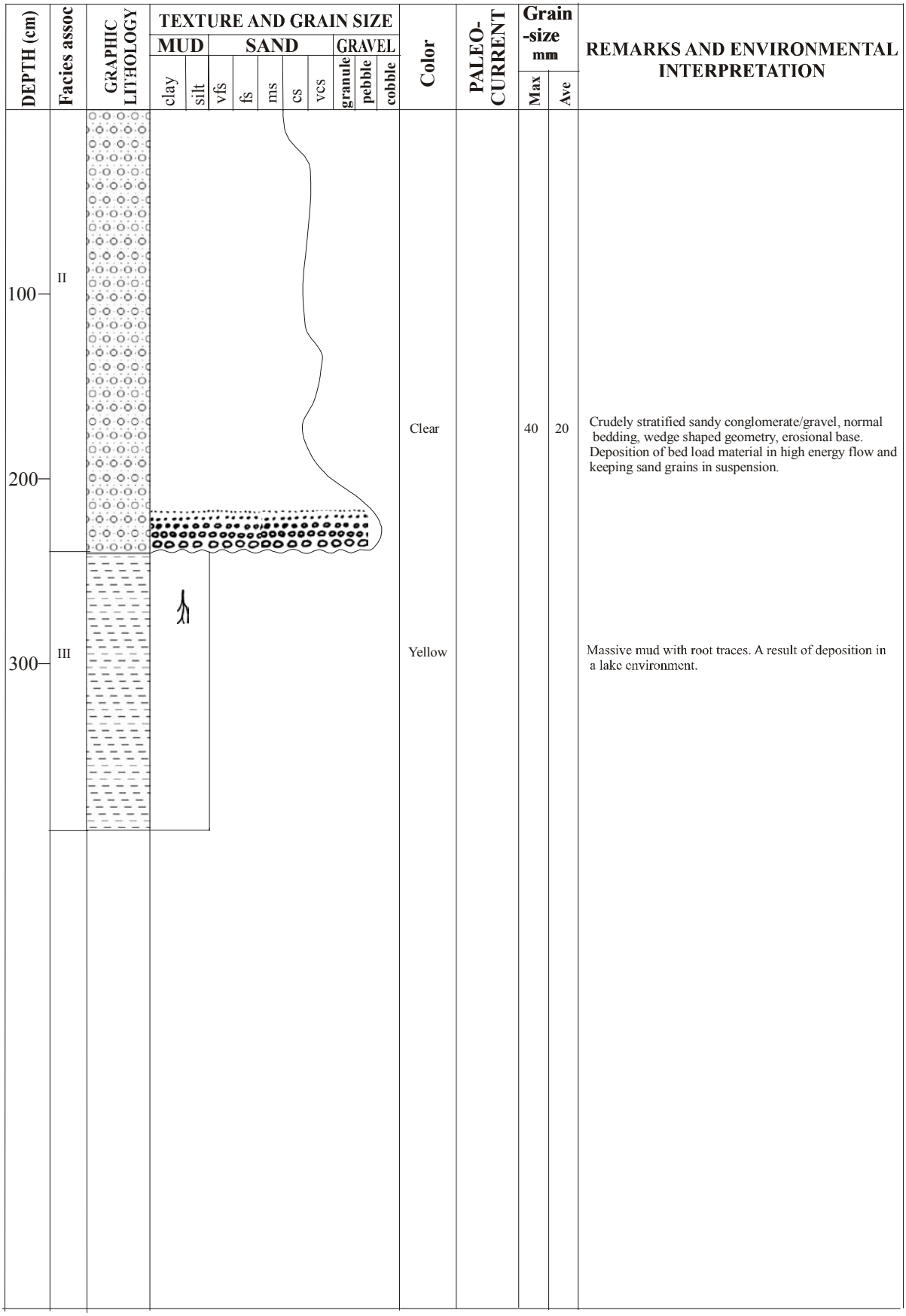

SECTION NO: G7
GEOLOGICAL SITUATION: Zayandeh river cut
SCALE: 1:30

LOCATION: 32⁰,21′,45″N 52⁰,47′,55″E
NAME: Varzaneh (10 km east of Varzaneh)
SHEET 9 OF 28

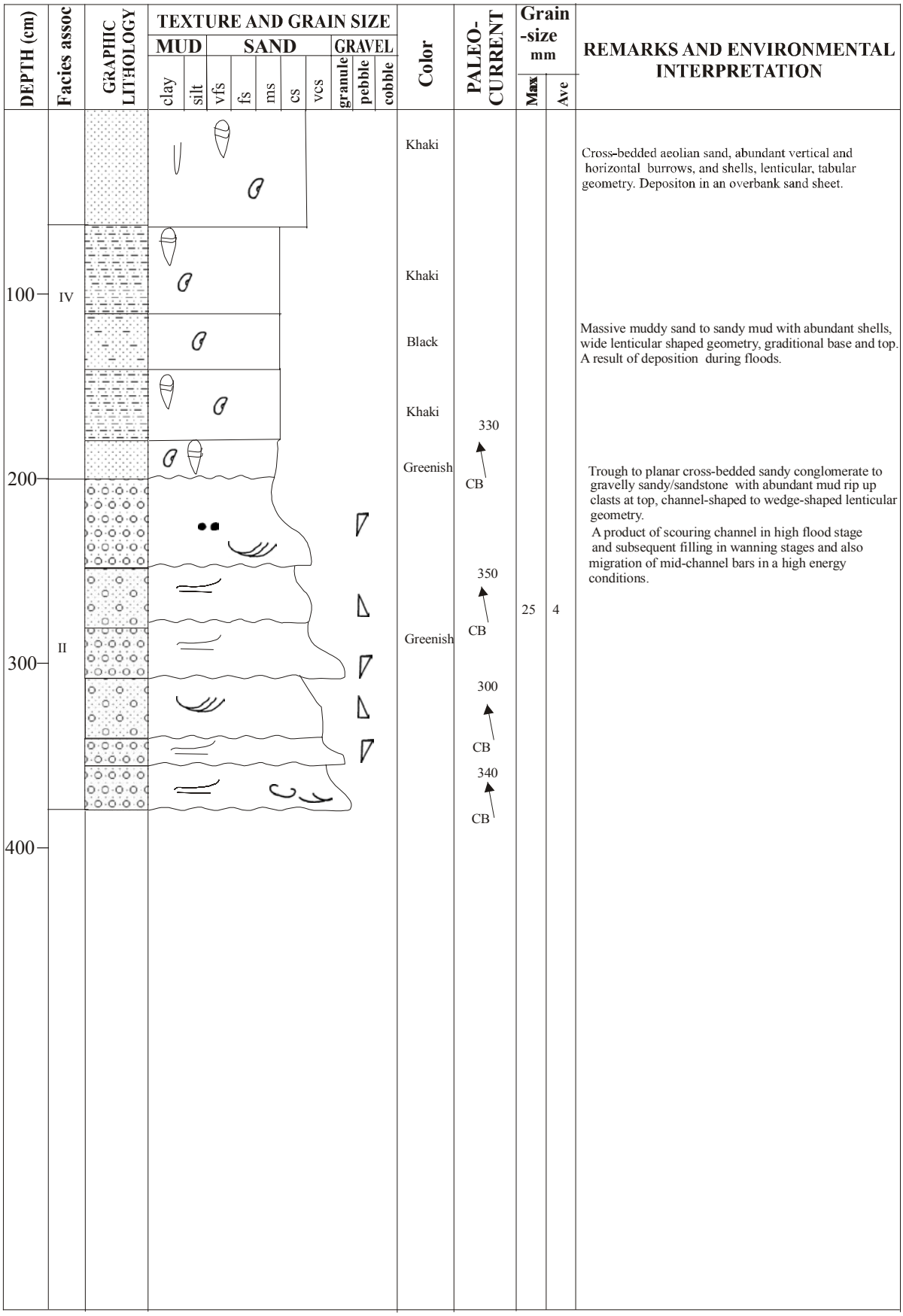

SECTION NO: G9
GEOLOGICAL SITUATION: Zayandeh river cut
SCALE: 1:30

LOCATION: 32⁰,29′,44″N 52⁰,25′,24″E
NAME: Ejieh (2 km east of Ejieh)
SHEET 10 OF 28

DEPTH (cm)	Facies assoc	GRAPHIC LITHOLOGY	TEXTURE AND GRAIN SIZE	Color	PALEO-CURRENT	Grain-size mm		REMARKS AND ENVIRONMENTAL INTERPRETATION
			MUD: clay, silt; SAND: vfs, fs, ms, cs, vcs; GRAVEL: granule, pebble, cobble			Max	Ave	
100	II	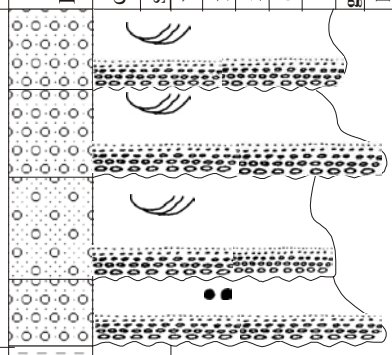		Clear		100	30	Trough cross-bedded asymmetrical, channel-shaped, concave base sandy conglomerate. A product of scoring an subsequent filling of bed load sediments in a channel. Massive sandy conglomerate with abundant mud rip up clasts, wedge-shaped lenticular geometry. Bed load deposition from high energy stream flow,
	III			Yellow				Massive yellow mud. Formation in a lacustrine environment. Massive mud with root traces. Formation in a lacustrine environment

SECTION NO: G10
GEOLOGICAL SITUATION: Trench
SCALE 1:30

LOCATION: 32º,30′,34″N 52º,24′,39″E
NAME: Sian (3km north of Ejieh)
SHEET 11 OF 28

DEPTH (cm)	Facies assoc	GRAPHIC LITHOLOGY	TEXTURE AND GRAIN SIZE: MUD (clay, silt)	SAND (vfs, fs, ms, cs, vcs)	GRAVEL (granule, pebble, cobble)	Color	PALEO-CURRENT	Grain-size mm: Max	Grain-size mm: Ave	REMARKS AND ENVIRONMENTAL INTERPRETATION
	IV		◇			Grey to black				Gypsiferous mud with a few fine gravel and sand. Deposition in a shallow lake and subsequent wind activity.
100	IV					Yellow to brown				Massive mud with root traces. Formation in a lacustrine environment
200										

SECTION NO: G11
GEOLOGICAL SITUATION: Irrigation channel
SCALE 1:30

LOCATION: 32⁰,31′,11″N 52⁰,21′,04″E
NAME: Gishi (7.5 km northwest of Ejieh)
SHEET 12 OF 28

DEPTH (cm)	Facies assoc	GRAPHIC LITHOLOGY	TEXTURE AND GRAIN SIZE	Color	PALEO-CURRENT	Grain-size mm	REMARKS AND ENVIRONMENTAL INTERPRETATION
			MUD: clay, silt; SAND: vfs, fs, ms, cs, vcs; GRAVEL: granule, pebble, cobble			Max / Ave	
100	II	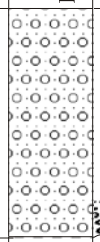	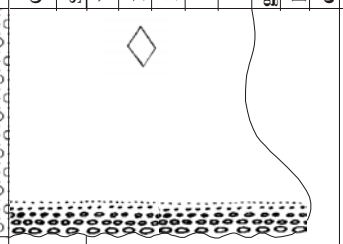	Clear		77 / 52	Massive to crudely stratified conglomerate/gravel, abundant gypsum crystals at top, normal graded bedding, lenticular, wedge-shaped geometry and erosional boundary. It records bed load deposition under high energy flow and sedimentation of subsequent of suspended sand material.
	III	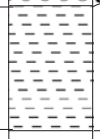		Yellow			Mud without any bedding. Deposition in a lacustrine sedimentary environment.

SECTION NO: G12
GEOLOGICAL SITUATION: Zayandeh river cut
SCALE 1:30

LOCATION: 32⁰,27/,10//N 52⁰,29/,10//E
NAME: Farfan (7.5 km east of Ejieh)
SHEET 13 OF 28

DEPTH (cm)	Facies assoc	GRAPHIC LITHOLOGY	TEXTURE AND GRAIN SIZE	Color	PALEO-CURRENT	Grain-size mm		REMARKS AND ENVIRONMENTAL INTERPRETATION
			MUD: clay, silt; SAND: vfs, fs, ms, cs, vcs; GRAVEL: granule, pebble, cobble			Max	Ave	
				Khaki				Laminated sandy mud to mud with abundant burrowing root traces, gastropod and ostracod shells. Broad lenticular, tabular geometry, graditional border with upper and lower layers. Deposition in a river overbank environment.
				Dark				
100	IV			Red				Massive mud with broad lenticular geometry, abundant root traces and gastropod and ostracod shells. A result of settling of suspended grains below water level of a lake.
200				Greenish				Massive sand/sandstone with abundant gastropod and ostracod shells. Broad lenticular, tabular geometry and normal graded bedding. Rapid deposition from suspension during floods.
				Greenish		40	20	Trough sandy conglomerate/gravel, channel shaped geometry, erosional scoured base. A product of scouring and filling in coarse-grained meandering or in braided river.
	II							
300				Greenish	45 CB			Planar cross-bedded sandy conglomerate/gravel, normal graded bedding with abundant mud rip-up clasts. It is resulted from migration of mid-channel bars.

SECTION NO: G13
GEOLOGICAL SITUATION: Zayandeh river cut
SCALE: 1:30

LOCATION: 32⁰,26′,44″N 52⁰,23′,02″E
NAME: Ejieh bridge
SHEET 14 OF 28

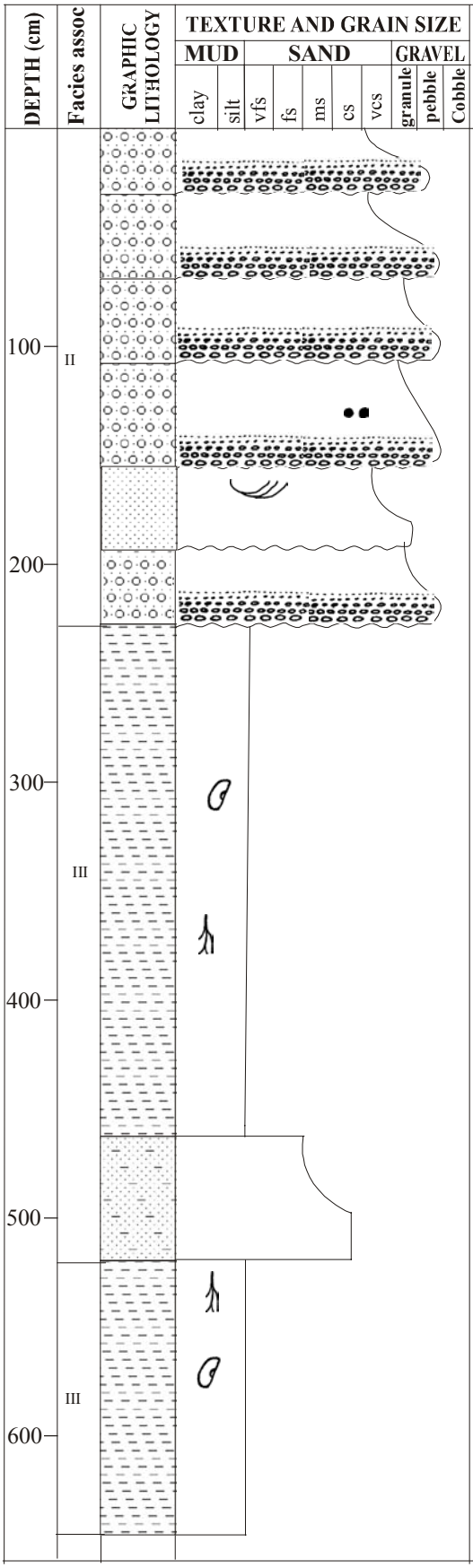

Color	PALEO-CURRENT	Grain-size mm Max	Grain-size mm Ave	REMARKS AND ENVIRONMENTAL INTERPRETATION
		180	36	Massive sandy conglomerate with a few mud rip up clasts in the lower part, graded bedding structure, channel shaped geometry. Bed load deposition from stream flow originated from high energy flow, transporting and accumulating coarse bed load and keeping sand material in suspension.
Clear				Trough cross-bedded sandstone with granules, lenticular wedge shaped geometry. A result of scouring channel and subsequent filling in wanning stages.
	55 FC			Strongly erosional scoured based massive sandy conglomerate. Deposition under high energy conditions in braided river.
Yellow				Massive mud to sandy mud with a few gastropod shells and abundant root traces, lenticular geometry. Deposition in a lacustrine environment accompanied period input of current transported sands.
Greenish				Massive sandstone/ sand with slightly mud, lenticular wedge shaped geometry, graditional base and top. Rapid deposition from suspension during floods.
Yellow				Massive mud with root traces and ostracod shells deposition in a lacustrine environment..

SECTION NO: G14
GEOLOGICAL SITUATION: Trench
SCALE 1: 30

LOCATION: 32⁰,13′,09″N 52⁰,40′,29″E
NAME: Dastgerd (7.5 km northwest of Hasanabad)
SHEET 15 OF 28

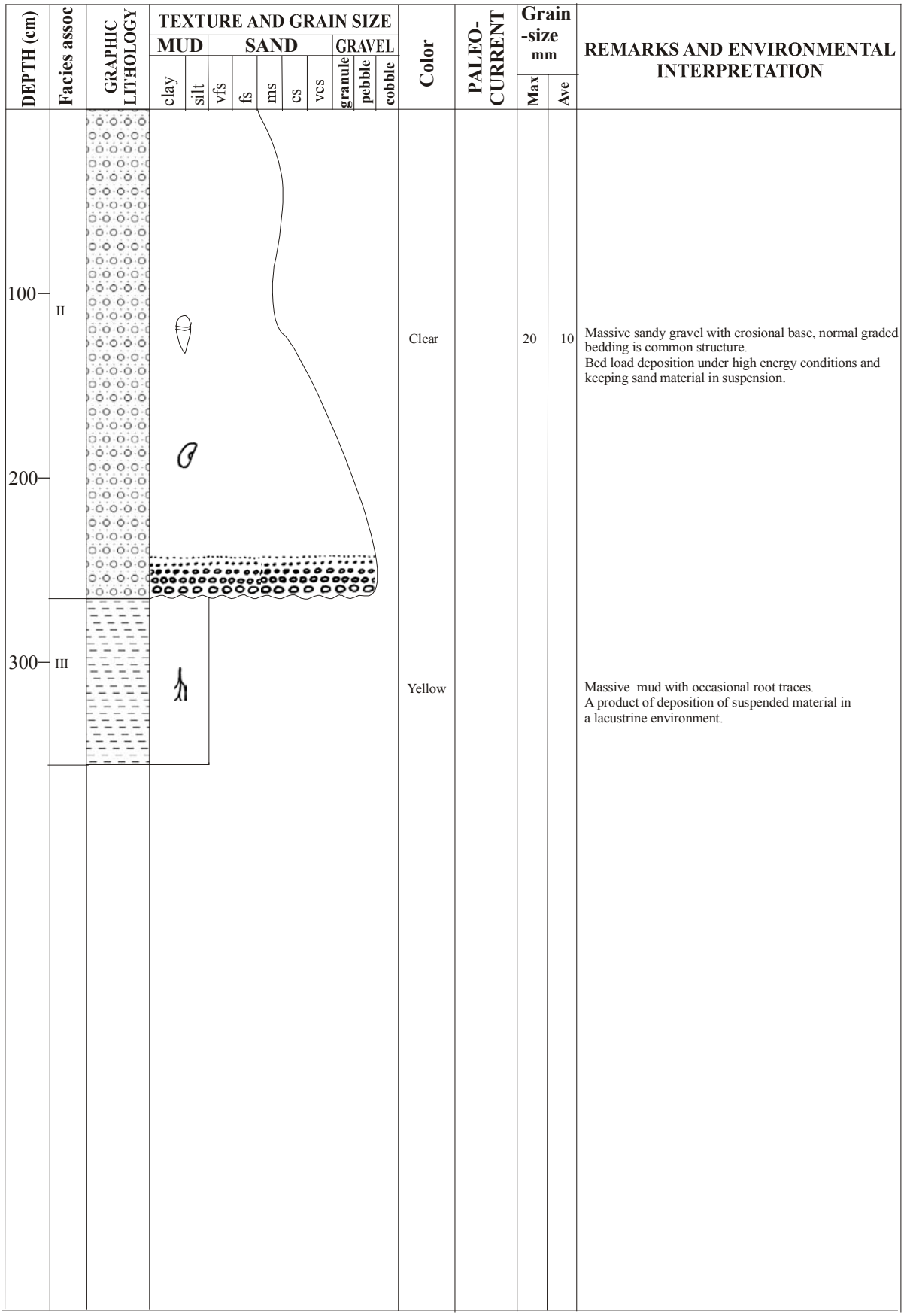

SECTION NO: G15
GEOLOGICAL SITUATION: Stream cut
SCALE 1:30

LOCATION: 32⁰,24′,34″N 52⁰,20′,56″E
NAME: Ejieh (5 km south of Ejieh)
SHEET 16 OF 28

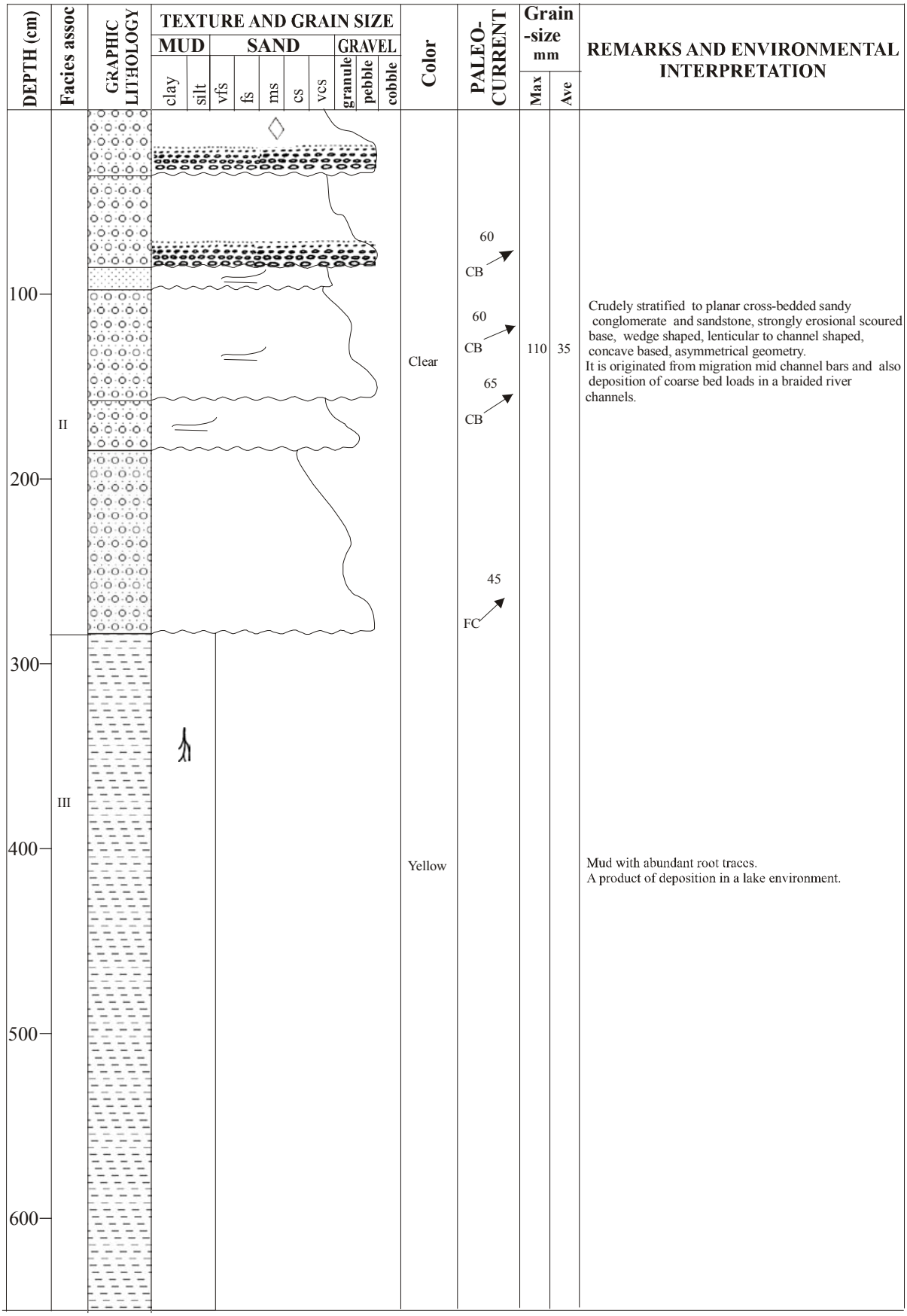

SECTION NO: G16
GEOLOGICAL SITUATION: Stream cut
SCALE 1:30

LOCATION: 32^0,23$^/$,25$^{//}$N 52^0,09$^/$,19$^{//}$E
NAME: Sian (11 km northwest of Yangabad)
SHEET 17 OF 28

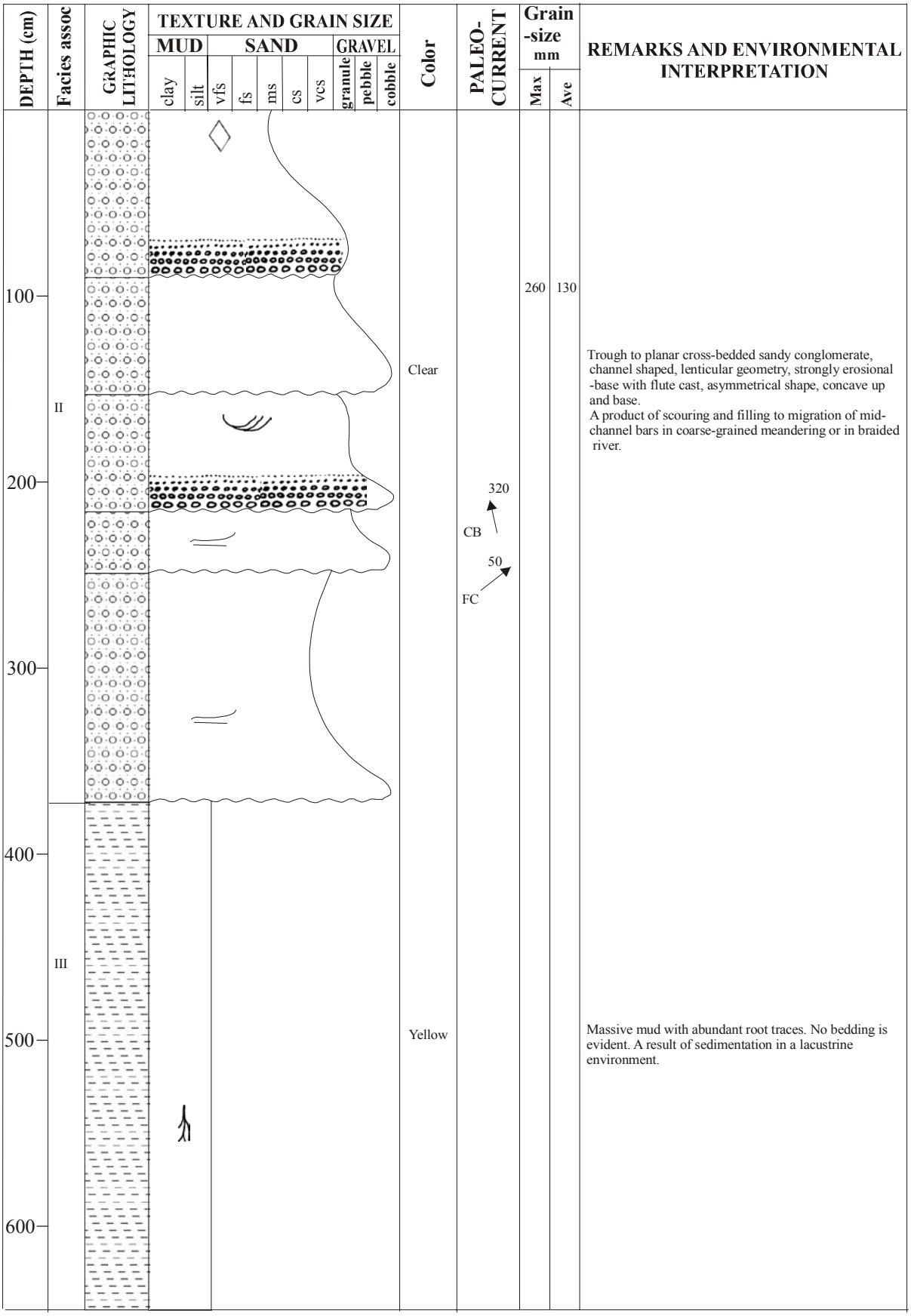

SECTION NO: G17
GEOLOGICAL SITUATION: Trench
SCALE 1:30

LOCATION: 32⁰,32′,08″N 52⁰,35′,52″E
NAME: Kamalabad (2.5 km northwest of Hasanabad)
SHEET 18 OF 28

DEPTH (cm)	Facies assoc	GRAPHIC LITHOLOGY	TEXTURE AND GRAIN SIZE	Color	PALEO-CURRENT	Grain-size mm		REMARKS AND ENVIRONMENTAL INTERPRETATION
			MUD: clay, silt; SAND: vfs, fs, ms, cs, vcs; GRAVEL: granule, pebble, cobble			Max	Ave	
100	I	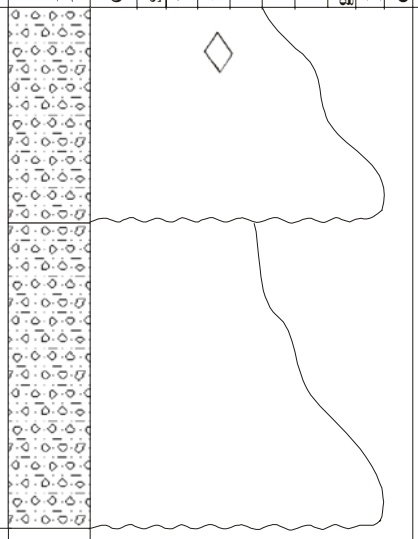		Red		35	29	Unstratified, matrix supported gravel, locally reverse graded bedding, wedge- shaped, broad lenticular geometry. A product of cohesive debris flow deposited in proximal alluvial fan environment.
200				Red				
300								

SECTION NO: G18
GEOLOGICAL SITUATION: Trench
SCALE 1:30

LOCATION: 32^{0},14$^{/}$,50$^{//}$N 52^{0},25$^{/}$,05$^{//}$E
NAME: Heydarabad (17.5 km northwest of Hasanabad)
SHEET 19 OF 28

DEPTH (cm)	Facies assoc	GRAPHIC LITHOLOGY	TEXTURE AND GRAIN SIZE	Color	PALEO-CURRENT	Grain-size mm		REMARKS AND ENVIRONMENTAL INTERPRETATION
			MUD: clay, silt; SAND: vfs, fs, ms, cs, vcs; GRAVEL: granule, pebble, cobble			Max	Ave	
100	I	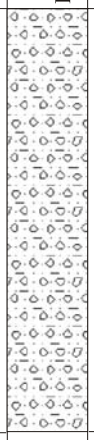		Red		40	19	Unstratified muddy sandy gravel with inverse graded bedding in some places. A result of cohesive debris flow deposited in proximal alluvial fan.

SECTION NO: G19
GEOLOGICAL SITUATION: Qnat well
SCALE 1:30

LOCATION: 32⁰,22′,30″N 52⁰,06′,45″E
NAME: Ganjabad (8 km northwest of Yangabad)
SHEET 20 OF 28

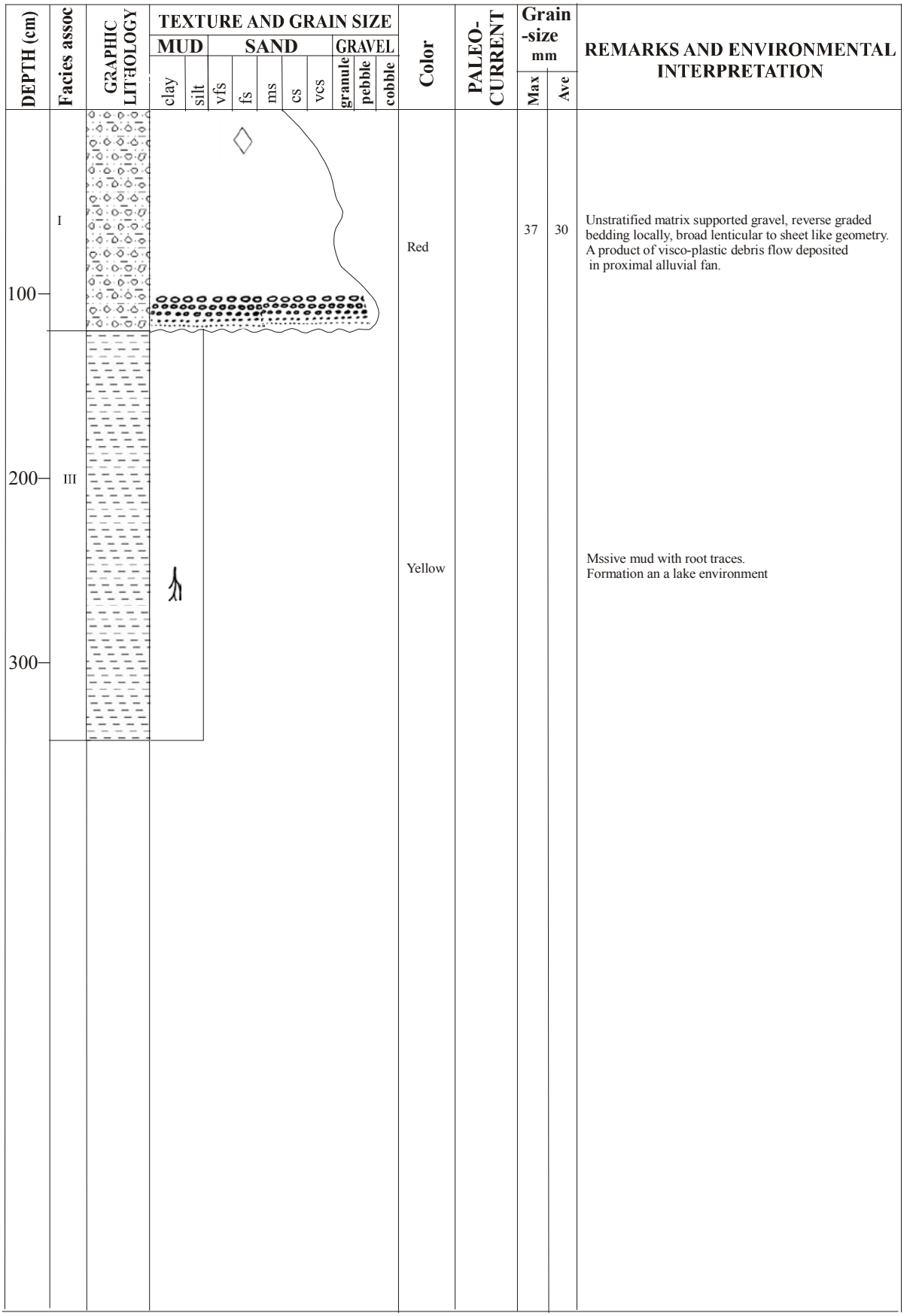

SECTION NO: G21
GEOLOGICAL SITUATION: Stream cut
SCALE 1:30

LOCATION: 32⁰,01′,02″N 52⁰,51′,49″E
NAME: Salt mine (25 km southeast of Hasanabad)
SHEET 21 OF 28

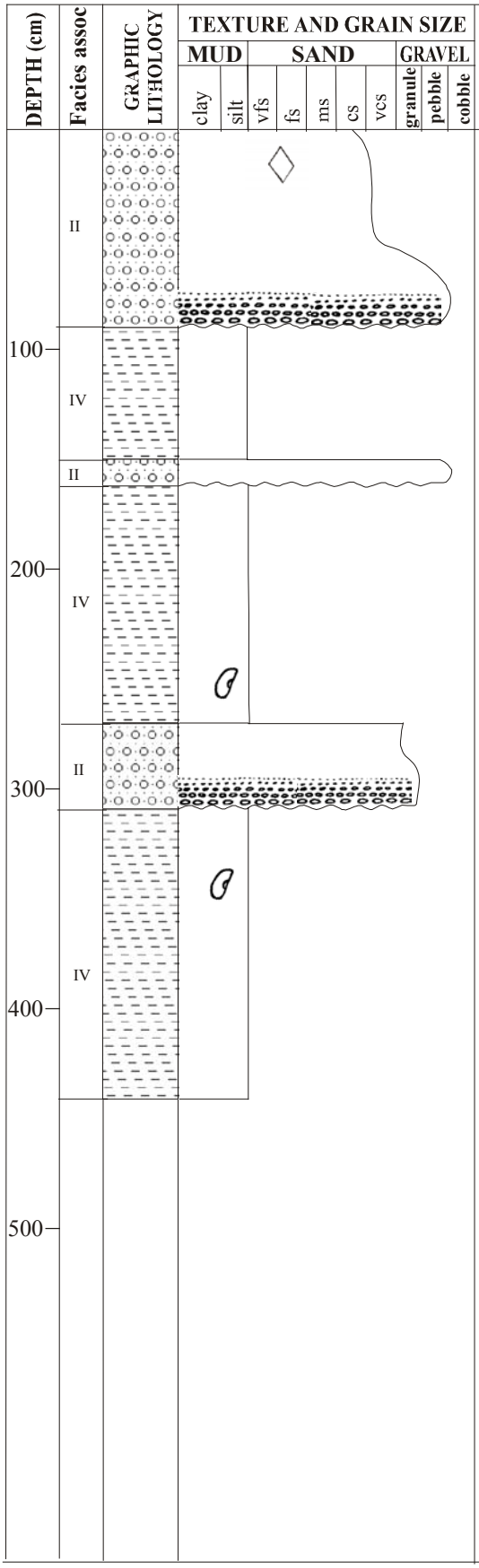

Color	PALEO-CURRENT	Grain-size mm Max	Grain-size mm Ave	REMARKS AND ENVIRONMENTAL INTERPRETATION
Clear		52	42	Massive sandy conglomerate/gravel, broad lenticular geometry with erosional base. Bed load deposition from stream flow under high energy conditions, transporting and accumulating coarse bed load and keeping sand material in suspension.
Khaki				Laminated mud to sandy mud with a few ostracod shells, lenticular geometry. Deposition in a river overbank.
Clear				Sandy conglomerate/gravel, lenticular, wedge- shaped geometry. Deposition of bed load material in high energy condition and keeping sand grains in suspension in a braided to meandering river.
Khaki				Laminated mud with occasional ostracod shells lenticular geometry. A product of deposition in a river overbank environment.
Clear		50	38	Sandy conglomerate/gravel, lenticular, wedge shaped geometry. Lenticular, wedge shaped geometry, erosional base. Deposition in channel under high energy flow and subsequent filling of sand material in suspension.
Khaki				Laminated mud to sandy mud with a few ostracod shells. Deposition in a river overbank environment.

SECTION NO: G22
GEOLOGICAL SITUATION: Stream cut
SCALE 1:30

LOCATION: 32⁰,12′,20″N 52⁰,07′,06″E
NAME: Peykan (10 km southwest of Yangabad)
SHEET 22 OF 28

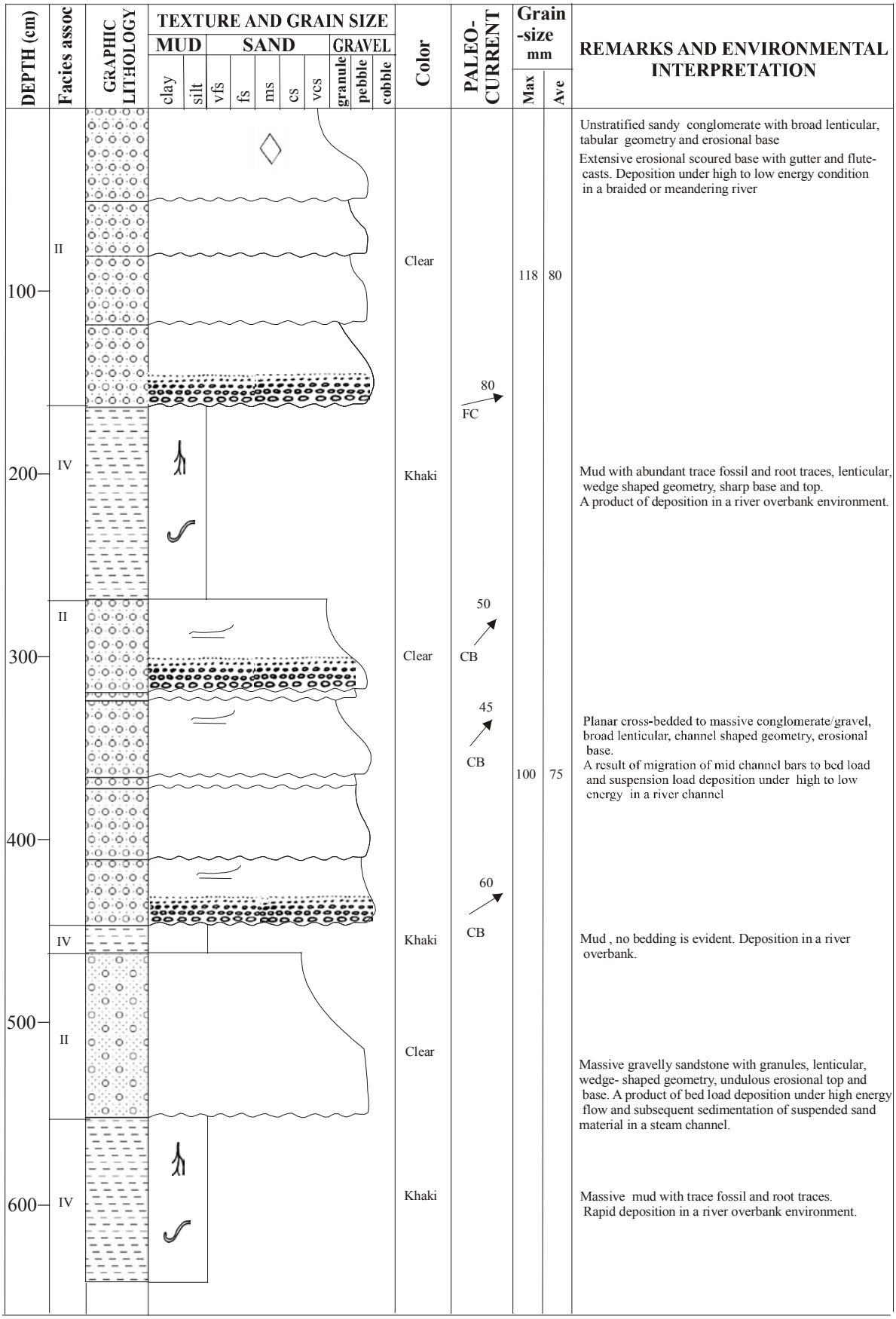

SECTION NO: I1
GEOLOGICAL SITUATION: Trench
SCALE1:15

LOCATION: 32⁰,07′,09″N 52⁰,40′,30″E
NAME: Khara (5 km southeast of hasanabad)
SHEET 23 OF 28

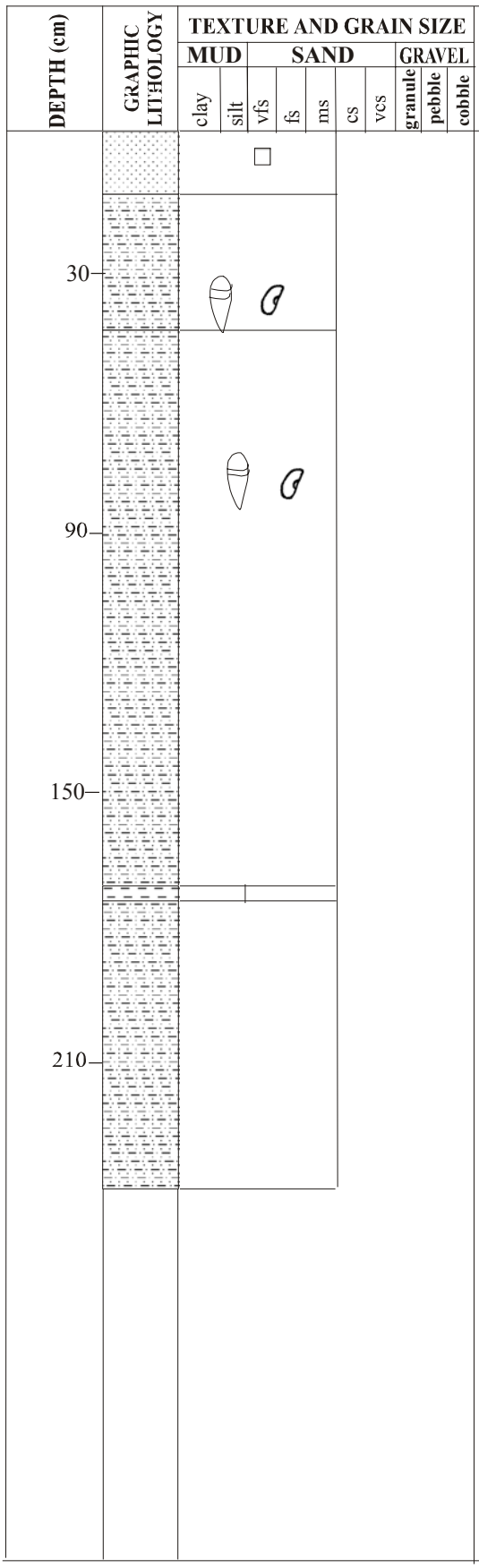

Color	REMARKS AND ENVIRONMENTAL INTERPRETATION
Khaki	Thin bedded fine to medium sand with fine halite crystals, tabular shaped geometry. Deposition in an interdune sub-environment by wind activity.
Grey to black	Massive sandy mud, abundant gastropod and ostracod shells, lenticular gypsum crystals in some places. A product of deposition in a shallow restricted freshwater-brackish lake in reduction conditions.
Off-white	Massive sandy mud, abundant gastropod and ostracod shells. Formation in a shallow fresh water-brackish lake and wind activity.
Brown to red	Brown mud with lenticular geometry. A result of deposition in a fresh water-brackish lake.
Off-white	Massive sandy mud, a few gastropod and ostracod shells. It is deposited in a fresh water -brackish lake with wind activity.

SECTION NO: I2
GEOLOGICAL SITUATION: Trench
SCALE1:15

LOCATION: 32⁰,06′,26″N 52⁰,41′,57″E
NAME: Khara (7 km east of Hasanabad)
SHEET 24 OF 28

Color	REMARKS AND ENVIRONMENTAL INTERPRETATION
Khaki	Thin bedded fine to medium sandy mud, a few gastropod and ostracod shells and fine halite crystals, tabular shaped geometry. Deposited in an interdune sub-environment.
Greenish	Massive sandy mud, a few gastropod and ostracod shells A product of deposition in a fresh water -brackish lake with wind activity..
Brown to red	Brown mud with lenticular geometry. Deposition i na shallow fresh water- brackish lake.
Greenish	Massive sandy mud without gastropod and ostracod shells.
Khaki	Fine to medium massive sandy mud, a few gastropod and ostracod shells. A result of rapid deposition in a shallow restricted lake.

SECTION NO: M1
GEOLOGICAL SITUATION: Trench
SCALE 1:15

LOCATION: 32^0,19$^/$,10$^{//}$N 52^0, 51$^/$, 53$^{//}$E
NAME: Shakhkenar (23 km east of Varzaneh)
SHEET 25 OF 28

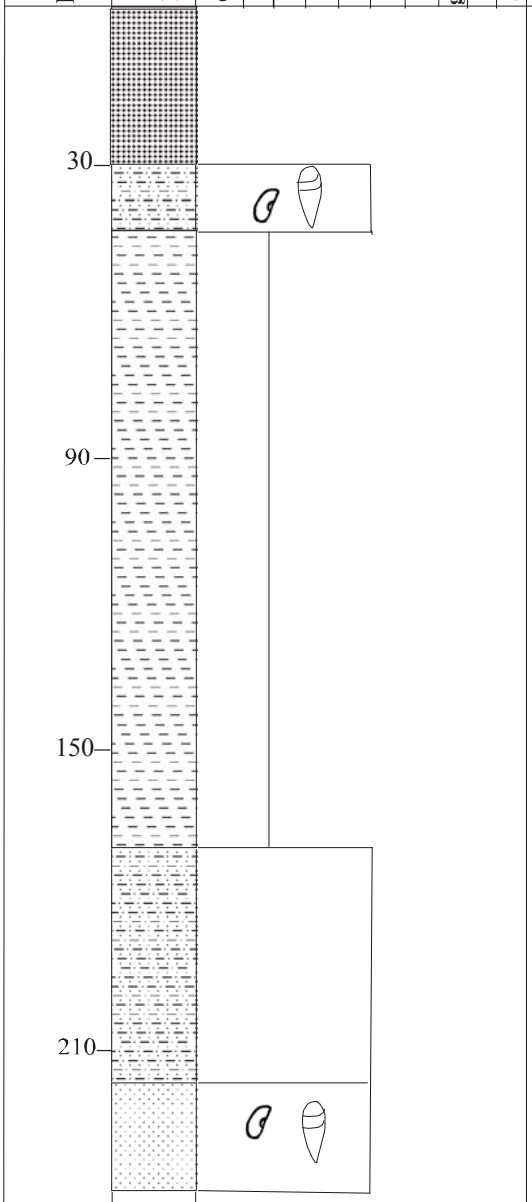

Color	REMARKS AND ENVIRONMENTAL INTERPRETATION
Khaki	Skeletal salt with minor mud, hard and porous surface. Originated from migration of water to surface by capillarity and precipitation after saturation in flood plain.
Khaki	Massive muddy sand with abundant gastropod and ostracode shells. A product of rapid deposition in flood sheets and shallow distributary channels.
Khaki	Massive mud, graditional boundary at base and top. Rapid deposition of suspended load in flood plain
Khaki	Massive muddy sand, graditional boundary at base and top . Deposition in flood plain and shallow distributary channels.
Khaki	Massive fine to medium sand with abundant gastropod and ostracod shells. A rapid deposition during thunderstorms in a shallow temporary lake or also directly as bottom load from the Zayandeh river.

SECTION NO: M2
GEOLOGICAL SITUATION: Trench
SCALE 1:15

LOCATION: 32⁰,18′,09″N 52⁰,53′,07″E
NAME: Kuh-e-Siah (28 km east of Varzaneh)
SHEET 26 OF 28

DEPTH (cm)	GRAPHIC LITHOLOGY	TEXTURE AND GRAIN SIZE										Color	REMARKS AND ENVIRONMENTAL INTERPRETATION
		MUD		SAND					GRAVEL				
		clay	silt	vfs	fs	ms	cs	vcs	granule	pebble	cobble		
			G									Khaki	Skeletal salt with minor mud, hard and porous surface, a few ostracod shells, gypsiferous mud in the eastern saline mud flat. A product of migration of water by capillarity and subsequent saturation in flood plain environment.
30													
												Khaki	Massive mud. Rapid deposition in flood sheet in a semi-arid to arid climate.
90													

SECTION NO: S3
GEOLOGICAL SITUATION: Trench
SCALE 1:15

LOCATION: 32⁰,06′,24″N 52⁰,48′,13″E
NAME: Salt mine
SHEET 27 OF 28

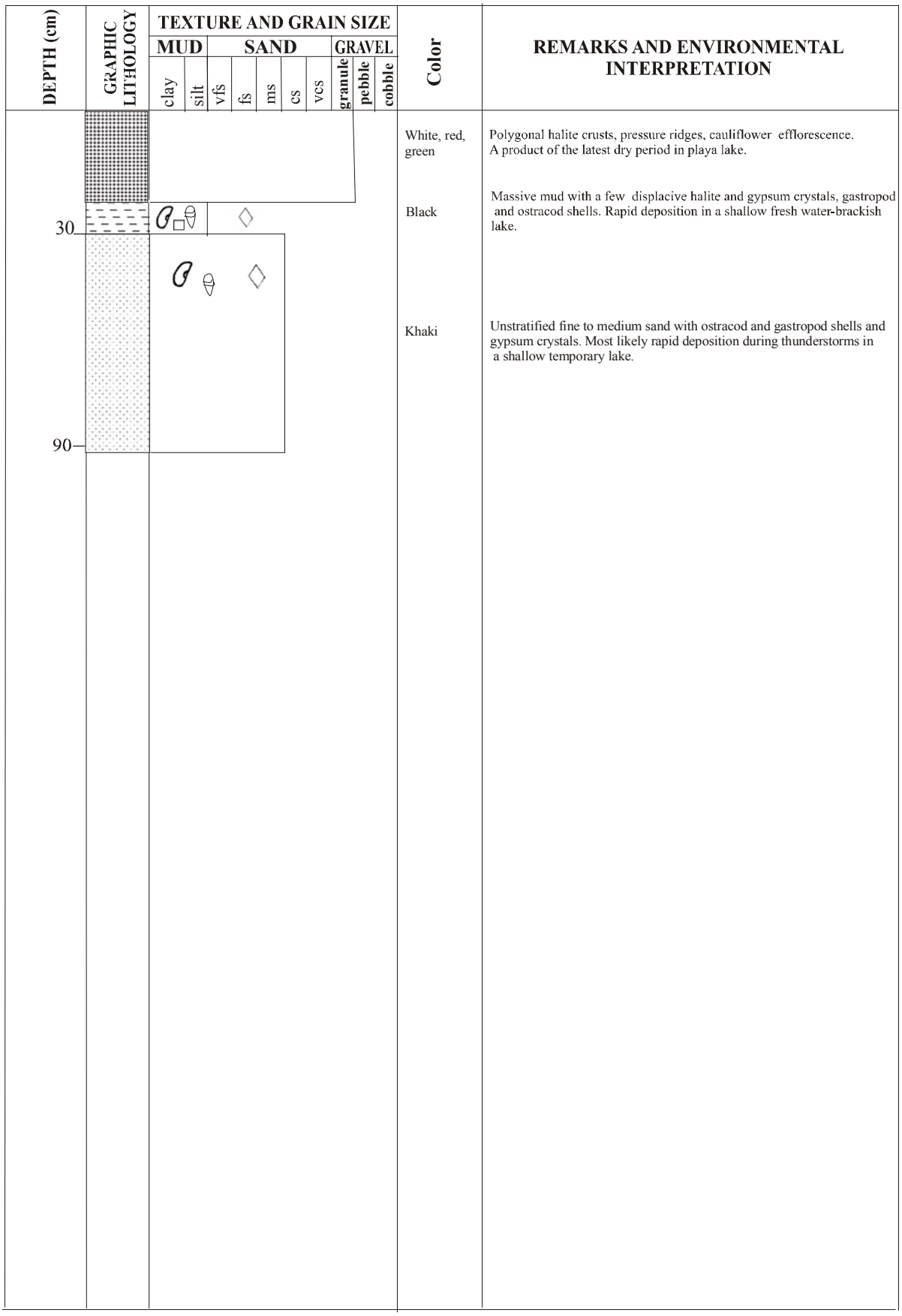

SECTION NO: S4
GEOLOGICAL SITUATION: Trench
SCALE 1: 150

LOCATION: 32⁰,01′,33″N 52⁰,52′,44″E
NAME: salt mine (15 km east of Hasanabad)
SHEET 28 OF 28

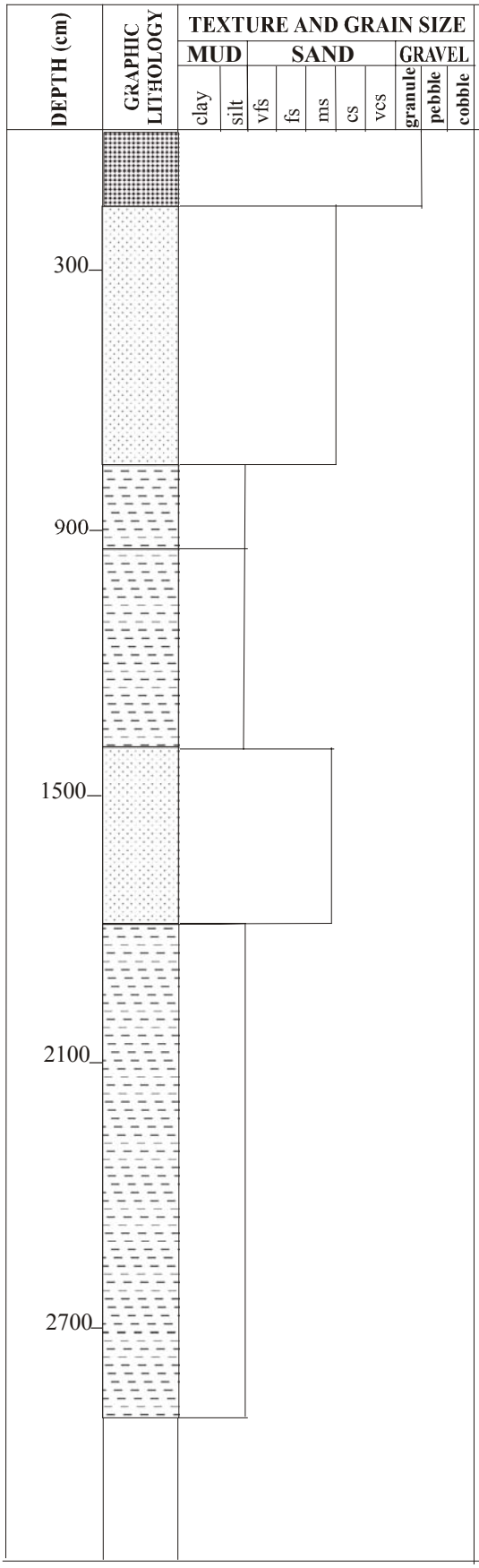

Color	REMARKS AND ENVIRONMENTAL INTERPRETATION
White	Polygonl halite crusts, pressure ridges, cauliflower efflorescence, interbedded with thin bedded black mud. A product of subaqueous crystallization and growth of salt in saline lake.
Khaki	Fine to medium sand. Deposition in a shallow temporary lake or transported by wind from sand dunes.
Greenish	Gypsiferous mud. Probably deposition in a shallow fresh water-brackish lake or flood sheet.
Yellow to brown	Brown mud without any bedding. A product of sedimentation in a shallow fresh water-brackish lake.
Khaki	Fine to medium sand. Most probably reflect deposition during thunderstorms in a shallow temporary lake or directly as bottom load from the Zayandeh river.
Yellow to brown	Mud without any bedding. Deposition in a shallow fresh water-brackish lake in a semi to arid climate.